UNIVERSITÄT TRIER – FACHBEREICH I

DOCTORAL THESIS

THE ROLE OF PHASE-AMPLITUDE COUPLING IN THE RELATIONSHIP BETWEEN ACUTE STRESS AND EXECUTIVE FUNCTIONS

BY

MAREIKE JOHANNA HÜLSEMANN

SUPERVISORS:

DR. RER. NAT. EWALD NAUMANN

PROF. DR. MED. HARTMUT SCHÄCHINGER

TRIER, SEPTEMBER 2016

Affiliation of the Supervisors

Dr. rer. nat. Ewald Naumann
Psychophysiological Laboratory – Department of Psychology
Trier University

Prof. Dr. med. Hartmut Schächinger
Department of Clinical Psychophysiology – Institute of Psychobiology
Trier University

The research leading to this doctoral thesis was funded by the Ministry of Science Rhineland-Palantine within the Research Focus “Psychobiology of Stress” of Trier University. The research leading to thesis was performed at and the thesis was written at Trier University.

WHAT I CANNOT CREATE, I DO NOT UNDERSTAND.

Richard Feynman

ACKNOWLEDGEMENT

Mein größter Dank gilt meinem Doktorvater, Herr Dr. Ewald Naumann, der mir die Chance gab und die Freiheit ließ, Wissenschaft zu betreiben. Seine Erfahrung und Führung haben es mir ermöglicht mein Promotionsprojekt durchzuführen. Herrn Prof. Dr. Hartmut Schächinger danke ich herzlich für seine wertvolle Unterstützung.

Mein Dank gilt Dr. Angelika Dierolf, die mich bei meinen ersten Schritten in der wissenschaftlichen Welt an die Hand genommen und geduldig meine ersten Versuche der EEG-Auswertung begleitet hat.

Den ehemaligen und gegenwärtigen Mitarbeitern des Psychophysiologischen Labors danke ich für ihre tatkräftige Unterstützung bei der Studie, die ich im Rahmen des Promotionsprojektes durchgeführt habe; außerdem für anregende Diskussionen und gemeinsame Reisen.

Linus Fuchs, Thorsten Brinkmann und Lua Kaiser danke ich ausdrücklich für die Revision dieser Arbeit.

I am deeply grateful to Scott Makeig and Makoto Miyakoshi for inviting me to visit the Swartz Center, sharing their expert knowledge with me, and introducing me to the famous tea time.

Ich bin meiner Familie für ihre Liebe und ihren Rückhalt dankbar, im Besonderen meinen Eltern und meinem großen Bruder. Dank gebührt zudem meinen vortrefflichen Freunden, insbesondere Tobi, der alles ins rechte Verhältnis zu rücken vermag.

GENERAL ABSTRACT

Acute stress leads to the release of cortisol which influences the brain in manifold ways. Presumably, it especially influences those structures that are active. Executive functions are a group of abilities which enable us to purposefully shape our behaviour, cognition, and emotion. Executive functions are crucial for a successful and healthy life in our modern society. A huge body of studies shows that stress can influence executive functioning, in essence having detrimental effects. Phase-amplitude cross-frequency coupling is a mechanism thought to facilitate communication between neuronal ensembles, as well as, separation of communication processes from one another and, thereby, enabling parallel processing. It seems to be a ubiquitous phenomenon in mammalian brains. This mechanism could underlie the implementation of complex cognitive processes, like executive functions, in the brain. This thesis contributes to answering the question, whether phase-amplitude cross-frequency coupling is a mechanism by which executive functioning is implemented in the brain and whether an assumed performance effect of stress on executive functioning is reflected in phase-amplitude coupling strength. Via simulation study the performance of two widely used phase-amplitude coupling measures was tested. Both measures were found to meet the requirements of being specific and sensitive to coupling strength and coupling width. The simulation study also drew attention to several confounding factors which influence phase-amplitude measures (e. g. data length, multimodality). In two independent studies, each being comprised of two core executive function tasks (flexibility and behavioural inhibition as well as cognitive inhibition and working memory), beta-gamma phase-amplitude coupling was found to be a robust phenomenon, detected in the left and right prefrontal hemispheres. Minor phase-amplitude coupling strength modulations have been detected in these studies. More importantly no systematic pattern of coupling strength modulation by either task demands or acute stress were detected. Beta-gamma coupling might also be present in more basic attention processes. This is the first investigation of the relationship between stress, executive functions and phase-amplitude coupling. There are many aspects that have not been explored yet, for example, studying phase precision instead of coupling strength as an indicator for phase-amplitude coupling modulations. Furthermore, data was analysed in source space (independent component analysis); comparability to sensor space has still to be determined. These as well as other aspects should be investigated, due to the promising finding of very robust and strong beta-gamma coupling for all executive functions.

CONTENT

INDEX OF FIGURES

INDEX OF TABLES

INDEX OF EQUATIONS

INDEX OF ABBREVIATIONS

ACTH	adrenocorticotropic hormone
Ag/AgCl	silver-silverchloride
ANOVA	analysis of variance
ANS	autonomic nervous system
ASR	artefact subspace reconstruction
BG	beta-gamma
BOLD	blood oxygenation level dependent
CBG	corticosteroid-binding globulin
CFC	cross-frequency coupling
CPT	cold pressor test
CRH	corticotropin-release hormones
DB	delta-beta
DBP	diastolic blood pressure
DG	delta-gamma
ECG	electrocardiography
EcOG	electrocorticogram
EEG	electroencephalography
EOG	electrooculography
ERPAC	event-related phase-amplitude coupling
FFT	fast Fourier transform
FIR	finite impulse response
fMRI	functional magnet resonance imaging
GR	glucocorticoid receptor
HPA	hypothalamus-pituitary-adrenal
IC	independent component
ICA	independent component analysis
LFP	local field potential
M	mean
MEG	magnetencephalography
MI	modulation index
MNI	Montreal Neurological Institute
MR	mineralocorticoid receptor
MRI	magnet resonance imaging
MVL	mean vector length
PAC	phase-amplitude coupling

PVN	paraventricular nucleus
R. V.	residual variance
S. D.	standard deviation
S. E.	standard error
SBP	systolic blood pressure
SECPT	socially evaluated cold pressor test
SNS	sympathetic nervous system
STN	subthalamic nulceus
tACS	transcranial alternating current stimulation
TB	theta-beta
TG	theta-gamma
TMS	transcranial magnetic stimulation
TSST	Trier social stress test
WHO	World Health Organisation

1 General Introduction

1.1 Cortisol and Its Effects on the Brain

> *Stress ist jedoch unser ständiger Begleiter, solange wir leben. Er sitzt mit uns zu Tisch, er geht mit uns schlafen, er ist dabei, wenn leidenschaftliche Küsse getauscht werden. Manchmal geht uns seine Anhänglichkeit ein wenig auf die Nerven; dennoch verdanken wir ihm jeden persönlichen Fortschritt und erreichen durch ihn immer höhere Stufen geistiger und körperlicher Weiterentwicklung. Er ist die Würze unseres Lebens.*
>
> Selye, 1977[1]

History of the stress concept.

Stress research slowly evolved at the beginning of the 20th century. Its origins date back to Claude Bernard (1813 – 1878), who formulated the concept of the *milieu intérieur* that was later on called homeostasis by Walter B. Cannon (1871 – 1945). The concept of homeostasis was derived from the ancient Greeks (Johnson, Kamilaris, Chrousos, & Gold, 1992). Homeostasis – Greek for *steady state* – designates a state of equilibrium within a system that is maintained by permanent adjustments. Examples include the acid-base balance, thermoregulation, and blood pressure. The concept of homeostasis was criticized because some of the systems, like blood pressure, are not constantly held within specific boundaries, but are adjusted according to the challenges the organism has to meet. Cannon himself noted "we should have to learn how steady are the steady states" (Cannon, 1935, p. 13). Thus allostasis was defined; a concept formulated by McEwen (2000a), describing that stability would be achieved through change (McEwen, 2007, p. 880). However, the concept of allostasis does not invalidate the concept of homeostasis. Even though deviations from homeostasis are inherent and even necessary, a "chronically increased allostasis can lead to pathophysiology" (McEwen, 2007, p. 880). Cannon was the first to use the term stress in a biological sense, when stating: "It will be pertinent, therefore, to survey some of the stresses of homeostasis to which we are not uncommonly subjected, in order to learn how well the organism meets them and how much strain is imposed" (Cannon, 1935, p. 8). The terms stress and strain were borrowed from material science, where stress is defined as the force per unit area and strain is defined as the amount of deformation caused by stress.

Hans Selye (1907 – 1982), who published his seminal work in 1936, developed his stress concept on the basis of observations on human patients in hospitals and laboratory animals. The animals showed largely similar symptoms when being mistreated by diverse noxious agents or maltreatment (Selye, 1936). Selye observed three phases in response to stress, and subsumed them under the term *general adaption syndrome:* the alarm reaction, comprising all non-specific physiologic responses to stimuli the organism is not adapted to; the stage of resistance, comprising all non-specific physiologic responses to stimuli to which the organism adapted due to unceasing exposure; and the stage of

[1] "As long as we live, stress is our constant companion. Stress sits down with us at table, it goes to bed with us, it is present when passionate kisses are exchanged. Sometimes its devotedness annoys us; however, we owe stress every personal progress and reach ever increasing levels of mental and physical development due to stress." (Translation M. J. H.)

exhaustion, comprising all non-specific physiologic responses to stimuli to which the organism previously adapted to, but can no longer sustain adaption (Selye, 1946, pp. 119–121). The general adaption syndrome obtained its name due to generally emerging in response to any stimulus, to which the organism is not yet adapted to. Using the term stress scarcely in the beginning (e. g. Selye & McKeown, 1935, Selye, 1939, and Selye & Pentz, 1943), Selye embraced it following World War II. At this time the US army popularized the term stress and also promoted biological and psychological research on it, aiming to find out why excellent pilots crashed their planes during distressing acts of war (Kury, 2012). Selye's work concentrated on the hypothalamus-pituitary-adrenal (HPA) axis response, which today is known to be much more specific than postulated by Selye (e. g. Sapolsky, Romero, & Munck, 2000, p. 56). In contrast, Cannon's work concentrated on the stress response of the autonomic nervous system (ANS), which in fact seems to be unspecific.

Definition of Stress.

Here stress and the stress response are defined according to Chrousos "as a state in which homeostasis is actually threatened or perceived to be so; homeostasis is re-established by a complex repertoire of behavioural and physiological adaptive responses of the organism" (Chrousos, 2009, p. 374). Instead of using the term homeostasis, one can speak more generally about "a real or interpreted threat to the physiological or psychological integrity of an individual" (McEwen, 2000b, p. 508). Further, a focus is led on the biochemical stress response, that is, the increase of adrenal glucocorticoids and catecholamines due to an experience (McEwen, 2000b, p. 508). The fact that "stress is also a subjective experience that may or may not correspond to physiological responses" (McEwen, 2000b, p. 508) plays a minor role in this thesis.

A stressor, defined as a stimulus or situation that induces stress, can be virtually anything, as long as it is severe enough to require major physiological or psychological adjustments (Lovallo, 1997). It can be useful to distinguish between physiological and psychological stressors. In contrast to physiological stressors, psychological stressors contain a higher degree of subjective appraisal processes. The literature implies that physical stressors, like the cold pressor test (CPT; Velasco, Gomez, Blanco, & Rodriguez, 1997), predominantly induce an autonomic stress response while the endocrine stress system is only marginally innervated (McRae et al., 2006; Velasco et al., 1997). Psychological stressors, like the Trier social stress test (Kirschbaum, Pirke, & Hellhammer, 1993), on the other hand lead to a marked autonomic and endocrine stress response (Dickerson & Kemeny, 2004). It was also found that physical stressors primarily recruit the brain stem and hypothalamus, while psychological stress recruits the amygdala, prefrontal cortex, and the hippocampus (Herman & Cullinan, 1997; Joëls & Baram, 2009).

The biochemical response.

The physiological stress response is composed of two biochemical cascades. Stressors which can be signals from the inner and outer environment, as well as appraisal processes, are able to stimulate the hypothalamus to trigger a fast stress response via the autonomic nervous system and a slow stress response via the HPA axis (Silbernagl & Despopoulos, 2012). Within seconds after stress onset, the sympathetic nervous system (SNS), a part of the autonomic nervous system innervates the adrenal medulla to secrete adrenalin and noradrenalin into the bloodstream. This fast autonomic stress response seems to be unspecific (i. e. activated by any stressor). Its main function is to mobilize chemically saved energy (e. g. lipolysis) and, at the same time, increase the cardiac output and inhibit gastrointestinal functions (Silbernagl & Despopoulos, 2012). In other words, it facilitates survival relevant functions (e. g. energy allocation) and inhibits survival irrelevant functions (e. g. digestion). Catecholamines, to which adrenalin and noradrenalin belong, cannot cross the blood brain barrier, but can nevertheless exert feedback on the brain via the vagus nerve (McGaugh, 2000).

Within minutes after stress onset, peaking about 20 to 40 minutes post stress onset (Dickerson & Kemeny, 2004), the HPA axis secrets its end-product cortisol into the bloodstream. Specifically, stress causes the secretion of corticotropin-release hormones (CRH) from the paraventricular nucleus (PVN) of the hypothalamus. CRH in turn induces the release of adrenocorticotropic hormones (ACTH) from the corticotroph cell of the anterior pituitary in the bloodstream via the hypophyseal portal veins, which then trigger the release of glucocorticoids (mainly cortisol in humans) from the adrenal cortex (Nestler, Hyman, & Malenka, 2009). Only 5 % of the exerted cortisol is biologically active; 95 % is bound to carrier proteins like the corticosteroid-binding globulin (CBG). Each component of the HPA axis exerts negative feedback on all previous sites of the HPA axis, thereby preventing an overshoot of the stress response (Keller-Wood, 2015; McEwen, de Kloet, & Rostene, 1986; Silbernagl & Despopoulos, 2012). The key effects of cortisol are an increase in blood glucose level and its immunosuppressive function. In contrast to catecholamines, which immediately help the organism to cope with a stressful situation, cortisol is responsible for regaining homeostasis. Tausk (1951, p. 16) compared stress with fire, stating that cortisol should be seen as the resource that curtails the water damage arising from fire-fighting operations; cortisol should not be seen as the fire-fighting operation itself.

Glucocorticoid receptors in the brain.

Once released into the blood stream, cortisol is distributed quickly throughout the whole body. Being a small and lipophilic hormone, biologically active cortisol readily diffuses across the blood-brain barrier and other cell membranes (Nestler et al., 2009). Theoretically, cortisol concentrations should rise especially in those brain regions to which most of the oxygenated blood is transported, i. e. to the active areas. This assumption is inferred by the same logic that underlies the blood oxygenation level dependent (BOLD) signal of functional magnet resonance imaging (fMRI) and is additionally supported by Makara

and Haller (2001), who state that "glucocorticoids in general can affect many processes, but the process actually affected is the one, which is active" (Makara & Haller, 2001, p. 379). Cortisol is only retained in cells which contain cortisol receptors (Joëls & de Kloet, 1994; McEwen, Weiss, & Schwartz, 1968). Genomic cortisol effects, acting via intra-cellular receptors, and non-genomic cortisol effects, acting via membrane receptors are differentiated.

The most well-known cortisol receptors are the intracellular glucocorticoid (GR) and mineralocorticoid (MR) receptors. Actions via these receptors are genomic. That is, the ligand-receptor complex, after translocating to the nucleus of the cell, induces or inhibits transcription and thereby translation of genes (de Kloet, Holsboer, & Joëls, 2005; Webster & Cidlowski, 1999). GRs and MRs can be found throughout the entire brain, concentrations being especially high in the hippocampus (McEwen et al., 1968; Meaney & Aitken, 1985; Patel et al., 2000; Sánchez, Young, Plotsky, & Insel, 2000; Sarrieau et al., 1986; Sarrieau et al., 1988). This discovery resulted in extensive research of cortisol effects on memory (Het, Ramlow, & Wolf, 2005; Sauro, Jorgensen, & Pedlow, 2003; Schwabe, Joels, Roozendaal, Wolf, & Oitzl, 2012).

Action via membrane receptors, contrary to intracellular GRs and MRs, is non-genomic and thereby rather short-termed and reversible: a ligand-receptor complex exerts its effect immediately, for example, by changing ion channel permeability. Existence of various membrane receptors throughout the brain and body has been confirmed (Dallman, 2005; Losel et al., 2003; Makara & Haller, 2001; Norman, Mizwicki, & Norman, 2004). Evidence exists that MRs and GRs can also be located within membranes, having a much lower affinity for glucocorticoids than their intracellular counterparts (de Kloet, 2013). Additionally, the intracellular GR is a candidate for non-genomic action. When cortisol binds to a GR, a heat-shock protein is detached from the receptor (Makara & Haller, 2001). While the receptor-ligand complex will induce genomic actions, the heat-shock protein could exert rapid effects on cell properties.

In the studies presented in this thesis, primarily non-genomic effects that evolve within minutes will be examined. Genomic effects, which have been shown to mainly evolve hours and up to days after stress onset (Joëls & de Kloet, 1994), are not fully covered. However, investigating behaviour up to 35 minutes after stress onset, the most rapid genomic effects cannot be excluded (Makara & Haller, 2001).

How does cortisol affect cell properties within the brain? Joëls and de Kloet (1994) discuss three possible mechanisms: alterations in ionic conductivities, alterations in transmitter systems (synthesis, turnover, release, uptake, receptor properties, changes in functional responses), and alterations in cell properties (metabolism, morphology). To give one concrete example for the second mechanism, cortisol has been shown to inhibit the catecholamine reuptake in the pre-synaptic neuron (Wang et al., 2013, but also see Lieberman, Stokes, Fanelli, & Klevan, 1980). Joëls and de Kloet (1994) gathered plenty of evidence for all three mechanisms via the genomic pathway, but these mechanisms equally apply for the non-genomic pathway (Groeneweg, Karst, de Kloet, & Joëls, 2011; Losel et al., 2003; Myers, McKlveen, & Herman, 2014; Norman et al., 2004). The experiments presented in this thesis are blind

to the exact mechanisms by which cortisol exerts its influence on neural transmission. For detailed reviews of these mechanisms the reader may refer to Joëls and de Kloet (1994), Haller, Mikics, and Makara (2008), and Makara and Haller (2001).

Knowledge about glucocorticoid receptors, their distribution, and their functionality has been gained primarily from in vitro studies and studies with rodents. Studies on non-human primates and humans are scarce in comparison. Following Leibniz who stated "[…] *la nature ne fait jamais des sauts*: ce que j'appellois la *Loy de la Continuité* […]" (Leibniz, 2013, XXVIII)[2], one can be rather confident that most basic mechanisms which are valid in rodents are also valid in primates, both belonging to placentals, a subdivision of the class of mammals. Nevertheless, evolution has progressed since speciation, and caution is appropriate. This is especially true for the prefrontal cortex, which seemed to have evolved massively from rodents to primates (Preuss, 1995).

Influence of stress on the prefrontal cortex.

Arnsten (2009) suggests that during the experience of stress, the usually present top-down regulation of brain regions by the prefrontal cortex is impaired. Amongst others, under non-stressful conditions the prefrontal cortex inhibits dopamine and noradrenaline producing cell bodies in the brain stem. Under stress this inhibition seems to collapse. Without inhibition, central catecholamines are released to larger extents. This causes bottom up attention, emotional habits, as well as rapid and reflexive behaviours, in contrast to purposeful behaviour, which dominates when the prefrontal cortex is in control. Arnsten's theory concentrates on the effects of catecholamines. However, glucocorticoid receptors are present in the monoamine producing cell bodies (Joëls & de Kloet, 1994), potentially influencing their activity. Both catecholamines and glucocorticoids are released and influence the brain during stress, especially psychological stress.

The fact that loss of control is essential for causing stress effects on the prefrontal cortex and also for the release of cortisol in stressful situations (Dickerson & Kemeny, 2004), suggests that cortisol is necessary for the occurrence of stress effects on the prefrontal cortex. Effects of cortisol might be indirect, e. g. by potentiating catecholamine effects by inhibiting their reuptake in the pre-synaptic neuron.

Influence of the prefrontal cortex on the hypothalamus-pituitary-adrenal axis.

It is not only cortisol that acts on the brain; at the same time the HPA axis is influenced by various brain structures (Dedovic, Duchesne, Andrews, Engert, & Pruessner, 2009; Nestler et al., 2009, p. 247). Thereby, the prefrontal cortex is the only neocortical structure that has direct efferents to the hypothalamus (Fuster, 1980). An initial misconception of a purely inhibitory effect of the prefrontal cortex on the HPA axis was later replaced by the assumption that, depending on the kind of stress (e. g. psychological or physical) and depending on the brain region which is exerting the influence, the HPA

[2] „Nature does not make leaps. That is what I call the Law of Continuity." (Translation M. J. H.)

axis can be inhibited or activated by the prefrontal cortex (Dedovic et al., 2009; Diorio, Viau, & Meaney, 1993; Kern et al., 2008). Because these studies are predominantly correlational, the direction of effects remains unclear and no causal relationship can be proven.

In summary, stress, especially psychological stress, triggers the release of cortisol which in turn influences neuronal processes in manifold brain regions and ways. Those processes that are active, seem to be especially influenced by cortisol.

1.2 Executive Functions

Brains are foretelling devices … . Even in the most complex animals, the goal of cognition is the guidance of action.
Buzsáki, 2006

Executive functions are a group of abilities which enable us to purposefully shape our behaviour, cognition, and emotion. Executive functions enable us to execute coordinated, planned, and adaptively optimized behaviour in specific situations or regarding a specific goal (Jäncke, 2013). They are needed when obstacles prevent automatic processes and they require attention and concentration. Executive functions are therefore effortful processes that modulate sub-processes (top-down influence).

Executive functions are crucial for a successful and healthy life in our modern society. Adele Diamond compiled an extensive list, backed up by several references, describing the aspects of life where executive functions are required (Diamond, 2013, p. 137, Table 1). Accordingly, impaired executive functions are associated with various mental disorders (addiction, attention deficit hyperactivity disorder, conduct disorder, depression, obsessive compulsive disorder, schizophrenia). Impaired executive functions are further associated with poor physical health (obesity, substance abuse, poor treatment adherence) and less quality of life. They predict school readiness even more than intelligence as well as school and job success. They are further relevant to interpersonal life, as people with good executive functions are easier to get along with and are more dependable. Executive functions potentially help to improve public safety: studies suggest that people with poor executive functions are more likely to commit crimes and behave violently and recklessly.

Two unique research approaches indicate that all the above listed abilities and processes, subsumed under the term executive function, rely on three core executive functions: flexibility, inhibition, and working memory (Miyake et al., 2000; Sabb et al., 2008). While some authors add additional abilities, these three basic abilities are widely accepted as being either the fundamental basic executive functions or at least belonging to them.

Flexibility represents the ability to switch between tasks, actions, demands, etc. When behaving flexibly, one has to disengage from A and engage in B. Reasons for having to switch are manifold and the alternative action B must not be known beforehand. For example, finding divergent ways for

problem solving requires flexible thinking. Adjusting ones behaviour according to potentially changing rules or different environments is another example. Goal-directedness is, as for all executive functions, a key characteristic. Flexibility can refer to cognition, behaviour, and emotion.

Inhibition describes the ability to withhold an automatic or dominant action, thought, or emotion. Typically, it is easier to execute the behaviour that needs to be inhibited. That is why active and demanding willpower is needed for inhibition. In the case of inhibition, actions are not driven by stimuli directly, which would be impulsive or automatic behaviour, but are instead deliberate. The kind of inhibition described here, needs to be actually intended, therefore – following the argumentation of Miyake et al. (2000) – inhibition processes like *negative priming* or *inhibition of return* are excluded.

Working memory describes a limited-capacity storage (Baddeley & Hitch, 1974). People usually can keep 7 ± 2 items in working memory (Miller, 1956). The duration of storage is normally restricted to a few seconds and can be prolonged by constant rehearsal. Wide agreement exists in the scientific community to differentiate between working memory and short-term memory. The only difference thereby is that short-term memory is engaged when material has to be simply held in mind and working memory is engaged when the memorized material has to be manipulated (Baddeley, 2000). For example, the reproduction of a series of numbers requires short-term memory, but the reverse reproduction of that series requires working memory. Working memory is essential for both of the former aspects of executive functioning (flexibility and inhibition): one must keep the goals or rules in mind in order to act flexibly or inhibit specific behaviours, cognitions, and emotions. As an example, higher working memory capacity was found to attenuate detrimental effects of stress on the ability to act flexibly (Edwards, Moore, Champion, & Edwards, 2015).

Miyake et al. (2000) defined these three concepts as basic processes serving executive functioning, first, because flexibility, inhibition and working memory[3] are well defined, low level functions that can be precisely operationalised. Secondly, several well validated tasks are available and widely used to measure each of these functions. Thirdly, all three functions combined are likely to support more complex executive functions. In a confirmatory factor analysis, which was replicated by Friedman et al. (2008), Miyake et al. (2000) found all three basic functions to be self-contained, while simultaneously being significantly correlated (Figure 1.1a). Analysis further showed that all tests that were used to operationalise the three basic executive functions load on one common executive function factor (Figure 1.1b). The common factor explains part of the variance generated by flexibility and working memory tasks. Nevertheless, there is still unique variance left which is explained by flexibility and working memory specific factors. In contrast, the common factor explains all variance generated by the inhibition tasks. This does not mean that one can omit the factor inhibition. It is a process independent from flexibility and working memory, which can be completely explained by a common executive function factor that also explains some of the variance of flexibility and working memory.

[3] Miyake et al. (2000) use the term shifting for flexibility and the term updating for working memory. These terms are used synonymously.

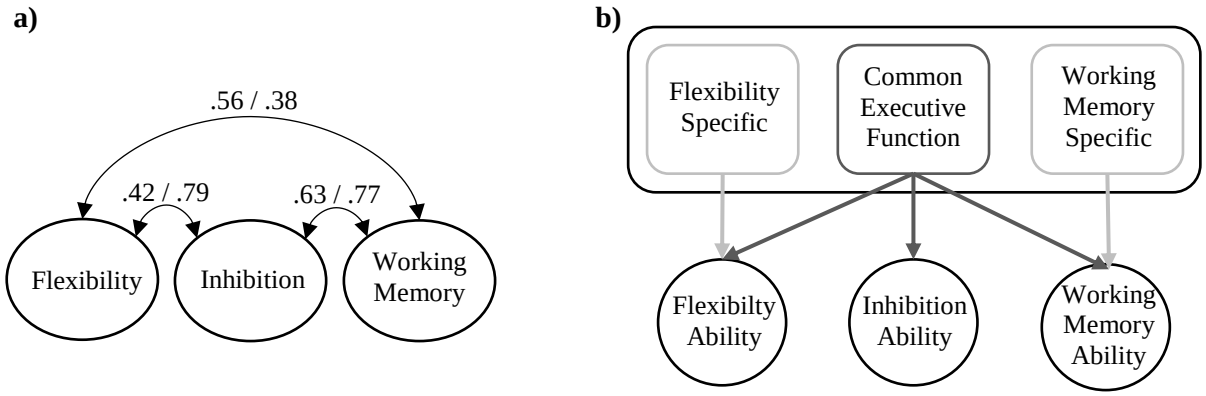

Figure 1.1: a) Correlation between three latent variables, reflecting the three basic executive functions. Correlation coefficients on the left are the results from the first analysis of Miyake et al. (2000) and correlation coefficients on the right are the results from a second sample reported in Friedman et al. (2008). b) Diagram of the unity (the common executive function related to all three basic executive functions) and diversity (specific functions; e. g. flexibility specific) of the three basic executive functions flexibility, inhibition, and working memory. Figure 1a is reprinted with permission from Elsevier (Cognitive Psychology (41), 49-100, Miyake et al., Copyright © 2000) and adapted with permission from the American Psychological Association (Copyright © 2008). Figure 1b is adapted from Miyake and Friedman (2012).

Sabb et al. (2008) searched the scientific literature for terms associated with the term "cognitive control", which is used synonymously with executive function. Working memory, task switching or set shifting (flexibility), response inhibition (inhibition), and response selection were the four terms most frequently associated with cognitive control. This review revealed that cognitive control truly is a generic term, as it was almost never measured directly but always indirectly via one of the four subtopics. Response selection will be subsumed under the term inhibition as it is operationalised by tasks which represent inhibition. There is "evidence that some of these constructs [especially working memory and inhibition] may be ontologically distinct, as reflected in the ability to accurately classify them on the basis of brain imaging data" (Lenartowicz, Kalar, Congdon, & Poldrack, 2010, p. 690).

Executive functions are supported by the prefrontal cortex.

Fuster (1980) suggested three nearly identical functions to those of Miyake et al. (2000) and Sabb et al. (2008) as core functions of the prefrontal cortex: anticipation, control of interference, and provisional memory. Control of interference and provisional memory can undoubtedly be equalised with inhibition and working memory, respectively. Even though not identical with flexibility, the concept of anticipation incorporates the precondition for flexible behaviour: "Because of past experience, therefore, the organism is able to prepare, with the assistance of the prefrontal cortex, for a certain range of possible contingencies" (Fuster, 1980, p. 134). Anticipation also incorporates attention processes and is especially related to the orienting system of the attention theory according to Posner and Petersen (Fan, McCandliss, Sommer, Raz, & Posner, 2002; Petersen & Posner, 2012; Posner & Petersen, 1990):

"Preparation involves the adjustment of the sensory and motor apparatus before each event, thus optimizing reception and setting effector systems for the anticipated movement" (Fuster, 1980, p. 134).

The first evidence for the localisation of executive functions in prefrontal cortex originated from lesion studies (Fuster, 1980). It was found that the larger the amount of damaged prefrontal cortex, the larger the adverse effects on executive functioning.

The ability to flexibly adjust action, cognition, and emotion evolves late in life. The same is true for inhibition and working memory capacity. Executive functions seem to mature until the end of adolescence. Moreover, flexibility and inhibition performance, as well as working memory capacity, decline in the elderly. This development is paralleled by the maturation of the prefrontal cortex up until and beyond the age of 20 (Gogtay et al., 2004; Jäncke, 2013)[4] and its subsequent decline in the elderly (Ziegler et al., 2012). Both executive functions and prefrontal cortex follow the "last in – first out" principle. Of course this parallel does not imply causality, but along with findings from lesion and electrophysiological studies (Fuster, 1980), it leaves little doubt as to the causal dependence of executive functions on prefrontal cortex structures.

Several meta-analyses confirm that prefrontal and parietal cortices are more active during the execution of flexibility tasks (Niendam et al., 2012; Wager, Jonides, & Reading, 2004; Yarkoni, Poldrack, Nichols, van Essen, & Wager, 2011), inhibition tasks (Cai, Ryali, Chen, Li, & Menon, 2014; Levy & Wagner, 2011; Nee, Wager, & Jonides, 2007; Niendam et al., 2012; Yarkoni et al., 2011), and working memory tasks (Cabeza & Nyberg, 2000; Niendam et al., 2012; Rottschy et al., 2012; Wager et al., 2004; Wager & Smith, 2003; Yarkoni et al., 2011) when compared with control tasks or resting conditions. Activations are generally bilateral, one exception being inhibition, which in two of the five meta-analyses was found to be associated solely with activation in the right hemisphere (Cai et al., 2014; Levy & Wagner, 2011). Executive functions are thus localised at the prefrontal and parietal cortices. Anatomical domains of each of the three basic executive functions are not clearly separable from one another (Lenartowicz et al., 2010; Yarkoni et al., 2011). Activations largely, but not fully, overlap. It seems that all executive functions share large parts of the prefrontal and parietal cortices, with individual focuses on some structures. This assumption is supported by two facts: first, deficits after prefrontal cortex lesions partly depend on the lesion location and, second, besides a common connectivity structure, parts of the prefrontal cortex have unique connections to other neural structures (Fuster, 1980).

In this thesis electroencephalography (EEG) is measured in the most common way, using a standardised electrode cap, positioned in a standardised way, but not localizing electrode positions exactly or having an individual magnet resonance imaging (MRI) scan. Therefore, all localization attempts in this thesis are coarse. Hence, results of the meta-analyses shall serve as rough estimation of where to look for stress effects on executive functioning, namely in the left, midline, and right fronto-parietal network as well as within the prefrontal cortex.

[4] The parietal cortex on the other hand matures much earlier. Gogtay et al. (2004) published, along with their paper, videos showing the myelinisation of the human cortex.

As a critical note, one should be aware that the fronto-parietal network is not specifically activated during executive functioning, but rather seems to be generally activated during cognitive and emotional tasks (Toro, Fox, & Paus, 2008). That is why it is also called the task-positive network, which can be clearly distinguished from the task-negative default mode network that is active during rest (Fox et al., 2005; Schwarz et al., 2013).

Stress and Executive Functions.

Former publications often argue that cortisol receptor density in the prefrontal cortex is especially high and therefore an association between stress and prefrontal cortex related processes is probable and worth to investigate. To my knowledge, there is no actual publication indicating an especially high cortisol receptor density in the prefrontal cortex, as it is the case for the hippocampus. The relationship between stress and executive functions is nevertheless reasonable to investigate, as this and the former section have shown. This is the case, first, because cortisol is likely to accumulate in those regions that are activated, i. e. in the prefrontal cortex during the use of executive functions. Second, the work of Arnsten (2009) strongly indicates that the prefrontal cortex is cut off during stress. Third, it was shown that cortisol receptors are present throughout the whole brain. An especially high density of receptors is thus not necessary for hypothesising cortisol effects on prefrontal structures.

Furthermore, illnesses like schizophrenia or mood disorders, of which onset is thought to be provoked by stress and which are associated with alterations in prefrontal MR and GR quantity, distribution, and activity compared to healthy controls, are repeatedly associated with executive dysfunction (Holmes & Wellman, 2009; Qi et al., 2013; Sinclair, Tsai, Woon, & Weickert, 2011; Webster, Knable, O'Grady, Orthmann, & Weickert, 2002).

The interplay of stress and executive functioning is intensively studied in humans (cf. sections 3.1 and 4.1). But despite the overwhelming amount of these studies, only a minor part measures EEG (e. g. Lai et al., 2014; Sänger, Bechtold, Schoofs, Blaszkewicz, & Wascher, 2014; Yildiz, Wolf, & Beste, 2014), let alone analysing cross-frequency coupling (CFC). Fuster emphasises that “the study of the neural mechanisms by which the prefrontal cortex fulfils its postulated role in anticipatory set, provisional memory, and suppression of interference” (Fuster, 1980, pp. 140–141) is “of paramount importance” (Fuster, 1980, p. 140). And in 2004 Ridderinkhof et al. still remark that “conspicuously little is known about how the brain determines and communicates the need to recruit cognitive control and how such signals instigate the implementation of appropriate performance adjustments” (Ridderinkhof et al., 2004, pp. 129–130). To overcome this state, this thesis investigates whether the construct of phase-amplitude cross-frequency coupling, being introduced in the next chapter, could be a mechanism by which the brain implements executive functioning, and whether this is influenced by stress.

1.3 Phase-Amplitude Cross-Frequency Coupling: A new Tool to investigate Neuronal Communication

> *We are like the prisoners in the cave [of Plato]. There are platonic 'biological bases of behaviour' that we want to discover (the figures walking on the pathway behind the prisoners), but all we can observe are the shadows cast on the wall (empirical data) by the flame in the back of the cave (methods and technologies); (…) However we have one important advantage over the prisoners in Plato's cave: We can, to some extent, control the flame. We can develop new technologies and methodologies, and we can combine methodologies in interesting, novel, and insightful ways.*
>
> Cohen, 2011

The oscillating brain.

Neurons are the basic unit of the central nervous system[5], being causal for neural communication via action potential generation and transfer (Thompson, 2000). Action potentials in turn are responsible for one important characteristic of the brain: its oscillating nature. When recording electrical activity emitted from the brain, one registers an oscillating electrical current. This was first shown in humans by Berger (1929). Three spatial scales exist: *microscopic oscillations* are spike trains from single cells, *mesoscopic oscillations* are local field potentials (LFP) including several ten thousands of nerve cells, and *macroscopic oscillations* are either recorded from subdural electrocorticogram (ECoG) summing up millions of cells or at an even broader scale from scalp recordings (EEG, magnetencephalography [MEG]) integrating several cortical areas (Canolty & Knight, 2010; Young & Eggermont, 2009).

The causal relationship between microscopic oscillations in the form of spike trains and neural communication is straightforward. It can be experimentally investigated by manipulating cells with substances; this manipulation leads to altered oscillations and, in turn, to an altered signal transmission from the manipulated neuron to its down-stream neurons (Joëls & de Kloet, 1992). In contrast, meso- and macroscopic oscillation are more complex and therefore more difficult to understand. They do not reflect action potentials generated by single neurons. Instead, one could say the "sounds" that neurons produce when "talking" to each other, can be "heard" as meso- or macroscopic oscillations. In the case of macroscopic oscillations, the sound is composed of the synchronous spiking of several millions of cells. Therefore, macroscopic oscillations are effectively epiphenomenal. They do not represent the direct neuronal information transfer, but instead are produced by the information transferring cells of the brain. Berger has already stated: "Wir sehen im Elektrenkephalogramm eine Begleiterscheinung der ständigen Nervenvorgänge, die im Gehirn stattfinden, genau wie das Elektrokardiogramm eine

[5] By saying this, the importance of glia cells, making up about 50 % of the brain (Herculano-Houzel, 2009), is neglected. Research on glia cells and on their contribution to neuronal information transfer is only in the beginning stages and should be integrated in all aspects of electrophysiology in the future.

Begleiterscheinung der Kontraktionen der einzelnen Herzabschnitte darstellt“ (Berger, 1929, p. 569)[6]. Notwithstanding being effectively epiphenomenal, macroscopic oscillations have a direct connection to neuronal information transfer and are correlated with behaviour (Buzsáki, 2006). By modulating macroscopic oscillations, e. g. via transcranial alternating current stimulation (Vosskuhl, Huster, & Herrmann, 2015) or transcranial magnetic stimulation (Meyer & Damasio, 2009), behaviour can be modulated. Mesoscopic oscillations were shown to predict concrete behaviour as well as spike trains (Mehring et al., 2003; Pesaran, Pezaris, Sahani, Mitra, & Andersen, 2002).

There are two compelling reasons for choosing to investigate macroscopic over microscopic and mesoscopic oscillations. First, macroscopic oscillation can be relatively economically, and most important, non-invasively measured in human brains. Second, networks of cells code information in the brain, not single cells alone (Buzsáki, 2006; Hebb, 1949; Meyer & Damasio, 2009; O'Reilly, 1998; Sporns, 2011); therefore the measurement of cell networks is essential to gain a full understanding of brain functioning. Saying this, research on microscopic or mesoscopic oscillation is by no means dispraised. For a full understanding of the brain, each spatial level has to be studied.

Macroscopic oscillations produce negative and positive far fields at the scalp. Negative far fields reflect increased excitability of neurons while positive far fields reflect decreased excitability of neurons. Why is this the case? Due to architecture and characteristics of cortical neurons and their synapses, macroscopic oscillations are mainly produced by excitatory synapses located in the region of apical dendrites of pyramidal neurons (see Hagemann, 1999, for an excellent and thorough disquisition; see also Jackson & Bolger, 2014). Signals arriving at synapses of apical dendrites evoke a relative reduction of positivity outside the neuron in the subsynaptical area, causing an ion flow in the extracellular space between the proportionally more positive cell soma (relative source) and the proportionally less positive apical dendrite (relative sink). Given that a large number of uniformly arranged neurons generate superimposed activity, the relative sink is measureable at the scalp level. Because propagation of electric current decreases with distance to the place of origin, action potentials arriving at the dendrites cannot nudge the downstream neuron to generate its own action potential, but solely influence the membrane potential of the downstream neuron by elevating it to a more positive charge (depolarisation) or lowering it to a more negative charge (hyperpolarisation). Action potentials which arrive at the cell soma, ideally close to the initial segment of the neuron, are capable of triggering an action potential in the downstream neurons. These are facilitated or obstructed by the membrane potential. Therefore signals should arrive at times when neuronal ensembles are most excitable, in order to be optimally decoded and transferred. Oscillations emitted from the brain at meso- or macroscopic scale indicate that neuronal networks constantly switch between states of increased excitability (negative far field) and decreased excitability (positive far field), i. e. facilitation and inhibition of spike generation, respectively.

[6] “In the electroencephalogram we see an epiphenomenon of the constantly ongoing nervous processes of the brain; just like the electrocardiogram is an epiphenomenon of the contractions of all heart segments” (Translation M. J. H.)

Oscillations span a wide range of frequencies from *ultra slow* fluctuations of about 0.05 Hz to *ultra fast* oscillations of up to and above 600 Hz (Penttonen & Buzsáki, 2003). Slower frequencies are more powerful than faster frequencies. Slow frequencies are thought to integrate activity of larger amounts of cells, while fast frequencies are expected to integrate activity of smaller amounts of cells:

> When a goal is scored in a football stadium, the coordinated roar of fans can be heard for miles, in contrast to uncoordinated local conversations, which are lost in the background noise. Similarly, slow rhythms involve very large numbers of cells and can be 'heard' over a long distance, whereas localized fast oscillations involving only a small fraction of neurons may be conveyed only to a few partners. (Buzsáki, 2006, p. 119)

Moreover, "different frequencies provide distinct temporal windows for processing" (Canolty & Knight, 2010, p. 506). With lower frequencies, the window within which information from other cells can be integrated (the duration of the on-stage) is larger than with fast oscillations that switch more rapidly between on and off states and can therefore only integrate information arriving in a short time-window. Consequently, low oscillations can integrate information of larger cell populations than fast oscillations are able to (Buzsáki, 2006, pp. 115–116). Accordingly, it was found that higher frequencies only synchronize in compact neuronal patches, whereas lower frequencies correlate highly between distant regions (Canolty et al., 2007; von Stein & Sarnthein, 2000).

The fast spike-based computation of neurons has to be coordinated and integrated at different spatial scales. Single neuron activity is integrated within networks which leads to two other important characteristics of the brain: its small-world architecture and its modularity.

The small-world network architecture of the brain.

Networks can effectively be investigated via graph theory. The most important concepts of graph theory are nodes, edges, and paths. A node is a unit of a network, e. g. a neuron in the brain or a person in a city. Edges are direct connections between two units, e. g. a direct axonal connection from one neuron to another or the direct friendship between two persons. Paths are connections that can include several edges. The length of a path is defined by the amount of edges, not by any physical distance. Instead of neurons and axonal connections, nodes can also represent neural regions of interest and edges can represent some statistical dependency between these regions. See Rubinov and Sporns (2010) for a concise and Sporns (2011) for a thorough description of neuronal network analysis.

Two parameters are especially important when describing small-world networks: clustering coefficient and characteristic path length. The *clustering coefficient* is best explained within a social network (Watts & Strogatz, 1998, p. 441): for each person it describes how many of the person's friends are also friends with each other. Averaged over all people in the network, the clustering coefficient describes the cliquishness of the network, and is therefore a simple measure of modularity (see below). For neuronal networks, the clustering coefficient specifies the fraction of a nodes direct neighbours that are also directly connected. The *characteristic path length* is the average length of all shortest paths between any two nodes, hence the mean length of all shortest paths.

A small-world network stands out due to its rich local connections (high clustering coefficient) and sparse long-range connections (low characteristic path length). This kind of network is located between a completely regular network (Figure 1.2a), where each node is only connected to its nearest neighbours (high clustering, long characteristic path length), and a completely random network (Figure 1.2c), where each node is randomly connected to a fraction of all possible nodes (low clustering, short characteristic path length). As Watts and Strogatz (1998) have shown, a regular network with a few long-range connections keeps its high clustering, but greatly reduces the average path length, hence forming a small-world network (Figure 1.2b).

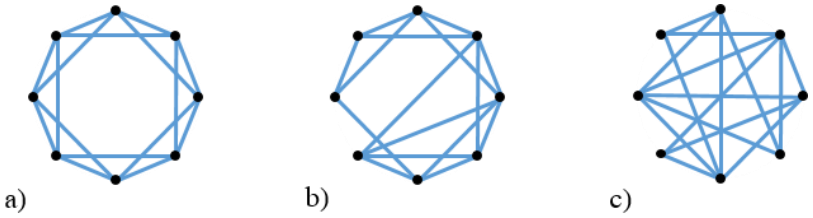

Figure 1.2: a) Example of a regular network. Each node is connected to its two nearest neighbours. b) Example of a small-world network. Two edges have been re-connected and become long-range connections. c) A random network. Each node is randomly connected to a fraction of all possible nodes. Adapted by permission from Macmillan Publishers Ltd: Nature, Watts & Strogatz, 1998, copyright 1998.

In the case of the brain, the small-world architecture provides a perfect network structure to reduce energetically expensive long-range connections and, at the same time, keep a fast information transfer between all brain areas. Long-range connections not only need to be restricted because they are energetically expensive, but also because they take up a large amount of space due to myelination. It has been shown, even though white matter grows disproportionally strong compared to grey matter in brains of increasing size (Zhang & Sejnowski, 2000), that as the number of neurons increases, the proportion of connections needed to keep the same level of connectivity decreases (Buzsáki, 2006). Not proportional (isometric) connectivity, but absolute (allometric) connectivity is maintained (Sporns, 2011), thereby restricting spatially and energetically expensive long-range connections. Watts and Strogatz (1998) proved that infectious diseases propagate very fast in small-world networks. Analogously, information should be able to be transferred easily in small-world networks (Bassett & Bullmore, 2006; Nishikawa, Motter, Lai, & Hoppensteadt, 2003).

Watts and Strogatz (1998) were the first to demonstrate that the central nervous system of the nematode *Caenorhabditis elegans* (*C. elegans*) had small-world properties at the cellular scale. With roughly 300 neurons and several thousand connections between these neurons (White, Southgate, Thomson, & Brenner, 1986), this nervous system could be completely analysed on the cellular scale. This project is unfeasible for the human brain, consisting of roughly 86 billion neurons (Herculano-Houzel, 2009).

Summing up, a neuronal small-world network is energy efficient, spatially efficient, and enables a fast and easy information transfer. In addition to being theoretically compelling, this network structure

has been shown empirically in neuronal networks of various species and at various network scales (Achard, Salvador, Whitcher, Suckling, & Bullmore, 2006; Bassett, Meyer-Lindenberg, Achard, Duke, & Bullmore, 2006; Eguiluz, Chialvo, Cecchi, Baliki, & Apkarian, 2005; Fair et al., 2009; He, Chen, & Evans, 2007; Salvador et al., 2005; Sporns & Zwi, 2004; Stam, 2004). Moreover, small-world networks are not only a fundamental characteristic for central nervous systems, but also occur ubiquitously in biological, social, and man-made systems like the U. S. power grid (Watts & Strogatz, 1998).

Modularity of the brain.

The third important characteristic of the brain is its modularity: modules are groups of nodes which possess strong interconnectivity and sparse connectivity to other nodes. A high clustering coefficient, which is a feature of small-world networks can, but does not have to, imply modularity. For example, Müller-Linow, Hilgetag, and Hütt (2008) found modularity in the nervous system of the cat, but no modularity in the nervous system of *C. elegans*, both proven to be small-world networks with high clustering coefficients.

Network modularity has been repeatedly found (Chen, He, Rosa-Neto, Germann, & Evans, 2008; Fair et al., 2009; Hagmann et al., 2008). However, results differ regarding location and functionality of networks. This might be due to differences in methodology, but presumably modules are subject to changes depending on subjects' activity. A meta-analysis of more than 1600 fMRI studies detected modularity at the whole-brain scale, including modules spanning the occipital lobe, central brain area (including sensorimotor areas), fronto-parietal network, and default mode network (Crossley et al., 2013). There are also indications that the typical modularisation of human brains is disturbed in persons suffering from mental disorders, e. g. childhood onset schizophrenia (Alexander-Bloch et al., 2010).

Revealingly, computer scientists started to program in a modularized form as soon as software started to become extensive (Boudreau, Tulach, & Wielenga, year unknown). Modularized programming had manifold advantages and is a core programming principle nowadays: different groups can work on parts of the same software independently. Neither group needs to be aware of the exact operating mode of other groups' modules; only common interfaces between modules are necessary. Additionally, modularized software has proven to be more robust to errors than non-modularized software. A software module contains basic processing, which can be used as elements of more complex functions. This is the same concept as assumed for neuronal modules, with functionally segregated local processing units which have to be globally integrated to implement complex functions (Park & Friston, 2013). Empirical data has shown that the relatively simple neuronal system of *C. elegans* is not modularized, but that more complex neuronal systems are indeed modular (Müller-Linow et al., 2008). This parallel is intriguing. Nature seemingly evolved modularity as size and complexity of biological systems increased. In the same manner, humans started to create modularized systems as the size and complexity of their systems increased.

Phase-Amplitude Cross-Frequency Coupling.

A fundamental aim of neuroscience is to elucidate how the above described modular structures of the brain cooperate and communicate. So far, research concentrated on the spatial localization of neuronal processes; the temporal course of neuronal activity received less attention: “In the analogy of Plato’s cave, our current approach to understanding the biological foundations of cognition is like looking at shadows cast on a region of the wall of the cave without observing how they change dynamically over time.” (Cohen, 2011, p. 1). EEG, having a “precise temporal resolution in the millisecond range” (Hülsemann, 2013, p. 7), being non-invasive and therefore applicable to large samples of human subjects, is an excellent tool for studying neural communication.

Cross-frequency coupling is a recent concept proposed to explain how neuronal networks cooperate and communicate. It is hypothesized to provide "hierarchical control of inter-areal synchrony" (Monto, 2012, p. 1) and being an “indicator of network coordination and functional integration” (Allen et al., 2011, 59-1). It is assumed to be a "mechanism for binding distributed neuronal activities" (Monto, 2012, p. 1), that is, the “integration of distributed information" (Jirsa & Müller, 2013, p. 1), a "mechanism for selectively routing information through neuronal networks" (van der Meij, Kahana, & Maris, 2012, p. 111), a "mechanism that is able to separate spatially distributed networks operating in parallel" (van der Meij et al., 2012, p. 111), as well as a "mechanism for the interaction of local and global processes" (Jirsa & Müller, 2013, p. 1). In essence, there seem to be three core functions of cross-frequency coupling:

1. Information transfer between distinct neuronal sites
2. Binding of distributed neuronal activity
3. Enabling parallel processing in time and space

All authors agree on cross-frequency coupling being a mechanism to facilitate communication between neuronal ensembles, as well as, separation of communication processes from one another and, thereby, enabling parallel processing.

Three forms of cross-frequency coupling can be distinguished: phase-amplitude coupling (PAC), phase-phase-coupling, and amplitude-amplitude coupling. As shown in the next paragraphs, the first mentioned attribute of cross-frequency coupling, “information transfer between distinct neuronal sites”, is represented by phase-amplitude coupling, while the second attribute, “binding of distributed neuronal activity”, is rather represented by phase-phase coupling. Amplitude-amplitude coupling is less well understood (Canolty & Knight, 2010).

In contrast to both other forms of cross-frequency coupling, phase-amplitude coupling implies a clear direction of action: it is defined as the phase of a comparatively slow oscillation modulating the amplitude of a comparatively fast oscillation. While this directionality is inherent to the definition of phase-amplitude coupling, technically it is a correlational measure and cannot imply causality. Phase-amplitude coupling is defined as the statistical dependence between the instantaneous phase of

frequency A and the instantaneous amplitude of frequency B of either the same or two distinct signals (see chapter 2 for a detailed description). This technical definition makes it easy to understand the other two forms of cross-frequency coupling. Phase-phase coupling is the statistical dependence between the instantaneous phase of frequency A and instantaneous phase of frequency B of either the same or two distinct signals. Amplitude-amplitude coupling describes the statistical dependence between the instantaneous amplitude of frequency A and instantaneous amplitude of frequency B of either the same or two distinct signals.

For now, cross-frequency coupling measured from scalp EEG remains a marker (cf. Figure 4 in Aru et al., 2015, p. 56), whose interpretation for neuronal communication exceeds what is currently known about the parameter. Nevertheless, these interpretations are based on reasonable assumptions and should therefore be investigated. This thesis will contribute to answering the question as to whether phase-amplitude coupling is present during the execution of cognitive control and whether an assumed performance effect of stress on executive functioning is reflected in phase-amplitude coupling strength.

Phase-amplitude coupling is a ubiquitously found phenomenon in mammalian brains. More than 80 studies[7], of which 90 % were published in the last decade, report phase-amplitude coupling measured via EEG (e. g. Nakatani, Raffone, & van Leeuwen, 2014), MEG (e. g. Kaplan et al., 2014), ECoG (e. g. Szczepanski et al., 2014), or LFP (e. g. Lopez-Azcarate et al., 2010). Phase-amplitude coupling is found in conscious (e. g. Roux, Wibral, Singer, Aru, & Uhlhaas, 2013) and unconscious states (e. g. sleep: Staresina et al., 2015; e. g. anaesthesia: Mukamel, Wong, Prerau, Brown, & Purdon, 2011), during rest (e. g. Foster & Parvizi, 2012) and activation (e. g. Yanagisawa et al., 2012). It is found during various experimental tasks, amongst others the oddball task (e. g. Allen et al., 2011), Sternberg task (e. g. Axmacher et al., 2010), go-nogo task (e. g. Dürschmid et al., 2014), t-maze (e. g. Tort et al., 2008), and attentional blink task (e. g. Mizuhara & Yamaguchi, 2011). So far rats (e. g. Li, Bai, Liu, Yi, & Tian, 2012), mice (e. g. Scheffzük et al., 2011), nonhuman primates (e. g. Spaak, Bonnefond, Maier, Leopold, & Jensen, 2012), and humans (e. g. Köster, Friese, Schöne, Trujillo-Barreto, & Gruber, 2014) have been studied. Sample sizes in these studies range from single cases (e. g. Miyakoshi et al., 2013) to up to 400 subjects (e. g. Kirihara, Rissling, Swerdlow, Braff, & Light, 2012).

In most studies, theta-gamma coupling, i. e. gamma amplitude nested within the theta cycle, is found (e. g. Canolty et al., 2006; Tang et al., 2016). One reason for the frequent discovery of theta-gamma coupling is that many studies exclusively analyse this frequency pair. But also in studies that scan broad frequency ranges (exploratory analysis), theta-gamma coupling is often evident and in some cases the only phase-amplitude coupling present (e. g. McGinn & Valiante, 2014). Nevertheless, virtually all other frequency combinations were also found to be engaged in phase-amplitude coupling (e. g. Cohen, Elger, & Fell, 2009). Importantly, not only the pure existence of phase-amplitude coupling,

[7] A complete list of these studies can be found in Appendix A. Certainly, this list of publications is not exhaustive, but it represents the majority of published studies on phase-amplitude coupling.

but also its association with behaviour was found (e. g. Köster et al., 2014; Mizuhara & Yamaguchi, 2011; Soto & Jerbi, 2012).

One prominent example of theta-gamma coupling and its relation to cognition shall be briefly reviewed. Jensen and Lisman (1998) formulated a neurobiological theory of working memory that incorporates phase-amplitude coupling (Jensen, 2006; Lisman & Jensen, 2013). As shown in Figure 1.3, gamma amplitude is strong during the rising phase, peak, and decreasing phase of a theta cycle and weak (depicted as not present in Figure 1.3) during the trough of the theta cycle. According to this theory, each memory item is coded by a unique set of neurons, which fire in union in gamma frequency. Each item that has to be kept in working memory fires for one gamma cycle and this gamma cycle takes up "one space" within the theta cycle (cf. Figure 1.3). The sets of neurons repeat firing at the same "space" in the next theta cycle. The first item to be held in working memory will fire first, then the second set of unique items representing memory item B will fire second etc. Overall 7 ± 2 gamma cycles fit into each theta cycle (depending on the exact frequency of theta and gamma)[8]. Intriguingly it is exactly 7 ± 2 items that humans normally can keep in working memory (Miller, 1956). Furthermore, Sternberg (1966) found that participants, when required to judge whether a test stimulus matches to a list of stimuli seen before, need about 38 milliseconds processing time for every item that was presented in the list.[9] That is, reaction times of participants become on average 38 milliseconds faster when there is one stimulus less in a list they have to remember. Additionally, if the target stimulus matches an early presented stimulus from the list, reaction times are correspondently faster, implying a serial search of memory items that stops if target and memory item match. Jensen and Lisman (1998) formally show that this theory can explain many of the empirical working memory phenomena. One assumption within this theoretical framework is that the theta cycle must slow-down in order to increase working memory capacity. Accordingly, Vosskuhl et al. (2015) showed that short term memory capacity is indeed increased when slowing down individual theta frequency via transcranial alternating current stimulation.

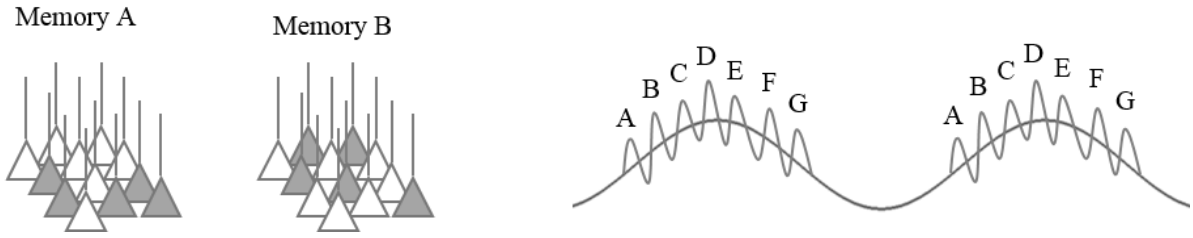

Figure 1.3: Memory items are represented by unique sets of neurons which fire in union in gamma frequency. Each unique set of neurons, representing a memory item, is active for one gamma cycle and takes up "one space" within the theta cycle. Active memory items are repeated in each theta cycle. Selection of memories are divided via a silent time during the trough of the theta cycle. Adapted and republished with permission of the Society for Neuroscience, from the Journal of Neuroscience, Jensen and Lisman, 18(24), 1998.

[8] In a theta cycle with a length of 200 milliseconds (5 Hz), 7 gamma cycles with a length of 21 milliseconds (about 48 Hz) can be fitted during the up state of theta, leaving 50 milliseconds refractory period (duration of the trough).
[9] In a theta cycle with a length of 250 milliseconds (4 Hz), 5 gamma cycles with a length of 38 milliseconds (about 26 Hz) can be fitted during the up state of theta, leaving 63 milliseconds refractory period (duration of the trough).

In relation to stress research, the finding that cortisol might modulate the coupling between delta and beta power (amplitude-amplitude coupling), is especially interesting. This form of cross-frequency coupling was found in approximately a dozen of studies (for a review see Schutter & Knyazev, 2012) and seems to vary systematically with cortisol and related concepts (e. g. anxiety). In this theoretical frame-work delta-beta coupling is interpreted as executive control, while decoupling is interpreted as behavioural disinhibition. So far all studies investigating delta-beta coupling (see Schutter & Knyazev, 2012 for an overview) calculated inter-individual correlation coefficients, but interpreted their results as intra-individual correlations: delta and beta power were correlated within a subsample of all participants (one coupling measure for each subsample) and not individually for each participant (one coupling measure for each subject). This is problematic, because the interpretation of the results as intra-individual coupling is not covered by the performed statistics. The only study also calculating intra-individual coupling was published by Knyazev (2011), though he could not find delta-beta coupling being related to cortisol or another direct stress measure.

It seems plausible that cross-frequency-coupling is a mechanism by which the brain exchanges information and parallels cognitive and emotional processes (Buzsáki, 2006; Canolty & Knight, 2010; Jensen & Colgin, 2007). Therefore, in this thesis the relationship between stress, executive functions, and cross-frequency coupling is explored with appropriate methods in the time-frequency domain. Using completely different methods, it would not be surprising if former findings regarding delta-beta coupling and stress (cf. Knyazev, 2011) cannot be replicated. That is why exploratory analyses are conducted with being open about the exact frequency bands and the location of coupling, but not about the general idea of a relationship between stress, executive functions, and cross-frequency coupling. Phase-amplitude coupling is chosen, because it is the most studied method for assessing cross-frequency coupling so far. This is of advantage when conducting an exploratory analysis, as it is helpful to compare findings with the results of other research areas. Secondly, phase-amplitude coupling implies a causal direction: it is assumed to reflect the modulation of one neuronal source by another. In contrast, phase-phase or amplitude-amplitude coupling rather reflect the cooperation between two neuronal sources. Thus, phase-amplitude coupling seems to be the adequate concept, as it corresponds to the concept of executive functioning in respect of directionality and modulation.

1.4 Summary

The relevance of stress, executive functions, and phase-amplitude cross-frequency coupling, as well as their interrelation, has been demonstrated. Stress, particularly cortisol, influences the brain in manifold ways. Presumably, it especially influences those structures that are active. The prefrontal cortex and the fronto-parietal network are hypothesized to support executive functions, which are crucial for purposeful and optimized behaviour. Not much is known about how exactly the brain implements

executive functions, but it could be by phase-amplitude cross-frequency coupling, a concept that provides a theoretical explanation about how one neuronal structure modulates another. Additionally, the brains modularized structure and the presence of oscillations of various frequencies require the assumption of a mechanism by which neuronal structures communicate. This mechanism could be phase-amplitude cross-frequency coupling. The aim of this work, therefore, is to investigate whether executive functions are implemented via phase-amplitude cross-frequency coupling in the prefrontal cortex and fronto-parietal network and whether stress modulates the ability to execute executive functions on a behavioural (at the level of executive functions) and neuronal (at the level of cross-frequency coupling) level. As described above, cross-frequency coupling seems to be a ubiquitous phenomenon in mammalian brains, and hence not the proof of its pure existence, but exploring its association with behaviour is essential. It is therefore expected to find phase-amplitude cross-frequency coupling and further hypothesized that it will vary with the behaviour of humans in executive functioning paradigms and is potentially moderated by stress.

2 Quantification of Phase-Amplitude Coupling

2.1 Introduction

Section 1.3 described the general idea behind cross-frequency phase-amplitude coupling and summarized previous findings regarding this concept. The section showed that phase-amplitude coupling is a promising method to study cognitive processes in EEG. There is no convention yet of how to calculate phase-amplitude coupling. This chapter is designed to give a short overview about the heterogeneity of phase-amplitude calculation methods used in the literature. Performance of two of the most widely used phase-amplitude coupling measures – mean vector length (MVL) by Canolty et al. (2006) and modulation index (MI) by Tort et al. (2008) – is thoroughly compared with the help of simulated data.

From a historical viewpoint, the first amplitude modulations that have been detected are amplitude fluctuations of specific frequency bands, becoming apparent in the fast Fourier transform (FFT) of constituents of these signals (Burgess & Ali, 2002; Novak, Lepicovska, & Dostalek, 1992; Pfurtscheller, 1976). Because the FFT approach can solely reveal that the amplitude of a higher frequency oscillates at a lower frequency (characteristic of one signal), these amplitude modulations should not be misinterpreted to account for true temporal coupling between the instantaneous phase of the lower frequency and the amplitude envelope of the higher frequency (association between two signals). Neither the lower frequency itself nor its instantaneous phase are extracted in this approach.

Some of the most widely used phase-amplitude coupling measures today are the phase-locking value [PLV] (Mormann et al., 2005; Vanhatalo et al., 2004), also called synchronization index [SI] by Cohen (2008), the modulation index [MI] (Tort et al., 2008), the mean vector length [MVL] (Canolty et al., 2006), the envelope-to-signal correlation [ESC] (Bruns & Eckhorn, 2004), the general linear model approach [GLM] (Kramer & Eden, 2013; Penny, Duzel, Miller, & Ojemann, 2008), phase binning combined with ANOVA [BA] (Lakatos et al., 2005), and the weighted phase locking factor [wPLF] (Maris, van Vugt, & Kahana, 2011). All of these measures use the instantaneous phase and amplitude of band-pass filtered signals to calculate a measure that represents coupling strength. However, conceptual ideas and mathematical principles differ substantially between measures. The FFT approach is also still used. Figure 2.1 depicts the application frequency of these measures in an extensive, but not exhaustive selection of 82 publications on phase-amplitude coupling (see Appendix A for references).

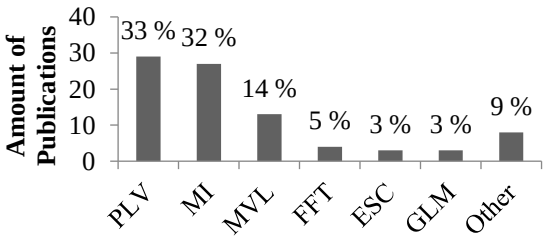

Figure 2.1: Frequency of various phase-amplitude coupling measures in 82 publications (five of which apply two measures). MI: modulation index; PLV: phase-locking value; MVL: mean vector length; FFT: FFT approach; ESC: envelope-to-signal correlation; GLM: general linear model approach. References of these publications can be found in Appendix A.

Several of these phase-amplitude coupling measures were compared with the help of simulated and real data in four reviews. Tort, Komorowski, Eichenbaum, and Kopell (2010) executed the most extensive comparison so far, including most of the above

listed measures and evaluating their performance pertaining to tolerance to noise, amplitude independence[10], sensitivity to multimodality, and sensitivity to modulation width. The modulation index, introduced by the same group (Tort et al., 2008), is well-rated in all aspects while, amongst others, the phase-locking value has poor ratings in all aspects. The mean vector length has good ratings in some aspects (e. g. tolerance to noise), but weaknesses in others (e. g. amplitude dependence).

Penny et al. (2008) introduced the GLM approach and compared it to the mean vector length, phase-locking value, and envelope-to-signal correlation in respect to noise level, coupling phase, epoch length, sample rate, signal non-stationarity, and multimodality. They found that the methods discriminated between data simulated with and without coupling to different extents, ranging from below chance level to perfect discrimination. Performance of the measures differed under poor conditions (high noise, low sampling rate, etc.), however, all measures performed equally well under good conditions (longer epochs, less noise, etc.).

Kramer and Eden (2013) introduced a new GLM cross-frequency coupling measure. It proves to be valid and performs equally well as the modulation index. The advantages of this method are that it can be interpreted as percentage change in amplitude strength due to modulation. Additionally confidence intervals are easily computed and the measure can detect biphasic coupling.

When Onslow, Bogacz, and Jones (2011), compared three phase-amplitude coupling measures, they found that "no one measure unfailingly out-performed the others" (Onslow et al., 2011, p. 56). They concluded that each measure seems to be particularly suited for specific data conditions. Mean vector length for example is suitable for noisy data, exploratory analyses (analysing a broad frequency spectrum) and when the power of the amplitude providing frequency band is low.

The above cited reviews do not point to a single optimal measure for calculating phase-amplitude coupling. They rather show that most – but not all – of the used measures perform well and are equally affected by various confounders. Despite the availability of manifold measures, 79 % of studies use the mean vector length, modulation index or phase-locking value adapted for phase-amplitude coupling. Why is this the case? Possibly the predominant application of mean vector length is due to its mathematical directness. The modulation index is conceptually intuitive. This will become evident in the following sections where both measures are explained in detail. The phase-locking value is derived from a long-used, phase-phase coupling measure that is easily adapted for the purpose of phase-amplitude measurement. Its familiarity in the scientific community might have promoted its application. Its usage is potentially problematic because phase information is extracted from the amplitude envelope of a signal. Phase information can only be correctly extracted from truly oscillating signals; this is not necessarily the case for an amplitude envelope. So far, no review evaluated this measure explicitly as positive.

[10] Amplitude independence denotes to the independence of the measure from the amplitude strength of the amplitude-providing frequency band.

The majority of reviews used very straightforward data simulation methods. Oftentimes, a sinusoidal oscillation is constructed at a lower phase-providing frequency and at a higher amplitude-providing frequency. Phase-amplitude coupling is introduced by multiplying both signals (cf. Onslow et al., 2011, p. 52). Amplitude is then extracted from the so constructed signal and phase is extracted from the pure sinusoidal oscillation of the lower frequency. White noise is added to both signals. There are two pitfalls in this approach. Both sinusoidal signals reflect a plain prototype of phase-amplitude coupling, but in real neuronal data, pure sinusoidal oscillation cannot be filtered; rather, frequency bands containing different amounts of various frequencies are extracted. Second, white noise is added to the simulated data, even though it is known that not white noise but Brownian noise is inherent to brain dynamics (He, Zempel, Snyder, & Raichle, 2010; Miller, Sorensen, Ojemann, & den Nijs, 2009).

Because none of the hitherto existing reviews simultaneously meet the requirements of realistic simulation of EEG data, providing inferential statistics for comparison of the measures, investigating moderators of phase-amplitude coupling, and including two of the most widely used measures (mean vector length and modulation index), a new comparison of both methods is presented in this chapter. It aims to combine the best aspects of all previous reviews. EEG data is simulated rather realistically according to the procedure described by Kramer and Eden (2013). The influence of several moderators (multimodality, data length, sampling rate, noise level, modulation strength, and modulation width) inspired by Tort et al. (2010) is investigated. Sensitivity and specificity of the phase-amplitude coupling measures are checked according to the methods described in Onslow et al. (2011). For all these comparisons inferential statistics are provided.

2.2 Methods

2.2.1 Extracting Frequency, Phase, and Amplitude from EEG Data

An oscillation carries three pieces of information:

(1) Frequency: specifying how many full cycles can be completed within one second; measured in Hz.

(2) Instantaneous Amplitude[11]: specifying how powerful the signal is at each instance; usually measured in microvolts (μV) in electrophysiology.

(3) Instantaneous Phase[12]: specifying which portion of the cycle has already been completed; ranging from 0° – 360° (0 – 2π radians).

In order to measure cross-frequency phase-amplitude coupling one needs to extract all of this information from raw data. This is done by the following preparatory steps.

[11] The term amplitude has two meanings: it signifies the vertical distance between the zero crossing and peak of each cycle of an oscillation and it signifies the amplitude envelope – often referred to as amplitude magnitude – as described above. Here, amplitude is used in the sense of the amplitude envelope.

[12] The term phase has two meanings: it signifies the phase offset of each cycle of an oscillation and it signifies the instantaneous phase as described above. Here, phase is used in the sense of instantaneous phase.

First, raw data (Figure 2.3A, grey thick line) **is band-pass filtered in the frequency bands of interest** (Figure 2.3A, red and blue line). When analysing phase-amplitude coupling, phase is extracted from a relatively slow oscillation while amplitude is extracted from a relatively fast oscillation (cf. p. 18). For simplicity, preparatory steps are illustrated only for the frequency band of 4 – 6 Hz.

Second, the real-valued band-pass filtered signal is transformed into a complex-valued analytic signal. This is commonly done by using the Hilbert transform. It transforms the signal into a time series of complex-valued numbers of the form a + bi, representing an oscillation of one specific frequency band (in this case 4 – 6 Hz). The imaginary part is a 90° shifted version of the original real-valued filtered signal; this becomes apparent when plotting the real and imaginary part of the analytic signal (Figure 2.3B). A complex number can be depicted as a vector in a polar plane (Figure 2.2A), which is a two-dimensional plane where the abscissa represents the real part (a) and the ordinate represents the imaginary part (bi). When analysing EEG data, there is not only one vector, but as many as the number of data points. One minute EEG data with a sampling rate of 1000 Hz produces 60000 data points. The representation of this signal in the polar plane would be a circulating arrow (Figure 2.2B), whose length depends on the amplitude strength of the signal. In Figure 2.2B, a constant amplitude strength is depicted. The vector circulates counter clockwise. By comparing Figure 2.2B and C, one can see the correspondence between the oscillating arrow in the polar plane and the regular wave in the Cartesian plane. One full cycle in the polar plane represents one full wave cycle.

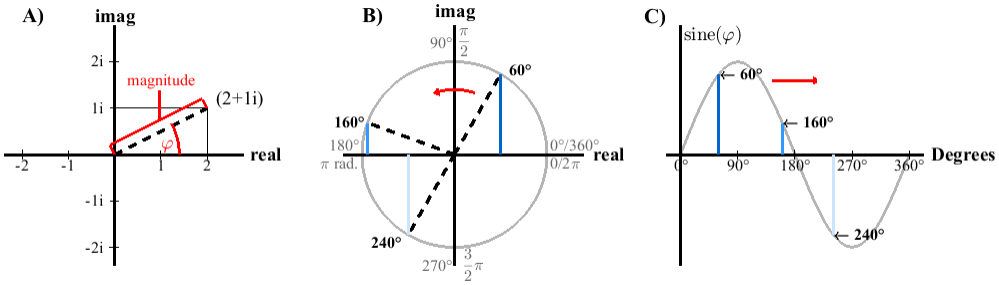

Figure 2.2: A) Representation of one data point (2 + 1i) of a complex analytic signal in the polar plane. The angle between vector and abscissa represents the instantaneous phase. The length of the vector (magnitude) represents the instantaneous amplitude of the signal. B) Representation of three data points and their corresponding instantaneous phases of the analytic signal in the polar plane; all data points have identical magnitude (amplitude strength). C) Data points from Figure 1.2B mapped onto the Cartesian plane. One full cycle in Figure 1.2B corresponds to one sine wave cycle.

Finally phase or amplitude is extracted from the complex-valued analytic signal. Phase is extracted by measuring the angle between the vector and the positive part of the abscissa (Figure 2.2A, Figure 2.3C). Phase is a circular variable (0° and 360° are identical). Amplitude is extracted by measuring the length (magnitude) of the vector (Figure 2.2A, Figure 2.3D). The precise mathematical operations are

for extraction of phase $\varphi = \tan^{-1}\frac{imag}{real}$ (Equation 1)

for extraction of amplitude $M = \sqrt{real^2 + imag^2}$ (Equation 2)

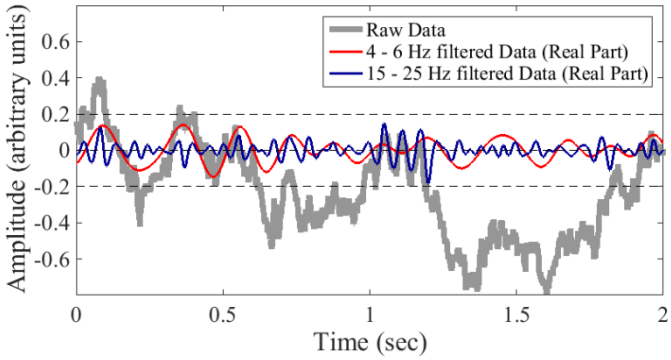

A) Raw data and two band-pass filtered signals extracted from the raw data. One can see how the filtered signals represent components of the raw data (e. g. at 0.4 to 0.6 seconds for the 4 – 6 Hz filtered data and at 1.0 to 1.2 seconds for the 15 – 25 Hz filtered data).

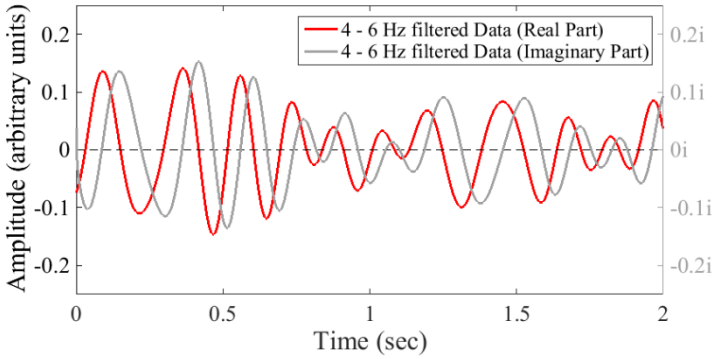

B) Representation of real and imaginary part of the complex-valued analytic signal derived from the raw data filtered at 4 – 6 Hz. The imaginary part is a 90° shifted version of the real part.

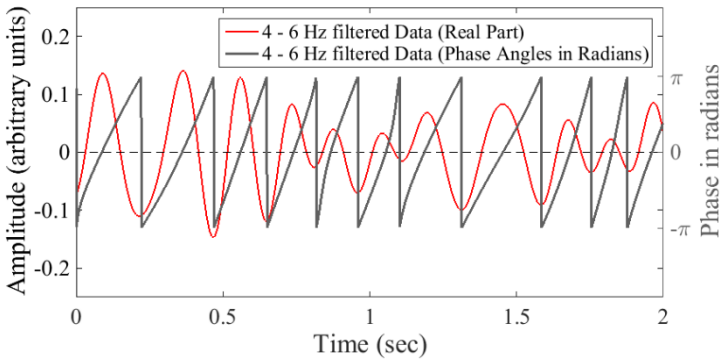

C) Depiction of the band-pass filtered signal and its corresponding instantaneous phase angles. Here phase angles range from –π radians to π radians (-180° – 180°; see next page for explanation). It can be seen that the oscillation has its peaks at 0 radians (0°), while it has its troughs at –π radians/π radians (180°/-180°).

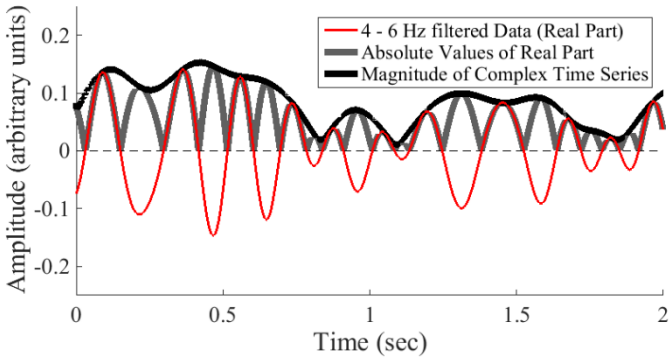

D) For understanding the genesis of the amplitude envelope (magnitude of complex time series; black line), fold up the negative parts of the band-pass filtered signal (red line); thereby bringing about the absolute values (grey line). Then adapt a smooth line to all peaks (amplitude envelope). The absolute height of the smooth line corresponds to the magnitude of the vector of this data point in the polar plane.

Figure 2.3: The steps to extract phase and amplitude from raw data are depicted graphically. See the text next to each figure for a detailed description.

All these steps are essentially implemented in MATLAB with four lines of code:

```
filtered_data = pop_eegfiltnew(raw_data,lower_frequency_bound,upper_frequency_bound);
hilbert_data  = hilbert(filtered_data);
amplitude     = abs(hilbert_data);
phase         = phase(hilbert_data);
```

In addition to the Hilbert transform, there are two other widely used methods to convert real-valued band-pass filtered signals to complex-valued analytic signals, namely the complex Morlet wavelet and the short-time fast Fourier transform. As Bruns (2004) has shown, the Hilbert transform, the Complex Morlet Wavelet, and the Short-Time Fast Fourier Transform can produce nearly identical results. Differences only arise from different filter characteristics. Therefore, neither method outperforms the other. A method should be chosen according to the aim of the analysis carried out. In this work, the Hilbert transform is used because it gives the researcher "more control over the frequency characteristics of the filter" (Cohen, 2014, p. 175) than both other methods.

Filtering can seriously distort raw data; it is therefore essential to take care of an optimal filtering routine (Widmann, Schröger, & Maess, 2015). To guarantee prevention of artefacts due to filtering, the following aspects were always taken into consideration: only continuous data was filtered and first and last samples, where edge artefacts can occur, were later on discarded. A zero-phase Hamming-windowed sinc finite impulse response (FIR) filter implemented in EEGLAB (pop_eegfiltnew.m; written by A. Widmann) was used. This function automatically chooses the optimal filter order and transition band width for a precisely selectable filter bandwidth.

Some authors, as well as MATLAB, choose degrees and radians to range from -180° to 180° (-π to π radians; relating to a cosine wave) instead of 0° to 360° (0 to 2π radians; relating to a sine wave; cf. Figure 2.4). Because MATLAB is used for all subsequent data analysis, this work complies with this practice, such that 0° (0 radians) represents the peak and -180°/180° (-π/π radians) represents the trough of an oscillation.

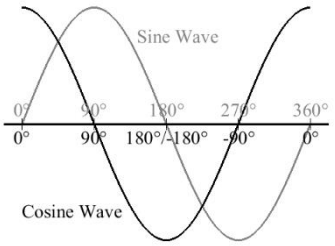

Figure 2.4: Relation between sine and cosine. Instead of defining a full cycle (0° to 360°), MATLAB assigns negative degrees (-180° to 0°) to the second half of the unit circle.

2.2.2 Mean Vector Length

The phase-amplitude coupling measure mean vector length (MVL) introduced by Canolty et al. (2006) utilizes phase angle and magnitude of the complex number in a quite direct way to estimate the degree of coupling. As described above, each complex value of the analytic time series is a vector in the polar plane. Phase-amplitude coupling is present, when the magnitude M of a fraction of all data points is especially high at a specific phase or at a narrow range of phases (Figure 2.5A). Averaging all vectors creates a mean vector with a specific phase and length (white arrow in Figure 2.5). The length of this vector represents the amount of phase-amplitude coupling. The direction represents the mean phase

where amplitude is strongest. When no coupling is present, all vectors cancel each other out and the mean vector will be short (Figure 2.5B). Then its direction does not represent any meaningful phase.

The mean vector length is calculated by the following formula:

$$MVL = \left|\frac{\sum_{t=1}^{n} a_t e^{i\theta_t}}{n}\right| \qquad \text{(Equation 3)}$$

where n is the total number of data points, t is a data point, a_t is the amplitude at time point t and θ_t is the phase angle at time point t. This value cannot become negative because it represents the length of the mean vector (white arrows in Figure 2.5). The length of a vector cannot be negative.

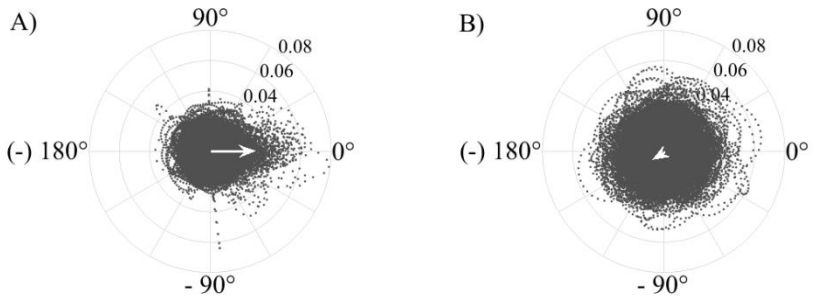

Figure 2.5: An idealized depiction of simulated phase-amplitude coupling (A) and no coupling (B). The white arrow indicates coupling strength (length of the arrow) and is pointing into the direction of the preferred phase in the case of coupling.

Three caveats come along with this measure: (1) the value is dependent on the general absolute amplitude of the amplitude providing frequency (independent of outliers), (2) amplitude outliers can strongly influence the mean vector length, and (3) phase angles are often not uniformly distributed. All caveats are simultaneously counteracted by nonparametric permutation testing (see Cohen, 2014, chapter 30.3, pp. 410-418 for detailed description). Additionally permutation testing allows an evaluation of the meaningfulness of the observed phase-amplitude coupling value. For permutation testing, the observed mean vector length is compared to a distribution of shuffled mean vector length. Shuffled mean vector lengths are constructed by calculating the mean vector length between the original phase time series and a permuted amplitude time series (or vice versa). The permuted amplitude time series is constructed by cutting the amplitude time series at a random time point and reversing the order of both parts (Figure 2.6). Generating surrogate data this way is most conservative, because it leaves all characteristics of the EEG data intact, except the studied one, namely the temporal relationship between phase angle and amplitude magnitude. Shuffling is usually repeated 200 to 1000 times[13]. The observed mean vector length is standardized to the distribution of the shuffled values according to the following formula:

[13] In the selection of 82 studies (Appendix A), 38 report permutation testing. Of these 14 (37 %) apply 200 permutations and 10 (26 %) apply 1000 permutations. Other amounts are ~50, 100, 300, 500, and 10 000 permutations.

$$MVL_z = \frac{MVL_{observed} - \mu_{MVL_{shuffled}}}{\sigma_{MVL_{shuffled}}} \qquad \text{(Equation 4)}$$

where μ denotes the mean and σ denotes the standard deviation (S. D.). Only when the observed mean vector length is larger than 95 % of shuffled values is it defined as significant. It is then assumed that the observed mean vector length value could not have been found, had the original signals been uncorrelated (like the surrogate data). That is, the standardized mean vector length should exceed a critical value, for example being larger than 95 % of the values expected under the null hypothesis of no coupling (surrogate mean vector length distribution). One of the reviews cited in the introduction (Tort et al., 2010) finds faults with the mean vector length being amplitude dependent. As this paragraph shows, this is only true for the raw, but not for the permuted mean vector length.

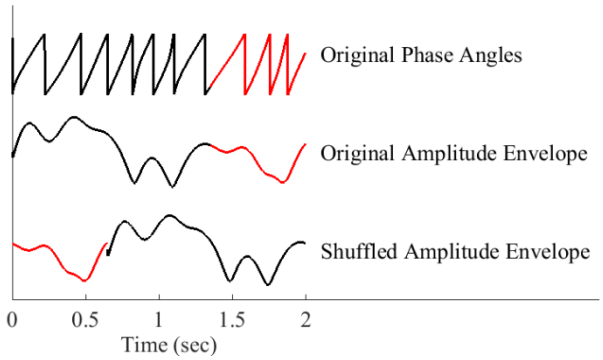

Figure 2.6: Depiction of shuffling the amplitude time series. The amplitude time series is cut at a random time point within a trial and the order of both parts is reversed. Thereby the temporal relationship between phase time series and amplitude time series is destroyed while all other characteristics of the time series are preserved.

In the interest of completeness, it should be mentioned that Özkurt and Schnitzler (2011) proposed a *direct mean vector length* which is amplitude-normalized and ranges between 0 and 1. When applying permutation testing to both mean vector length and direct mean vector length return essentially the same values. That is, when applied along with permutation testing, both measures are exchangeable. Without permutation testing, the direct mean vector length is recommended because it takes care of the possible amplitude differences in raw data. However, it is strongly recommended to apply permutation testing. Firstly, in order to verify the meaningfulness of the observed coupling. Secondly, to make one's own measure comparable to other studies' measures. Thirdly, to counteract all three caveats of the raw mean vector length simultaneously, not only the amplitude dependency.

2.2.3 Modulation Index

Tort et al. (2008) suggests a very different way of computing phase-amplitude coupling, which anyways is based on the same parameters of the analytic signal, amplitude magnitude and phase angle. For calculating the modulation index (MI) according to Tort et al. (2008), all possible phases from -180° to 180° are first binned into a freely chosen amount of bins. Tort et al. (2008) established to use 18 bins

of 20° each, which many authors follow. The amount of bins can influence the results, as will be explained below. The average amplitude of the amplitude-providing frequency in each phase bin of the phase-providing frequency is computed and normalized by the following formula:

$$p(j) = \frac{\bar{a}}{\sum_{k=1}^{N} \bar{a}_k} \qquad \text{(Equation 5)}$$

where ā is the average amplitude of one bin, k is the running index for the bins, and N is the total amount of bins; p is a vector of N values. With the help of these calculations, one obtains the data for the phase-amplitude plot which depicts the actual phase-amplitude coupling graphically (Figure 2.7).

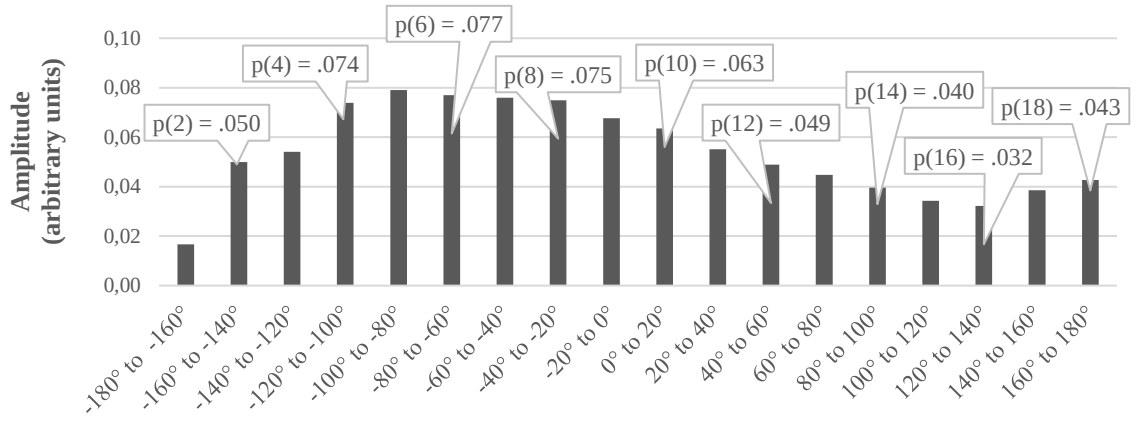

Figure 2.7: Detailed depiction of a phase-amplitude plot.

Subsequently Shannon entropy is computed; a measure that represents the inherent amount of information of a variable. If Shannon entropy is not maximal, there is redundancy and predictability in the variable. Shannon entropy is maximal, if the amplitude in each phase bin is equal (uniform distribution, Figure 2.8). Shannon entropy is computed by the following formula:

$$H(p) = -\sum_{j=1}^{N} p(j) \log p(j) \qquad \text{(Equation 6)}$$

where p is the vector of normalized averaged amplitudes per phase bin and N is the total amount of bins. It does not matter which logarithm base is used if permutation testing is applied later on (Cohen, 2014). Like in Tort et al. (2008) the natural logarithm is used here. Shannon entropy is dependent on the amount of bins used and this is why the modulation index is likewise dependent on the number of bins. The higher the amount of bins, the larger Shannon entropy can become. There are different ways of calculating the optimal number of bins, most of which depend on data length (cf. Cohen, 2014, pp. 391–394). Complying with the original author and most other studies, 18 bins have been employed here. However, squeezing different amounts of data into the same mask of 18 bins will not produce most comparable results. The more data we squeeze into a fixed mask the more information is lost. The ideal procedure for choosing the amount of bins cannot be determined in this work. Hence, the compliance with 18 bins.

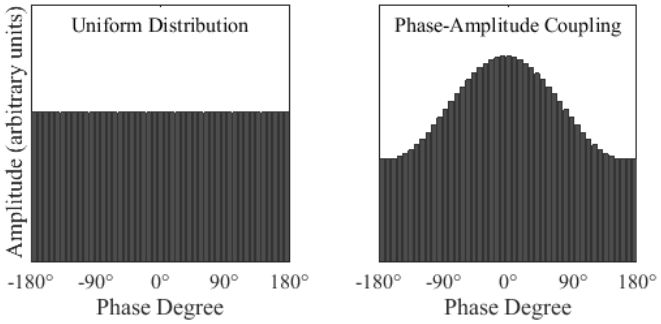

Figure 2.8: Shannon entropy is maximal for uniform distributions (left panel). The Kullback-Leibler distance measures how much a distribution X (right panel) deviates from the uniform distribution (left panel).

Phase-amplitude coupling is defined by a distribution that significantly deviates from the uniform distribution. Kullback-Leibler distance, a measure for the disparity of two distributions is calculated by the following formula:

$$KL\ (U,X) = \log N - H(p) \qquad \text{(Equation 7)}$$

where U is the uniform distribution, X is the distribution of the data, N is the total amount of bins, and H(p) is the Shannon entropy according to equation 6. The uniform distribution is represented by log(N). The final modulation index is calculated by the following formula:

$$MI = \frac{KL\ (U,X)}{\log N} \qquad \text{(Equation 8)}$$

where KL(U,X) is the Kullback-Leibler distance according to equation 7 and N is the total amount of bins. Like the mean vector length, the modulation index is subjected to permutation testing in order to quantify the meaningfulness of the derived value.

2.2.4 Preliminary Summary

The logic of both measures is very different. Due to the phase-amplitude plot, the modulation index is intuitively understandable, but combines manifold mathematical concepts. The mean vector length on the other side involves just a single formula, but requires an understanding of complex numbers. Both are reasonable measures from a theoretical point of view. Furthermore, both measures are widely used in the literature. This is why the performance of these two measures will be extensively tested in this chapter to give empirical reasons for choosing one of the measures for application on EEG data.

2.2.5 Simulation of EEG Data and Implementation of Phase-Amplitude Coupling

A characteristic of natural EEG data is the proportionality of its frequency spectrum to a power law $P(f) \sim (1/f^{\beta})$. Namely, the higher the frequency f, the weaker the amplitude P(f) (Figure 2.9). The exponent β defines the strength of the amplitude decrease. White noise is defined by β = 0, pink noise by β = 1 and Brownian (red noise) by β = 2. Different investigations have shown that the frequency

spectrum of human brain activity relates to Brownian (red) noise, with $2 < \beta < 3$ (He et al., 2010; Miller et al., 2009). Because of this, Brownian noise was generated using MATLAB code provided by Zhivomirov (2013), in order to simulate EEG data.

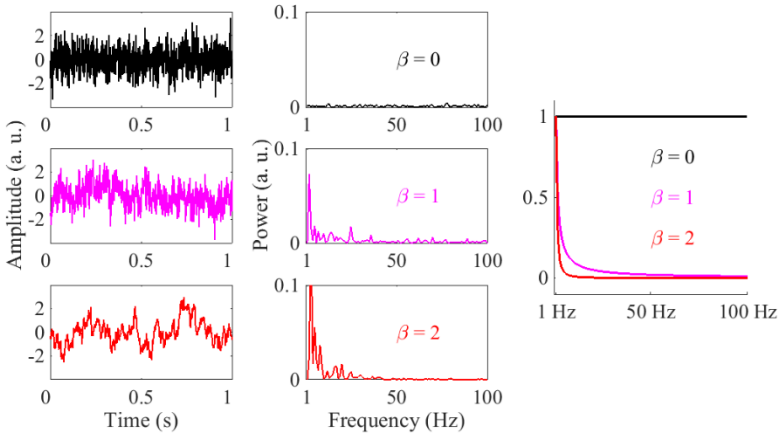

Figure 2.9: White (first row), pink (second row), and Brownian (red) noise (third row) in the left column and its corresponding frequency spectrum in the middle column. The right subplot depicts the amplitude decrease with increasing frequency of white, pink, and Brownian noise.

Simulated data was then filtered at a low phase-providing frequency, from here on referred to as phase time series, with a constant and narrow bandwidth of 2 Hz. The same data was filtered at a high amplitude-providing frequency, from here on referred to as amplitude time series, with a broad bandwidth. The exact bandwidth of the amplitude time series depended on the frequency of the phase time series. As Berman et al. (2012) have shown and is illustrated in Figure 2.10:

> […] amplitude-modulated signals have a complex frequency spectrum with a bandwidth that is related to the frequency of modulation. […] the consequence of an inappropriately narrow filter bandwidth is the unintentional elimination of the signal's amplitude modulation. If the high-frequency amplitude-modulated signal is either distorted or attenuated by the filter, then the CFC metric will not be accurate. (Berman et al., 2012, p. 156)

For this reason data was filtered, such that the sidebands of the modulating frequency were always included (i. e. centre frequency of amplitude-providing frequency band ± upper boundary of phase-providing frequency band). Data was filtered by using the EEGLAB function pop_eegfiltnew.m provided by A. Widmann. Low frequency was set to 8 – 10 Hz and high frequency to 50 – 70 Hz.

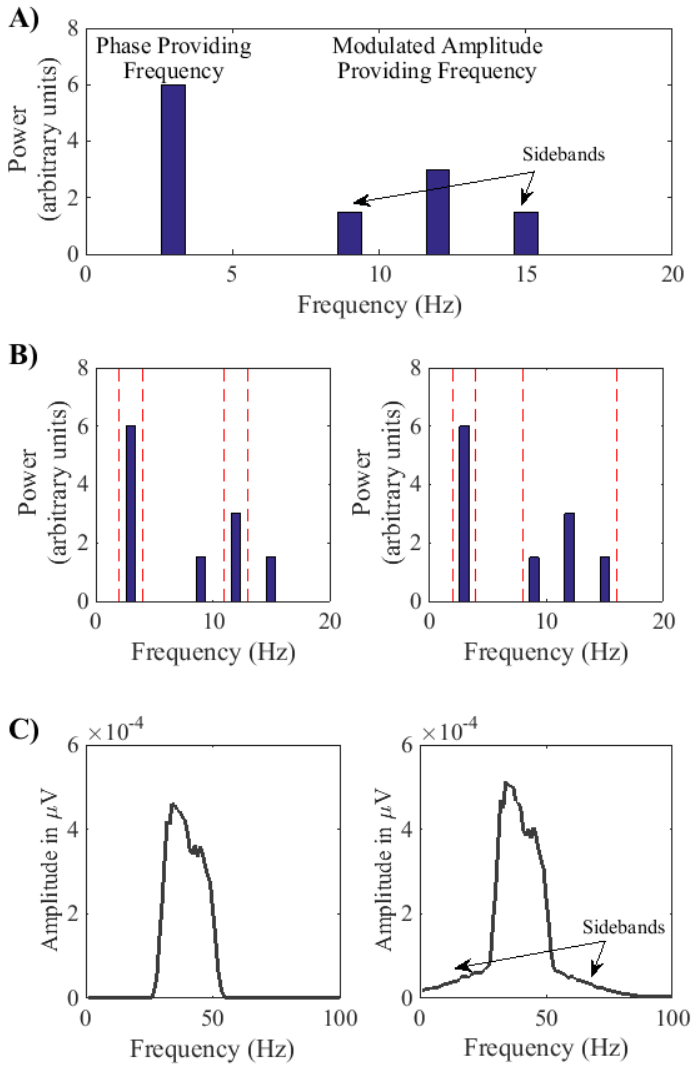

Figure 2.10: A) Idealized frequency spectrum of a signal containing a pure 3 Hz sinusoidal and a 12 Hz oscillation modulated by the 3 Hz oscillation. B) Narrow filtering for both frequency bands leaves out the modulating side bands of the upper frequency band (left side). Broad band filtering for the upper frequency band includes the modulating side bands and leaves the frequency spectrum of the modulated frequency intact. C) Simulated data show the side bands of a modulated frequency band (right side), which are not present in the same unmodulated frequency band (left side). (A) and B) adapted from Berman et al., 2012).

To introduce coupling, the procedure of Kramer and Eden (2013) was followed. A Hanning window plus one[14] (black curve in Figure 2.11) was multiplied with the amplitude time series. This multiplication of the Hanning window with the amplitude time series was not done continuously, but centred at specific time points (see Figure 2.11 for the example of one time point). These specific time points are either the relative maxima (peaks) or the relative maxima and minima (peaks and troughs) of the phase time series, in order to simulate monophasic and biphasic coupling, respectively (see Figure 2.12 for monophasic coupling). Extremum times are chosen because they are easy to detect. They relate to phase angles of 0° and 180°/-180°. Phase-amplitude coupling measures would not change if the coupling was to be introduced at another phase angle. Examples for monophasic and biphasic coupling

[14] "Hanning window plus one", denotes that each data point of the Hanning window is added with one.

are displayed in Figure 2.13A. The Hanning window itself is multiplied with the factor I to graduate the intensity of phase-amplitude coupling (Figure 2.13B). To double the amplitude of the time series at the specified time I = 1.0 is chosen. I = 0.0 reflects no phase-amplitude coupling (i. e. not modulating the amplitude time series; uniform distribution; cf. Figure 2.8). The length of the Hanning window was also modulated to simulate different "widths" of phase-amplitude modulation (Figure 2.13C). Parameters chosen are specified below. In a final step, additional noise was added to the phase and amplitude time series. Therefore, Brownian noise of the same length was simulated, band-pass filtered at the same frequencies as the phase and amplitude time series, and added to the original phase and modulated amplitude time series, respectively. Frequency matched noise is disruptive to the modulated phase-amplitude coupling and therefore allows to check for the robustness of the phase-amplitude coupling measures.

Subsequently, phase and amplitude were extracted from the correspondent time series via Hilbert transform, using the Signal Processing Toolbox of MATLAB. Then continuous phase and amplitude time series were segmented. This was done to introduce data discontinuities which are present in real data as well. Filtering, Hilbert transform, and phase or amplitude extraction were always conducted on continuous data, to prevent filtering or other artefacts in the later analysed data epochs.

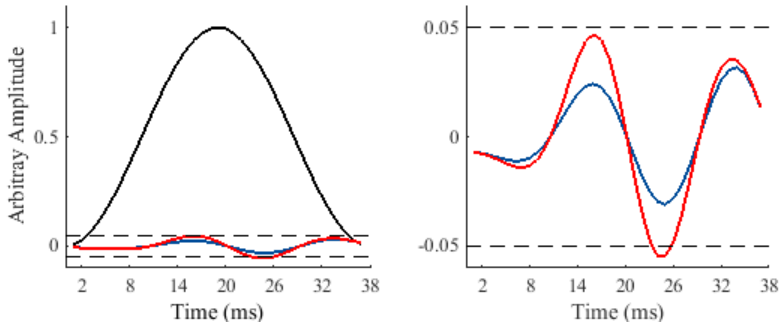

Figure 2.11: Original (blue line) and modulated (red line) amplitude time series. Modulation was realised by multiplying the original data (blue line) with a Hanning window (black line). The right subplot is an enlarged duplication of the left subplot without depiction of the Hanning window.

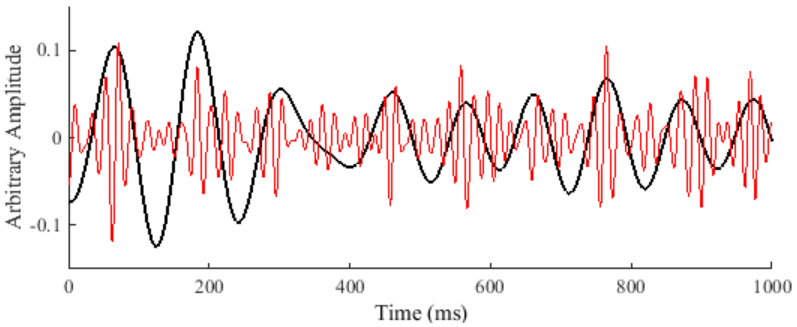

Figure 2.12: Example of monophasic coupling. Amplitude of the modulated upper frequency (red line) is higher during the peaks of the lower frequency band (black line).

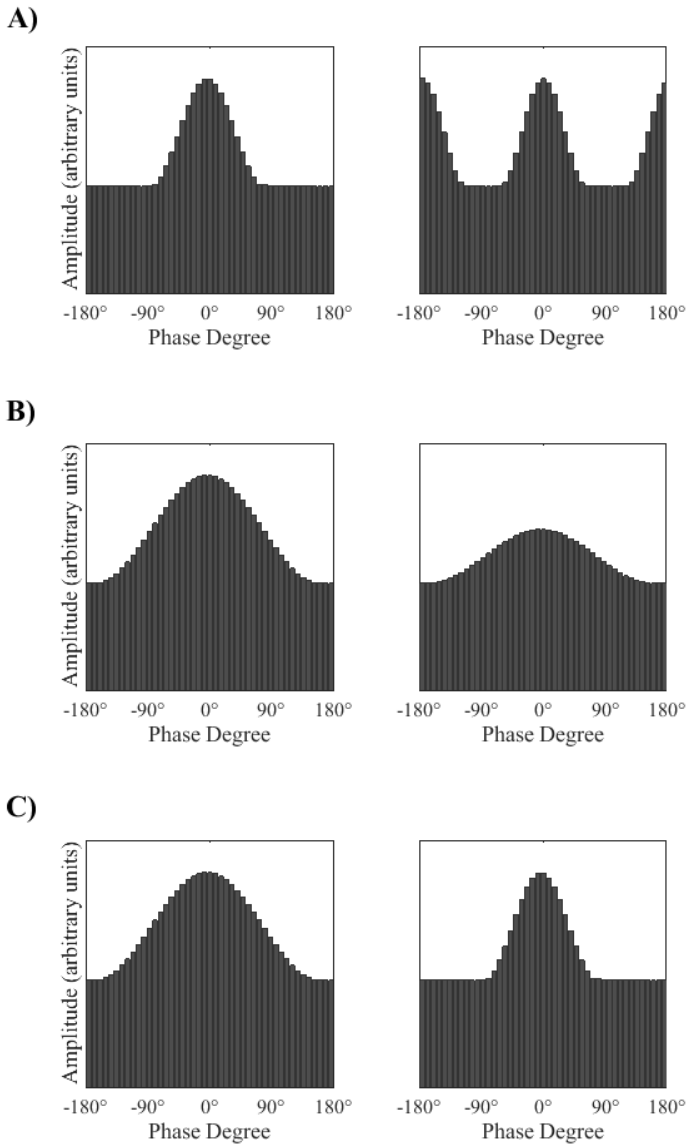

Figure 2.13: A) Monophasic (left) versus biphasic (right) phase-amplitude coupling. B) Strong (left) versus weak (right) phase-amplitude coupling. C) Broad (left) versus narrow (right) phase-amplitude coupling.

Data sets with a length of 42, 105, and 180 seconds were simulated. This amount of data is sufficient to simulate 30 trials with a length of 400, 2500 and 5000 milliseconds plus additional 30 seconds to introduce data discontinuities when segmenting the data. These parameters were chosen to mirror the properties of EEG data analysed in chapters 3 & 4: (1) at least 30 trials per unique condition for which phase-amplitude coupling will be calculated, (2) trial length between 400 and 5000 milliseconds, and (3) data discontinuities between trials. Sampling rate was set to 1000 Hz, identical to the sampling rate of the EEG data analysed later on. In addition, simulated data was resampled to 500 Hz in order to investigate to influence of sampling rate. Noise was scaled by the factor 0.9, 1.0, and 1.1 in order to simulate different signal-to-noise ratios. Scaling factor 0.9, 1.0, and 1.1 correspond to a noise signal strength of 90 %, 100 %, and 110 % compared to the data signal strength. Four modulation

strengths were realised: I = 0.0 for no coupling and I = 0.9, I = 1.0, and I = 1.1 for increasing coupling strength (I = 1.0 doubling the original amplitude strength). These values lie within the range of former studies (e. g. Kramer & Eden, 2013). The length of the Hanning Window ranged between 22.5 % and 27.5 % of one low frequency cycle to modulate different "widths" of phase-amplitude modulation. This width is equivalent to about a quarter of one cycle and therefore covers the peak (or trough) phases of that low frequency cycle (Figure 2.14). At these phases amplitude of the higher frequency was increased. All parameters were realised for mono- and biphasic coupling (factor multimodality).

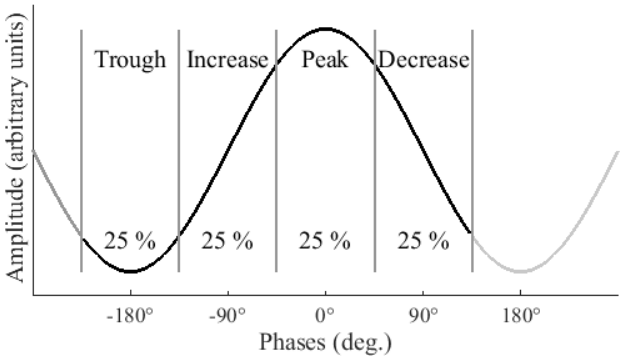

Figure 2.14: Partition of one wave cycle into quarters: first quadrant (trough), second quadrant (increase), third quadrant (peak), and fourth quadrant (decrease).

2.2.6 Statistical Analyses

All statistical analyses were conducted with IBM Statistics for Windows Version 23 (SPSS, Inc., IBM company), except otherwise specified. Significance level were set to $p_{two\text{-}tailed} < .05$. Violations of sphericity were, whenever appropriate corrected by Greenhouse-Geisser ε (Geisser & Greenhouse, 1958). Further analyses of significant results were conducted post hoc with Dunn's multiple comparison procedure (Dunn, 1961). Effect size measure ω^2 is reported for significant results (Hays, 1973). It is an estimator for the population effect Ω^2, which specifies the systematic portion of variance in relation to the overall variance (Rasch, Friese, Hofmann, & Naumann, 2006). According to Cohen (1988) $\Omega^2 = .01$ is considered a small, $\Omega^2 = .06$ a medium, and $\Omega^2 = .14$ a large effect. However, here, only significant effects larger than $\omega^2 > .05$ are considered relevant and reported here (Schweisthal, 2007).

Specificity of phase-amplitude coupling measures

In a first step 1000 data sets without coupling were simulated by setting the modulation strength to I = 0. Simulations were carried out for the frequency pair 8 – 10 Hz for phase time series and 50 – 70 Hz for amplitude time series. Phase-amplitude coupling values were generally compared in a 2 x 3 x 2 x 3 analysis of variance (ANOVA) with the repeated measurement factors phase-amplitude coupling measure (mean vector length, modulation index), data length (400 ms, 2500 ms, 5000 ms), sampling rate (500 Hz, 1000 Hz), and noise level (90 %, 100 %, 110 %).

As described above, for both measures nonparametric permutation testing was performed. Thereby one can test "how the phase-amplitude coupling value compares to a distribution of [phase-

amplitude coupling] values expected under the null-hypothesis" (Cohen, 2014, p. 414), i. e. the assumption of no coupling. Normal z-values directly imply p-values; a value of 1.64 corresponds to a p-value of 5 %. The phase-amplitude coupling value distribution which is expected under the null-hypothesis does not have to match the standardised normal distribution. Therefore, significance was not inferred from the standardised normal distribution, but instead by that phase-amplitude coupling value, at which 5 % of simulated data (with no coupling) was classified as false positive. Shuffling for permutation testing was done within trials because later analysis will also be conducted within trials. Coupling measures were then calculated on concatenated trials.

Specificity of measures was analysed by counting false positives (significant coupling, even though it was not engineered into the simulated data) depending on (1) data length, (2) sampling rate, and (3) noise level. To be able to conduct an ANOVA, the 1000 simulations were divided into 10 subsamples of 100 simulations each. For each subsample false negatives (dependent variable) were counted and each subsample was treated as a case in the subsequent 2 x 3 x 2 ANOVA with the repeated measurement factors data length (400 ms, 2500 ms, 5000 ms), sampling rate (500 Hz, 1000 Hz), and noise level (90 %, 100 %, 110 %). ANOVAs were carried out for both phase-amplitude coupling measures separately.

Sensitivity of phase-amplitude coupling measures as a function of moderating variables

Performance of phase-amplitude coupling measures were quantified by simulating 100 independent data sets and modifying the parameters (1) multimodality, (2) data length, (3) sampling rate, (4) noise level, (5) modulation strength, and (6) modulation width within each dataset. A 2 x 2 x 3 x 2 x 3 x 3 x 3 ANOVA with repeated measurement factors phase-amplitude coupling measure (mean vector length, modulation index), multimodality (monophasic, biphasic), data length (400 ms, 2500 ms, 5000 ms), sampling rate (500 Hz, 1000 Hz), noise level (90 %, 100 %, 110 % compared to signal strength), modulation strength (90 %, 100 %, 110 %), and modulation width (22.5 %, 25.0 %, 27.5 % of one low frequency cycle) was calculated. Because overall magnitude of phase-amplitude coupling values was highly different for both measures, the 7-way ANOVA was split into two 6-way ANOVAs excluding the factor phase-amplitude coupling measure.

Simulations were carried out for two frequency pairs (8 – 10 Hz/50 – 70 Hz and 16 – 18 Hz/202 – 238 Hz). Only results of one frequency pair (8 – 10 Hz/50 – 70 Hz) are reported in detail, because effects in both frequency pairs are highly similar. SPSS datasets, syntax, and outputs for all simulations are available from the author.

2.3 Results

2.3.1 Specificity of Phase-Amplitude Coupling Measures

Phase-amplitude coupling values did not differ depending on phase-amplitude coupling measures, data length, sampling rate, or noise level. Because of the high number of simulations (n = 1000), some main effects and interactions became significant. But all effect sizes were below $\omega^2 < .002$, therefore these differences are irrelevant.

Figure 2.15 shows the phase-amplitude coupling value distribution for the mean vector length and the modulation index. At a value of 1.86 for the mean vector length and 1.99 for the modulation index, five percent of the simulated data were classified as containing coupling (false positive). These values were therefore defined as critical z-values to imply significance. Values larger than the critical z-value are defined as reflecting significant coupling. Values smaller than the critical z-value are defined as not reflecting any coupling.

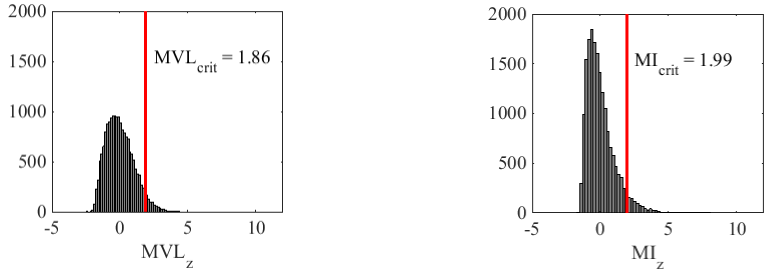

Figure 2.15: Phase-amplitude coupling value distribution of mean vector length (left panel) and modulation index (right panel). The red line marks the critical phase-amplitude coupling value. 18 000 values contribute to each distribution due to 1000 simulations in 18 conditions (data length [3] x sampling rate [2] x noise level [3]).

Amount of false positives did not differ depending on data length, sampling rate, or noise level in neither measure. One interaction in each analysis became significant, but effect sizes were below $\omega^2 < .02$, and are therefore considered negligible.

2.3.2 Sensitivity of Phase-Amplitude Coupling Measures as a Function of Moderating Variables

The 7-factor analysis showed that mean vector length (2.13 ± .08) and modulation index (12.02 ± .71) differed in their absolute magnitude independently of any other factor (main effect phase-amplitude coupling measure: $F_{(1,99)} = 241.99$, $p < .001$, $\omega^2 = .55$). For simplicity further analysis were conducted for each phase-amplitude coupling measure separately.

Mean Vector Length by Canolty et al. (2006)

All included factors contributed with a significant main effect. In contrast to biphasic coupling (.02 ± .01), monophasic coupling could be found (4.22 ± .15) by the mean vector length ($F_{(1,99)} = 824.83$, $p < .001$, $\omega^2 = .80$). Mean vector length increased with increasing data length ($F_{(2,198)} = 1041.07$, $p < .001$, $\omega^2 = .87$, $\text{Dunn}_{crit} = .29$). Mean vector length slightly increased with increasing sampling rate ($F_{(1,99)}$

= 20.26, p < .001, ω^2 = .09). Mean vector length decreased with increasing noise ($F_{(2,198)}$ = 400.60, p < .001, ω^2 = .73, $\text{Dunn}_{\text{crit}}$ = .06). Mean vector length increased with increasing modulation strength ($F_{(2,198)}$ = 173.02, p < .001, ω^2 = .53, $\text{Dunn}_{\text{crit}}$ = .06). Mean vector length increased with increasing modulation width ($F_{(2,198)}$ = 160.47, p < .001, ω^2 = .51, $\text{Dunn}_{\text{crit}}$ = .06). All factor levels in all effects are significantly different from each other according to Dunn's post hoc test.

Multimodality interacted with noise level, modulation strength, and modulation width (all *p's* < .001). Comparably data length interacted with noise level, modulation strength, and modulation width (all *p's* < .001). Multimodality and data length also interacted (p < .001). Sampling rate was the only factor that did not interact with any other factor. Further, three-way interactions of multimodality and data length with noise level ($F_{(4,396)}$ = 103.99, p < .001, ω^2 = .19, $\text{Dunn}_{\text{crit}}$ = .13), modulation strength ($F_{(4,396)}$ = 60.06, p < .001, ω^2 = .12, $\text{Dunn}_{\text{crit}}$ = .14), and modulation width ($F_{(4,396)}$ = 62.25, p < .001, ω^2 = .12, $\text{Dunn}_{\text{crit}}$ = .14) were significant.

These interactions had a monotone pattern, following the pattern of each main effect. For example, mean vector length increased with increasing modulation strength, but it increased even more when modulation width also increases. This pattern was true for each added factor. Mean vector length did not find biphasic coupling at all. Because of this, the described pattern is only valid for monophasic, but not for biphasic coupling. Patterns for each main effect are depicted in Figure 2.16. Three-way interactions are depicted in Table 2.1, Table 2.2, and Table 2.3.

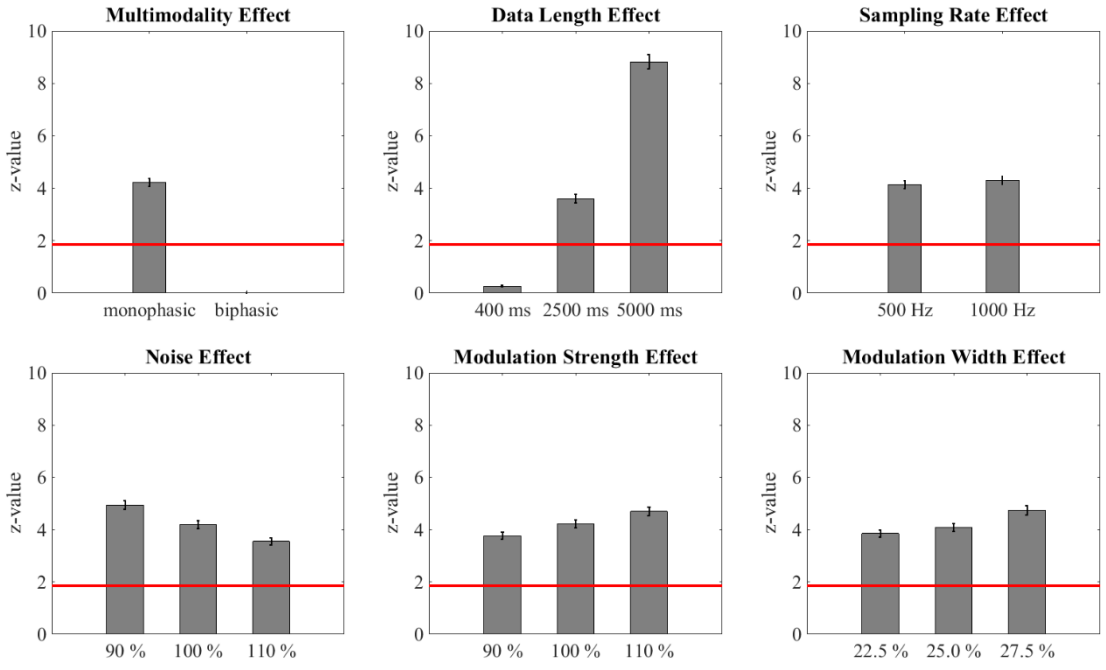

Figure 2.16: Mean (± S. D.) phase-amplitude coupling values for the mean vector length for each main effect. All effects, except the modularity effect, are solely depicted for monophasic coupling. The red line marks the significance level. All values above this line represent significant phase-amplitude coupling. All factor levels in all effects are significantly different from each other according to Dunn's post hoc test.

Table 2.1: Mean and standard error of mean vector length for the three-way interaction of multimodality, data length and modulation width. Significant phase-amplitude coupling values are printed in bold.

	Monophasic			**Biphasic**		
	Modulation Width			**Modulation Width**		
Data Length	**22.5 %**	**25.0 %**	**27.5 %**	**22.5 %**	**25.0 %**	**27.5 %**
400 ms	.219 (.037)	.275 (.035)	.304 (.037)	.060 (.024)	-.003 (.027)	.050 (.024)
2500 ms	**3.318** (.155)	**3.437** (.160)	**4.056** (.179)	.027 (.029)	.047 (.026)	.023 (.028)
5000 ms	**8.047** (.255)	**8.547** (.269)	**9.858** (.306)	-.008 (.025)	-.006 (.026)	-.004 (.029)

Table 2.2: Mean and standard error of mean vector length for the three-way interaction of multimodality, data length and modulation strength. Significant phase-amplitude coupling values are printed in bold.

	Monophasic			**Biphasic**		
	Modulation Strength			**Modulation Strength**		
Data Length	**90 %**	**100 %**	**110 %**	**90 %**	**100 %**	**110 %**
400 ms	.239 (.036)	.274 (.038)	.285 (.036)	.022 (.024)	.037 (.028)	.048 (.028)
2500 ms	**3.160** (.153)	**3.543** (.163)	**4.109** (.178)	.022 (.027)	.059 (.029)	.016 (.028)
5000 ms	**7.899** (.253)	**8.840** (.285)	**9.713** (.293)	-.005 (.031)	-.018 (.026)	.006 (.024)

Table 2.3: Mean and standard error of mean vector length for the three-way interaction of multimodality, data length and noise. Significant phase-amplitude coupling values are printed in bold.

	Monophasic			**Biphasic**		
	Noise Level			**Noise Level**		
Data Length	**90 %**	**100 %**	**110 %**	**90 %**	**100 %**	**110 %**
400 ms	.341 (.045)	.258 (.037)	.199 (.028)	.030 (.030)	.026 (.026)	.051 (.025)
2500 ms	**4.438** (.187)	**3.507** (.151)	**2.867** (.156)	.041 (.032)	.054 (.028)	.003 (.023)
5000 ms	**10.041** (.286)	**8.819** (.277)	**7.592** (.268)	-.006 (.026)	.010 (.030)	-.022 (.025)

Modulation index by Tort et al. (2008)

All included factors contributed with a significant main effect. Modulation index was larger in monophasic than in biphasic coupling ($F_{(1,99)} = 488.978$, $p < .001$, $\omega^2 = .71$). Modulation index increased with increasing data length ($F_{(2,198)} = 324.20$, $p < .001$, $\omega^2 = .68$, $\text{Dunn}_{\text{crit}} = 3.79$). Modulation index slightly increased with increasing sampling rate ($F_{(1,99)} = 23.98$, $p < .001$, $\omega^2 = .10$). Modulation index decreased with increasing noise ($F_{(2,198)} = 323.32$, $p < .001$, $\omega^2 = .68$, $\text{Dunn}_{\text{crit}} = .70$). Modulation index increased with increasing modulation strength ($F_{(2,198)} = 161.32$, $p < .001$, $\omega^2 = .52$, $\text{Dunn}_{\text{crit}} = .52$). Modulation index increased with increasing modulation width ($F_{(2,198)} = 160.68$, $p < .001$, $\omega^2 = .52$, $\text{Dunn}_{\text{crit}} = .48$). All factor levels in all effects are significantly different from each other according to Dunn's post hoc test.

Data length interacted with multimodality ($F_{(2,198)} = 325.69$, $p < .001$, $\omega^2 = .52$, $\text{Dunn}_{\text{crit}} = .90$), noise level ($F_{(4,396)} = 229.21$, $p < .001$, $\omega^2 = .50$, $\text{Dunn}_{\text{crit}} = 1.49$), modulation strength ($F_{(4,396)} = 108.00$, $p < .001$, $\omega^2 = .32$, $\text{Dunn}_{\text{crit}} = 1.23$), and modulation width ($F_{(4,396)} = 99.32$, $p < .001$, $\omega^2 = .30$, $\text{Dunn}_{\text{crit}} = 1.27$). Additionally there was a multimodality with modulation width interaction ($F_{(2,198)} = 21.05$, $p < .001$, $\omega^2 = .06$, $\text{Dunn}_{\text{crit}} = .68$), which was small compared to the other effects found here. Sampling rate was the only factor that did not interact with any other factor.

Like for mean vector length, these interactions had a monotone pattern, following the pattern of each main effect. For example, modulation index increased with increasing modulation strength, but it increased even more when modulation width also increases. Patterns for each main effect are depicted in Figure 2.17. Two-way interactions are depicted in Table 2.4 to Table 2.8.

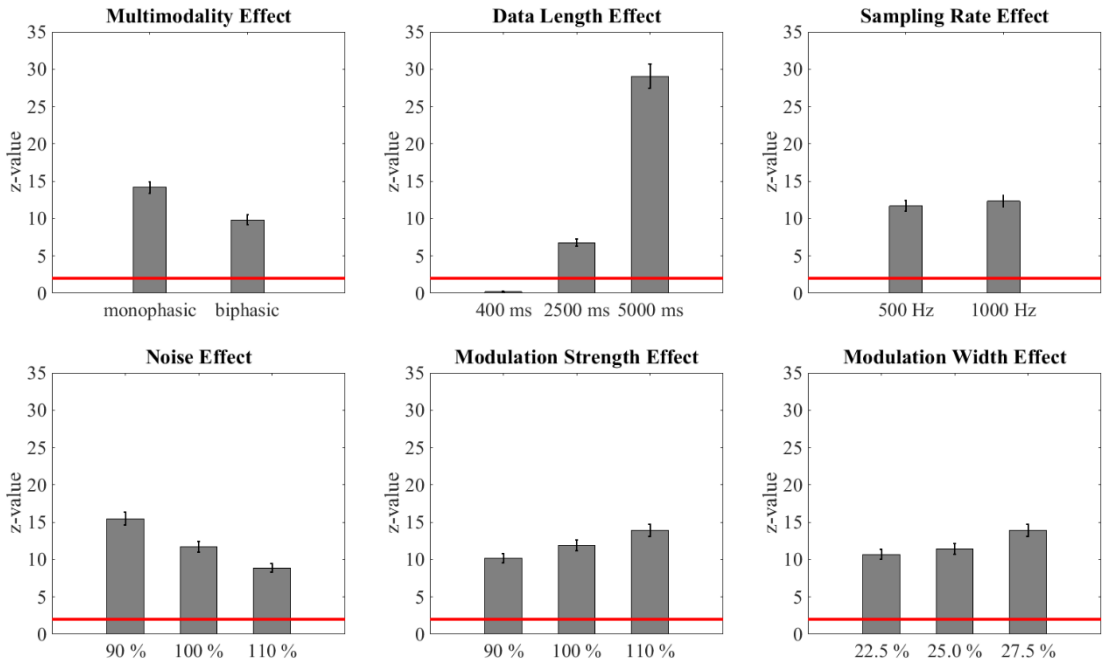

Figure 2.17: Mean (± S. D.) phase-amplitude coupling values for the modulation index for each main effect. The red line marks the significance level. All values above this line represent significant phase-amplitude coupling. All factor levels in all effects are significantly different from each other according to Dunn's post hoc test.

Table 2.4: Mean and standard error of modulation indices for the interaction of multimodality and data length. Significant phase-amplitude coupling values are printed in bold.

	Multimodality	
Data Length	**Monophasic**	**Biphasic**
400 ms	.283 (.035)	.045 (.022)
2500 ms	**8.477** (.541)	**5.083** (.423)
5000 ms	**33.816** (1.755)	**24.300** (1.553)

Table 2.5: Mean and standard error of modulation indices for the interaction of noise and data length. Significant phase-amplitude coupling values are printed in bold.

	Noise Level		
Data Length	**90 %**	**100 %**	**110 %**
400 ms	.307 (.039)	.198 (.030)	.154 (.023)
2500 ms	**9.112** (.609)	**6.442** (.461)	**4.786** (.372)
5000 ms	**36.993** (2.010)	**28.490** (.372)	**21.690** (1.375)

Table 2.6: Mean and standard error of modulation indices for the interaction of modulation strength and data length. Significant phase-amplitude coupling values are printed in bold.

	Modulation Strength		
Data Length	**90 %**	**100 %**	**110 %**
400 ms	.148 (.028)	.249 (.032)	.262 (.032)
2500 ms	**5.710** (.415)	**6.557** (.459)	**8.073** (.572)
5000 ms	**24.693** (1.480)	**29.001** (1.650)	**33.479** (1.857)

Table 2.7: Mean and standard error of modulation indices for the interaction of modulation width and data length. Significant phase-amplitude coupling values are printed in bold.

	Modulation Width		
Data Length	**22.5 %**	**25 %**	**27.5 %**
400 ms	.191 (.032)	.226 (.028)	.241 (.032)
2500 ms	**6.164** (.452)	**6.328** (.464)	**7.848** (.535)
5000 ms	**25.720** (1.481)	**27.726** (1.579)	**33.727** (1.913)

Table 2.8: Mean and standard error of modulation indices for the interaction of modulation width and multimodality. Significant phase-amplitude coupling values are printed in bold.

Modulation Width	**Multimodality**	
	Monophasic	**Biphasic**
22.5 %	**12.401** (.687)	**8.982** (.626)
25 %	**13.421** (.734)	**9.432** (.651)
27.5 %	**16.753** (.919)	**11.125** (.735)

Table 2.9: Effect sizes ω² for all significant main effects and interactions for mean vector length.

Main Effects	**9 Hz / 60 Hz**	**17 Hz / 220 Hz**
Multimodality	.80	.81
Data Length	.87	.88
Sampling Rate	.09	.82
Noise	.73	.76
Modulation Strength	.53	.61
Modulation Width	.52	.67
Interaction with Multimodality		
Multimodality * Sampling Rate	-	.59
Multimodality * Noise	.56	.64
Multimodality * Modulation Strength	.36	.44
Multimodality * Modulation Width	.38	.49
Interaction with Data Length		
Data Length * Multimodality	-	.79
Data Length * Sampling Rate	-	.48
Data Length * Noise	.32	.36
Data Length * Modulation Strength	.21	.26
Data Length * Modulation Width	.22	.28
Interaction with Multimodality and Data Length		
Multimodality * Data Length * Sampling Rate	-	.33
Multimodality * Data Length * Noise	.19	.21
Multimodality * Data Length * Modulation Strength	.12	.15
Multimodality * Data Length * Modulation Width	.12	.16
Interaction with Sampling Rate		
Sampling Rate * Modulation Width	-	.06

Table 2.10: Effect sizes ω² for all significant main effects and interactions for modulation index.

Main Effects	**9 Hz / 60 Hz**	**17 Hz / 220 Hz**
Multimodality	.71	.74
Data Length	.68	.68
Sampling Rate	.10	.58
Noise	.68	.67
Modulation Strength	.52	.53
Modulation Width	.52	.55
Interaction with Multimodality		
Multimodality * Modulation Strength	-	.08
Multimodality * Modulation Width	.06	.16
Interaction with Data Length		
Data Length * Multimodality	.52	.53
Data Length * Sampling Rate	-	.45
Data Length * Noise	.50	.52
Data Length * Modulation Strength	.32	.35
Data Length * Modulation Width	.30	.34
Interaction with Sampling Rate		
Sampling Rate * Noise	-	.12
Sampling Rate * Modulation Width	-	.07

Effect of sampling rate on phase-amplitude coupling measures

The factor sampling rate stands out because of its comparatively small effect size and lack of interaction with all other factors. A second set of data was simulated testing mean vector length and modulation index at 16 – 18 Hz for modulating frequency and 202 – 238 Hz for the modulated frequency. This analysis showed that sampling rate is indeed important, but only if the investigated frequencies approach the Nyquist frequency. Table 2.9 and Table 2.10 list all significant effect sizes for both simulations, of 8 – 10 Hz/50 – 70 Hz (9 Hz/60 Hz) and 16 – 18 Hz/202 – 238 Hz (17 Hz/220 Hz) for mean vector length and modulation index respectively.

2.4 Discussion

Specificity of phase-amplitude coupling values. Neither raw mean vector length nor raw modulation index can become negative. This is reflected in the positive skewed phase-amplitude coupling z-value distribution. Both measures have slightly more false positives than expected under the standardised normal distribution. This is corrected by increasing the critical z-value for both measures individually. The absolute phase-amplitude coupling value, as well as the amount of false positives, does not differ between measures and is not modulated by data length, sampling rate, and signal-to-noise ratio.

Multimodality influences both measures very differently. The mean vector length cannot find biphasic coupling as it was implemented here (amplitude of the higher frequency was increased at peak and trough of the lower frequency). Because of its mathematic construct (Equation 3, Figure 2.18), this is not surprising. Peak and trough appear on opposite sides in the polar plane: their mean will cancel each other out. If other forms of biphasic coupling would be present, the mean vector length could be able to find it, but would probably underestimate its strength and would furthermore return distorted phase information. Therefore, it is important to have a look at the polar plot before interpreting one's results. The modulation index is able to find biphasic coupling, but biphasic coupling leads to a reduction in the phase-amplitude coupling value. The selection of 82 studies cited earlier, indicates that biphasic coupling plays a minor role in empiric data. Only three studies (~ 3 %) report biphasic coupling (Lega, Burke, Jacobs, & Kahana, 2016; Leszczynski, Fell, & Axmacher, 2015; van der Meij et al., 2012), and two further studies report biphasic coupling in a single subject (Friese et al., 2013; Köster et al., 2014). Nearly 70 % of studies report monophasic coupling and nearly 30 % do not reveal the nature of coupling.

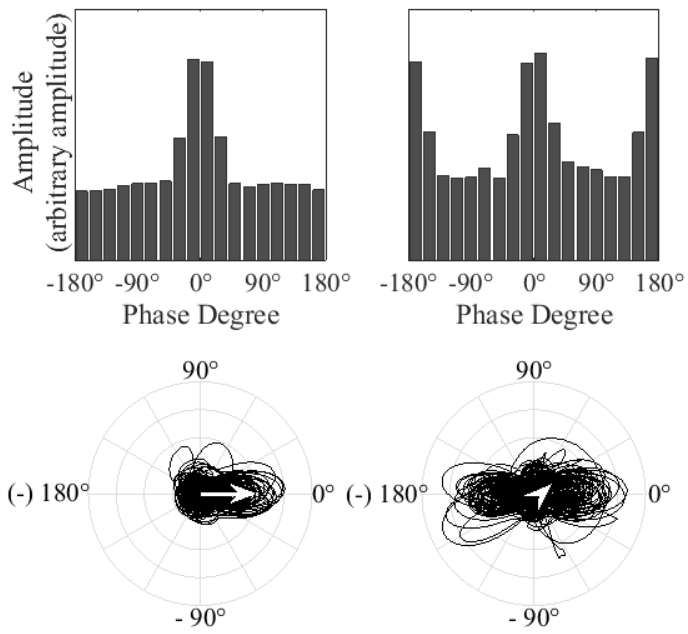

Figure 2.18: Idealized depiction of monophasic (left column) and biphasic (right column) phase-amplitude coupling. The white arrows are an idealized representation of the mean vector length.

The longer the data, the larger mean vector length and modulation index are. This association was found in the data presented here, but must not generally apply. Because coupling was simulated continuously into the data, there was proportionally more coupling in longer data epochs. If coupling is transient and does not proportionally vary with data length, this relationship does not need to apply. Potentially, the general rule is that the longer the data epochs where coupling occurs, the stronger the phase-amplitude coupling values. This should be tested in a follow-up analysis. This analysis further showed that a minimal data length is required for finding coupling, which should exceed at least 400 milliseconds per trial when including 30 trials. Neither modulation index nor mean vector length were able to detect coupling in the shortest simulated epoch of 400 milliseconds. It might be useful to develop a correction factor for data length, to make phase-amplitude coupling values more comparable across studies.

The noisier the data, the lower mean vector length and modulation index are. This aspect is not desired but logical. Noise obscures the relation between the phase of the lower frequency and amplitude of the higher frequency. The data as a whole contains phase-amplitude coupling to a lesser extent, as the relative amount of noise compared to the relative amount of signal increases.

The stronger the coupling, the larger mean vector length and modulation index are. As Tort et al. (2010) has shown, this behaviour is not inherent to all phase-amplitude coupling measures. Since researchers do not only want to prove the existence of phase-amplitude coupling, but also differentiate its strength, a measure which can do this is indispensable. Both increasing and decreasing

amplitudes are conceivable. Only increasing amplitude was simulated. The modulation index should be able to detect phase-amplitude coupling with decreasing amplitudes: The phase-amplitude plot will equally deviate from the uniform distribution, no matter if amplitude strength is increased or decreased at specific phases. The mean vector length, on the other hand, can only correctly detect "bumps" at narrow phase angles, and would therefore supposedly not detect amplitude decreases for a narrow range of phase angles, because this pattern implies a broad range of phase angles with strong amplitudes, which drive the estimate of the mean vector length.

The broader the coupling width, the larger mean vector length and modulation index are. Width of coupling was defined as either 22.5 %, 25 %, or 27.5 % of one slow frequency cycle. The relation of broader coupling with stronger phase-amplitude coupling values might be reversed if the phase-amplitude coupling width becomes too broad (Figure 2.19).

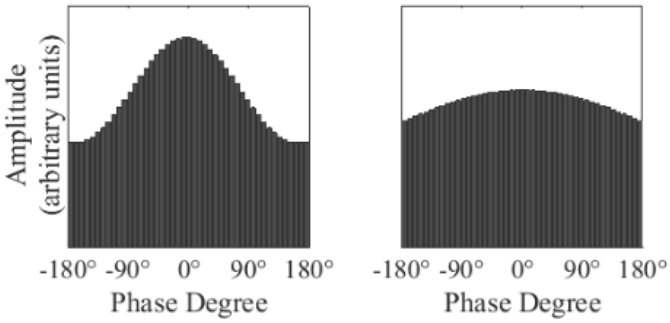

Figure 2.19: Illustration of two modulation width: narrow (left) and broad (right).

Sampling Rate has a minor effect on mean vector length and modulation index. It seems to be only important if investigated frequencies approach the Nyquist frequency.

All interactions are ordinal, that is, they simply add up: phase-amplitude coupling measures decrease as modulation width decreases, and they decrease even faster when modulation strength decreases additionally. Therefore, the potentially complex 6-way analysis of variance becomes comprehensible. The higher the interaction, the more the effect size decreases. The generally large effects sizes are owed to choices of data simulation. Apparently, varying modulation strength about 10 percentage points is easily detectable for either coupling measure. This implies that even smaller differences in modulation strength and modulation width can be easily detected by both measures (depending on sample size). Detection depends, as this analysis shows, on confounding variables like data length, signal-to-noise ratio, modulation width, etc.

2.5 Conclusion

Analyses indicate that both measures behave as desired, by differentiating coupling strength and coupling width. In addition, other factors like data length, signal-to-noise-ratio, sampling rate when approaching Nyquist frequencies, and multimodality of coupling also influences the level of the phase-amplitude coupling values. In the worst case, this can lead to insignificant measures, even though coupling is present. Comparing absolute coupling strength across studies might be difficult because of the confounding variables. Comparisons within one study, on the other hand, can be done with confidence. Nevertheless, one should make sure that signal-to-noise ratio is comparable within all experimental conditions and over the course of the experiment.

If it is not clear whether cross-frequency coupling will be mono- or biphasic, the modulation index by Tort et al. (2008) should be used. Literature suggests that biphasic coupling can be neglected, but it is not yet clear if this is due to the lack of its existence or methodological reasons (e. g. usage of mean vector length). Consequently, mean vector length by Canolty et al. (2006) should only be used when restricting analysis to monophasic coupling. This measure cannot detect multiphasic coupling. Besides that it seems to be negligible which measure is used, as both are equally good in indicating coupling strength and coupling width, while being equally prone to data length, sampling rate, and signal-to-noise ratio.

The modulation index, even though its calculation is less intuitive than that of the mean vector length, proved to be a valid measure. Both phase-amplitude coupling measures lead to comparable results. The modulation index is quantitatively larger. But even despite substantial quantitative differences in values, the qualitative decision for significance of phase-amplitude coupling is the same for both measures. Nevertheless, comparison of coupling strength between both measures is problematic. Because of the lack of comparability between measures, it would be advisable for the research community to either report both measures or select one obligatory measure for future analyses.

Generally, it is advisable to work with standardized phase-amplitude coupling measures via permutation testing. It facilitates the interpretation of the measures, first and foremost, by giving the researcher knowledge about the probability that the observed modulation index would have been also found under the assumption of the null-hypothesis. This aspect is often ignored in the literature.

Kramer and Eden (2013) stated that “an optimal analysis method to assess this cross-frequency coupling (CFC) does not yet exist” (p.64). Even if it would be ideal, to have a measure that is less susceptible to confounding variables – especially data length – summarizing this analysis, it should be rather concluded that at least two reasonable analysis methods exist. For further analyses in this work the modulation index is chosen, firstly, because the existence of biphasic coupling cannot be excluded and secondly, because most former studies (about one third) used this measure. Therefore, the results presented here are comparable to a majority of former studies.

3 Flexibility and Inhibition under Acute Stress: a Phase-Amplitude Coupling Study

3.1 Introduction

The relevance of investigating the relation between stress, executive functions, and cross-frequency coupling has been extensively discussed in chapter 1. This chapter will present data about effects of stress on flexibility and inhibition as well as its relation to phase-amplitude cross-frequency coupling. So far there are no studies examining all three components (stress, executive functions, phase-amplitude coupling) simultaneously.

3.1.1 Flexibility, Stress, and Phase-Amplitude Coupling

The majority of studies exploring the effect of acute psychological or physical stress on flexibility in healthy subjects found detrimental effects of stress on flexibility (Alexander, Hillier, Smith, Tivarus, & Beversdorf, 2007; Hillier, Alexander, & Beversdorf, 2006; Liston, McEwen, & Casey, 2009; Plessow, Kiesel, & Kirschbaum, 2012; Renner & Beversdorf, 2010; Seehagen, Schneider, Rudolph, Ernst, & Zmyj, 2015; Shields, Trainor, Lam, & Yonelinas, 2016; Yildiz et al., 2014). A minority found no or small, negligible effects (Ishizuka, Hillier, & Beversdorf, 2007; Renner & Beversdorf, 2010; Steinhauser, Maier, & Hübner, 2007). Alternately, some beneficial effects of stress on flexibility performance were also found (Beste, Yildiz, Meissner, & Wolf, 2013; Delahaye et al., 2015; Kofman, Meiran, Greenberg, Balas, & Cohen, 2006). While direction of effects differed, effect sizes showed considerable conformity ranging around 10 % explained variance[15] in both cases of detrimental and beneficial effects of stress on flexibility. The studied populations are young, healthy individuals of both sexes with a sample size between 20 to 50 subjects in all but two cases. The first exception included 75 female and 38 male students and found that only men exhibited less flexibility after being stressed, while women's behaviour was not modulated by stress (Shields et al., 2016). None of the other studies reported sex differences. Due to highly unequal group sizes, results should be interpreted carefully. The second exception examined infants, finding more habitual behaviour after having them stressed in comparison to a non-stressed control group (Seehagen et al., 2015).

A potential explanation for the heterogeneity of results could be the diversity of stressors as well as flexibility measures. However this seems not to be the case as no single stressor or flexibility tasks can be exclusively associated with beneficial or detrimental effects of stress.

The classification of stressed participants into low and high responders could be important and will be applied in this study. Low responders are subjects that physiologically barely respond to a stress induction procedure, while high responders show a marked physiological stress response. Other studies have already shown that the separation of low and high responders can be useful because variance in cortisol response is large (Elzinga & Roelofs, 2005) or effects can only be found in one of the two groups (al'Absi, Hugdahl, & Lovallo, 2002).

[15] This value was extracted by quantifying F- and t-values with the effect size measure ω^2. As is described in Rasch et al. (2006) ω^2 estimates the population effect size Ω^2. It specifies the percentage of explained variance of the total variance.

The induced physiological stress response could be another aspect explaining differences between study results. The Trier social stress test (TSST), and to a lesser extent the SECPT, are known to reliably and significantly elevate cortisol levels (Dickerson & Kemeny, 2004) and also lead to a significant autonomic stress response. This is not the case for noise (Andren, Lindstedt, Bjorkman, Borg, & Hansson, 1982), movies (Qin et al., 2012) and the CPT (Schwabe, Haddad, & Schachinger, 2008). Not all studies measured the physiological stress response. Of those who did report cortisol levels, which were solely the studies using TSST and SECPT, all measured significant cortisol increases in response to the stressor. Three studies showed less flexibility in the stressed group compared to the control group (Plessow et al., 2012; Shields et al., 2016; Yildiz et al., 2014) and one showed increased flexibility in stressed versus control subjects (Beste et al., 2013); another study did not find significant differences between stressed female subjects and female controls (Shields et al., 2016). Neither absolute cortisol level nor time of task in relation to stress induction procedure seem to explain the different effects.

Like the majority of reviewed studies, a recent meta-analysis concludes that acute stress impairs flexibility (Shields, Sazma, & Yonelinas, 2016). They further found that the greater the stress severity, the greater the detrimental effects. Sex seems to not influence this effect; however this result should be interpreted cautiously, because statistical tests lacked power. In a meta-analysis of pharmacological cortisol effects on flexibility, no effects were found, indicating that not just cortisol, but the entire psychophysiological stress response causes detrimental stress effects on flexibility behaviour (Shields, Bonner, & Moons, 2015).

Assuming that for complex behaviours like the core executive function flexibility several basic processing units have to be integrated, the occurrence of phase-amplitude coupling is expected during flexible behaviour. Voloh, Valiante, Everling, and Womelsdorf (2015) empirically showed this association. Two monkeys executing an attention shifting task, in which relevant information had to be selected and combined in a flexible manner, showed phase-amplitude coupling in prefrontal cortex and anterior cingulate cortex when successfully executing this task, but not when failing. Furthermore, phase-amplitude coupling was found to be higher during a task switching paradigm, than during a simple stimulus-response mapping task in four humans (Voytek et al., 2015). This effect was found within the prefrontal cortex and between prefrontal and primary motor as well as premotor cortex, respectively.

These findings suggest that if flexible behaviour decreases – which can be assumed under stress – strength of phase-amplitude coupling should also decrease. Behavioural findings are in accordance with Arnsten's theory regarding stress signalling pathways (Arnsten, 2009; see section 1.2). Phase-amplitude coupling findings are also capable of being integrated in Arnsten's theory. She assumes that the top-down control of the prefrontal cortex over other brain regions (e. g. the parietal cortex) collapses during stress. So if phase-amplitude coupling, being a mechanism that could represent this top-down control, collapses due to stress, top-down control equally collapses, causing behavioural stress effects.

3.1.2 Inhibition, Stress, and Phase-Amplitude Coupling

Behavioural Effects.

Three groups investigated how examination stress influences performance of Stroop (Kofman et al., 2006; Pattyn et al., 2014) and go-nogo task (Wu et al., 2014). Cognitive inhibition testing was executed under basal cortisol levels. It was expected that stress would be generally exaggerated in the exam period compared to a control period without exams. In none of the studies was cortisol directly assessed, but all reported elevated subjective stress ratings during the exam period compared to the control period. Sympathetic activation during the exam period was at least descriptively elevated in Kofman et al. (2006) and Pattyn et al. (2014). It was not measured in Wu et al. (2014). Even though Kofman et al. (2006) found overall increased reaction times in participants in an exam period compared to participants having no exams, no group differences regarding inhibition performance (interference effect) were found in these studies. Also Wu et al. (2014) did not find influences of stress on inhibition. Pattyn et al. (2014) found increased error rates in a Stroop version which used emotional stimuli especially relevant to the subject group and thereby increased interference for personally relevant emotional stimuli. Significant effects explained about eight to nine percent of variance in these studies.

Six studies investigated how acute psychosocial stress (TSST or SECPT) influences inhibition ability (Plessow, Fischer, Kirschbaum, & Goschke, 2011; Plessow, Schade, Kirschbaum, & Fischer, 2012; Sänger et al., 2014; Scholz et al., 2009; Schwabe, Höffken, Tegenthoff, & Wolf, 2013; Yildiz et al., 2014). All of these six studies used a between-subject design with young, healthy participants and ran their study in the afternoon (except Yildiz et al., 2014, who tested their subjects in the morning hours; personal communication).[16] Sample sizes ranged between 25 and 56 subjects of either solely male participants or mixed samples. All studies induced a significant HPA axis activation and ANS activation as well as higher subjective stress ratings in the stress compared to the control condition. Cognitive tasks were executed mostly immediately after the stress procedure and lasted at most until 50 minutes post stress onset. Therefore, all cognitive tasks laid roughly in the phase of rising and peaking cortisol levels. However, length of stress induction procedures (about 15 minutes for TSST, about 5 minutes for SECPT) and length of cognitive testing differed. For example Sänger et al. (2014) applied the SECPT three times and tested 20 minutes after each SECPT onset; cognitive tasks lasting 15 minutes. Other participants were tested for 50 minutes without repeated induction of stress after the first time (Yildiz et al., 2014). Schwabe et al. (2013) waited 30 minutes before cognitive testing took place, just after cortisol levels peaked.

Irrespective of stressor (TSST, SECPT), time lag of cognitive testing relating to stress onset, and potentially irrespective of task, positive (Plessow et al., 2011; Schwabe et al., 2013), negative (Plessow et al., 2012; Sänger et al., 2014; Scholz et al., 2009), and no effects (Yildiz et al., 2014) of stress on inhibition were found. Sex differences were not found in studies using both sexes (Plessow et

[16] Due to the diurnal rhythm of cortisol this factor might influence results. Cortisol levels are highest shortly before awakening and decrease over the course the awake period (Weitzman et al., 1971).

al., 2011; Plessow et al., 2012; Schwabe et al., 2013), nor did a recent meta-analysis on this topic report sex differences (Shields et al., 2016). Effect sizes ranged from 4 to 22 % explained variance in the case of detrimental effects and from 7 to 14 % explained variance in the case of beneficial effects. Like for flexibility there is a tendency for more studies to show detrimental effects, whereas the recent meta-analysis (Shields et al., 2016) found that stress enhanced response inhibition (e. g. assessed via go-nogo task), but impaired cognitive inhibition (e. g. assessed via Flanker task). The qualitative review conducted here did not differentiate between response and cognitive inhibition. Because of the quantitative meta-analysis and the heterogeneous results from the qualitative review, beneficial effects of stress on behavioural inhibition are expected in the go-nogo task applied in this thesis.

Phase-Amplitude Coupling Effects.

At least four studies directly explored the relationship between inhibition and phase-amplitude coupling (Dürschmid et al., 2014; Popov, Steffen, Weisz, Miller, & Rockstroh, 2012; Tang et al., 2016; van Wingerden, van der Meij, Kalenscher, Maris, & Pennartz, 2014). Except for one study (Popov et al., 2012), all solely investigated and found theta-gamma phase-amplitude coupling.

In an MEG study, Popov et al. (2012) analysed and found alpha-gamma coupling in a sample of 24 healthy human subjects during an emotion regulation task. Gamma amplitude was strongest at alpha phase peaks. They found stronger phase-amplitude coupling while participants regulated their feelings towards unpleasant pictures versus passively watching them but do not provide significance testing for the coupling per se. A repeated measurement design was used, showing that coupling strength varies intra-individually with task demands. Coupling was found within the medial prefrontal cortex.

In a go-nogo task executed by three subjects, phase-amplitude coupling strength increased in parallel with reaction time decreases (Dürschmid et al., 2014). Only correct go-trials were analysed and therefore simply motor responses were investigated, not the inhibition of behaviour. Coupling was primarily found in motor regions. Simultaneously, three additional subjects, who performed purely non-inhibitory tasks also requiring a motor response to a stimulus, were analysed. Theta-gamma coupling was found to be associated to performance in all six subjects. Therefore coupling appears to be a mechanism by which motor responses are programmed and optimized. In a previous study, Dürschmid et al. (2013) manipulated the needed amount of cognitive control for a motor learning task and found significant theta-gamma phase-amplitude coupling following the motor responses in the nucleus accumbens contralateral to the used hand. Coupling only reached significance in blocks of high cognitive control, but not during blocks of low cognitive control. Additionally, preferred coupling phase between blocks of high and low cognitive control varied. Phase-amplitude coupling was further diminished in error trials, as a negative correlation between the phase-amplitude measure and error probability appeared.

Tang et al. (2016) detected significant theta-gamma coupling while 15 participants executed a Stroop task. Coupling was evident in half of the recorded electrodes. Strength of coupling was not modulated by trial type (congruent versus incongruent) and no correlation with behaviour was reported.

Recording LFPs from the orbitofrontal cortex of three awake rats executing an odour discrimination go-nogo task, van Wingerden et al. (2014) found manifold associations between behaviour and theta-gamma coupling. Phase-amplitude coupling appeared to be time locked to odour sampling and was found to be higher in correct trials compared to incorrect ones. Furthermore the preferred coupling phase differed between correct and incorrect trials and showed more consistency in correct trials than in incorrect trials. In correct trials, no matter whether a go- or nogo-response was expected, coupling strength correlated positively with behavioural performance. Phase-amplitude coupling strength differed between regions within the orbitofrontal cortex, being strongest between posteromedial phase-providing channels and posterolateral amplitude-providing channels.

The association between inhibition and phase-amplitude coupling was indirectly measured by Lee and Yun (2014) in an EEG study, comparing intoxicated and sober human subjects. Alcohol consumption is thought to decrease executive control (cf. Quinn & Fromme, 2016). Delta-gamma and theta-gamma coupling were reduced in intoxicated subjects compared to the sober ones. This was true for a resting state but no group differences were found during an arithmetic task. Coupling strength was found to decrease at frontal and parietal regions. Unfortunately Lee and Yun (2014) do not provide significance testing for phase-amplitude coupling and do not relate coupling directly to behaviour.

The review of these studies gives an idea of what to expect when looking for phase-amplitude coupling in inhibition paradigms. Some of the studies have a rather loose relationship with inhibition as defined in section 1.2. So far, no study investigated phase-amplitude coupling at scalp EEG level in healthy human subjects providing significance testing and associating inhibition with performance. This is why no strong hypotheses are inferred from these studies but an exploratory phase-amplitude cross-frequency analysis is conducted. Nevertheless, if an association between phase-amplitude coupling and inhibition was found (four of six studies; Dürschmid et al., 2013; Lee & Yun, 2014; Popov et al., 2012; van Wingerden et al., 2014), it always pointed towards stronger coupling during increased need of inhibition. Summing up, increased response inhibition is expected under stress which should be mirrored in increased phase-amplitude coupling when executing inhibition (e. g. nogo trials) compared to a control task (e. g. go trials).

3.1.3 Hypotheses

Exploratory phase-amplitude coupling analyses are conducted across a broad frequency range to investigate whether flexibility and inhibition are reliably accompanied by phase-amplitude coupling. This first step is necessary to establish knowledge whether phase-amplitude coupling is actually present during executive functioning. Furthermore, phase-amplitude coupling strength will be analysed to

address the question as to whether coupling strength might be associated with task demands and stress level of participants. For behaviour and coupling strength the following hypotheses are formulated:

1.1 Reaction times will be faster and error rates lower in switch compared to repeat trials for the task switching design and error rates lower in the go trials compared to the nogo trials in the go-nogo paradigm.
1.2 Groups will not differ in their flexibility and inhibition performance before the SECPT.
1.3 a) Stressed participants, especially those with a marked physiological stress response, will perform less flexibly after the SECPT than before SECPT and worse than the control group after the SECPT.
b) Stressed participants, especially those with a marked physiological stress response, will show better behavioural inhibition behaviour after the SECPT than before SECPT and better inhibition than the control group after the SECPT.

2.1 Phase-amplitude coupling strength will be stronger in switch compared to repeat trials for the task switching design and stronger in the nogo trials compared to the go trials in the go-nogo paradigm.
2.2 Groups will not differ in their coupling strength before the SECPT.
2.3 a) Stressed participants, especially those with a marked physiological stress response, will show less coupling after the SECPT than before the SECPT and less coupling than the control group in the flexibility task after the SECPT.
b) Stressed participants, especially those with a marked physiological stress response, will show increased coupling after the SECPT than before the SECPT and stronger coupling than the control group in the inhibition task after the SECPT.
2.4 Phase-amplitude coupling should correlate negatively with reaction times in the flexibility task.

3.2 Material and Methods

3.2.1 Participants

The final sample size was comprised of 33 male students from Trier University. Mean age ± standard deviation was 24 ± 3 years and ranged from 19 to 30 years. Initially 41 subjects were invited to participate in the study. Two participants had to be discarded because of technical problems which lead to an interruption of EEG recording. Another six subjects were discarded for the following reason: as will be described below, raw EEG data was transformed from sensor to source level (independent component analysis; ICA). When analysing sensor level data, sensors (F3, Fz, etc.) are construed as being equivalent across subjects. When analysing source level data, equivalent sources (independent components; ICs) across subjects have to be defined. Because ICs differ between subjects, it is not always possible to find equivalent sources for all subjects. Subjects that did not contribute with a source to all required regions of interest were therefore excluded in order to keep the sample identical for all

statistical analyses. Excluded subjects did not differ from included subjects regarding age, task order, or experimental manipulation.

Preconditions for eligibility were the following: (1) age between 18 and 30 years, (2) body mass index between 18 and 30, (3) being a non-smoker, (4) no use of illegal and legal drugs or substances possibly influencing cortisol levels, (5) right-handedness, (6) absence of any acute and chronic mental disorder or physical disease (especially the Raynaud syndrome), as well as absence of a history of mental disorders, (7) native German speaker, (8) normal or corrected-to-normal vision, and (9) not studying psychology. Preconditions were to ensure that cortisol levels were to the greatest possible extent within the normal range (1-4), participants had similar hemispheric specialisation[17] (5), had no problems understanding instructions and complying with the experimental procedure (6-8), and guaranteeing unbiased behaviour in the experiment (9).

Participants gave written informed consent prior to participation. The study was approved by the local ethics committee and is in accordance with the Declaration of Helsinki (World Medical Association, 2013). Participants received either course credits or 35 euros for participation.

3.2.2 Experimental Procedure

Subjects were invited for an initial screening session. There eligibility was determined with a structured interview. The aim of the study was explained and detailed information about experimental procedure was provided. A battery of personality questionnaires as well as additional information and sampling devices for measuring the cortisol awakening response (Fries, Dettenborn, & Kirschbaum, 2009), were handed out to eligible participants. Analysis of this data can be found in Fechtner (2012). Participants conducted the experiment another day at 1200h, 1430h, or 1700h to guarantee comparably low cortisol levels across subjects (Kirschbaum & Hellhammer, 2000). They had refrained from physical exercise and alcohol consumption on the day of the experiment and from caffeinated drinks and meals one hour prior the experimental session.

Immediately after arrival, subjects provided their first saliva sample (#01, approximately 48 minutes prior to the stress induction procedure). Participants were seated in a dimly lit, sound-attenuated, and electrically shielded recording cabin and prepared for EEG, electrooculography (EOG), and electrocardiography (ECG) recordings. Participants were left alone in the recording cabin; all instructions were given via computer screen. They provided their second saliva sample (#02, 37 minutes prior to the stress induction procedure), practiced the first task (64 or 16 practice trials for the task switching paradigm or go-nogo paradigm respectively; feedback was given during practice) and subsequently executed the baseline block of this task. After a one minute break, they practiced the second task and subsequently executed the baseline block of this task before providing the third saliva sample (#03, 2 minutes prior to the stress induction procedure).

[17] According to Galin, Ornstein, Herron, and Johnstone (1982) handedness affects hemispheric specialization and can thus lead to differences in EEG measurement.

Participants were then exposed to the socially evaluated cold pressor test or a socially evaluated warm water control procedure (SECPT). A female investigator, unknown to the participant, entered the room and led the participant through the stress induction procedure. After the stress induction procedure, participants were again left alone in the recording cabin, rated their subjective stress perception and conducted another block of each task, providing salivary samples before and after each task (#04 – #06, 8 – 39 minutes after SECPT). Order of tasks was completely randomized between subjects resulting in four possible task orders: TG|TG, TG|GT, GT|GT, GT|TG (T represents task switching while G represents the go-nogo task; | represents the SECPT). After removal of all recording devices, participants were debriefed by the investigator who conducted the stress induction procedure, provided a last saliva sample (#07, 50 minutes after SECPT), and were compensated with course credits or monetarily. The whole experimental procedure took about two hours. Throughout the experiment, subjects filled out several state questionnaires (Figure 3.1) whose results are not analysed here.

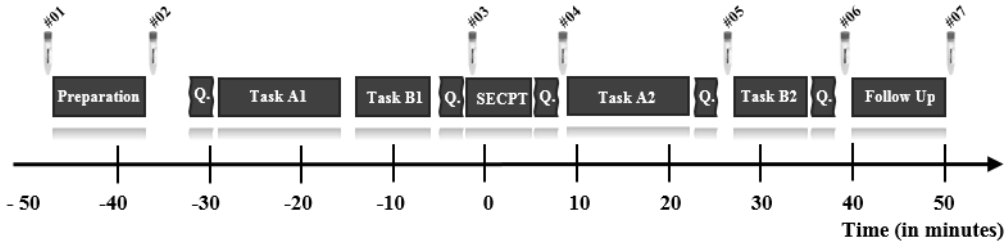

Figure 3.1: Experimental procedure for the task order TG|TG (task switching, go-nogo, task switching, go-nogo). Tasks were practiced once before the first execution of each task. Times of practicing the tasks are not depicted in this overview. The subjective stress rating reported in this study, was given immediately after the SECPT. Q.: Questionnaires; Task A: task switching; Task B: go-nogo paradigm.

3.2.3 Cognitive Tasks

Cognitive tasks were presented on a 20" LCD monitor (Eizo FlexScan, S2031W) with a 60 Hz refresh rate using E-Prime presentation software (Eprime 2.0, Psychological Software Tools, Pittsburgh, PA). Participants had a distance of 100 cm to the computer screen.

3.2.4 Task Switching Paradigm

In this study, a task-cueing paradigm was used to investigate cognitive flexibility. That is, participants have to switch between two categorization tasks. Which task is required is indicated by one of two cues. This paradigm is often used and well validated (Kiesel et al., 2010; Monsell, 2003).

One trial consisted of a sequence of three slides (Figure 3.2). First, the cue was presented for 200 ms (20 % of trials) or 1200 ms (80 % of trials). The second slide consisted of the target letter (A, E, I, U, a, e, i, u, G, B, T, D, g, b, t, d). It was presented until the participant responded. The third slide appeared simultaneously as they responded, showing a fixation cross for a variable time interval (3600 ms – cue slide presentation time in ms minus reaction time in ms). The duration of one trial was always 3600 ms.

A total of 208 trials were presented before and another 208 trials were presented after the stress induction procedure. Each block of 208 trials took approximately 12.5 minutes, resulting in 416 trials and 25 minutes of total processing time for the task switching paradigm. Subjects could not decrease the duration by answering especially fast.

In each trial subjects had to classify the target according to the cue. A circle indicated to classify whether the target is an upper- or lowercase letter. A triangle indicated to classify whether the target is a vowel or consonant. The target letter was never the same in consecutive trials. There were no more than four repetitions of the same cue in a row. Fifty percent of trials were repeat trials and 50 % of trials were switch trials. This was balanced across cue-target intervals (200 vs. 1200 ms). Subjects could not predict 'repeat' and 'switch' trials. The cue-target interval of 200 ms was realised for exploratory reasons beyond the scope of this investigation. Therefore only trials with a cue-target interval of 1200 ms were further analysed resulting in a total amount of 333 trials for each participant. Participants responded with a key press on the left or right arrow key. Mapping of response keys to vowel/consonant and lower-/uppercase was counterbalanced across subjects, but kept constant within subjects. Participants were meant to respond as fast and accurately as possible. They always responded with the index finger of the right hand. Subjects were meant to rest their index finger in between the response keys, i. e. at the down arrow, to guarantee unbiased reaction times in each trial.

Slides were always black with white stimuli. Cues were either a filled triangle or a filled circle. The triangle had a total horizontal visual angle of 1.146° and a vertical deviation of 0.974°. The circle had a total horizontal and vertical visual angle of 0.917°. Target letters were presented in typeface Courier New and font size 36. This is equivalent to an approximate horizontal and vertical visual angle of 0.458°. All stimuli were centred horizontally and vertically.

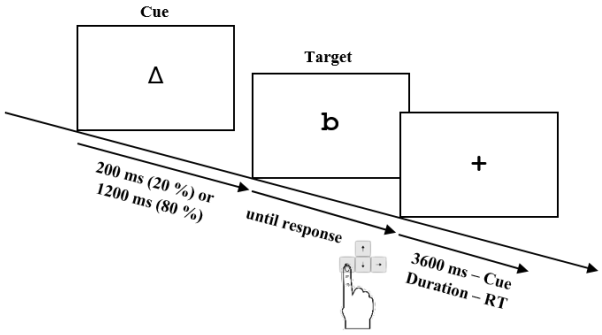

Figure 3.2: One trial of the task switching paradigm. Only trials with a 1200 ms presentation duration for the cue (cue duration) were analysed here. Participants responded by either pressing the left arrow or right arrow key.

3.2.5 Go-Nogo Paradigm

A go-nogo task was used to investigate cognitive inhibition. Participants were shown two stimuli: To one they had to respond as fast as possible and to the other had to withhold a response. This is an often used and well validated inhibition paradigm (Criaud & Boulinguez, 2013).

One trial consisted of three slides (Figure 3.3). The first slide contained the target and is presented for 400 ms or until the participant responded. If participants responded slower than 400 ms an empty slide was shown until the participant responded in the case of a go task or for 1100 ms in the case of a nogo task. The last slide contained a fixation cross and was presented for 2500 ms minus reaction time in the case of a go task and for 1000 ms in the case of a nogo task.

A total of 180 trials were presented before and another 180 trials were presented after the stress induction procedure. Each block of 180 trials took approximately 7.5 minutes, resulting in 360 trials and 15 minutes of total processing time for the go-nogo paradigm. Subjects could not decrease the duration by answering especially fast.

In each trial, participants had to respond as fast as possible to go trials by pressing the down arrow key on the keyboard, while withholding a reaction to nogo trials. There were no more than three repetitions of go or nogo trials in a row. Fifty percent of trials were go trials and 50 % of trials were nogo trials. Mapping of go and nogo letter to X and Y were counterbalanced across subjects but held constant within subjects. Participants were meant to respond as fast and accurately as possible. They always responded with the index finger of the right hand.

Slides were always black with white stimuli. Target letters X and Y had a horizontal and vertical visual angle of 0.458°. Target letters were presented in typeface Courier New and font size 36. All stimuli were centred horizontally and vertically.

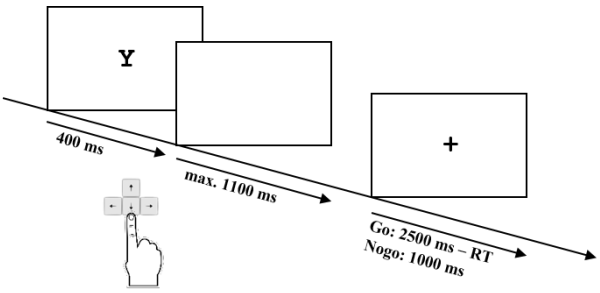

Figure 3.3: One trial of the go-nogo paradigm. Participants responded as fast as possible in go-trials by pressing the downward arrow key or withheld a response in the case of a nogo-trial.

3.2.6 Socially Evaluated Cold Pressor Test

Aside from minor changes, the socially evaluated cold pressor test was conducted in accordance to the protocol of Schwabe et al. (2008). An investigator of female sex and unfamiliar to the participant entered the recording cabin, wearing a white lab coat, greeting the subject briefly. The investigator adjusted the camera and started the video recordings, requesting the subject to look into the camera at all times during hand immersion in order to be able to analyse facial expression and gesture. Participants

were already informed about the videotaping and analysis of their gesture and facial expressions in the screening interview. Written informed consent was obtained, stating that recordings could be presented to a scientific community.

The water container was brought in and placed on the left hand side of the subject. Subjects were informed about the duration of hand immersion (three minutes) at the initial screening session. Immediately before hand immersion, subjects were informed that the investigator would tell them when to remove the hand from the water. Participants were then asked to immerse their hand up to and including the wrist into the water container and hold their hand completely still. The investigator measured the time, watched the participants all the time throughout the test, and took notes about their behaviour in addition to the videotaping. She corrected behaviour of the participants that was not desired, like looking away from the camera, moving the hand, or moving excessively with short standardized sentences; e. g. "Please look into the camera at all times." Behaviour of the investigator was neutral and reserved. After three minutes participants were instructed to take their hand out of the water. If they had removed the hand beforehand they were informed that the hand should still be immersed and asked to immerse the hand again. Regardless of whether participants re-immersed their hand or not, observation and videotaping was always executed for three minutes. The investigator then turned off the camera, removed the water container from the recording cabin and left the subject alone in the recording cabin. Participants completed the subjective stress rating and then proceeded with the second part of the experiment.

Procedures for the socially evaluated cold pressor test and the warm water control procedure were identical. The only difference was the water temperature and appearance of the water, being between 1 – 4 °C for the cold pressor test with some ice cubes in the water and between 36 – 38 °C in the warm water condition. Because it is known that the socially evaluated cold pressor test does not lead to cortisol elevation in all participants (Schwabe et al., 2008), two thirds of the subjects were exposed to the cold water, while one third was exposed to the warm water. That way three equally numbered groups could be formed post hoc via median split of the cold water group: the warm water control group, the stress group with no or a low cortisol response (low responders), and the stress group with a substantial cortisol increase (high responders). Time of investigation and order of tasks was counterbalanced across cold water and warm water conditions, controlling for potential influences of this variables. In the following text the abbreviation SECPT is used generally for both warm and cold water condition if statements over both groups are made, e. g. "After the SECPT, participants provided the fourth saliva sample".

3.2.7 Endocrine Stress Response

In total 7 saliva samples were collected and subsequently analysed: approximately -48 min (#01), -37 min (#02), -2 min (#03), +8 min (#04), +21/26 min (#05), +39 min (#06), and +50 min (#07) in reference to the start of the SECPT. Depending on task order participants provided the fifth saliva

sample 21 minutes after SECPT (order TG**GT**/GT**GT**) or 26 minutes after SECPT (order TG**TG**/GT**TG**). This was due to different task lengths: duration of task switching was approximately 12.5 minutes and duration of go-nogo was approximately 7.5 minutes.

Samples acquired before and after the first block of tasks served as baseline measurement of cortisol activity (samples #02, #03). To determine stress reactivity, the mean of baseline cortisol levels were subtracted from the mean of cortisol levels between 20 and 40 minutes after SECPT onset (samples #05, #06), as this is period when cortisol level are generally highest (Dickerson & Kemeny, 2004).

Saliva samples were obtained using Salivette® collection devices (Sarstedt, Nürnbrecht, Germany). Sampling instructions were given via computer screen and adherence was monitored. Samples were frozen immediately after the experiment at -20 °C for later biochemical analyses. Salivary cortisol was analysed with a time-resolved immunoassay with fluorescence detection as described in detail in Dressendörfer, Kirschbaum, Rohde, Stahl, and Strasburger (1992). Intra- and interassay variability was less than 10 % and 12 % respectively.

3.2.8 Subjective Stress Ratings

Participants rated their perception of the SECPT on several items, from which six were analysed here. Participants responded on a scale from strongly disagree (1) to strongly agree (6) to items about how stressful the SECPT was, how painful the SECPT was, how tense they felt during the SECPT, and how they coped with the situation (three items: encouraging themselves, pulling themselves together, distancing from the pain).

3.2.9 EEG Recording and Quantification

EEG was recorded with an Easy-Cap electrode system (EasyCap GmbH, Herrsching, Germany) from 28 sites positioned according to the 10-10 electrode reference system (Chatrian, Lettich, & Nelson, 1985): Fp1, Fpz, Fp2, F7, F3, Fz, F4, F8, FC3, FC4, T7, C3, Cz, C4, T8, CP3, CPz, CP4, P7, P3, Pz, P4, P8, O1, Oz, O2, A1, and A2. EOG was recorded from four positions: centred above and below the left eye (m. orbicularis oculi, pars palpebralis and m. orbicularis oculi, pars orbitalis respectively) as well as from each temple (close to the lateral canthus). All sites of EEG and EOG were online referenced to FCz. AFz served as ground. Silver-silver chloride (*Ag/AgCl*) were utilized for EEG and EOG (Falk Minow Services, Munich, Germany).

EEG and EOG was amplified by a BrainAmp amplifier with an input impedance of 10 MΩ (Brain Products GmbH, Munich Germany). Recordings, in AC mode, were sampled at 1000 Hz. Impedances of EEG electrodes were kept below 15 kΩ. The pass-band was set to .016 to 499 Hz (-12 dB/octave roll-off). Recorded data was stored to hard disk for later processing using MATLAB® 2014b (MathWorks, Natick, USA), including its Statistics and Signal Processing toolbox, and EEGLAB v13.4.4b (Delorme & Makeig, 2004).

One of the biggest challenges in analysing macroscopic oscillations is that, due to volume conduction, one can only record a mixture of all neural activity at the scalp level. In other words, data recorded at one sensor includes activity from different neuronal sources potentially scattered across the entire brain. One has to disentangle the distinct neuronal sources that contribute to the mixture by post hoc applied algorithms. In order to extract unique neuronal processes, the ICA, a blind source separation algorithm, was applied to raw EEG data. Debener, Makeig, Delorme, and Engel (2005) very concisely described why there is good reason to apply ICA to EEG data:

> ICA exploits temporal independence to perform blind source separation … [Bell & Sejnowski, 1995; Makeig, Bell, Jung, & Sejnowski, 1996; Makeig, Jung, Bell, Ghahremani, & Sejnowski, 1997]. It finds a square unmixing matrix that maximizes the joint entropy of zero-mean input vectors, and can decompose linearly mixed processes having non-gaussian distributions. The fitness of this approach for the analysis of EEG data has been demonstrated repeatedly (e.g., Refs. … [Delorme & Makeig, 2003; Jung et al., 2000; Jung et al., 2001; Makeig et al., 1999; Makeig et al., 2002]). ICA decomposition of EEG data provides spatially fixed and temporally independent components without a priori assumptions on the temporal dynamics or spatial structure of the underlying processes. (Debener et al., 2005, p. 311)

That is, by applying ICA, raw EEG data, where each channel records a mixture of various brain sources (due to volume conduction), is separated into independent components. ICA achieves a separation of physiologically reasonable sources even though not knowing anything about physiology. Further background knowledge about ICA and its application to EEG data can be gained from Onton, Westerfield, Townsend, and Makeig (2006) and Debener, Thorne, Schneider, and Viola (2010). A more technical report on ICA and its mathematical principles can be found in Hyvärinen, Karhunen, and Oja (2001).

Preprocessing and Independent Component Analysis.

Stationarity of raw data is a prerequisite for ICA, but low-frequency drifts can be spatiotemporally non-stationary. Therefore raw data was **high-pass filtered at 1 Hz** before running the ICA algorithm (Miyakoshi, 2016; Winkler, Debener, Muller, & Tangermann, 2015) using a zero-phase Hamming-windowed sinc FIR filter implemented in EEGLAB (pop_eegfiltnew.m; Widmann et al., 2015). **No resampling** was carried out. A high sampling rate can be beneficial when analysing phase-amplitude coupling at frequencies close to the Nyquist frequency (cf. chapter 2). Then **data was segmented into experimental parts**. Block 1 (before SECPT) and 2 (after SECPT) of each paradigm (task switching, go-nogo) were segmented and concatenated. From now on, data of both paradigms was analysed separately but analogously. This was done to account for possibly unique processes, reflected in unique ICs within each paradigm. Channels were checked for **flatline periods exceeding 5 seconds** via artefact subspace reconstruction (ASR) method (Kothe, 2013). Flatlines never occurred, except in one channel of one subject for the task switching paradigm; this channel was discarded. EEG and EOG channels were **re-referenced offline to average reference** and online-reference FCz was restored. Even though preconditions for average reference, namely high density equidistant electrode arrangement and

electrodes on upper and lower part of the head were violated, average-reference seemed to be the better option compared to common reference (e. g. linked-mastoids). Criterion for decision of performance was non-activeness of the reference. Cz was discarded after re-referencing to match amount of channels and rank of data for ICA. Cz was chosen because its activity is best captured by neighbouring electrodes, and presumably least information will be lost by discarding this electrode. Data was temporally segmented into one-second epochs and **artefactual epochs were rejected automatically** (Delorme, Sejnowski, & Makeig, 2007). Epochs were rejected if activations exceeded amplitude thresholds of -500 and 500 µV (EEGLAB function pop_eegthresh). In order to not capture eye blinks – which will be separated by the ICA decomposition – this criterion was not applied to channels Fp1, Fpz, and Fp2. Furthermore a probability distribution of data points for each epoch was calculated for single electrodes and for the entirety of electrodes. Supposing artefacts are improbable, improbable epochs were rejected (EEGLAB function pop_jointprob). Improbability was determined by means of standard deviations of the probability distribution. The threshold was 5 standard deviations for single channels and 2 standard deviations for all channels. Criteria were chosen to aim for a rejection rate of roughly 10 % (Delorme et al., 2007). Rejection of a trial always led to rejection of this trial in all channels. This automatic procedure led to an average of 7.66 ± .87 %[18] rejected epochs for task switching and an average of 7.92 ± .84 % for the go-nogo task. Remaining segments were concatenated in order to **run AMICA**, the best performing ICA algorithm available (Delorme, Palmer, Onton, Oostenveld, & Makeig, 2012). AMICA itself is applying another artefact rejection procedure to the data before starting the decomposition. The ICA algorithm returns as many independent components as included sensors (square unmixing matrix).

Equivalent Dipole Fitting.

After running ICA raw data was reloaded, this time *not* filtered, again not resampled, experimental parts were extracted, and data re-referenced as described above. Finally ICA weights were applied to the so processed data and all following processing was done on IC components (source level) instead of electrodes (sensor level). **Equivalent dipole source localization** of independent components was done by using Dipfit2, an EEGLAB plug-in, contributed by R. Oostenveld (Donders Institute for Brain, Cognition and Behaviour, Netherlands). A standardized boundary element head model (Oostendorp & van Oosterom, 1989) was used. EOG channels were excluded from the fitting procedure, because their positions were not standardized. Source-level data was saved as continuous data and then temporarily segmented into epochs of trial length for **automatic artefact rejection on component data**. For task switching, epochs were segmented -200 ms to +3400 ms with reference to cue onset. For go-nogo, epochs were segmented -200 ms to +2300 ms with reference to target onset. Artefactual epochs were rejected according to criteria described above (threshold, probability). Trial indices of rejected trials were saved for later rejection of these trials. Component artefact rejection led to an average of 11.05 ± .48 % rejected epochs for task switching and an average of 10.67 ± .78 % for the go-nogo task.

[18] Statistical data is reported as mean ± standard error (S. E.) except otherwise specified.

Clustering and Reclustering components.

In order to identify ICs that represent functionally equivalent sources across subjects, all available ICs of reasonable quality were clustered by a k-means algorithm implemented in EEGLAB (Onton & Makeig, 2014). Reasonable IC quality is defined by a residual variance[19] of less than 15 % and a dipole location within the brain. The validity and reliability of the residual variance criteria was confirmed by Artoni, Menicucci, Delorme, Makeig, and Micera (2014). The within brain dipole localization criteria guaranteed the exclusion of all ICs which dipole was localized outside of the brain and therefore presumably represents a non-physiological source.

For the task switching paradigm, from a total of 1247 ICs, 682 ICs of reasonable quality remained (mean residual variance: 7.02 %; range: 0.33 - 14.94 %). Each subject contributed on average 17 ICs (range: 12 - 23). For the go-nogo task, from a total of 1248 ICs, 674 ICs of reasonable quality remained (mean residual variance: 7.4 %; range: 0.76 - 14.97 %). Each subject contributed on average 17 ICs (range: 10 - 22). These statistics relate to all 39 subjects whose IC's were initially clustered.

Criteria for clustering were dipole position and frequency spectra (see Appendix B for a diagram of the k-means clustering process). Although k-means clustering is not an ideal approach (Bigdely-Shamlo, Mullen, Kreutz-Delgado, & Makeig, 2013; Spadone, Pasquale, Mantini, & Della Penna, 2012), it is widely used and gives back reasonable results (Onton et al., 2006; Onton & Makeig, 2006). The amount of clusters is one critical parameter regarding the cluster solution. There is no statistical way to derive an optimal number of clusters (Bigdely-Shamlo et al., 2013). Therefore a number was chosen that made it likely that each cluster included on average at least one IC per subject.

Visual inspection of the automatic cluster solution revealed several possibilities of improvement and furthermore reclustering was necessary because exactly one IC of each subject in each cluster was required for calculating phase-amplitude coupling. Reclustering criteria were dipole location, frequency spectra, topography, and residual variance of the ICs. In the majority of the cases, these criteria unanimously lead to one IC, underlining the practicality of the criteria. Furthermore, in the majority of the cases these criteria pointed to the originally clustered IC. In the task switching paradigm on average 16 % of ICs were manually selected, ranging from 3 % to 29 % for all relevant clusters. In the go-nogo paradigm on average 17 % of ICs were manually selected, ranging from 10 % to 30 % for the all relevant clusters. The majority of manually picked ICs were from one or two other clusters, meaning that according to k-means criteria these ICs were very similar to each other. Clear rules, which were applied here (and can be found in Appendix C), guarantee a minimum of objectivity for the reclustering process. To further increase objectivity reclustering results should be validated via calculation of interrater reliability.

[19] Residual variance (R. V.) designates the amount of deviation of the actual IC scalp map from the scalp map that would be produced by the estimated equivalent dipole.

Six participants were excluded after the reclustering process because for these participants a suitable IC had not been found for each of the relevant clusters (cf. section 3.2.1). The six relevant clusters are localized left, midline, and right frontal as well as left, midline and right parietal (Figure 3.4). These regions of interest were chosen because they are reliably associated with executive functioning (see section 1.2)

Filtering data and applying Hilbert transform.

Subsequently, continuous data for each chosen IC from all subjects and clusters was filtered in the relevant frequency bands using a zero-phase Hamming-windowed sinc FIR filter implemented in EEGLAB (pop_eegfiltnew.m; Widmann et al., 2015). Data was filtered from 3 – 19 Hz in 2 Hz steps with a fixed bandwidth of 2 Hz (2 – 4 Hz, 4 – 6 Hz, 6 – 8 Hz, etc.) for extracting instantaneous phases (phase time series) and from 15 – 100 Hz in 5 Hz steps with a variable bandwidth (cf. Berman et al., 2012; also compare section 2.2.5) for extracting the amplitude envelope (amplitude time series). Phase-amplitude coupling investigated here, is defined as elevated amplitude of a higher frequency at a specific phase of a lower frequency. Coupling was only calculated for frequency pairs where the lower bound of the amplitude-providing frequency band is absolutely higher than the upper bound of the phase-providing frequencies, avoiding overlapping frequency bands (Berman et al., 2015). Hilbert transform was applied to filtered data and phase or amplitude information was extracted from the continuous complex-valued analytical signal in exactly the same way as described in chapter 2. Subsequently phase and amplitude time series were segmented: For task switching, epochs were segmented -200 ms to +3400 ms with reference to cue onset. For go-nogo, epochs were segmented -200 ms to +2300 ms with reference to target onset. Artefactual trials, according to the automatic cleaning procedure described above, were discarded.

Exploratory analysis of phase-amplitude coupling.

Overall nine networks were screened for phase-amplitude cross-frequency coupling by calculating the modulation index (Tort et al., 2008) as described in chapter 2. Networks were left, midline, and right fronto-frontal network (coupling within the same source), left, midline, and right fronto-parietal network (phase at the frontal source drives amplitude at the parietal source), and left, midline, and right parieto-frontal network (phase at the parietal source drives amplitude at the frontal source; Figure 3.4). To identify networks displaying significant coupling permutation testing with 200 iterations was applied. Two hundred permutations mark the lower bound of iterations used by most studies (Appendix A). The amount was chosen in order to keep calculation time in reasonable terms. Networks that showed significant coupling averaged over the whole sample and all conditions were further analysed. Phase-amplitude coupling in these networks was recalculated with 1000 iterations. One thousand permutations mark the upper bound of iterations used by most studies (Appendix A). Significance was derived via permutation testing (cf. section 2.2.2). According to findings from chapter

2 a z-value larger than 1.99 is considered significant ($p < .05$). Because in the screening analysis it became evident that significant coupling emerged at the borders of the analysed frequency range, the phase frequency range was broadened from 3 Hz – 19 Hz to 3 Hz – 29 Hz in the follow up calculation. It was not broadened at the amplitude frequency range because this would have massively exceeded the available calculation time and memory space. Furthermore it can be argued that frequencies above 100 Hz are not ideally recorded via scalp EEG.

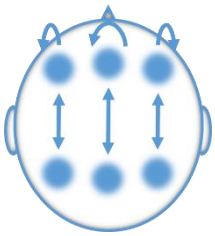

Figure 3.4: Graphical depiction of all nine screened networks: left, midline, and right fronto-frontal network (coupling within the same source); left, midline, and right fronto-parietal network (phase at the frontal source drives amplitude at the parietal source); left, midline, and right parieto-frontal network (phase at the parietal source drives amplitude at the frontal source).

3.2.10 Statistical Analyses

Statistical analyses were conducted according to descriptions given in section 2.2.6. Literature reveals small to medium empirical effects (see section 3.1.1 and 3.1.2). Hence, effect sizes from $\omega^2 > .03$ were considered meaningful and are reported. The basic hypotheses assume a block by responder group interaction in the case of behavioural data and a frequency pair by block by responder group interaction in the case of electrophysiological data. Given the sample size of 33 subjects and a significance level of $p = .05$, the two- and three-way interactions can detect a relative small effect of $\Omega^2 \geq .03$ with a probability $1\text{-}\beta > .95$. This calculations assume a plausible population correlation of $\rho = .90$ for reaction time measures and $\rho = .30$ for electrophysiological data (supported by the empirical data). Power even increases for higher order interactions. Because the population correlation for errors was lower than for reaction times ($\rho = .62$), only effects of $\Omega^2 \geq .05$ could be found with a probability of $1\text{-}\beta > .85$. All power calculations were done by hand according to Rasch et al. (2006) using tables provided by Hager (1987). Starting time of the experimental session and task order were balanced over experimental conditions (warm water, cold water). These factors were therefore controlled for and not included in statistical analyses. Data is always presented as mean ± standard error (S. E.) except otherwise specified.

Manipulation Check Cortisol Profile. The success of the experimental manipulation, i. e. change of cortisol levels during the experiment was checked via a 7 x 3 ANOVA with the within-subjects factor measurement time (-48, -37, -2, 8, 21/26, 39, 50 minutes from SECPT onset) and between-subjects factor responder group (warm water control, low responders, high responder).

Subjective Stress Rating. Subjective stress was analysed with a 4 x 3 ANOVA with the within-subjects factor question type (stress, pain, tension, coping effort) and between-subjects factor responder

group (warm water control, low responders, high responder). The dependent variable was participants' rating ranging from 1 (no stress, no pain etc.) to 6 (strong pain, stress etc.).

Task Switching Paradigm. Behavioural results (dependent variables: reaction time, error rate) in the task switching paradigm were analysed by a 2 x 2 x 3 ANOVA with the within-subjects factors block (block 1 – before SECPT, block 2 – after SECPT) and trial type (switch, repeat) as well as the between-subjects factor responder group (warm water control, low responders, high responder). For reaction time analysis only trials with correct responses were included. Furthermore reaction time distributions for each subject were calculated. Reaction times exceeding the third quartile of the corresponding distribution (Tukey, 1977) or were faster than 200 ms were deemed outliers and removed for statistical analyses. Switch costs (reaction time in switch trials minus reaction time in repeat trials) in correct trials were analysed by a 2 x 3 ANOVA with the within-subjects factors block and with the between-subjects factor responder group.

Go-Nogo Task. Behavioural results (dependent variable: reaction time) in the go-nogo task were analysed by a 2 x 3 ANOVA with the within-subjects factor block (block 1 – before SECPT, block 2 – after SECPT) and between-subjects factor responder group (warm water control, low responders, high responder). Only trials with correct responses were included. Because in nogo trials there are no responses, only go trials could be included in the reaction time analysis. Reaction time distributions for each subject were calculated. Reaction times exceeding the third quartile of the corresponding distribution (Tukey, 1977) or were faster than 100 ms were deemed outliers and removed for statistical analyses. Participants made on average 1.99 % errors. Error rates ranged from .28 to 6.67 %. This error rate was considered too low to analyse.

Exploratory phase-amplitude coupling. After inspection of the comodulograms it was decided to split the comodulogram into five distinct frequency pairs, namely delta-beta coupling, delta-gamma coupling, theta-beta coupling, theta-gamma coupling, and beta-gamma coupling (Figure 3.5). The chosen division is in accordance with the natural logarithmic relationship between brain oscillations (Penttonen & Buzsáki, 2003) and will be further justified by the found coupling pattern (cf. Figure 3.11 and Figure 3.15). Coupling values within these frequency pairs were averaged and subsequently submitted to a 2 x 5 x 2 x 2 x 3 ANOVA with the repeated measurement factors hemisphere (left, right)[20], frequency pair (delta-beta, delta-gamma, theta-beta, theta-gamma, beta-gamma), block (before SECPT, after SECPT), and trial type (switch vs. repeat in the case of the task switching paradigm; go vs. nogo in the case of the go-nogo paradigm) as well as the between-subjects factor responder group (warm water controls, low responders, high responders).

[20] In anticipation of the results: because only coupling within frontal sources became significant, the factor caudality can be omitted in these analyses.

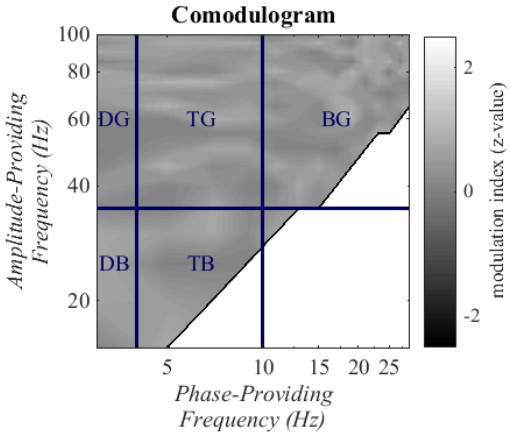

Figure 3.5: A simulated comodulogram and its division into five distinct frequency pairs: delta-beta (DB), delta-gamma (DG), theta-beta (TB), theta-gamma (TG), beta-gamma (BG). Frequency pairs within the white triangle at the right bottom corner were not calculated because they represent frequency pairs where frequency bands overlap (Berman et al., 2012; Berman et al., 2015). X- and y-axis display the centre frequencies of the corresponding frequency bands. As described before, bandwidth of amplitude-providing frequencies depend on the corresponding phase-providing frequency.

Correlation between modulation indices and reaction times. Reaction times in the task switching paradigm were correlated with the corresponding modulation indices separately for hemispheres, frequency pair, block, and trial type (Spearman's rho). Correlations between modulation indices and error rates were not calculated, because phase-amplitude coupling was only calculated for correct trials. Correlations between reaction times and modulation indices in the go-nogo paradigm could only be calculated for go trials, because there are no responses in nogo trials. Correlations were calculated across the whole sample.

3.3 Results

3.3.1 Manipulation Check: Endocrine Stress Response

Participants completing the SECPT were split into low and high responders according to a median split of their cortisol reactivity as described in section 3.2.7 (median: -0.17 nmol/l). Low responders (n = 12) had a mean increase of -2.13 ± .62 nmol/l. High responders (n = 11) had a mean increase of 3.99 ± 1.34 nmol/l. The warm water control group (n = 10) had a mean increase of -1.18 ± .39 nmol/l. The median split is justified, because all low responders and no high responder had absolute cortisol decreases in response to the SECPT. Furthermore eight of eleven high responders had a biologically significant cortisol increase (Miller, Plessow, Kirschbaum, & Stalder, 2013).

Cortisol level showed a significant interaction of time of measurement and responder group ($F_{(12,180)} = 6.06$, $p < .01$, $\omega^2 = .21$, $\text{Dunn}_{crit} = 3.20$). Post hoc tests revealed that cortisol levels of the warm water control group and low responder group did not change significantly over the course of the experiment. Only high responder's cortisol levels increased significantly after the stress procedure (from

+ 8 minutes onward) until they peaked 21 to 26 minutes after the stress procedure (Figure 3.6). Cortisol level of the warm water control group and low responders differed significantly between 20 and 40 minutes after SECPT onset. High responders thereby constantly having the highest and the warm water control group constantly having the lowest levels. Low responders and warm water control group did not differ significantly in their cortisol level. Additionally groups did not differ significantly in their cortisol levels before the onset of the stress procedure and at the last measurement 50 minutes after the stress procedure. Cortisol data did not depend on task order (TG|TG, TG|GT, GT|GT, GT|TG; data not shown).

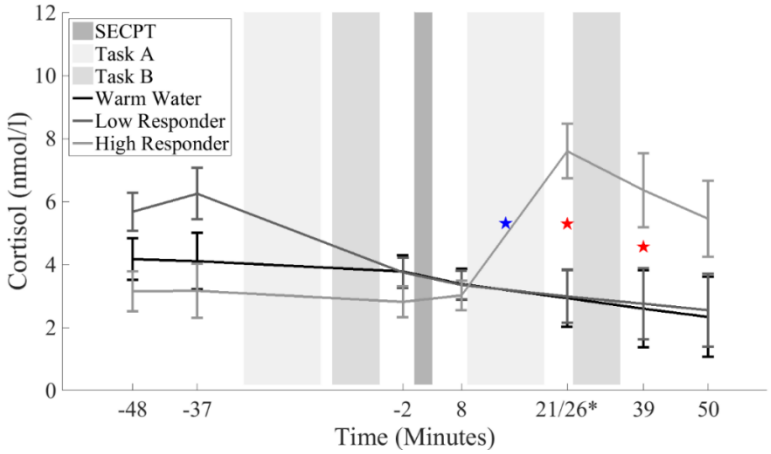

Figure 3.6: Cortisol profile (mean ± S. E.) for each experimental group over the course of the experiment. One of four possible task orders is depicted (task switching, go-nogo, task switching, go-nogo). Red stars mark significant differences between high responders and both low responders as well as warm water controls. The blue star marks the only significant change in cortisol levels within a group.
* Depending on task order participants provided the fifth saliva sample 21 minutes after SECPT (order TG|**GT**, GT|**GT**) or 26 minutes after SECPT (order TG|**TG**, GT|**TG**). This is due to different task length.

3.3.2 Manipulation Check: Subjective Stress Ratings

Amongst others participants rated how stressful and painful they perceived the SECPT, rated their tension and effort to cope with the situation. There were significant main effects question type ($F_{(3,90)} = 10.02$, $p < .01$, $\omega^2 = .17$, $\text{Dunn}_{\text{crit}} = .54$) and responder group ($F_{(2,30)} = 16.99$, $p < .01$, $\omega^2 = .49$, $\text{Dunn}_{\text{crit}} = 1.09$), which were further qualified by a question type by responder group interaction ($F_{(6,90)} = 3.04$, $p < .01$, $\omega^2 = .08$, $\text{Dunn}_{\text{Krit}} = 1.14$).

Groups differed significantly from each other in each rating (Figure 3.7), except for tension were only the warm water control group differed from high responders. Differences were larger than one point on the rating scale in all differences. The warm water control group rated stressfulness, painfulness, tension and coping effort constantly lowest, low responders had constantly medium ratings, while high responders rated stressfulness, painfulness, tension and coping effort constantly highest. The warm water control group rated tension and coping effort significantly higher than pain.

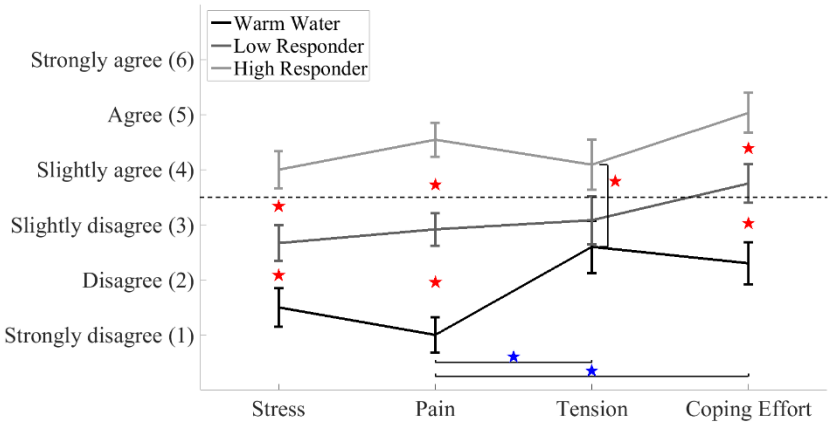

Figure 3.7: Mean subjective stress ratings (mean ± S. E.) of each experimental group in perceived stress, pain, tension and coping effort. Red stars mark significant differences between groups (upper line of red stars: difference between low and high responders; lower line of red stars: difference between warm water controls and low responders; for tension only ratings between warm water controls and high responders differ significantly). Blue stars mark significant differences within the warm water control group.

3.3.3 Task Switching Paradigm

Behavioural Data

Task Switching Paradigm – Reaction Times. Replicating typical task switching results, participants responded about 29 ms faster to repeat (767.38 ± 26.55 ms) than to switch (795.96 ± 29.56 ms) trials ($F_{(1,30)} = 16.85$, $p < .01$, $\omega^2 = .19$). Subjects responded significantly faster in the second (760.71 ± 28.58 ms) compared to the first block (802.63 ± 29.22 ms), suggesting a mere practice effect ($F_{(1,30)} = 7.59$, $p = .01$, $\omega^2 = .09$). This effect was further qualified by responder group ($F_{(2,30)} = 3.98$, $p = .03$, $\omega^2 = .08$, $\text{Dunn}_{crit} = 78.60$), showing that only low responders had significantly decreased reaction times in the second compared to the first block, being about 90 ms faster (Figure 3.8). Low and high responders responded faster than the warm water control group in the second block. Low and high responders did not differ from each other. Groups did not differ in reaction times in the first block.

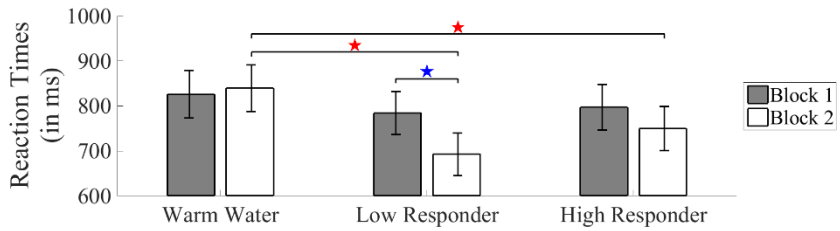

Figure 3.8: Reaction times (mean ± S. E.) averged over switch and repeat trials for each block (block 1: before SECPT, block 2: after SECPT) and experimental group. Red stars mark signifcance differences between experimental groups. The blue star marks the significance difference between reaction times of both blocks in low responders.

Task Switching Paradigm – Switch Costs. Switch costs significantly decreased from block 1 (40.39 ± 9.33 ms) to block 2 (16.76 ± 8.05 ms; $F_{(1,30)} = 5.09$, $p = .032$, $\omega^2 = .06$). Even though the block

by responder group interaction did not become significant ($p > .05$), switch costs descriptively differed between blocks and responder groups (Figure 3.9). Because repeated measurements did not correlate strongly for switch costs ($\rho \sim .20$), this analysis had too little power to find a small theoretical effect of $\Omega^2 = .03$ ($1 - \beta = .24$). Only large theoretical effects of $\Omega^2 = .14$ (according to Cohen, 1988) could have been found with sufficient power of $1 - \beta = .88$. Switch costs can either change due to reaction time changes in switch trials or due to reaction time changes in repeat trials. Here it became evident that low responders became generally faster from block 1 to block 2, without displaying changes in switch costs (Table 3.1). High responders descriptively decreased switch costs by becoming especially faster in switch trials (Table 3.1). Warm water controls on the contrary, reduced their switch costs by becoming descriptively slower in repeat trials (Table 3.1).

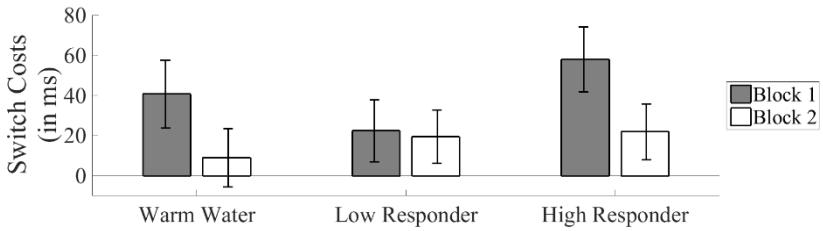

Figure 3.9: Switch costs (mean ± S. E.) for each block (block 1: before SECPT, block 2: after SECPT) and for each experimental group.

Table 3.1: Mean reaction times (S. E.) in ms for the task switching paradigm separately for each block, trial type, and responder group. Reaction times differences are not significant.

		Warm Water	Low responders	High Responder
Block 1	Switch	846.52 (57.55)	795.56 (52.53)	826.41 (54.87)
	Repeat	805.79 (49.34)	773.11 (45.04)	768.42 (47.04)
Block 2	Switch	844.09 (53.41)	702.28 (48.76)	760.91 (50.93)
	Repeat	835.12 (51.15)	682.82 (46.69)	739.05 (48.77)

Task Switching Paradigm – Errors. Participants made on average 5.6 % errors. Error rates ranged from .6 to 15.6 %. Participants made more errors in switch (6.4 ± 0.8 %) than in repeat (4.8 ± 0.7 %) trials ($F_{(1,30)} = 11.29$, $p = .002$, $\omega^2 = .13$). Participants made more errors in block 1 (6.6 ± 1.0 %) than in block 2 (4.5 ± 0.6 %; $F_{(1,30)} = 9.40$, $p = .005$, $\omega^2 = .11$). These effects were not moderated by responder group. They reflect typical task switching results.

Electrophysiological Data

Task Switching Paradigm – Clustering Results. Average scalp maps of all ICs of each cluster and their corresponding residual variance are shown in Figure 3.10. Dipole locations for all ICs in these clusters are depicted in Appendix D.

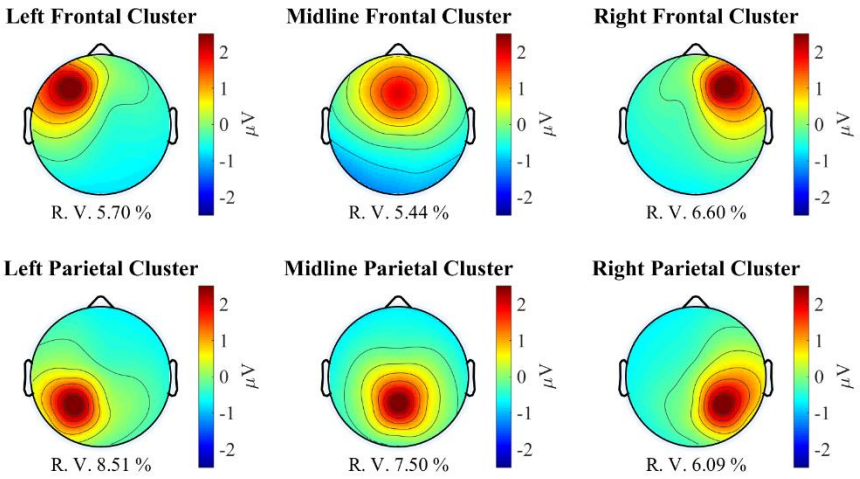

Figure 3.10: Final clusters of independent components found for the task switching paradigm for all six regions of interest. For ICs in these clusters phase-amplitude coupling was calculated either within the frontal clusters or between frontal and parietal clusters.

Task Switching Paradigm – Initial Screening for Phase-Amplitude Coupling. Only coupling within the left and right fronto-frontal network (i. e. coupling within one source) was found to be significant over the whole sample and all conditions (Figure 3.11). The screening indicated that gamma amplitude was nested within the beta cycle. Also delta-beta coupling within these two fronto-frontal networks showed the tendency for significance. Based on these screening analyses, all further analyses were restricted to the left and right fronto-frontal networks.

Task Switching Paradigm – Phase-Amplitude Coupling in Fronto-Frontal Networks. Coupling between beta and gamma (27.87 ± 7.69) was significant and significantly different from all other frequency pairs (delta-beta [1.77 ± .34], delta-gamma [1.74 ± .95], theta-beta [.97 ± .20], theta-gamma [1.47 ± .59]; $F_{(4,120)} = 11.98$, $p = .001$, $\omega^2 = .21$, $\text{Dunn}_{crit} = 13.75$). Neither of the other frequency pairs exhibited significant coupling nor differed in their coupling strength (Figure 3.12).

The preferred phase of beta-gamma coupling is 40° to 80°, representing the range of decreasing phases of the low-frequency oscillation; amplitudes are lowest at -140° to -100°, representing the range of increasing phases of the low-frequency oscillation (Figure 3.13).

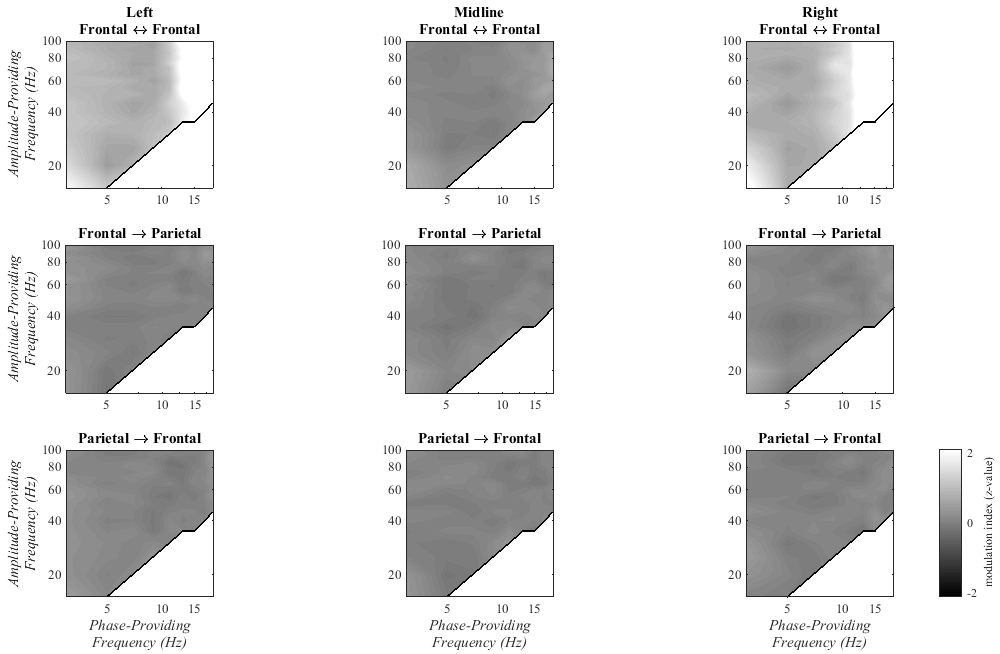

Figure 3.11: Screening of nine networks for phase-amplitude coupling within the task switching paradigm (see titles of panels for network name). Frequency pairs within the white triangle at the right bottom corner were not calculated because they represent frequency pairs where phase-providing and amplitude-providing frequency bands overlap. Only the left and right fronto-frontal network exhibit significant phase-amplitude coupling between beta and gamma frequencies (upper right corner) as well as indicate potential coupling between delta and beta (lower left corner). Z-values > 1.99 are considered as significant coupling. Here greyscale shading is chosen to enhance the difference between significant and nonsignificant coupling.

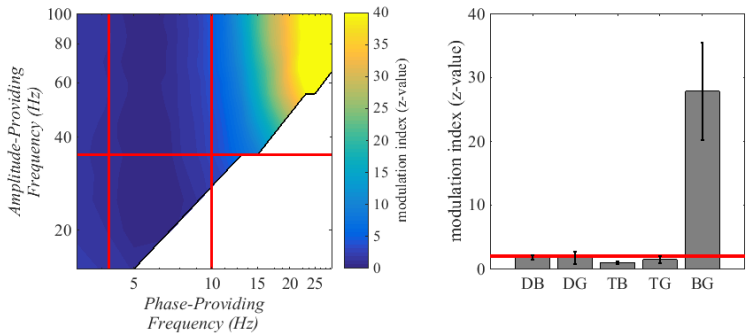

Figure 3.12: Comodulogram during the task switching paradigm of the fronto-frontal network averaged over hemispheres, blocks, trial types, and experimental groups. The bar plot shows mean modulation indices ± S. E. for each frequency pair. The red line marks the significance threshold. Please note that axes scaling for the comodulogram is different from that in Figure 3.11. Here coloured shading is chosen to enhance visibility of modulation index graduation. DB: Delta-Beta; DG: Delta-Gamma; TB: Theta-Beta; TG: Theta-Gamma; BG: Beta-Gamma.

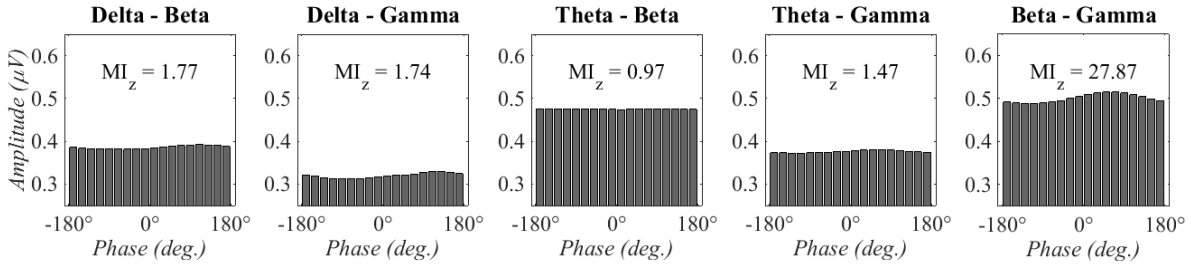

Figure 3.13: Phase-amplitude plots for each frequency pair and its corresponding standardised modulation index value (MI_z) for the task switching paradigm. Mean amplitudes are averaged over all participants, hemispheres, blocks, and trials types.

There was a significant frequency pair by trial type by responder group interaction ($F_{(8,120)} = 3.01$, $p = .04$, $\omega^2 = .05$, $Dunn_{crit} = 1.69$; Table 3.2). Only for beta-gamma coupling within the warm water control group, a significant difference in coupling strength between trial types were found: switch trials displayed more coupling (37.23 ± 14.16) than repeat trials (35.16 ± 13.71). In no other frequency pair nor in any other experimental group did switch and repeat trials differ in coupling strength. However, groups generally differed in their coupling strength. In both switch and repeat trials, the warm water control group had highest, low responders had medium, and high responders had lowest beta-gamma coupling strength. For theta-gamma coupling the warm water control group was the only group displaying significant coupling and had higher values than low and high responders, which did not differ from each other in their coupling strength. Finally, high responders were the only group displaying significant delta-gamma coupling, having higher coupling strength than warm water controls and low responders, which did not differ significantly in their coupling strength from each other.

Table 3.2: Mean modulation indices (S. E.) in the task switching paradigm for each frequency pair, trial type, and responder group. Averaged over both hemispheres and blocks. Values printed in bold represent significant coupling. Differences exceeding $Dunn_{crit} = 1.69$ are significant.

		Warm Water Controls	Low Responder	High Responder
Delta-Beta Coupling	Switch	1.85 (.61)	1.40 (.56)	**2.21 (.58)**
	Repeat	**2.03 (.64)**	1.31 (.59)	1.80 (.61)
Delta-Gamma Coupling	Switch	1.87 (1.62)	.29 (1.48)	**3.32 (1.54)**
	Repeat	.86 (1.84)	.36 (1.68)	**3.75 (1.75)**
Theta-Beta Coupling	Switch	.92 (.34)	1.01 (.31)	.71 (.32)
	Repeat	1.29 (.46)	1.35 (.42)	.55 (.44)
Theta-Gamma Coupling	Switch	**2.50 (1.05)**	1.19 (.96)	.76 (1.00)
	Repeat	**2.56 (1.10)**	1.08 (1.00)	.73 (1.05)
Beta-Gamma Coupling	Switch	**37.23 (14.16)**	**27.37 (12.93)**	**19.16 (13.50)**
	Repeat	**35.16 (13.71)**	**27.61 (12.52)**	**20.67 (13.07)**

Task Switching Paradigm – Correlations between Modulation Indices and Reaction Times. Behaviour, in form of reaction times, significantly and positively correlated with modulation indices within the left fronto-frontal network for beta-gamma coupling. Correlations did only become significant within the first block, explaining 31 % and 24 % of variance for switch and repeat trials respectively (according to r^2). In the second block, this correlation decreased and did not become significant anymore. No other correlation became significant (Table 3.3). Here positive correlations reflect that the higher the modulation indices, the longer the reaction times.

Table 3.3: Spearman's rho correlation between modulation index and reaction times in the task switching paradigm for each network, frequency pair, block, and trial type. Significant correlations are printed in bold.

			Frequency Pair				
			Delta-Beta (N = 33)	Delta-Gamma (N = 33)	Theta-Beta (N = 33)	Theta-Gamma (N = 33)	Beta-Gamma (N = 33)
Left Hemisphere	Block 1	Switch	-.08	.14	-.07	.05	**.55****
		Repeat	.03	.05	-.08	.05	**.49****
	Block 2	Switch	.08	.30	.08	.31	.22
		Repeat	.15	-.18	-.24	.03	.20
Right Hemisphere	Block 1	Switch	-.07	.07	-.03	.15	.19
		Repeat	-.03	.08	.13	.03	.25
	Block 2	Switch	.17	.26	-.15	.22	.07
		Repeat	.06	.26	-.31	.08	-.03

**$p < .01$.

3.3.4 Go-Nogo Paradigm

Behavioural Data

Go-Nogo Paradigm – Reaction Times. Because participants have to withhold from responding to nogo-trials, only reaction times in go-trials can be analysed. Neither the factor responder group nor block did influence reaction times in go trials. As reported in the methods section (p. 69), power to detect small effects was sufficient.

Electrophysiological Data

Go-Nogo Paradigm – Clustering Results. Scalp maps of the mean IC activations of each cluster and their corresponding residual variance can be found in Figure 3.14. Dipole locations are depicted in Appendix D.

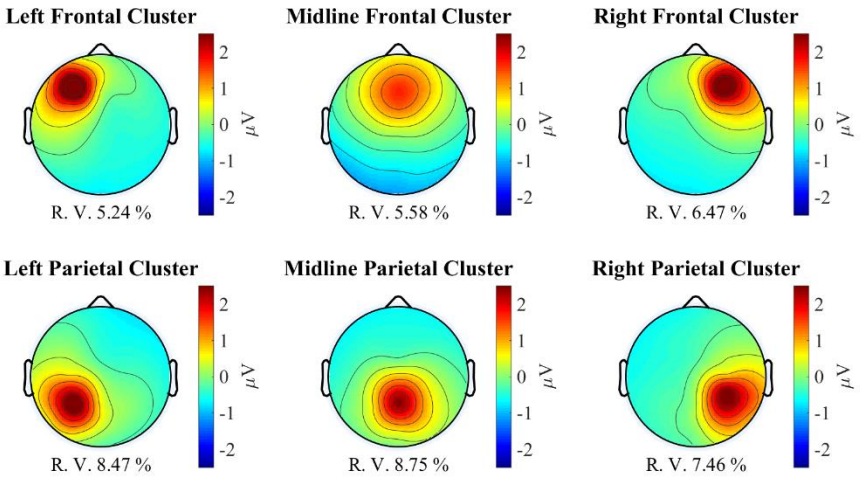

Figure 3.14: Final clusters of independent components found for the go-nogo task for all six regions of interest. For ICs in these clusters phase-amplitude coupling was calculated either within the frontal clusters or between frontal and parietal clusters.

Go-Nogo Paradigm – Initial Screening for Phase-Amplitude Coupling. Similarly to flexibility, only coupling within the left and right fronto-frontal network (i. e. coupling within one source) was found to be significant over the whole sample and all conditions (Figure 3.15). Based on these screening analyses, all further analyses were restricted to the left and right fronto-frontal networks.

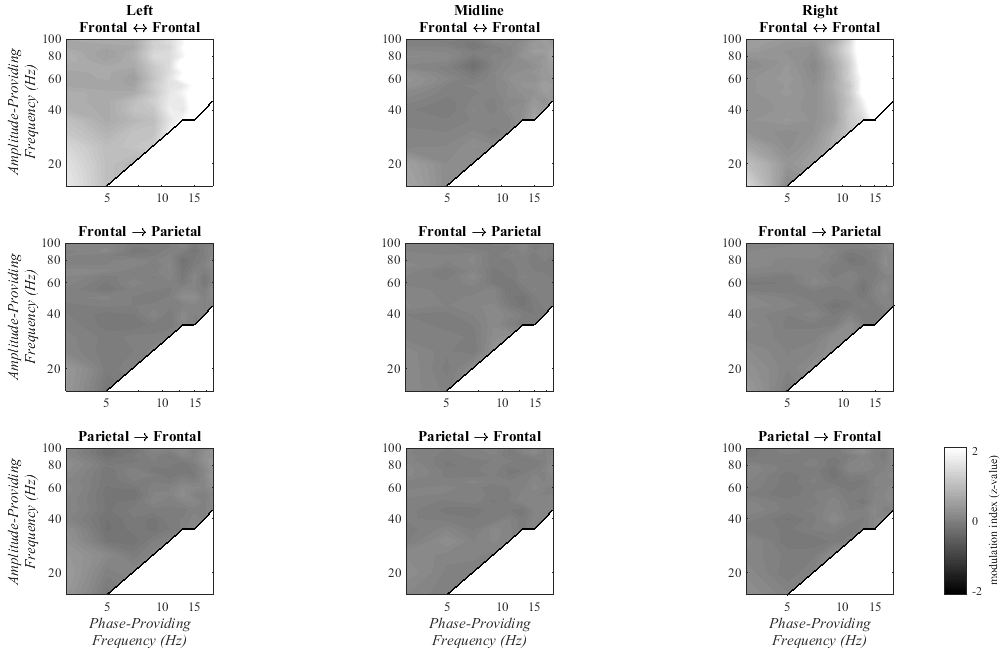

Figure 3.15: Screening of nine networks for phase-amplitude coupling within the go-nogo paradigm (see titles of panels for network name). Frequency pairs within the white triangle at the right bottom corner were not calculated because they represent frequency pairs where phase-providing and amplitude-providing frequency bands overlap. Only the left and right fronto-frontal network exhibit significant phase-amplitude coupling between beta and gamma frequencies (upper right corner) as well as indicate potential coupling between delta and beta (lower left corner). Z-values > 1.99 are considered as significant coupling. Here greyscale shading is chosen to enhance the difference between significant and nonsignificant coupling.

Go-Nogo Paradigm – Phase-Amplitude Coupling in Fronto-Frontal Networks. Coupling between beta and gamma (21.78 ± 6.21) was significant and significantly different from all other frequency pairs (delta-beta [1.50 ± .30], delta-gamma [.49 ± .16], theta-beta [1.04 ± .33], theta-gamma [.56 ± .11]; $F_{(4,120)} = 11.28$, $p = .002$, $\omega^2 = .20$, $\text{Dunn}_{crit} = 11.23$). Neither of the other frequency pairs exhibited significant coupling nor differed in their coupling strength (Figure 3.16).

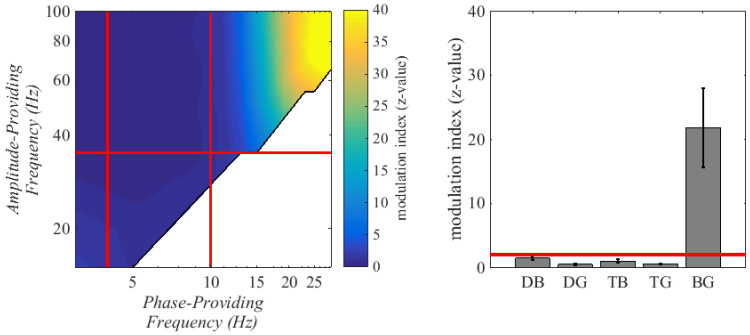

Figure 3.16: Comodulogram during the go-nogo paradigm of the fronto-frontal network averaged over hemispheres, blocks, trial types, and experimental groups. The bar plot shows mean modulation indices ± S. E. for each frequency pair. The red line marks the significance threshold. Please note that axes scaling of the comodulogram is different from that in Figure 3.15. Here coloured shading is chosen to enhance visibility of modulation index graduation. DB: Delta-Beta; DG: Delta-Gamma; TB: Theta-Beta; TG: Theta-Gamma; BG: Beta-Gamma.

The preferred phase of beta-gamma coupling is 40° to 80°, representing the range of decreasing phases of the low-frequency oscillation; amplitudes are lowest at -120° to -100°, representing the range of increasing phases of the low-frequency oscillation (Figure 3.17).

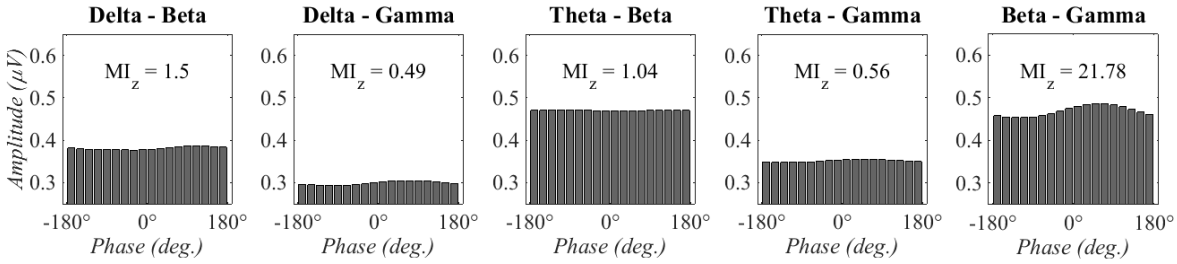

Figure 3.17: Phase-amplitude plots for each frequency pair and its corresponding standardised modulation index value (MI_z) for the go-nogo paradigm. Mean amplitudes are averaged over all participants, hemispheres, blocks, and trials types.

The hemisphere by frequency pair by block by responder group interaction ($F_{(8,120)} = 3.76$, $p = .033$, $\omega^2 = .03$, $\text{Dunn}_{crit} = 8.53$; Table 3.4) became significant. It explained 3 % of variance and showed that within the left hemisphere, the warm water control group showed significantly increasing beta-gamma coupling from block 1 to block 2. Low and high responders showed no significant difference in beta-

gamma coupling strength, despite a descriptive tendency of decreasing coupling strength over the blocks. The warm water control group had generally higher beta-gamma coupling strength within the left hemisphere than low and high responder, which did not differ in their coupling strength. For the right hemisphere, none of the groups showed differences in coupling strength over the course of the experiment, even though low and high responders had descriptively increasing beta-gamma coupling. For the right hemisphere high responders had generally the highest coupling strength, warm water controls had medium coupling strength, and low responders had the lowest coupling strength. High responders significantly differed from low responders in both blocks and from warm responders in the second block. The warm water control group and low responders did not differ significantly in their coupling strength in neither block. Warm water controls and high responders additionally showed significant delta-beta and theta-beta coupling in the left hemisphere (data not shown). However coupling strength did not differ between blocks or groups.

Table 3.4: Mean modulation indices (S. E.) in the go-nogo paradigm for each hemisphere, block, and responder group averaged over both trial types. All phase-amplitude coupling values represent significant coupling. Differences exceeding $Dunn_{crit} = 8.53$ are significant.

		Beta-Gamma Coupling	
		Left Hemisphere	Right Hemisphere
Warm Water Controls	Block 1	38.53 (17.86)	15.92 (7.19)
	Block 2	56.98 (20.13)	15.64 (6.85)
Low Responder	Block 1	19.73 (16.30)	8.77 (6.56)
	Block 2	18.14 (18.38)	10.95 (6.25)
High Responder	Block 1	19.17 (17.02)	20.90 (6.86)
	Block 2	11.44 (19.20)	25.22 (6.53)

Two other interactions became marginally significant, explaining at most 4 % of variance. Trial type interacted with responder group ($F_{(2,30)} = 2.49$, $p = .100$, $\omega^2 = .04$, $Dunn_{crit} = .62$) and was further qualified by frequency pair and block ($F_{(8,120)} = 2.85$, $p = .056$, $\omega^2 = .02$, $Dunn_{crit} = 2.48$; Figure 3.18). It revealed that only within beta-gamma coupling and within the warm water control group did task conditions influence coupling strength. Warm water controls showed significant more coupling in go compared to nogo trials in block 1. In block 2 trial type did no longer influence coupling strength. Coupling strength generally increased from block 1 to block 2 in both trial types for warm water controls. Warm water controls showed generally stronger coupling than high responders, which in turn showed significantly stronger coupling than low responders.

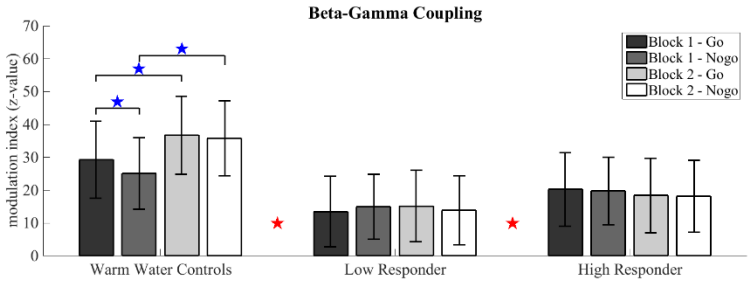

Figure 3.18: Coupling strength (mean modulation index ± S. E.) for beta-gamma coupling averaged over both hemispheres. Red stars signify that all groups differ significantly between each other in coupling strength. Blue stars mark the significant differences within the warm water control group.

Go-Nogo Paradigm – Correlations between Modulation Indices and Reaction Times. There were no significant correlations between modulation indices and reaction times in go trials.

3.4 Discussion

This study examined whether stress influences flexibility and inhibition behaviour, both being core executive functions. Furthermore, it was examined whether phase-amplitude cross-frequency coupling is a physiological marker of executive functions and is similarly influenced by stress in the way behavioural measures are expected to be.

The stress manipulation was successful and also the division of participants into low and high responders is justified by the data. Each low responder exhibited an absolute decrease of cortisol level in response to the SECPT (actually being a non-responder), while high responders all exhibited absolute cortisol increases. Eight of eleven high responders had biologically significant cortisol increases, defined as a cortisol increase of at least 1.5 nmol/l (Miller et al., 2013). As desired, participants did not differ in their cortisol level before the SECPT. The warm water control group was neither physiologically, nor psychologically stressed. Low responders, who were nearly indistinguishable from warm water controls in their physiological stress response, were psychologically more stressed than warm water controls. Nevertheless, they generally displayed only moderate distress while indicating the need for coping with the situation. High responders were psychologically and physiologically highly stressed. They had a marked cortisol increase in response to the SECPT and following the SECPT significantly higher cortisol levels than warm water controls and low responders. Additionally, they felt significantly more stressed, experienced more pain, and indicated higher coping effort than both warm water controls and low responders. They also experienced more tension than warm water controls. Differences in the psychological stress experience between groups are insofar interesting as in most studies low and high responders indicated no difference in subjective stress experience, but are clearly distinguishable in the physiological stress response. Here, low and high responders exhibited differences in subjective stress ratings which mirror the physiological stress response.

3.4.1 Flexibility, Stress, and Phase-Amplitude Coupling

In the task switching paradigm, which assessed the core executive function flexibility, typical results were found: participants needed significantly longer to respond to and made more errors in switch compared to repeat trials (switch costs). These results underline the validity of the task switching paradigm by showing that participants need more time and make more errors in the conceptually more difficult task of switching, than in the conceptually easier task of repeating an action.

Analyses further revealed that low responders which psychologically as well as physiologically successfully coped with the stressor seemed to profit from the cold water stress: They markedly increase their reaction times after the stress induction procedure without committing any more errors than before. High responders showed a tendency for a benefit, while warm water controls showed virtually no reaction times differences. Due to these reaction time modifications, low and high responders were significantly faster than warm water controls in the second block; groups did not differ in their reaction times in the first block. Looking at reaction times in more detail, it became evident that low responders equally increased reaction times in switch and in repeat trials (no switch costs modification). High responders became especially faster in switch trials (reduced switch costs). Warm water controls slowed down in repeat trials (reduced switch costs); their performance cannot be announced to have improved. Taking all aspects into account, performance was enhanced by the cold water condition of the SECPT; low responders enhanced their general reaction times and high responders enhanced their flexibility.

It can be therefore concluded that in this study cortisol enhanced flexibility, while stress generally improved performance. These results contradict the findings of a recent meta-analysis (Shields et al., 2016). However, this study is not the first to report beneficial effects of stress on flexibility (Beste et al., 2013; Delahaye et al., 2015; Kofman et al., 2006). When comparing the present and former studies, no parameter sticks out that might be causal for the beneficial effects. How can it be explained that low and high responders become significantly faster than the warm water controls in the second block? Derived from participants' comments, it was especially difficult to stay focused during the rather monotone experiment. The SECPT, as stressful and painful it is during hand immersion, might pull participants out of their monotony, increase arousal to an optimal level, and thereby provides a benefit for subjects in the cold compared to the warm water condition, whose arousal is too low for an optimal performance (Hebb, 1955; Radvansky, 2015). This potential benefit does translate into better performance when participants cope well with the stressor and do not experience a significant physiological stress response. Differences in results might also be explained by the rather long cue-stimulus interval of 1200 ms (but see General Discussion).

Are the behavioural effects reflected in the phase-amplitude coupling data? Only within warm water controls did beta-gamma coupling differ significantly between switch and repeat trials. As expected, coupling strength was stronger for switch than for repeat trials, suggesting that more cognitive control (higher coupling) is implemented during switch compared to repeat trials. This pattern was

expected to occur generally in the whole sample. Potential group differences were not expected to occur before the experimental stress induction.

Coupling strength indeed differed according to block. A block by trial type by responder group interaction occurred (further qualified by hemisphere and frequency pair). But these interactions became only marginally significant and did not explain more than 1 % of variance. Even though Cohen (1988) considers $\Omega^2 = .01$ a small effect, here this effect size is regarded being too small to be relevant. Because this pattern is only true for warm water controls, further interpretations are difficult.

The overall pattern of highest beta-gamma coupling in warm water controls, medium coupling in low responders, and lowest coupling in high responders is not reflected by the behavioural data, even though there was a tendency of generally longer reaction times in warm water controls compared to low and high responders. There is no explanation yet why groups differed in their coupling strength for theta-gamma, delta-gamma, and beta-gamma coupling. Trait differences can only serve as an explanation when warm water controls (consisting of potential low and high responders) show intermediate coupling values between low and high responders. This was never the case here. The group differences in coupling strength that are found are therefore hard to explain and await replication.

Lastly, looking into correlations between modulation indices and performance measures, it was found that only for the left prefrontal hemisphere there was a significant correlation between beta-gamma coupling and flexibility performance, even though the pattern was similar for the right hemisphere. This indicates that the left hemisphere was more directly involved with flexibility behaviour than the right hemisphere. These correlations were only significant in the first block for both trial types. Assuming that coupling strength reflects the amount of cognitive control that is implemented, it had been expected that reaction times would decrease with increasing cognitive control (high modulation indices). Instead reaction times increased with increasing modulation indices. Therefore this result is conflicting. On the other hand, if one interprets cognitive control as a wilful process, which needs active control, it would be conceivable that the more active control is needed, the longer the reaction times will become. Wilful, intended behaviour helps to avoid errors and becomes necessary in paradigms like task switching. Wilful behaviour is slower than automatic behaviour. In this study participants did not know beforehand, which trial they have to execute and therefore they need to keep up a certain amount of cognitive control the whole time, irrespective of switch or repeat trials.

Voloh et al. (2015) had found stronger theta-gamma coupling in correct compared to error trials in a flexibility task. Because error trials were rare in comparison to correct trials, phase-amplitude coupling was only calculated for correct trials in this analysis. It could be useful to design a flexibility task that leads to higher error rates, such that the findings of Voloh et al. (2015) can be replicated (see General Discussion).

Voytek et al. (2015), on the other hand, compares coupling in a flexibility task to coupling in a simple stimulus-response mapping task. They found theta-gamma coupling specifically in the flexibility task. This study also found coupling within the flexibility task – even though beta-gamma coupling –

but did not realise a task where no executive functions are needed. To overcome this, the following study (chapter 4) will include a paradigm covering the attention system and check the specificity of beta-gamma coupling across different cognitive domains.

3.4.2 Inhibition, Stress, and Phase-Amplitude Coupling

For the go-nogo paradigm, by which the core executive function inhibition was assessed, no significant effects of block or responder group were found. Errors could not be analysed because of minimal occurrence. A meta-analysis indicated that stress should have improved response inhibition (Shields et al., 2016). However, this is not the first study to report null findings (Kofman et al., 2006; Wu et al., 2014; Yildiz et al., 2014). One can be confident that these are true null findings as power for the main effect block and the interaction block by responder group exceeded 97 %. Presumably inhibition was not required extensively in the here realised go-nogo paradigm. The go response was probably not established to be a prepotent response, as participants faced go and nogo trials equally often. This could explain the lack of stress effects in behavioural inhibition results and further could explain why no clear pattern regarding coupling strength was found (see below). A detailed discussion of possible reasons for these null findings can be found in Dierolf (2014, pp. 33–36).

Regardless of behavioural results, the same pattern of strong beta-gamma coupling was evident during the inhibition task as during the flexibility task. Similar to the flexibility task, none of the other frequency pairs showed significant coupling. Contrary to the flexibility task, coupling strength in the inhibition task did differ between the hemispheres: coupling strength was markedly stronger for the left than for the right hemisphere in the inhibition task. This is surprising considering the meta-analyses that either found no hemispheric differences in prefrontal activation during inhibition (Nee et al., 2007; Niendam et al., 2012; Yarkoni et al., 2011) or found stronger right hemispheric activation (Cai et al., 2014; Levy & Wagner, 2011). However, processes that can be seen in neuroimaging data are solely those processes that consume more energy than a control process. Coupling occurs due to a temporal association between two aspects of ongoing neural oscillations, namely phase and amplitude of specific frequencies. For signals with the same amount of energy expenditure, coupling could be present or absent. These findings are therefore not contradicting but instead reveal methodological differences.

Beta-gamma coupling strength depended not only on hemisphere, but also on block and responder group. Within the left hemisphere, warm water controls showed a significant increase in coupling strength from block 1 to block 2 which was not mirrored in behavioural data. Low and high responders did not exhibit such a coupling strength increase. The cold water stress could have prevented the coupling increase that was seen in warm water controls. This coupling increase might occur when cognitive control is more easily implemented due to task practice or because more cognitive control is needed in the second block to keep performance at the same level, even though participants might experience fatigue. However, warm water controls were not just the only group exhibiting a coupling strength increase; they also had generally higher coupling strength than low and high responders.

In the right hemisphere, low responders showed lowest, high responders highest, and warm water controls intermediate beta-gamma coupling strength. In this specific case, coupling strength could be interpreted as a trait factor: people with low coupling strength would be more stress resistant than people with high coupling strength. The warm water control group assumingly consists of both responder types, therefore they display on average intermediate coupling strength. It can be speculated that more stress resistant people should have lower coupling because less coupling, interpreted as insufficient coordination between brain regions or processes (low coupling strength), hinders the full processing of stressful stimuli and thereby leads to a reduced stress response. Stress sensitive people should have higher coupling, because good coordination between brain regions or processes (high coupling strength), on the other hand, could facilitate processing of stressful stimuli and thereby lead to an enhanced stress response. When saying this, it should be kept in mind that the basic assumption of more coupling indicating better neural communication has not been verified yet; in fact, even the opposite pattern has been found (de Hemptinne et al., 2015). Furthermore, both causal directions are conceivable: low coupling leading to stress resistance or stress resistance leading to low coupling. The pattern of low coupling in low responders, high coupling in high responders, and intermediate coupling for the warm water control groups (supposedly a mix of potential low and high responders), was only evident in the right hemisphere. Hemispheric specialisation is a well-established fact in science (Behrmann & Plaut, 2015; Hopkins, Misiura, Pope, & Latash, 2015). So it is conceivable that differences regarding coupling strength, which might represent traits, only occur in specific brain regions or hemispheres. The effect size of this interaction is 3 % and thereby very small.

Even though explaining as little as 2 % of variance, another interesting effect occurred. Only warm water controls showed a modulation of coupling throughout the experiment. In block 1, before the SECPT and when the task was still new, they showed markedly stronger coupling in go, compared to nogo trials. This kind of result, namely coupling strength reflecting the optimization of a motor response, had been shown before (Dürschmid et al., 2014). In block 2, after the SECPT – when the task was already familiar – coupling strength in warm water controls significantly increased in both go and nogo trials. Now, trial types did not differ anymore in their coupling strength. In both low and high responders, coupling strength was not at all modulated by task conditions. Additionally, these groups generally showed markedly lower coupling strength than warm water controls and also differed in their coupling strength between each other. As stated above, these general group differences are difficult to explain.

The association between inhibition and phase-amplitude coupling had been shown in previous studies, but was, for example, restricted to emotion regulation (Popov et al., 2012) and disinhibition due to alcohol consumption (Lee & Yun, 2014) or had also only been shown to exist but not to vary with task demands (Tang et al., 2016), as is the case in the present study. Another study reported time-locked phase-amplitude coupling and differences of the preferred coupling phase between correct and incorrect responses. In the present thesis, phase-amplitude coupling was averaged across the entire trial length.

Preferred coupling phase seemed to be stable (40° – 80°), not only within the go-nogo task but also for the flexibility task. However, no concrete analysis of this parameter was yet conducted.

3.4.3 Preliminary Conclusion

Beta-gamma coupling strength was markedly higher than coupling strength for all other frequency pairs; frequency pair explaining about 20 % of variance in coupling strength. All other effects regarding phase-amplitude coupling were rather small, explaining between 3 to 5 % of variance. These effects partly showed the expected modulation of phase-amplitude coupling strength due to task requirements but also displayed general group differences which require results to be interpreted carefully until they have been replicated.

That beta-gamma coupling did only occur within one source might be explained by the circumstance that different frequency bands are thought to represent different spatial scales (cf. section 1.3): slower frequencies synchronize broader neuronal assemblies than faster frequencies, which are more localized. Therefore it is not expected to find beta-gamma coupling between two sources that are as far apart as the prefrontal and parietal cortex; here rather delta- or theta-gamma coupling would be expected. It has already been shown that phase synchrony between cortical areas occurs between delta, theta, and alpha frequencies while phase synchronisation within cortical areas occurred in gamma frequency (von Stein & Sarnthein, 2000).

When combining findings and interpretations of both the flexibility and inhibition tasks, it is revealed that results do not show a consistent, easily attributable phase-amplitude coupling strength pattern. Furthermore, trying to explain the findings shows that contradicting explanations can be logically derived by slightly changing the concrete definition of phase-amplitude coupling strength. First, one could assume that more coupling strength emerges because of task difficulty or task novelty; to meet the task requirements sufficient process coordination (coupling) is needed. Second, one could assume that more coupling strength emerges when processes or brain regions are well coordinated and thereby task requirements are easily met. These different explanations have to be empirically tested in order to be verified or falsified.

To summarize, stress induction was successful. Flexibility behaviour benefitted from cold water stress, which was not expected (Shields et al., 2016), but is definitely allegeable (arousal theory). The inhibition task, initially designed for an event-related potential study, was not ideal for the purposes of this study, which is why little conclusion can be drawn from behavioural data. Phase-amplitude coupling was consistently found during the flexibility and inhibition tasks, but it was not consistently modulated by task demands or by stress induction. The group differences found have to be cautiously examined in follow-up studies. That is, the exploratory analyses indeed revealed significant phase-amplitude coupling, but hypotheses regarding phase-amplitude coupling drawn from the literature could not be verified. Before refusing these hypotheses, more evidence needs to be gathered (see General Discussion).

4 Working Memory and Attention under Acute Stress: a Phase-Amplitude Coupling Study

4.1 Introduction

In the previously presented study, the relationship between stress, executive function, and phase-amplitude cross-frequency coupling had been studied for the first time in a rather large group of healthy male subjects with scalp EEG. Replications are needed to confirm the results (Open Science Collaboration, 2015; Schmidt, 2009). For a first step, it was chosen to not directly replicate the previous study, but to explore other aspects of this topic. Therefore, this experiment investigates the two remaining core executive functions – working memory and cognitive inhibition. Simultaneously, specificity of beta-gamma coupling for being a physiological marker of executive functions will be tested by investigating the entire attention system. This study will not only include male participants but will be extended to female subjects.

4.1.1 Working Memory, Stress, and Phase-Amplitude Coupling

Behavioural Effects.

Effects of acute stress on working memory are investigated with a huge variety of stressors; accordingly working memory is assessed by various tasks. All tasks used are accepted to properly assess working memory. In contrast, the various stressors differ in their ability to induce psychological and physiological stress. Therefore, the literature review is grouped according to the stressors used.

Cold pressor stress was found to cause detrimental effects on working memory, explaining 12 % of variance (Schoofs, Wolf, & Smeets, 2009). But faster and more error-prone responses were also found in the stressed group compared to the control group, explaining 3 – 4 % of variance and indicating a speed-accuracy trade off (Duncko, Johnson, Merikangas, & Grillon, 2009). Three experiments found no effects of cold pressor stress on working memory (Ishizuka et al., 2007; Porcelli et al., 2008). However, power in these experiments was insufficient for finding effects of the size reported above.

Heat stress reduced working memory performance in a study with 8 subjects, evoking a huge effect of $\omega^2 > .54$ (McMorris et al., 2006). With such a small sample, only large effects can be found (Button et al., 2013a, 2013b); results should be carefully interpreted. Schlader et al. (2015), studying subjects of about 30 and 70 years, found no effects of heat stress on working memory, while having virtually perfect statistical power for medium sized effects.

Stress elicited by movies[21] caused detrimental (Gärtner, Rohde-Liebenau, Grimm, & Bajbouj, 2014; Qin et al., 2012) and negligibly small or no effects (Cousijn, Rijpkema, Qin, van Wingen, & Fernández, 2012; Qin, Hermans, van Marle, Luo, & Fernández, 2009) of stress on working memory performance. Detrimental effects were not generally present but were constricted to specific conditions or groups (e. g. high works loads). Problematically, three of these studies (Cousijn et al., 2012; Gärtner et al., 2014; Qin et al., 2012) used a within-study design with a single experimental session, such that

[21] All studies reported here use short segments of the film "Irreversible" by Gaspar Noé (2002) for stressing participants and segments of "Comment j'ai tué mon père" by Anne Fontaine (2001) as control condition.

endocrinological stress effects, which were reported in all studies, would be carried over from the stress to the rest condition, in the case of watching stressful movies first.

Three studies used natural, stress arousing training to measure stress effects on memory. One of them, a military training, is highly successful in inducing stress and causes a twofold larger increase in cortisol than the TSST (Taverniers, van Ruysseveldt, Smeets, & Grumbkow, 2010). Stressed subjects made more errors than controls in a Digit Span Backward test ($\omega^2 = .14$). Robinson, Sünram-Lea, Leach, and Owen-Lynch (2008) also found detrimental effects of stress ($\omega^2 = .21$), even though no HPA axis activation was elicited in response to an underwater helicopter evacuation training. They investigated solely male participants in the morning hours. Robinson, Leach, Owen-Lynch, and Sünram-Lea (2013) found no effects of stress on a grammatical reasoning task, even though cortisol increased significantly in response to a simulated firefighting emergency. Statistical power was sufficient for large effects, but not for medium ones.

Examinations causing psychological stress and elevated cortisol levels had a small beneficial effect ($\omega^2 = .06$) on working memory performance (Lewis, Nikolova, Chang, & Weekes, 2008). Even though cortisol levels in the examination period are higher than in the control period, they are still basal levels and do not represent an acute HPA axis response. Performance pressure caused only negligibly small detrimental effects, insofar as under stress higher working memory capacity did no longer increase accuracy scores, as it does under rest (Beilock & Decaro, 2007). There was no manipulation check whether performance pressure was actually perceived as stressful by subjects.

Studies using the TSST (in one case TSST combined with SECPT; Lai et al., 2014) found equally often beneficial (al'Absi et al., 2002; Buckert, Kudielka, Reuter, & Fiebach, 2012; Lai et al., 2014; Schoofs, Pabst, Brand, & Wolf, 2013; Stauble, Thompson, & Morgan, 2013; Weerda, Muehlhan, Wolf, & Thiel, 2010), detrimental (Luethi, Meier, & Sandi, 2008; Oei, Everaerd, Elzinga, van Well, & Bermond, 2006; Olver, Pinney, Maruff, & Norman, 2015; Schoofs et al., 2013; Schoofs, Preuss, & Wolf, 2008), and null effects of stress on working memory (Cornelisse, Joëls, & Smeets, 2011; de Veld, Riksen-Walraven, & de Weerth, 2014; Elzinga & Roelofs, 2005; Gathmann et al., 2014; Hoffman & al'Absi, 2004; Oei et al., 2012; Smeets, Jelicic, & Merckelbach, 2006). Overall, these studies consistently induced significant cortisol increases. They found – if measured – heightened sympathetic activation and worse mood in response to the stress procedure compared to a control procedure (between-subject design) or compared to baseline measurements (within-subject design). All but one study, who investigated children (de Veld et al., 2014), included young healthy subjects, either all male or mixed-sex. These studies procedures produced a heterogeneous picture, neither indicating a clear direction of effects nor identifying parameters that are crucial for explaining the variation in results and effects sizes (summarized in Table 4.1). Studies using male samples tend to be more likely to find beneficial effects of stress on working memory performance. Within-subjects comparisons tend to find beneficial or no effects, while between-subjects designs tend to find detrimental effects. Time of testing might also play a role, insofar as basal cortisol levels, which are higher in the morning hours than in the

afternoon hours (Weitzman et al., 1971), might influence acute cortisol effects. It has already been shown that the influence of cortisol on flexibility behaviour differs according to the cortisol awakening reaction, a measure for basal cortisol level (Dierolf et al., 2016). Most studies conducted in the morning showed detrimental effects, while most studies conducted in the afternoon showed beneficial effects.

A meta-analysis investigating how acute stress influenced working memory performance concludes that stress impairs working memory performance (Shields et al., 2016). Even more so in male compared to female subjects, contrary to the conclusion of the qualitative review reported here. Detrimental stress effects become worse the longer the delay between the acute stressor and the execution of the working memory task is. Furthermore the more intense the stress, the stronger are the detrimental effects. Detrimental effects are especially present in high compared to low workloads. The meta-analysis did not investigate whether time of day of testing and experimental design (within and between) explained differences in findings. Again, the classification into low and high responders could be helpful for explaining results and will be conducted in this study, as was done in the previous study.

Table 4.1: Acute psychosocial stress effects (caused by the TSST) on working memory performance.

	Beneficial Effects (n = 7)	Detrimental Effects (n = 6)	No Effects (n = 7)
Tasks	n-back (3x) Sternberg (2x) Change-Detection Task (1x) Dichotic Listening (1x)	n-back (4x) Sternberg (1x) Operation Span (1x)	n-back (2x) Sternberg (1x) Digit Span Backward (4x)
Explained Variance	4 – 20 %	4 – 19 %	–
Sex of Sample	Male (4x) Both (3x)[1]	Male (3x) Both (3x)[2]	Male (2x) Both (5x)
Sample Size	12 – 109 (median = 40)	20-109 (median = 36)	23-158 (median = 44)
Time lag between stressor and task	< 20 min (2x) < 40 min (4x) > 40 min (1x)	< 20 min (1x) < 40 min (4x) > 40 min (1x)	< 20 min (2x)[3] < 40 min (4x) > 40 min (2x)[3]
Time of Testing	Morning (2x) Afternoon (5x)	Morning (4x) Afternoon (1x) All Day (1x)	Morning (2x) Afternoon (3x) All Day (1x)
Experimental Design	Within-subjects (5x) Between-subjects (2x)	Within-subjects (1x) Between-subjects (5x)	Within-subjects (5x) Between-subjects (2x)

[1] Two of these three studies find effects only for males (Schoofs et al., 2013).
[2] Two of these three studies find effects only for females (Schoofs et al., 2008).
[3] One study examines effects < 20 min and > 40 min post stress (Elzinga & Roelofs, 2005).

Phase-Amplitude Coupling Effects.

Regarding phase-amplitude coupling and working memory, the largest study so far was conducted by Rajji et al. (2016), investigating 70 healthy human subjects via scalp EEG on the association between theta-gamma phase-amplitude coupling and working memory assessed via n-back task. Rajji et al. (2016) particularly showed that theta-gamma coupling strength increased as a function of the need for ordering information. However, this association also independently applied for theta and gamma power. Coupling was measured within frontal electrodes and averaged over them.

Mizuhara and Yamaguchi (2011) found that during successful maintenance of items in a delayed-match-to-sample task, significant coupling between the phase of a 3 Hz oscillation at fronto-central sites and gamma amplitude at left fronto-lateral as well as left occipito-lateral sites occurred. There was no direct comparison between coupling strength at successful and unsuccessful maintenance trials. Coupling was measured during the retention period in 12 healthy humans via scalp EEG. They conclude that their "results supported the theoretical prediction that slow oscillation rehearsed the sensory inputs represented by the gamma oscillation" (Mizuhara & Yamaguchi, 2011, p. 1933), as was proposed by Jensen (2006).

Two further studies report theta-gamma coupling in healthy subjects measured via scalp EEG (Park, Jhung, Lee, & An, 2013; Park, Lee, & Lee, 2011). They explored the interrelation between working memory performance and theta-gamma phase-amplitude coupling during the maintenance period of this task in older adults (Park et al., 2011). Phase-amplitude coupling positively correlated with the accuracy rate at one (Fp2) of 19 electrodes ($r^2 = .32$; partial correlation controlling for subjects age). Reaction times did not correlate with phase-amplitude coupling strength. In a younger sample, they found theta-gamma coupling at Fp2 to be higher in a working memory compared to a vigilance task (Park et al., 2013). However, when analysing theta-gamma coupling at higher gamma frequencies (above 40 Hz), coupling was more often found to be higher in the vigilance compared to the working memory task. Because these studies omitted permutation testing, one cannot be confident that the reported coupling is meaningful (Cohen, 2008). Moreover, coupling differences between tasks, or as in the first study its correlation with behaviour, is found at a seemingly arbitrary electrode.

Five additional studies examine phase-amplitude coupling while subjects execute working memory tasks (Axmacher et al., 2010; Bruns & Eckhorn, 2004; Leszczynski et al., 2015; Maris et al., 2011; van der Meij et al., 2012). In these studies ECoG and LFPs were recorded from human subjects diagnosed with epilepsy. Sample sizes range between 7 and 27 subjects. All studies assess statistical significance of the empirical phase-amplitude coupling values. Theta-gamma coupling was found to be stronger in the maintenance than in the baseline period of a working memory task ($\omega^2 = .37$; (Axmacher et al., 2010). Coupling strength did not vary with workload. However, theta frequency was slower for high loads than for low loads, supporting the working memory theory of Lisman and Jensen (2013). In contrast to this finding, Leszczynski et al. (2015) observed decreased phase-amplitude coupling (over a broad range of frequencies) during the maintenance period compared to remaining interleaved periods

of the working memory ($\omega^2 = .24$). Furthermore, they found an increased amplitude-providing frequency for high workloads, not a decreased phase-providing frequency[22]. Both studies measured LFPs from the hippocampus and used 1000 permutations for significance testing; thus these factors cannot explain the opposing findings. Depending on the neuronal location Maris et al. (2011) found both increased and decreased phase-amplitude coupling in encoding and retention periods compared to baseline periods. This was similarly found for episodic memory: some regions in the hippocampus show increased phase-amplitude coupling during successful encoding and others during unsuccessful encoding (Lega et al., 2016).

Leszczynski et al. (2015), Maris et al. (2011), and van der Meij et al. (2012) found phase-amplitude coupling to be present at many frequency pairs – not solely at theta-gamma. van der Meij et al. (2012) reports phase-amplitude coupling to be distributed across the entire scalp, including various preferred coupling phases. They conclude that these findings support the idea that phase-amplitude coupling is a mechanism that separates "spatially distributed networks operating in parallel" (van der Meij et al., 2012, p. 111). In a case study, delta-gamma coupling was found to be present during the encoding period of a working memory task between an early visual area (modulator) and a higher visual area (modulated; Bruns & Eckhorn, 2004).

Not only working memory literature, but also long-term memory research, repeatedly finds theta-gamma coupling, preponderantly indicating stronger coupling to be associated with successful learning, encoding, or remembering (e. g. Friese et al., 2013; Kaplan et al., 2014; Köster et al., 2014; Mormann et al., 2005). Memory research almost exclusively investigates theta-gamma coupling. Nevertheless, even if broader frequency ranges are investigated, theta-gamma coupling is frequently, but not necessarily exclusively, present.

4.1.2 Attention, Cognitive Inhibition, Stress, and Phase-Amplitude Coupling

It has been shown that it is important to distinguish between cognitive and behavioural inhibition when investigating stress effects on inhibition (Shields et al., 2016). In that meta-analysis, behavioural inhibition was found to be enhanced by stress, whereas cognitive inhibition was found to be impaired. This suggests the presence of better motor control and a broader attention focus under stress compared to control conditions. Because cognitive and behavioural inhibition should be distinguished and behavioural inhibition has already been investigated in the previous study, this study investigated stress effects on cognitive inhibition via the attention network test (Fan et al., 2002). The attention network test combines a flanker paradigm (Eriksen & Eriksen, 1974) with the Posner cueing task (Posner, 1980). It is therefore possible to investigate cognitive inhibition while simultaneously testing the entire attention system of the human brain according to Posner and Petersen (1990). The objective of studying

[22] Rather than any phase-amplitude coupling parameter (e. g. coupling strength), it was the alternation between increased and decreased cross-frequency coupling that predicted successful maintenance. But not only the alternation between increased and decreased cross-frequency coupling predicted successful maintenance, but alpha-band power fluctuations did as well.

the entire attention system is to probe the specificity of stress effects on executive functioning and the specificity of phase-amplitude coupling patterns found for executive functions in contrast to a second cognitive domain, namely attention.

Posner and Petersen (1990) formulated and subsequently validated (Fan et al., 2002; Fan et al., 2007; Fan, McCandliss, Fossella, Flombaum, & Posner, 2005; Petersen & Posner, 2012) the existence of three discrete attention networks (alerting, orienting, and executive control [= cognitive inhibition]). Two other groups appraised the attention network test and attested to its reasonable quality, while stating that the three attention networks are to a certain amount dependent, and reliability of the test is only high for the executive control network (Ishigami & Klein, 2010; MacLeod et al., 2010). Low reliability for alerting and orienting and high reliability for executive control could hint that alerting and orienting are more state-dependent while executive control is more trait-dependent (MacLeod et al., 2010).

Alerting is defined as a high sensitivity or readiness to perceive and process impending stimuli (Posner & Rothbart, 2007; Raz & Buhle, 2006; Worden, 2011). It is dissociated from arousal, insofar as arousal refers to intrinsic attentiveness while altering refers to task specific phasic attentiveness (Raz & Buhle, 2006). Alerting is manipulated in the attention network test by either not presenting a warning cue (not alerted, diffused attention) or presenting a warning cue that does not tell the subject where to expect a subsequent target (alerted, diffused attention). Following a warning cue, subjects orient and respond faster to the subsequent target (Worden, 2011).

Orienting has been described as selection and prioritizing of sensory information, for example, by selecting a location to which to attend to (Fan et al., 2002; Petersen & Posner, 2012; Posner & Petersen, 1990; Worden, 2011). Processing of attended items is usually faster and more accurate than processing of unattended items (Worden, 2011, p. 296). Orienting is manipulated by presenting warning cues that are either predictive or non-predictive of the spatial target location (Fan et al., 2002).

Executive control was first introduced as detecting signals or focusing attention on narrow in contrast to wide areas (Posner & Petersen, 1990, p. 29). Today it is defined as monitoring and resolving of and adapting to conflicting information (Fan et al., 2002; Worden, 2011). Executive control requires mental effort and is comparable to the core executive function inhibition. The same cognitive task is used to measure both concepts (Eriksen flanker paradigm).

All three systems have been associated with distinct anatomical brain regions (Fan et al., 2005), distinct set of EEG activations (Fan et al., 2007), and distinct chemical modulators (Posner & Rothbart, 2007). Anatomical regions lie roughly within frontal and parietal areas, as was already reported for executive functions. Interestingly, alerting and orienting were found to be located within frontal and parietal areas while executive control was solely found to be located in frontal brain regions (Posner & Rothbart, 2007).

Stress effects on attention, specifically on the three attention networks, alerting, orienting, and executive control, are not well studied. It was found that heat stress had detrimental effects on executive control ($\omega^2 = .13$; Sun et al., 2012). However, no physiological or subjective stress effects were reported.

In another study heat stress, here reported to go along with an autonomic nervous system stress response, was found to improve some aspects of attention and have no effect on others (Schlader et al., 2015). Acute psychosocial stress (TSST) was found to have no effect on selective attention in young adults (Cornelisse et al., 2011), but to improve performance of executive control ($\omega^2 = .05$) and marginally improve orienting performance in children (Fairbairn, 2007). The TSST for children did not elicit an endocrine stress response, but elevated subjective stress ratings.

In summary, relying on the meta-analysis of Shields et al. (2016), one can expect negative effects of stress on the executive control network. Regarding alerting and orienting, non-significant effects have been found, but positive and negative stress effects were also reported. Literature on this subject is sparse. From a theoretical viewpoint, cortisol could be able to modulate attention processes because, as mentioned in the General Introduction, cortisol is able to influence many processes, but actually influences those that are active. Furthermore, during stress it is of fundamental importance to be alert and rapidly orient attention to relevant stimuli. Saying this, one would rather expect positive than negative stress effects on alerting and orienting. Narrowing attention during stress might be disadvantageous, leading an organism to miss relevant environmental stimuli. These assumptions fit to the findings of decreased executive control. In the case of the flanker paradigm, decreased executive control represents a decreased ability to block task-irrelevant peripheral stimuli.

To my knowledge, no study investigated phase-amplitude coupling within the attention network test yet. Additionally, studies investigating phase-amplitude coupling with other attention tasks are scarce. Studies examining phase-amplitude coupling and inhibition have been reviewed in section 3.1.2, where the focus centred on behavioural inhibition. However, some studies were reported investigating cognitive inhibition. These indicated that phase-amplitude is either only present or stronger when cognitive inhibition is required in a task (Dürschmid et al., 2013; Popov et al., 2012; Tang et al., 2016).

The fronto-parietal network is not only associated with executive functions, but also with attention processes. Szczepanski et al. (2014) reports delta-gamma coupling when targets had to be allocated; measured via ECoG data recorded from human subjects diagnosed with epilepsy during a spatial-cuing task, which resembles the Posner cueing task (Posner, 1980). Coupling was calculated within electrodes and found in the majority of these. Coupling strength negatively correlated with reaction times. Another study found that stimulus detection depended on ultra slow frequencies (.01 – .10 Hz), where amplitudes of faster frequencies (1 – 40 Hz) varied according to these ultra slow frequencies (Monto, 2012). These studies indicate that phase-amplitude coupling might also be present during basic attention processes.

4.1.3 Hypotheses

The previous chapter had shown that the straight hypotheses of stronger phase-amplitude coupling representing better executive functioning, in turn reflected in better performance, is not entirely

supported by the empirical data. Even though the hypotheses formulated in the previous chapter were not clearly verified, they shall serve as guiding principles in the investigation presented here.

Phase-amplitude coupling is thought to be a mechanism by which different brain regions or different neuronal processes are coordinated. Higher cognitive functions, to which executive functions (e. g. working memory, cognitive inhibition) belong but basic attention processes (e. g. alerting, orienting) do not, presumably require this kind of coordination in order to be successfully implemented. Basic processes are assumed to either not need this coordination, or at least to a lesser extent. Stress has been shown to modulate the performance of executive functions, and even though beneficial, detrimental, and null effects have been found so far, a recent meta-analysis concluded that stress has detrimental effects on working memory performance and cognitive inhibition. The following hypotheses are formulated:

1.1 Groups will not differ in their working memory and attention performance before the SECPT.
1.2 Stressed participants, especially those with a marked physiological stress response will show less cognitive inhibition and worse working memory performance after SECPT compared to before SECPT and after SECPT compared to the control group. Alerting and orienting are hypothesized to be left rather unaffected or to benefit from stress.

2.1 Phase-amplitude coupling strength will vary according to task demands: stronger coupling in incongruent trials than congruent or neutral trials, no variation according to cue types, and stronger coupling in high compared to low works loads.
2.2 Groups will not differ in their coupling strength before the SECPT.
2.3 Stressed participants, especially those with a marked physiological stress response will show less coupling in executive control, no change in alerting and orienting, and less coupling in working memory after SECPT compared to before SECPT and after SECPT compared to the control group.
2.4 Phase-amplitude coupling should correlate negatively with reaction times in the working memory and executive control tasks; it should not correlate with reaction times in alerting and orienting tasks.

The experiment presented in this chapter is an indirect replication study in the widest sense. It shall explore, whether the hypotheses can be verified in the other executive functioning domains which were not targeted in chapter 3. It shall further explore if the phase-amplitude pattern found in the previous experiment (beta-gamma coupling) is specific to executive functioning or can also be found in another cognitive domain (attention).

4.2 Material and Methods

4.2.1 Participants

The final sample size was comprised of 55 (29 female, 26 male) students from Trier university and young employed persons. Mean age ± standard deviation was 23 ± 3 years and ranged from 19 to 30 years. Initially 77 subjects were invited to participate in the study. Four subjects (2 female, 2 male) had to be excluded from analysis because they did not feel well after the SECPT (condition 1-4 °C) and reported to be about to faint. Three subjects (1 female, 2 male) had to be excluded because they did not adhere to the instructions and reacted with two fingers instead of only the index finger of their dominant hand, possibly influencing reaction times. One male subject was excluded because his cortisol profile was highly dissimilar to all other participants, with elevated level before the stress procedure and decreased level after the stress procedure (cold water condition). The reasoning for excluding this participant is justified by the research question: the aim of the present study is to explore whether stress, quantified via cortisol level, modulates cognition. Accordingly this participant is highly stressed during the baseline blocks, and rather relaxed during the experimental blocks. This is why he cannot be grouped with the other subjects. One more male subject was excluded due to strong perspiration EEG artefacts and additional technical problems during the socially evaluated cold pressor test. As was the case in the former reported experiment, thirteen subjects were excluded because they did not contribute an IC to each required region of interest. The exclusion of thirteen subjects due to the choice of applying independent component analysis might appear unjustifiable high. Analyses including these thirteen subjects were conducted, showing that neither behavioural nor physiological results were influenced by the decision to exclude these subjects.

Preconditions for eligibility were the following: (1) age between 18 and 40 years, (2) BMI between 18 and 30, (3) being a non-smoker, (4) at most moderate alcohol consumption according to world health organisation (WHO) guidelines, (5) no use of illegal and legal drugs or substances possibly influencing cortisol level, (6) right-handedness, (7) absence of any acute and chronic mental disorder or physical disease (especially the Raynaud syndrome) as well as a history of mental disorders, (8) speak and understand German fluently, (9) normal or corrected-to-normal vision, and (10) naivety to psychological stress induction procedures (e . g. TSST, CPT, SECPT). Women had to take hormonal contraceptives[23] and were neither pregnant nor breast-feeding. Preconditions were to ensure that cortisol level were to the greatest possible extent within the normal range (1-5), participants had similar hemispheric specialisation[24] (6), had no problems understanding instructions and complying with the experimental procedure (7-9), and to guarantee unbiased behaviour in the experiment (10).

[23] Women taking contraceptives containing drospirenone were excluded. Drospirenone is an antagonist for the mineralocorticoid receptor and might therefore alter cortisol effects in the brain (Genazzani, Mannella, and Simoncini, 2007).

[24] According to Galin et al. (1982) handedness affects hemispheric specialization and can thus lead to differences in EEG measurement.

Participants guaranteed completeness and accuracy of the information they provided and gave written informed consent prior to participation. The study was approved by the local ethics committee and is in accordance with the Declaration of Helsinki (World Medical Association, 2013).

4.2.2 Experimental Procedure

Subjects were received for an initial screening session. There eligibility was determined with a structured interview. Information about the aim of the study and experimental procedures were provided. Participants returned to the laboratories on another day at 1400 h, 1600h, or 1800h. They refrained from physical exercise and alcohol 24 hours prior the experimental session, refrained from caffeinated drinks at the day of the experiment, and did not eat one hour prior to the experimental session. All participants woke up before 0900h at that day and female participants, taking oral contraceptives made sure that the experimental session did not take place during their break from active pills.

They practiced the attention network test (24 practice trials with feedback) and the Sternberg task (12 practice trials with feedback) and provided the first saliva sample (#01) during an exercise session. Order of task was the same as later on in the experiment. After participants had understood and practiced the cognitive tasks they were led into the psychophysiological laboratory, seated in a dimly lit, sound attenuated, and electrically shielded recording cabin and prepared for EEG, EOG and ECG recordings. After preparations participants were left alone and got all instructions via computer screen. They executed the baseline blocks of both tasks, each split into two subunits and provided salivary samples before and after each subunit (#02 – #06). Participants were then exposed to the socially evaluated cold pressor test or a socially evaluated warm water control procedure. An investigator of opposite sex and unknown to the participant entered the room, prepared the subject for blood pressure measurements and subsequently led the subject through the stress induction procedure. After the stress induction procedure, subjects were again left alone in the recording cabin, rated their subjective stress experience and then conducted another block of each task, providing salivary samples before and after each subunit (#07 – #11). Order of tasks was randomized between subjects but held constant within subjects. Because exercising both cognitive tasks was hold when participants arrived and took place in another room than the recording cabin, experimental procedures before and after the stress procedure were identical. After removal of all recording devices participants were debriefed by the investigator who conducted the stress induction procedure, provided a last saliva sample (#12), and were compensated monetarily or with course credits. The whole experimental procedure (Figure 4.1) took about two hours.

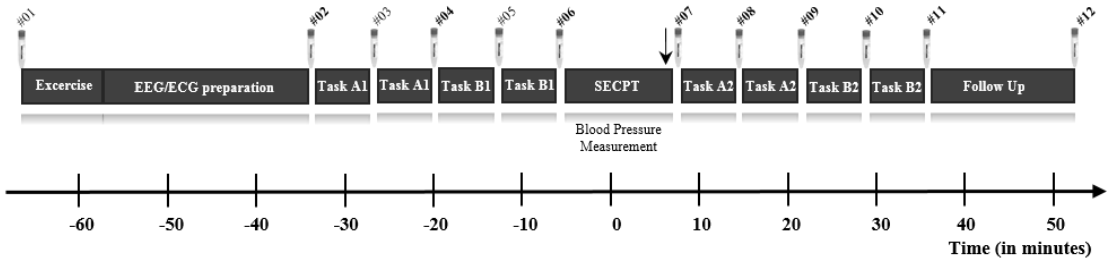

Figure 4.1: Graphical depiction of the experimental procedure. Measurement points of saliva cortisol are consecutively numbered from #01 to #12. Only saliva samples printed in bold were later on analysed. The down-head arrow indicates the time when participants rated their subjective stress experience. Task A and B can be either the attention network test or the Sternberg task. SECPT: socially evaluated cold pressor test.

4.2.3 Cognitive Tasks

Cognitive tasks were presented on a 19" LCD monitor (Eizo FlexScan, S1931) with 1280 x 1024 resolution and a 60 Hz refresh rate using E-Prime presentation software (Eprime 2.0, Psychological Software Tools, Pittsburgh, PA). Participants had a distance of 100 cm to the computer screen.

4.2.4 Sternberg Working Memory Task

A version of the Sternberg task was used to measure working memory performance (Sternberg, 1966, 1975). It is an often used and well validated paradigm (e. g. Brookes et al., 2011; Jensen & Tesche, 2002; Roznowski & Smith, 1993). In this task, participants have to judge, whether a probe stimulus did (match) or did not (non-match) appear in a list they had seen immediately before.

One trial consisted of a sequence of ten or fourteen slides, depending on the workload of the trial (Figure 4.2). In the first six or ten slides an uppercase consonant[25] was presented for 300 ms. The consonant was centred vertically and horizontally. A blank screen was shown for 200 ms. These two slides were repeated three or five times in total, depending on the condition workload (low: 3 consonants; high: 5 consonants). After the last blank screen, the retention interval began (a slide with a centred star) and lasted for 1200 ms. The probe letter was presented subsequently for a maximum of 2000 ms or until the participant responded. After participants' response a blank screen was shown for 2000 ms minus the reaction time. A variable inter-trial-intervals of 500 – 1000 ms (mean 750 ms) was represented by a slide showing a fixation cross centred vertically and horizontally.

A total of 120 trials were presented before the stress induction procedure, split into two subunits of 60 trials each. Another 120 trials, split into two subunits of 60 trials were presented after the stress induction procedure. Each block of 120 trials took approximately 12 minutes, resulting in 240 trials and 24 minutes of total processing time for the Sternberg task. Subjects could not decrease the duration by answering especially fast.

[25] Consonants T, D, H, L, C, G, M, B, W, F, K, Z, P, V, and J were used during the experiment. They were chosen, because they are neither the most frequent nor the least frequent consonants in German language (Beutelspacher, 2015). The remaining six consonants of the alphabet (N, S, R, Y, X, Q) were used during practice trials.

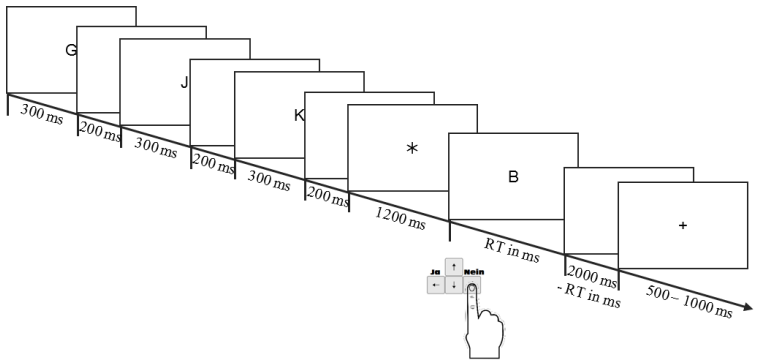

Figure 4.2: One trial of the Sternberg task with a workload of three letters and a non-match target.

Half of trials had a workload of three consonants, which in turn were to 50 % match trials and to 50 % non-match trials. The other half had a workload of five consonants, which also were to 50 % match trials and 50 % non-match trials. A match is a trial, where the test stimulus is part of the consonant list seen before. A non-match is a trial, where the test stimulus is not part of the consonant list seen before

Participants were meant to respond as fast and accurate as possible, by pressing either the left or right arrow key on the keyboard indicating whether the test stimulus was a match (left arrow key) or was a non-match (right arrow key). They always responded with the index finger of the right hand. Mapping of response keys was not varied between subjects. Subjects were ought to rest their index finger in between the response keys, i. e. at the down arrow, to guarantee unbiased reaction times in each trial.

Slides were always black with white stimuli. Consonants were present in Arial Font Size 40 and had horizontal visual angle of 0.573° and a vertical visual angle of 0.688°.

4.2.5 Attention Network Test

To measure the entire attention system the attention network test was used (Fan et al., 2002). It is an often used and well validated paradigm (MacLeod et al., 2010; Raz & Buhle, 2006). The attention network test measures the entire attention system according to Posner's theory of attention (Petersen & Posner, 2012; Posner & Petersen, 1990). Included in the attention network test is the measurement of cognitive inhibition (executive control).

One trial consisted of a sequence of five slides (Figure 4.3). First, a fixation cross was presented, centred horizontally and vertically. This slide was presented for 400 – 1600 ms, mean presentation time over all trials was 1000 ms. Subsequently one cue condition was realized (Figure 4.4, upper row). Cue slides were presented for 100 ms. Another slide with only a centred fixation cross follows for 400 ms. The next slide presented the target (Figure 4.4, lower row) above or below the centred fixation cross, which was also part of this slide. It was presented at most for 1700 ms, and disappeared at the end of the 1700 ms or as soon as the participant responded. If the participant did not respond within this time,

their response was marked as missing. The last slide only consisted of a centred fixation cross and was visible for a variable time depending on reaction time of the participant ('Waitfill' = 1700 ms – RT in ms + 525 ms). Duration of one trial was between 3125 and 4325 ms (mean: 3725 ms). Adding 525 ms to the waitfill duration is explained by the need to have a minimal trial length of 3000 ms for later EEG analysis and to construct almost identical block length for attention network test and Sternberg task.

A total of 192 trials were presented before the stress induction procedure, split into two subunits of 96 trials each. Another 192 trials, split into two subunits of 96 trials were presented after the stress induction procedure. Each block of 192 trials took approximately 12 minutes, resulting in 384 trials and 24 minutes of processing time for the attention network test. Subjects could not decrease the duration by answering especially fast.

Participants were meant to respond as fast and accurate as possible, by pressing either the left or right arrow key on the keyboard indicating the direction of the central arrow. They always responded with the index finger of the right hand. Response-keys were not varied between subjects, because responding to a left-pointing arrow with a relatively left key (especially the left arrow key) is intuitive while the opposite would be contra-intuitive and therefore possibly increasing reaction times. The same is true for a right arrow and right keys. Subjects were ought to rest their index finger in between the response keys, i. e. at the down arrow, to guarantee unbiased reaction times in each trial.

Cue condition, position of cue in the spatial cue condition, target condition, position of target (below or above the fixation cross), as well as direction of the central arrow (left vs. right) were counterbalanced across all trials.

Slides were always black with white stimuli. The target consisted of five lines or arrows (see Figure 4.4, lower row) with a total horizontal visual angle of 3.093° and a 1.146° vertical deviation from the centre of the screen. One line or arrow had a horizontal visual angle of 0.573° and a gap of 0.057° horizontally to the next line or arrow. Background colour was black, while all stimuli were presented in white colour.

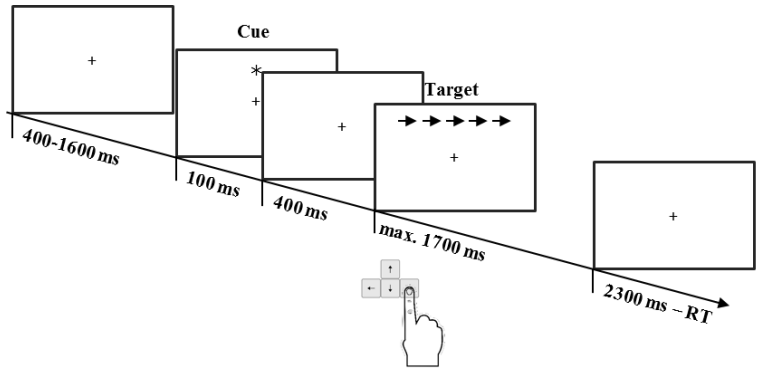

Figure 4.3: One trial of the attention network test.

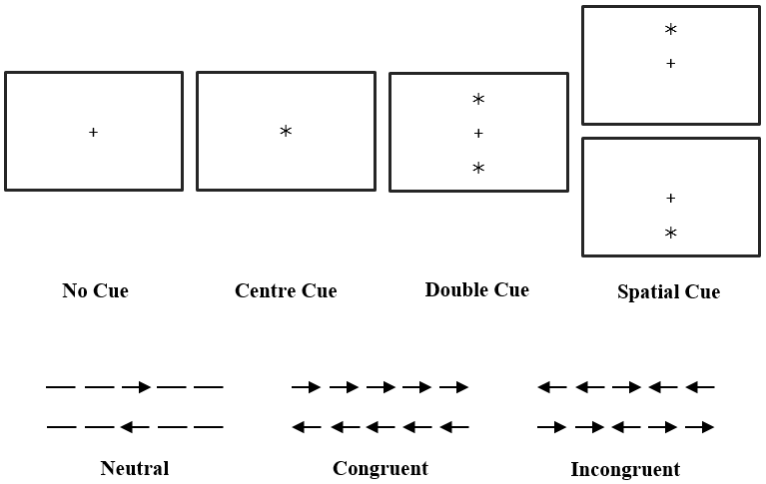

Figure 4.4: The upper row shows all four cue conditions (no cue, centre cue, double cue, spatial cue). The lower row shows all three target conditions (neutral, congruent, incongruent).

4.2.6 Socially Evaluated Cold Pressor Test

The socially evaluated cold pressor test was conducted in accordance to the protocol of Schwabe et al. (2008) with minor changes, described in section 3.2.6. The investigator leading the subject through the SECPT was always of opposite sex to the participant. Therefore two different investigators were needed. Sex, time of investigation and order of tasks were counterbalanced across cold water and warm water conditions, controlling for potential influences of this variables.

4.2.7 Endocrine Stress Response

In total twelve saliva samples were collected, of which nine were subsequently analysed (Sample #02, #04, #06, #07, #08, #09, #10, #11, and #12; cf. Figure 4.1). Samples provided immediately before the first block of the first task (#02), immediately before the first block of the second task (#04), and immediately before the SECPT (#06) served as baseline measure for cortisol level. Samples collected after the SECPT served for measuring cortisol response to the SECPT (#07 -#12). The remaining three samples were collected in order to keep the experimental procedure identical before and after the SECPT. Subjects who completed the socially evaluated cold pressor test were divided into two groups by a median split of their cortisol reactivity in response to the stressor. Reactivity was measured by subtracting baseline cortisol activity (mean of samples #02, #04, #06) from mean cortisol level between 21 and 28 minutes after SECPT onset (samples #09, #10), as this is period when cortisol level are generally highest (Dickerson & Kemeny, 2004). Thus three groups were distinguished: warm water control group, low responder, and high responder. Saliva samples were obtained using Salivette® collection devices (Sarstedt, Nürnbrecht, Germany). Sampling was practiced during the exercise session at the beginning of the experiment. This is why this probe was not analysed subsequently. Sampling instructions were given and adherence monitored via computer. Samples were frozen immediately after the experiment at -20 °C for later biochemical analyses. Salivary cortisol was analysed with a time-

resolved immunoassay with fluorescence detection as described in detail in Dressendörfer et al., 1992. Intra- and interassay variability was less than 10 % and 12 % respectively.

4.2.8 Cardiovascular Stress Response

In total six blood pressure measurements were recorded. Two measurements with a time lag of 90 seconds were recorded while the investigator prepared the cabin for the stress induction procedure. Two measurements were taken during hand immersion, 30 and 120 seconds after initially immersing the hand; another two measurements were taken after hand immersion, 210 and 300 seconds after initially immersing the hand. Time lag between the second and third measurement was at least 90 seconds. Systolic and diastolic blood pressure (SBP, DBP), were recorded with a Dinamap vital signs monitor (Critikon, Tampa, Florida). The cuff was placed on the upper right arm. It was not placed at the left arm, because the left hand was immersed into the water, for participants being able to respond with their right, dominant hand to the cognitive tasks before and after the stress induction procedure.

4.2.9 Subjective Stress Rating

Subjective perception of the SECPT was reviewed with four questions, which participants answered subsequent to the SECPT procedure. Participants rated (1) how difficult it was to keep the hand in the water, (2) how unpleasant the whole situation felt, (3) how stressed they felt during the procedure, and (4) how painful it was to keep the hand in the water. Rating scale ranged from 0 (not at all difficult/unpleasant/stressful/painful) until 100 (very much difficult/unpleasant/stressful/painful) in steps of 10. The rating scale was provided by Lars Schwabe and is identical to the one used in the original procedure (Schwabe et al., 2008).

4.2.10 EEG Recording and Quantification

EEG was recorded with an Easy-Cap electrode system (EasyCap GmbH, Herrsching, Germany) from 62 sites positioned according to the 10-10 electrode reference system (Chatrian et al., 1985): Fp1, Fpz, Fp2, AF7, AF3, AFz, AF4, AF8, F9, F7, F5, F3, Fz, F4, F6, F8, F10, FT7, FC5, FC3, FC1, FC2, FC4, FC6, FT8, T7, C5, C3, C1, Cz, C2, C4, C6, T8, TP9, TP7, CP5, CP3, CP1, CPz, CP2, CP4, CP6, TP8, TP10, P7, P5, P3, P1, Pz, P2, P4, P6, P8, PO9, PO3, PO4, PO10, O1, Oz, O2, and Iz. EOG was recorded from two positions: centred above and below the left eye (m. orbicularis oculi, pars palpebralis and m. orbicularis oculi, pars orbitalis respectively). All sites of EEG and EOG were online referenced to FCz. POz served as ground. Recording, digitalization and processing of data followed the same scheme as for the experiment described in chapter 3. Only deviating steps are described here.

Preprocessing and Independent Component Analysis. No deviations (cf. section 3.2.9, p. 64 ff.). The automatic artefact rejection procedure for sensor-level data led to an average of 10.34 ± .89 % (mean ± S. E.) rejected epochs for the Sternberg task and an average of 10.61 ± 1.11 % for the attention network test.

Equivalent Dipole Fitting. For the Sternberg task, epochs were segmented from -2900 ms to +2300 ms with reference to probe onset. For the attention network test, epochs were segmented from -200 ms to +2900 ms with reference to cue onset. There were no other deviations from the procedure described in section 3.2.9, p. 64 ff. Component artefact rejection led to an average of 18.83 ± .44 (mean ± S. E.) rejected epochs for the Sternberg task and 19.56 ± .54 attention network test.

Clustering and Reclustering components. No deviations (cf. section 3.2.9, p. 64 ff.). For the Sternberg memory task, from a total of 4345 components, 2063 components with reasonable quality remained (mean residual variance: 6.48 %; range: 0.30 – 15.00 %). Each subject contributed on average 30 components (range: 19 - 43). For the attention network test, from a total of 4345 components, 2001 components with reasonable quality remained (mean residual variance: 6.32 %; range: 0.39 - 14.99 %). Each subject contributed on average 29 components (range: 15 - 41). These statistics relate to all 68 subjects whose IC's were initially clustered. In the Sternberg task on average 40 % of ICs were manually selected for the relevant cluster, ranging from 17 % to 56 % for all relevant clusters. In the attention network test on average 32 % of ICs were manually selected, ranging from 5 % to 52 % for the all relevant clusters. The majority of manually picked ICs were from one or two other clusters, meaning that according to k-means criteria these ICs were very similar to each other.

Filtering data and applying Hilbert transform. No deviations (cf. section 3.2.9, p. 64 ff.).

Exploratory analysis of phase-amplitude coupling. No deviations (cf. section 3.2.9, p. 64 ff.).

4.2.11 Statistical Analyses

Statistical analysis were conducted as described in sections 2.2.6 and 3.2.10. The basic hypotheses assumed a block by responder group interaction in the case of behavioural data and a frequency pair by block by responder group interaction in the case of electrophysiological data. Given the sample size of 55 subjects and a significance level of $p = .05$, the two- and three-way interactions could detect a relative small effect of $\Omega^2 \geq .03$ with a probability of $1\text{-}\beta > .90$. These calculations assumed a plausible population correlation of $\rho = .80$ for reaction times and $\rho = .15$ for electrophysiological data (supported by the empirical data). Because the population correlation for errors was much lower than for reaction times ($\rho = .20$), only medium to large effects of $\Omega^2 \geq .08$ could be found with a probability of $1\text{-}\beta > .80$.

Manipulation Check Cortisol Profile. The success of the experimental manipulation, i. e. change of cortisol level during the experiment was checked via a 9 x 3 x 2 ANOVA with the within-subjects factor measurement time (-33, -19, -5, 7, 14, 21, 28, 35, 51 minutes from SECPT onset) and the between-subjects factors responder group (warm water control, low responder, high responder) and sex (male, female) in a repeated measurement factorial design.

Cardiovascular Stress Response (Blood Pressure Measurement). The six blood pressure measurements were combined into three measures before, during, and after the stress. The cardiovascular stress response was measured with the dependent variables systolic and diastolic blood

pressure. Changes were assessed with a 3 x 3 x 2 ANOVA with the within-subjects factor measurement time (before, during, after) and the between-subjects factors responder group (warm water control, low responder, high responder) and sex (male, female) in a repeated measurement factorial design.

Subjective Stress Rating. Subjective stress ratings were analysed with a 4 x 3 x 2 ANOVA with the within-subjects factor question type (difficulty, unpleasantness, stress, pain) and the between-subjects factors responder group (warm water control, low responder, high responder) and sex (male, female) in a repeated measurement factorial design. The dependent variable was participants rating ranging from 0 (not difficult, not unpleasant etc.) to 100 (very difficult, very unpleasant etc.) in steps of 10.

Sternberg Task. Behavioural results (dependent variable: errors, reaction time) in the Sternberg task were analysed by a 2 x 2 x 2 x 3 x 2 ANOVA with the within-subjects factors block (block 1 – before SECPT, block 2 – after SECPT), workload (low, high), and probe type (match, non-match) and the between-subjects factors responder group (warm water control, low responder, high responder) and sex (male, female) in a repeated measurement factorial design. Only trials with correct responses were included in the reaction time analysis. Furthermore reaction time distributions for each subject were calculated. Reaction times exceeding the third quartile of the corresponding distribution (Tukey, 1977) or were faster than 200 ms were deemed outliers and removed for statistical analyses.

Attention Network Test. Behavioural results (dependent variable: reaction time) in the attention network test were analysed by a 2 x 4 x 3 x 3 x 2 x ANOVA with the within-subjects factors block (block 1 – before SECPT, block 2, after SECPT), cue type (no cue, centre cue, double cue, spatial cue), and target type (neutral, congruent, incongruent) and the between-subjects factors responder group (warm water control, low responder, high responder) and sex (male, female) in a repeated measurement factorial design. Only trials with correct responses were included. Furthermore reaction time distributions for each subject were calculated. Reaction times exceeding the third quartile of the corresponding distribution (Tukey, 1977) or were faster than 200 ms were deemed outliers and removed for statistical analyses. Due to very low error rates, errors were not further analysed. Participants made on average 1.50 % errors, ranging from 0.00 to 4.43 %.

Exploratory phase-amplitude coupling. Identical to the procedure in chapter 3, the comodulogram was split into five distinct frequency pairs, namely delta-beta coupling, delta-gamma coupling, theta-beta coupling, theta-gamma coupling, and beta-gamma coupling (Figure 3.5). The chosen division is in accordance with the natural logarithmic relationship between brain oscillations (Penttonen & Buzsáki, 2003) and will be further justified by the found coupling pattern (cf. Figure 4.12 and Figure 4.22). Coupling values within these frequency pairs were averaged and subsequently submitted to a 2 x 5 x 2 x 2 x 2 x 3 x 2 ANOVA with the repeated measurement factors hemisphere (left, right), frequency pair (delta-beta, delta-gamma, theta-beta, theta-gamma, beta-gamma), block (before SECPT, after SECPT), workload (low, high), and probe type (match, non-match) as well as the between-subjects factors responder group (warm water controls, low responders, high responders) and

sex (male, female) in the case of the Sternberg task. In contrast to reaction times for the attention network test, phase-amplitude coupling for the attention network test was not calculated separately for all cue and target conditions, but only for each cue condition, averaged over all target conditions, and for each target condition averaged over all cue conditions. This was done in order to reduce calculation time and to increase the amounts of trials per condition (max. 48 trials for each cue condition and max. 64 trials for each target type versus max. 16 trials for a fully crossed design). Therefore, averaged coupling values were submitted to a 2 x 5 x 2 x 2 x 3 x 2 ANOVA with the repeated measurement factors hemisphere, frequency pair, block, and cue type (no cue, double cue), as well as the between-subjects factors responder group and sex in the case of the alerting network of the attention network test. Averaged coupling values were submitted to a 2 x 5 x 2 x 2 x 3 x 2 ANOVA with the repeated measurement factors hemisphere, frequency pair, block, and cue type (centre cue, spatial cue), as well as the between-subjects factors responder group and sex in the case of the orienting network of the attention network test. Averaged coupling values were submitted to a 2 x 5 x 2 x 3 x 3 x 2 ANOVA with the repeated measurement factors hemisphere, frequency pair, block, and target type (neutral, congruent, incongruent), as well as the between-subjects factors responder group and sex in the case of the executive control network of the attention network test.

Correlations between modulation indices and reaction times. Reaction times in the Sternberg task and attention network test were correlated with the corresponding modulation indices (Spearman's rho). Correlations between modulation indices and error rates were not calculated, because phase-amplitude coupling was only calculated for correct trials.

4.3 Results

4.3.1 Manipulation Check: Endocrine Stress Response

Participants completing the cold water condition of the SECPT were split into low and high responders according to a median split (median: 1.80 nmol/l) of their cortisol reactivity as described in section 4.2.7. Low responders (n = 17) had a mean increase ± S. E. of .05 ± .19 nmol/l. High responders (n = 18) had a mean increase ± S. E. of 5.36 ± .85 nmol/l. The warm water control group (n = 20) had a mean increase ± S. E. of -.63 ± .17 nmol/l.

Cortisol level showed a significant main effect time of measurement ($F_{(8,392)} = 22.79$, $p < .001$, $\omega^2 = .26$) and main effect responder group ($F_{(2,49)} = 12.25$, $p < .001$, $\omega^2 = .29$) which were further qualified by a time of measurement and responder group interaction ($F_{(16,392)} = 27.90$, $p < .001$, $\omega^2 = .47$, $\text{Dunn}_{\text{crit}} = 1.32$). Also the main effect sex ($F_{(1,49)} = 5.40$, $p < .001$, $\omega^2 = .07$) reached significance.

Post hoc tests revealed that cortisol level of the warm water control group and low responder group did not change significantly in the course of the experiment. Only high responder's cortisol level increased significantly after the stress procedure (from + 7 minutes onward), had a plateau between 21 and 35 minutes after the stress procedure and then decreased from 35 minutes onwards after stress onset

(Figure 4.5). Cortisol level of high responders on the one side and both warm water controls and low responders on the other side differed significantly between 14 and 51 minutes after SECPT onset. High responders thereby constantly having the highest and the warm water control group constantly having the lowest level. Low responders exhibited significantly higher cortisol level than warm water controls between 14 and 21 minutes after the stress procedure. Men (4.09 ± .33 nmol/l) exhibited overall higher cortisol level than women (3.01 ±. 32 nmol/l), but sexes did not show a generally different stress response.

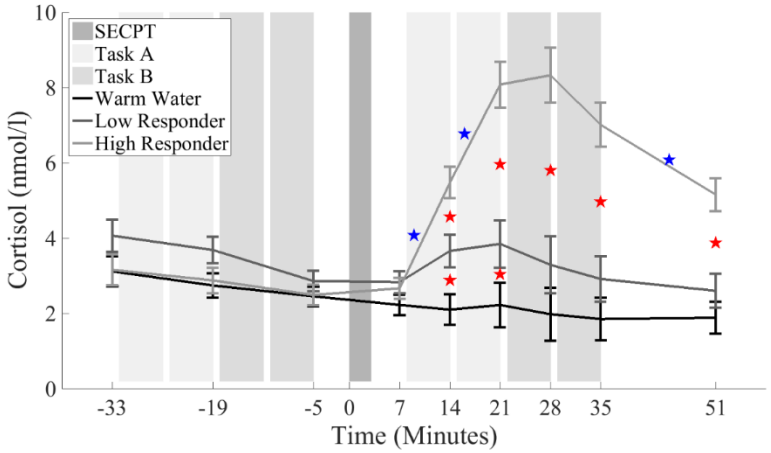

Figure 4.5: Cortisol profile (mean ± S. E.) for each experimental group over the course of the experiment. The experimental procedure was identical for both possible task orders (ANT first, Sternberg first) because the length of task was identical. Red stars mark significant differences between high responders and both low responders and warm water controls (upper row of red stars) and between low responders and warm water controls (lower row of red stars). Blue stars mark significant changes in cortisol level within high responders.

4.3.2 Manipulation Check: Cardiovascular Stress Response

Males had overall lower diastolic blood pressure than females (males: 73.73 ± 1.59 mmHg; females: 78.80 ± 1.52 mmHg; $F_{(1,49)} = 5.33$, $p = .025$, $\omega^2 = .07$). For both systolic and diastolic blood pressure, there were significant main effects measurement time (DBP: $F_{(2,98)} = 139.45$, $p < .001$, $\omega^2 = .63$; SBP: $F_{(2,98)} = 93.03$, $p < .001$, $\omega^2 = .53$) and responder group (DBP: $F_{(2,49)} = 10.43$, $p < .001$, $\omega^2 = .26$; SBP: $F_{(2,49)} = 4.40$, $p = .018$, $\omega^2 = .11$), which were further qualified by a measurement time by responder group interaction (DBP: $F_{(4,98)} = 20.91$, $p < .001$, $\omega^2 = .33$, $\text{Dunn}_{\text{crit}} = 4.86$; SBP: $F_{(4,98)} = 16.20$, $p < .001$, $\omega^2 = .27$, $\text{Dunn}_{\text{crit}} = 7.01$; Figure 4.6).

These interactions revealed that both systolic and diastolic blood pressure, were significantly elevated during the stress procedure for low and high responders but did not change for the warm water control group. Low responders' diastolic blood pressure was still elevated after the stress procedure compared to before the stress procedure, while high responders diastolic blood pressure after the SECPT did not differ from the values before the SECPT. The increase of blood pressure in low and high responders led to significant group differences between warm water controls on the one side and low and high responders on the other side during and after the stress induction procedure. Groups did not

differ in their blood pressure level before the stress induction procedure, but during and after the SECPT. Low and high responders thereby had higher level than warm water controls, but did not differ between each other.

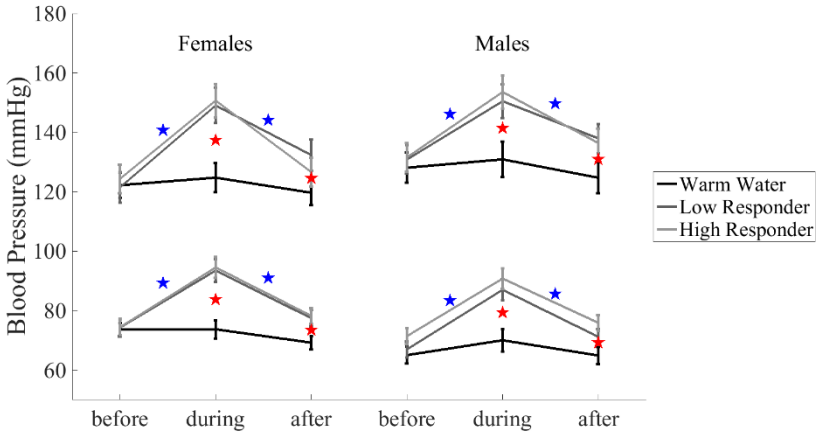

Figure 4.6: Cardiovascular profile (mean ± S. E.) for each experimental group and sex before, during, and after the SECPT. Red stars mark significant differences between warm water controls and both low and high responders. Blue stars mark significant changes within low and high responders. Low responders diastolic blood pressure was still significantly elevated after the stress procedure compared to before the stress procedure, but is not labelled with a star in this figure.

4.3.3 Manipulation Check: Subjective Stress Ratings

Male participants rated their subjective experience as significantly less aversive than females (males: 43.57 ± 3.60; females: 55.93 ± 3.45; $F_{(1,49)} = 6.14$, $p = .017$, $\omega^2 = .09$). There was a small main effect for question type ($F_{(3,147)} = 3.06$, $p = .042$, $\omega^2 = .03$) and a large main effect for responder group ($F_{(2,49)} = 68.63$, $p < .001$, $\omega^2 = .71$). These effects were further qualified by a question by responder group interaction ($F_{(6,147)} = 4.75$, $p = .001$, $\omega^2 = .09$, $\text{Dunn}_{\text{crit}} = 15.01$; Figure 4.7).

The warm water group rated averseness of the procedure in all questions significantly lower than low and high responders. Low and high responders did not differ significantly in their ratings. The warm water control group rated their experience as significantly less painful and difficult then unpleasant. Low responders rated their experience as significantly less stressful than painful. High responders' ratings did not differ with regards to question type.

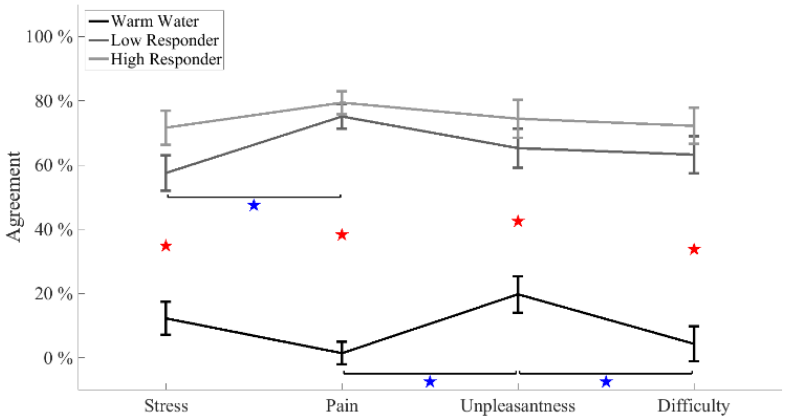

Figure 4.7: Subjective stress rating profile (mean ± S. E.) for each experimental group. Red stars mark significant differences between warm water controls and both low and high responders. Blue stars mark significant differences within experimental groups.

4.3.4 Sternberg Working Memory Task

Behavioural Data

Sternberg Task – Reaction Times. Subjects responded on average 28 ms faster in the second compared to the first block (block 1: 736.92 ± 18.80 ms; block 2: 708.54 ± 15.04 ms; $F_{(1,49)} = 10.00$, $p = .003$, $\omega^2 = .08$), indicating a practice effect. Typical results of Sternberg paradigms were replicated. On average higher workload slowed reaction times down by 49 ms (low workload: 698.40 ± 16.04 ms; high workload: 747.06 ± 17.07 ms; $F_{(1,49)} = 126.15$, $p < .001$, $\omega^2 = .53$). Subjects responded on average 31 ms faster to matches than non-matches (matches: 707.00 ± 17.03 ms; non-matches: 738.46 ± 16.53 ms; $F_{(1,49)} = 20.82$, $p < .001$, $\omega^2 = .15$). Workload and probe type were further qualified by an ordinal interaction ($F_{(1,49)} = 23.17$, $p < .001$, $\omega^2 = .09$; Figure 4.9) which was in turn qualified by a workload by probe type by responder group interaction ($F_{(2,49)} = 3.89$, $p = .027$, $\omega^2 = .03$, $\text{Dunn}_{\text{crit}} = 26.12$; Figure 4.8; Table 4.2). These interactions revealed that reaction time differences between match and non-match trials within high workload trials were much smaller – and even insignificant in the three-way interaction – compared to low workload trials. Participants responded always, i. e. in both workload conditions, significantly faster to matches than to non-matches. Lastly, warm water controls responded faster than both low and high responders, in low workload – non-match and high workload – match trials. Low and high responders did not differ significantly from each other in their reaction times.

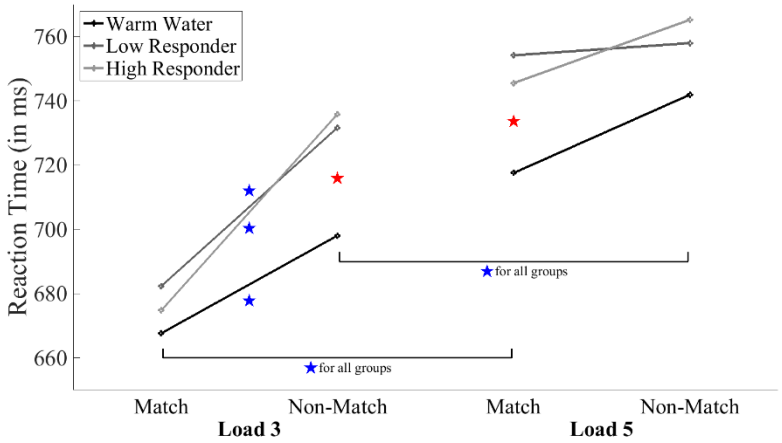

Figure 4.8: Mean reaction times for the workload by probe type by responder group interaction. Standard error bars are omitted here, because they obstruct the clarity of the figure. Standard errors can be found in Table 4.2. Red stars mark differences between warm water controls and both low and high responders. Blue stars mark differences within responder groups between different workload and probe type conditions.

Table 4.2: Mean reaction times (S. E.) in ms in the Sternberg task for the workload by probe type by responder group interaction. Differences exceeding $Dunn_{crit}$ = 26.12 are significant.

		Responder Group		
		Warm Water Controls	Low Responders	High Responders
Load 3	Match	667.64 (28.16)	682.33 (29.98)	674.78 (29.08)
	Non-Match	698.07 (27.03)	731.67 (28.78)	735.89 (27.92)
Load 5	Match	717.55 (29.72)	754.18 (31.64)	745.52 (30.69)
	Non-Match	741.90 (29.02)	757.98 (30.89)	765.23 (29.97)

Sternberg Task – Errors. Error rates ranged from .83 to 23.75 % (median: 6.25 %). Higher workload led to more errors (load 3: 2.51 ± .30 %; load 5: 4.84 ± 39 %; $F_{(1,49)} = 90.81$, $p < .001$, $\omega^2 = .45$). Subjects made more errors when responding to matches than to non-matches (match: 4.92 ± .52 %; non-match: 2.43 ± .22 %; $F_{(1,49)} = 28.88$, $p < .001$, $\omega^2 = .20$). These effects were further qualified by an ordinal interaction ($F_{(1,49)} = 16.31$, $p < .001$, $\omega^2 = .07$, $Dunn_{crit} = .56$ [critical difference relates the absolute amount of errors]; Figure 4.9). Sex and probe type (match vs. non-match) interacted significantly ($F_{(1,49)} = 6.57$, $p = .014$, $\omega^2 = .05$, $Dunn_{crit} = 1.03$ [critical difference relates the absolute amount of errors]). Only males made significantly more errors to matches (5.27 ± .75 %) than to non-matches (1.58 ± .32 %). The pattern in females was the same but error rates did not differ significantly between matches (4.58 ± .72 %) and non-matches (3.27 ± .31 %). Males and females did not differ in their total amount of errors.

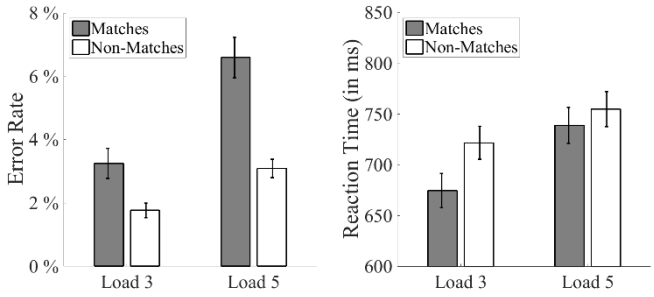

Figure 4.9: Mean error rates ± S. E. (left panel) and mean reaction times ± S. E. (right panel) for the workload by probe type interaction. All differences within each dependent variable domain are significant.

Electrophysiological Data

Sternberg Task – Clustering Results. Average scalp maps of all ICs of each cluster and their corresponding residual variance are shown in Figure 4.10. Dipole locations for all ICs in these clusters are depicted in Appendix E.

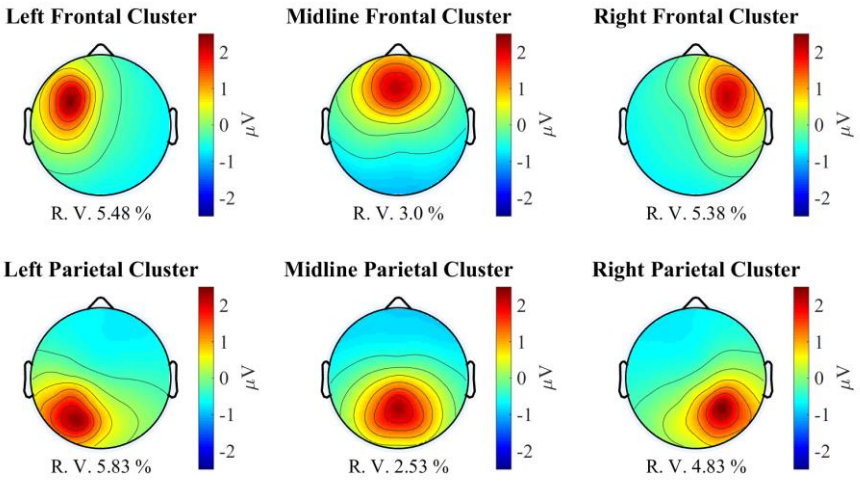

Figure 4.10: Final clusters of independent components found for the Sternberg task for all six regions of interest. For ICs in these clusters phase-amplitude coupling was calculated either within the frontal clusters or between frontal and parietal clusters.

Sternberg Task – Initial Screening for Phase-Amplitude Coupling in Nine Networks. Only coupling within the left and right fronto-frontal network (i. e. coupling within one source) was found to be significant over the whole sample and all conditions (Figure 4.11). The screening indicated that gamma amplitude was nested within the beta cycle. Also delta-beta coupling within these two fronto-frontal networks showed the tendency for significance. Based on these screening analyses, all further analyses were restricted to the left and right fronto-frontal networks. In addition to the here evident

pattern of beta-gamma coupling, some subjects also showed theta-beta coupling. However this was not a characteristic of the majority of subjects.

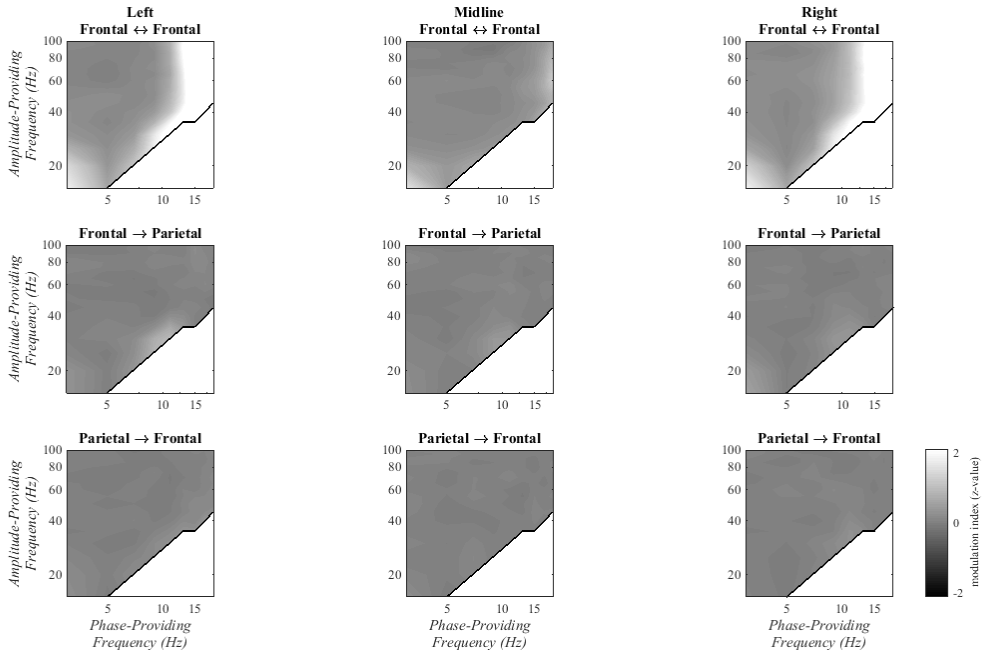

Figure 4.11: Screening of nine networks for phase-amplitude coupling within the Sternberg task (see titles of panels for network name). Frequency pairs within the white triangle at the right bottom corner were not calculated because they represent frequency pairs where phase-providing and amplitude-providing frequency bands overlap. Only the left and right fronto-frontal network exhibit significant phase-amplitude coupling between beta and gamma frequencies (upper right corner) as well as indicate potential coupling between delta and beta (lower left corner). Z-values > 1.99 are considered as significant coupling. Here greyscale shading is chosen to enhance the difference between significant and nonsignificant coupling.

Sternberg Task – Phase-Amplitude Coupling in Fronto-Frontal Networks. Coupling between beta and gamma was significant (5.40 ± 1.15) and significantly different from all other frequency pairs (delta-beta [1.07 ± .19], delta-gamma [.18 ± .05], theta-beta [.78 ± .24], theta-gamma [.24 ± .07]; $F_{(4,196)} = 17.05$, $p < .001$, $\omega^2 = .19$, $\text{Dunn}_{\text{crit}} = 2.15$). Neither of the other frequency pairs exhibited significant coupling nor differed between each other in their coupling strength (Figure 4.12).

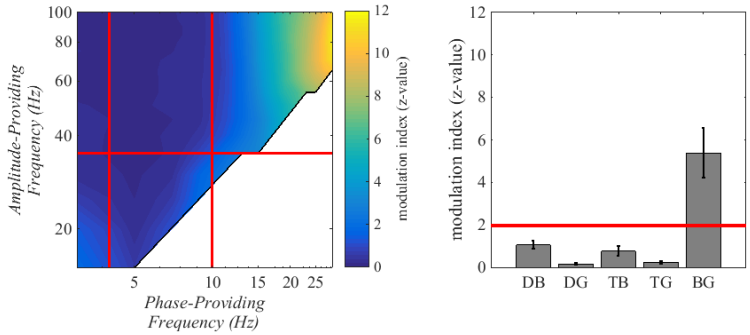

Figure 4.12: Comodulogram during the Sternberg task of the fronto-frontal network averaged over hemispheres, blocks, trial types, and experimental groups. The bar plot shows mean modulation indices ± S. E. for each frequency pair. The red line marks the significance threshold. Please note that axes scaling for the comodulogram is different from that in Figure 4.11. Here coloured shading is chosen to enhance visibility of modulation index graduation.

The preferred phase of beta-gamma coupling is 40° to 60°, representing the range of decreasing phases of the low-frequency oscillation; amplitudes are lowest at -140° to -120°, representing the range of increasing phases of the low-frequency oscillation (Figure 4.13).

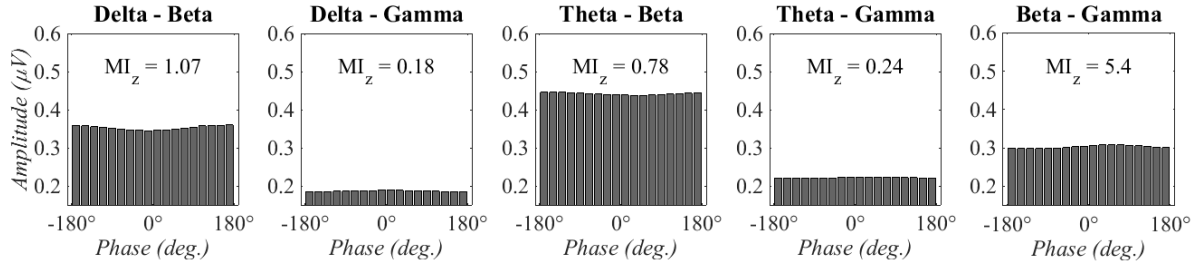

Figure 4.13: Phase-amplitude plots for each frequency pair and its corresponding standardised modulation index value (MI_z) for the Sternberg task. Mean amplitudes are averaged over all participants, hemispheres, blocks, and trials types.

Furthermore there was a small block by probe by responder group interaction ($F_{(2,49)} = 4.23$, $p = .020$, $\omega^2 = .03$, $Dunn_{crit} = .54$; Figure 4.14, Table 4.3). Please note that for reaction times there was a workload by probe by responder group interaction, here however block interacted with probe and responder group.

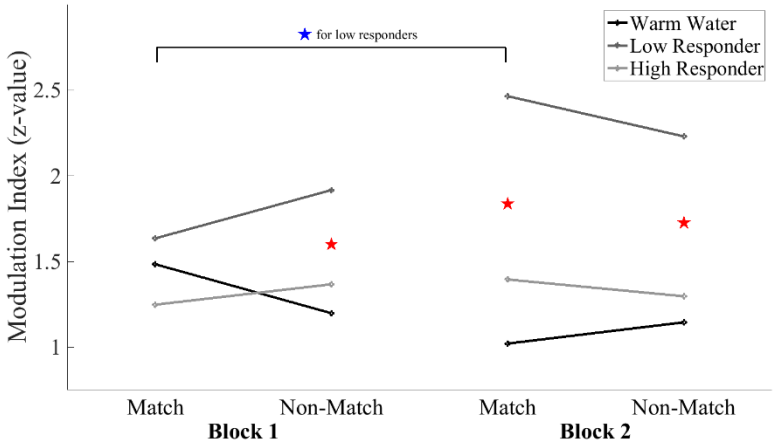

Figure 4.14: Mean modulation indices for the block by probe type by responder group interaction. Standard error bars are omitted here, because they obstruct the clarity of the figure. Standard errors can be found in Table 4.3. Red stars mark differences between warm low responders and both water controls and high responders. The blue star marks the difference within low responders between block 1 and block 2 for the match condition.

Table 4.3: Mean modulation indices (S. E.) in the Sternberg task for each block, probe type, and responder group. Averaged over hemispheres, frequency pairs, workloads, and sexes. Values printed in bold represent significant coupling. Differences exceeding $Dunn_{crit}$ = .54 are significant.

		Responder Group		
		Warm Water Controls	Low Responders	High Responders
Block 1	Match	1.48 (.41)	1.64 (.43)	1.25 (.42)
	Non-Match	1.20 (.43)	1.92 (.46)	1.37 (.44)
Block 2	Match	1.02 (.46)	**2.47 (.49)**	1.40 (.47)
	Non-Match	1.15 (.45)	**2.23 (.48)**	1.30 (.47)

There was a small interaction between hemisphere, block, responder group and sex ($F_{(2,49)}$ = 4.07, p = .023, ω^2 = .03, $Dunn_{crit}$ = 1.85; Figure 4.15, Table 4.4), which revealed that only male low responders had significantly increased phase-amplitude coupling strength in the second compared to the first block in the left fronto-frontal network. Because of this increase, in block 2, their coupling strength was significantly higher in the left compared to the right hemisphere. Furthermore, because of this increase, in block 2, low responders had significantly stronger coupling than both warm water controls and high responders. There were no other significant responder group differences, neither in females nor in males. Furthermore, neither females nor males exhibited any other significant differences in coupling strength between left and right hemisphere or coupling strength changes from block 1 to block 2. There were however differences between sexes in their coupling strength. Males and females of the low responder group differed in their coupling strength in block 2 for both left and right hemisphere. Males had stronger coupling than females in the left hemisphere, while females had stronger coupling than males in the right hemisphere. High responders showed significant sex differences in the right hemisphere during block 1, where females exhibited stronger coupling than males. These coupling

values are averaged over all frequency pairs, as the factor frequency pair did not contribute to this interaction.

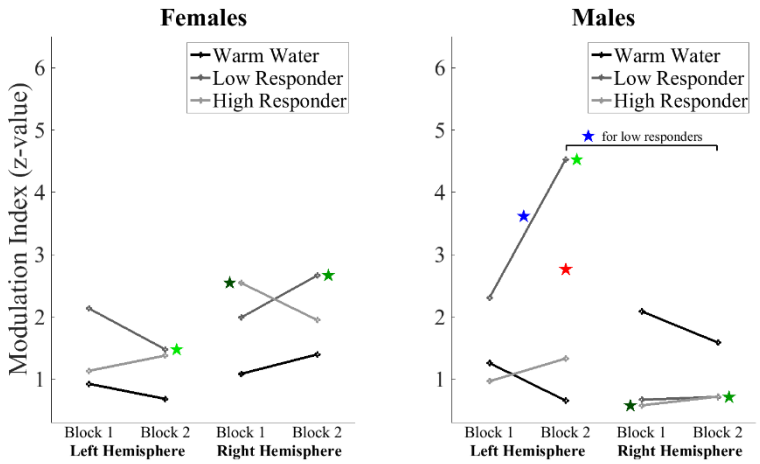

Figure 4.15: Mean modulation indices for the hemisphere by block by responder group by sex interaction. Standard error bars are omitted here, because they obstruct the clarity of the figure. Standard errors can be found Table 4.4. The red star marks the difference between low responders and both warm water controls and high responders. Blue stars mark significant coupling strength differences within low responders. Green stars mark differences in coupling strength between sexes for otherwise constant conditions (light green: low responders, left hemisphere, block 2; medium green: low responders, right hemisphere, block 2; dark green: high responders, right hemisphere, block 1). For a simplified graphical depiction of this effect see Figure 4.23.

Table 4.4: Mean modulation indices (S. E.) in the Sternberg task for each hemisphere, block, responder group, and sex. Averaged over frequency pairs, workloads, and probe types. Values printed in bold represent significant coupling. Differences exceeding $Dunn_{crit} = 1.85$ are significant.

			Responder Group		
			Warm Water Controls	Low Responders	High Responders
Males	Left Hemisphere	Block 1	1.26 (.93)	**2.31 (.87)**	.97 (.87)
		Block 2	.66 (1.22)	**4.53 (1.15)**	1.33 (1.15)
	Right Hemisphere	Block 1	**2.09 (.69)**	.67 (.65)	.58 (.65)
		Block 2	1.59 (.63)	.72 (.59)	.72 (.59)
Females	Left Hemisphere	Block 1	.93 (.76)	**2.13 (.93)**	1.14 (.87)
		Block 2	.69 (1.00)	1.48 (1.22)	1.38 (1.15)
	Right Hemisphere	Block 1	1.09 (.56)	**1.99 (.69)**	**2.55 (.65)**
		Block 2	1.40 (.51)	**2.67 (.63)**	1.95 (.59)

Sternberg Task – Correlations between modulation indices and reaction times. Behaviour, in form of reaction times, significantly and positively correlated with modulation indices within the left hemisphere for beta-gamma coupling. This was only true for match trials, except match trials in block 2 for high workload. Significant correlations explained 7 to 16 % of variance (according to r^2). Correlations for non-match trials and match trial in block 2 for load 5 did not become significant. Furthermore, theta-beta coupling modulation indices were consistently negatively correlated with

reaction times in the left hemisphere. In both blocks these correlations became only significant for high workloads (load 5). Additionally some correlations in other frequency pairs became significant. However, no specific patterns emerged. Positive correlations reflect that the higher the modulation indices, the longer the reaction times. Negative correlations reflect that the higher the modulation indices, the shorter the reaction times. All exact correlation values can be found in Table 4.5.

Calculating correlations separately for responder groups did not reveal systematically different correlations patterns (data not shown). Calculating correlations separately for sexes however did reveal systematically different correlations patterns for beta-gamma coupling (Figure 4.16). Females' reaction times and modulation indices were significantly correlated within the left hemisphere explaining 15 to 34 % of variance. Two correlations (block 1/low workload/non-match and block 2/high workload/non-match) did not reach significance. In the right hemisphere correlations were weaker explaining between 1 and 11 % of variance but nevertheless were consistently positive. Males did not show any significant coupling between reaction times and modulation indices, but descriptively showed a very different pattern of correlation strength than females did. For males, especially the right hemisphere showed a consistent pattern of correlation strength than females did. For males, especially the right hemisphere showed a consistent pattern of negative correlations in block 1 and zero correlations in block 2.

Table 4.5: Spearman's rho correlations between modulation indices and reaction times in the Sternberg task for each hemisphere, frequency pair, block, and trial type. Significant correlations are printed in bold.

				Frequency Pair				
				Delta-Beta (N = 55)	Delta-Gamma (N = 55)	Theta-Beta (N = 55)	Theta-Gamma (N = 55)	Beta-Gamma (N = 55)
Left Hemisphere	Block 1	Load 3	Match	.12	-.08	-.14	.15	**.27***
			Non-match	.07	**-.47****	-.10	.15	.11
		Load 5	Match	.11	.17	-.24†	-.5	**.40****
			Non-match	-.05	-.17	**-.32***	.07	.11
	Block 2	Load 3	Match	-.08	-.23†	-.06	.06	**.28***
			Non-match	.02	-.11	-.19	.19	.05
		Load 5	Match	-.05	.07	**-.30***	.04	.11
			Non-match	-.10	.11	**-.28***	.12	.10
Right Hemisphere	Block 1	Load 3	Match	.12	.16	.12	-.11	.14
			Non-match	.00	-.11	-.01	.08	-.01
		Load 5	Match	.01	.17	.04	.21	.08
			Non-match	**.28***	-.04	.26†	-.24†	-.03
	Block 2	Load 3	Match	-.08	.01	-.03	-.16	.07
			Non-match	.07	**.34***	.02	-.06	.11
		Load 5	Match	.12	.15	.04	.16	.18
			Non-match	.21	.00	.15	.02	.08

**$p < .01$. *$p < .05$. †$p < .10$.

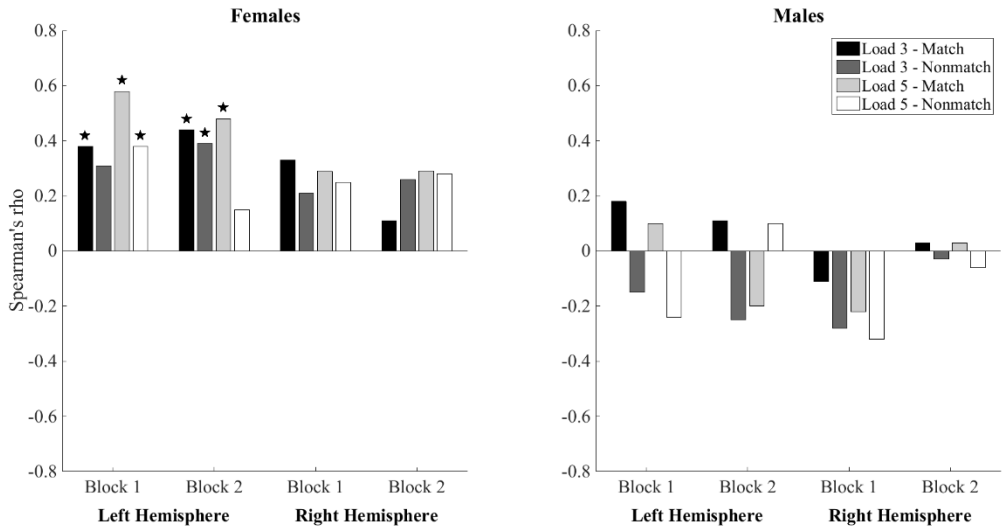

Figure 4.16: Spearman's rho correlations between modulation indices and reaction times in the Sternberg task for beta-gamma coupling in each hemisphere, block, and trial type separately listed for females and males. Significant correlations are marked with a black star ($p < .05$).

4.3.5 Attention Network Test

Behavioural Data

Attention Network Test – Reaction Times. There was a significant main effect block ($F_{(1,49)} = 7.97$, $p = .007$, $\omega^2 = .06$), indicating a practice effect: participants became on average 13 seconds faster in the second (618.86 ± 8.55 ms) compared to the first block (631.73 ± 9.70 ms). There was a significant main effect cue type ($F_{(3,147)} = 534.69$, $p < .001$, $\omega^2 = .88$) with monotonically decreasing reaction times from no cue over central and double to spatial cue. All differences were significant. Additionally there was a significant main effect target type ($F_{(2,98)} = 145.15$, $p < .001$, $\omega^2 = .64$) with monotonically decreasing reaction times from incongruent over congruent to neutral targets. All differences were significant. These two effects were further qualified by a small ordinal interaction cue by target ($F_{(6,294)} = 4.94$, $p < .001$, $\omega^2 = .03$, $\text{Dunn}_{crit} = 10.42$). Mean reaction times and standard error for this interaction are depicted in Figure 4.17. All differences are significant except the following three: reaction times between centre and double cue did not differ for neutral and congruent trials and reaction times between neutral and congruent trials did not differ for spatial cues. The block by target type interaction became significant ($F_{(2,98)} = 7.47$, $p = .001$, $\omega^2 = .04$, $\text{Dunn}_{crit} = 6.81$; Table 4.6), displaying smaller reaction time differences between target types in block 2, compared to block 1. Furthermore reaction time differences were larger for incongruent than for neutral and congruent trials. The main effect sex ($F_{(1,49)} = 5.41$, $p = .024$, $\omega^2 = .07$) was further qualified by a cue type by sex interaction ($F_{(3,147)} = 7.33$, $p < .001$, $\omega^2 = .08$, $\text{Dunn}_{crit} = 12.20$), showing that male participants (604.71 ± 12.78 ms) are generally 41 seconds faster than females (645.89 ± 12.26 ms). Additionally males do not show reaction time differences between centre and double cue, while females do (Figure 4.17). Other significant effects did not explain more than 3 % of variance and are therefore not reported here.

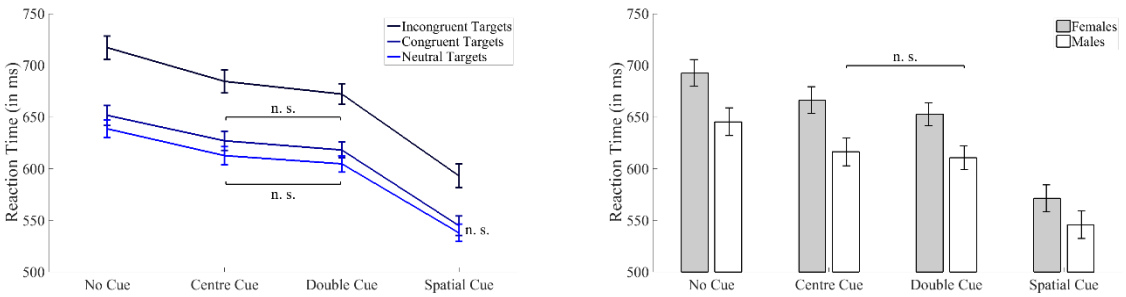

Figure 4.17: The left panel shows mean reaction times ± S. E. for the cue type by target type interaction. All differences except the labelled ones are significant. Right panel shows mean reaction times ± S. E. for the cue type by sex interaction. All differences except the labelled ones are significant.

Table 4.6: Mean reaction times (S. E.) in ms for the attention network test for the block by trial type interaction. All differences are significant ($Dunn_{crit}$ = 6.81). However, differences between target types become smaller in the second compared to the first block. Furthermore difference is largest for incongruent trials compared to both other target types.

	Trial Type		
	Neutral	Congruent	Incongruent
Block 1	603.03 (8.87)	615.11 (9.29)	677.07 (11.94)
Block 2	594.11 (7.87)	605.87 (8.78)	656.60 (9.86)

Electrophysiological Data

Attention Network Test – Clustering Results. Scalp maps of the mean IC activations of each cluster and their corresponding residual variance can be found in Figure 4.18. Dipole locations are depicted in Appendix E.

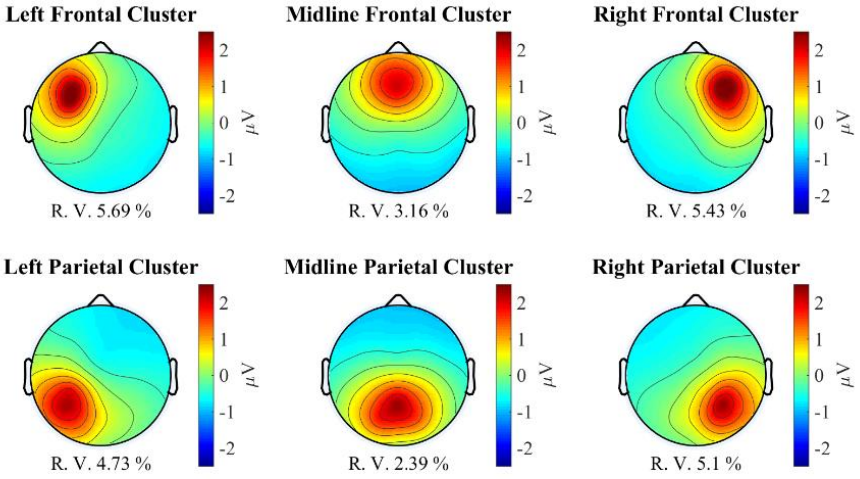

Figure 4.18: Final clusters of independent components found for the attention network test for all six regions of interest. For ICs in these clusters phase-amplitude coupling was calculated either within the frontal clusters or between frontal and parietal clusters.

Attention Network Test – Initial Screening for Phase-Amplitude Coupling in Nine Networks. Only coupling within the left and right fronto-frontal network (i. e. coupling within one source) was found to be significant over the whole sample and all conditions for alerting, orienting, and executive control (Figure 4.19, Figure 4.20, Figure 4.21). The screening indicated that gamma amplitude was nested within the beta cycle. For executive control, also delta-beta coupling within these two fronto-frontal networks showed the tendency for significance. Based on these screening analyses, all further analyses were restricted to the left and right fronto-frontal networks.

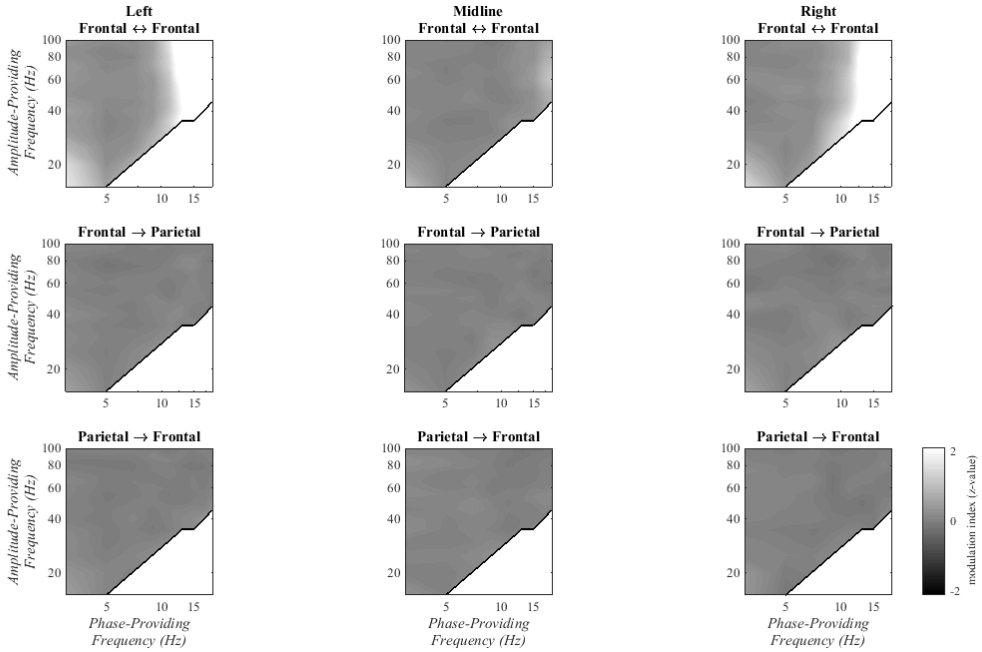

Figure 4.19: Screening of nine networks for phase-amplitude coupling within the alerting network of the attention network test (see titles of panels for network name). Frequency pairs within the white triangle at the right bottom corner were not calculated because they represent frequency pairs where phase-providing and amplitude-providing frequency bands overlap. Only the left and right fronto-frontal network exhibit significant phase-amplitude coupling between beta and gamma frequencies (upper right corner). Z-values > 1.99 are considered as significant coupling. Here greyscale shading is chosen to enhance the difference between significant and nonsignificant coupling.

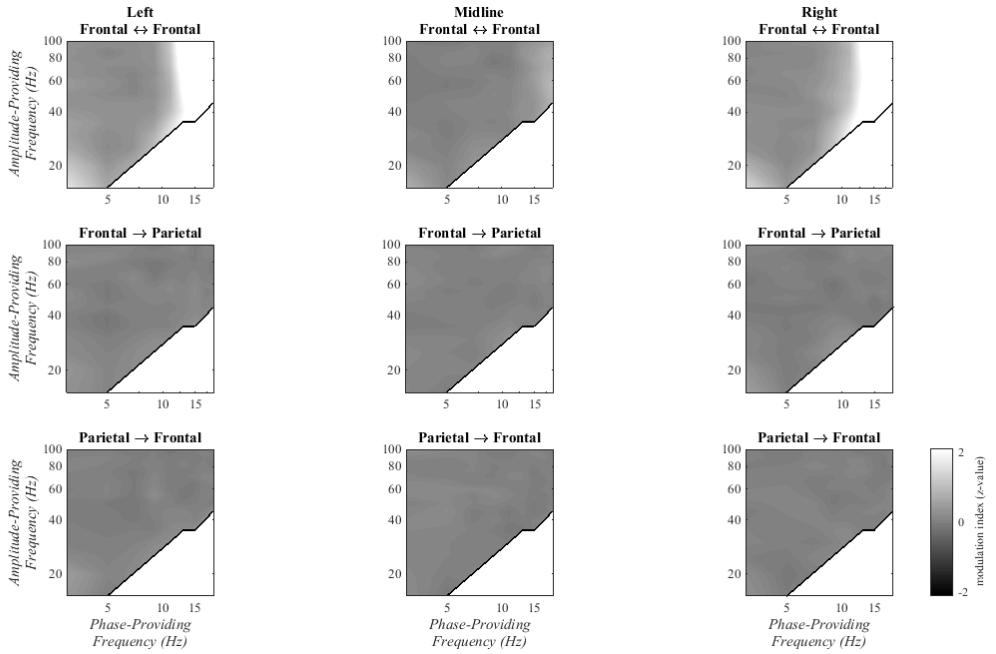

Figure 4.20: Screening of nine networks for phase-amplitude coupling within the orienting network of the attention network test (see titles of panels for network name). Frequency pairs within the white triangle at the right bottom corner were not calculated because they represent frequency pairs where phase-providing and amplitude-providing frequency bands overlap. Only the left and right fronto-frontal network exhibit significant phase-amplitude coupling between beta and gamma frequencies (upper right corner). Z-values > 1.99 are considered as significant coupling. Here greyscale shading is chosen to enhance the difference between significant and nonsignificant coupling.

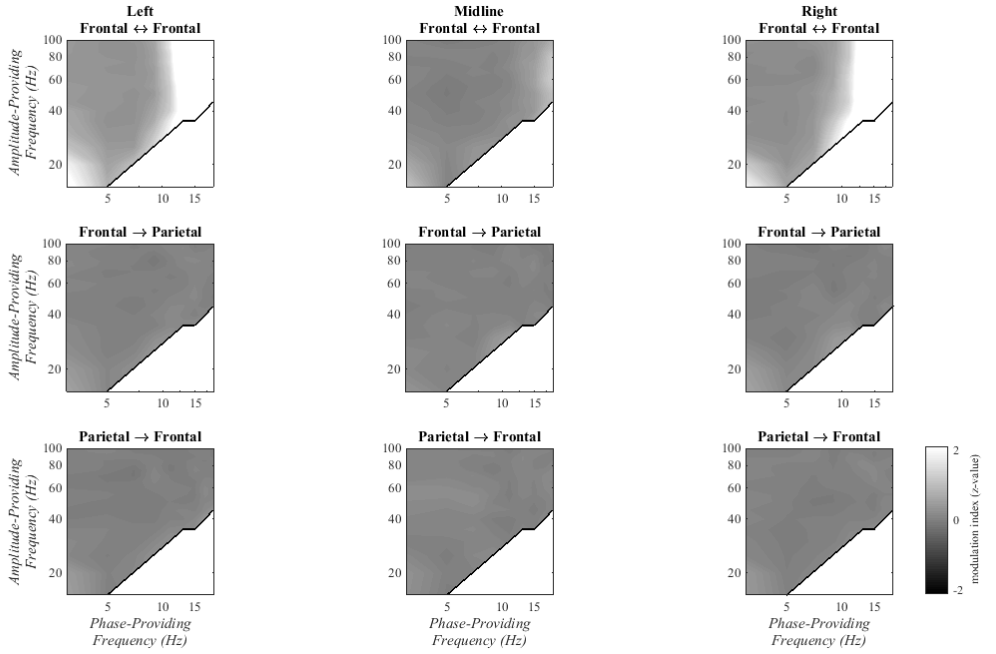

Figure 4.21: Screening of nine networks for phase-amplitude coupling within the executive control network of the attention network test (see titles of panels for network name). Frequency pairs within the white triangle at the right bottom corner were not calculated because they represent frequency pairs where phase-providing and amplitude-providing frequency bands overlap. Only the left and right fronto-frontal network exhibit significant phase-amplitude coupling between beta and gamma frequencies (upper right corner) as well as indicate potential coupling between delta and beta (lower left corner). Z-values > 1.99 are considered as significant coupling. Here greyscale shading is chosen to enhance the difference between significant and nonsignificant coupling.

Attention Network Test – Phase-Amplitude Coupling in Fronto-Frontal Networks. Coupling between beta and gamma was significant and significantly different from all other frequency pairs (alerting: $F_{(4,196)} = 25.45$, $p < .001$, $\omega^2 = .26$, $\text{Dunn}_{\text{crit}} = 2.24$; orienting: $F_{(4,196)} = 24.95$, $p < .001$, $\omega^2 = .26$, $\text{Dunn}_{\text{crit}} = 2.28$; executive control: $F_{(4,196)} = 26.54$, $p < .001$, $\omega^2 = .27$, $\text{Dunn}_{\text{crit}} = 2.86$; Figure 4.22, upper row). Neither of the other frequency pairs exhibited significant coupling nor differed between each other in their coupling strength. Men exhibited overall stronger coupling than women (alerting: $F_{(1,49)} = 4.38$, $p = .042$, $\omega^2 = .06$; orienting: $F_{(1,49)} = 5.50$, $p = .023$, $\omega^2 = .08$; executive control: $F_{(1,49)} = 5.18$, $p = .027$, $\omega^2 = .07$). The main effects were qualified by a frequency pair by sex interaction (alerting: $F_{(4,196)} = 4.01$, $p = .049$, $\omega^2 = .04$, $\text{Dunn}_{\text{crit}} = 3.54$; orienting: $F_{(4,196)} = 4.68$, $p = .034$, $\omega^2 = .05$, $\text{Dunn}_{\text{crit}} = 3.60$; executive control: $F_{(4,196)} = 4.22$, $p = .044$, $\omega^2 = .04$, $\text{Dunn}_{\text{crit}} = 4.51$; Figure 4.22, lower row), revealing that men solely exhibited stronger beta-gamma coupling than women, while sexes did not differ in their coupling strength of other frequency pairs.

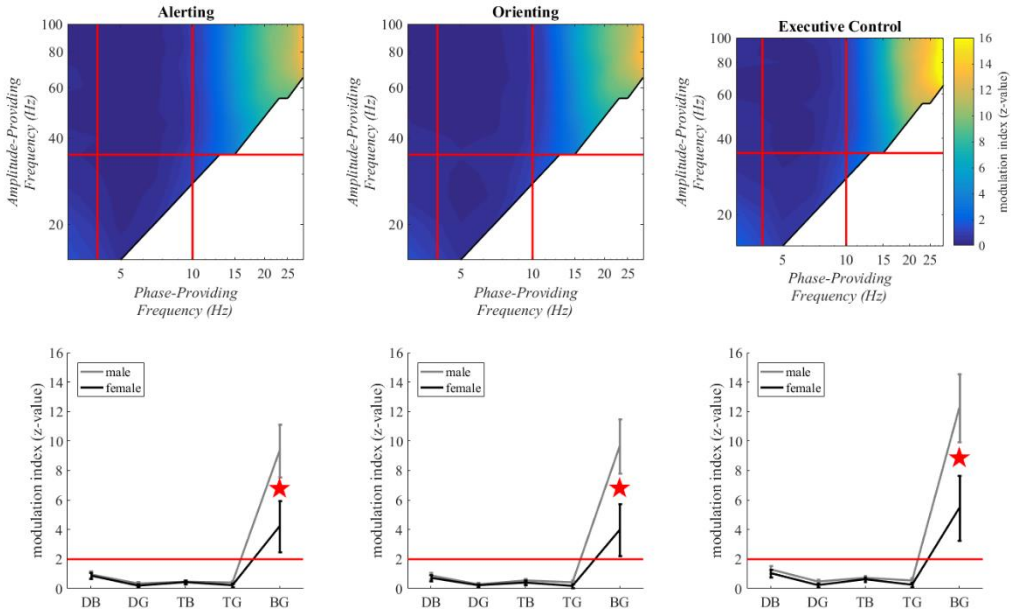

Figure 4.22: Comodulogram during the attention network test of the fronto-frontal network averaged over hemispheres, blocks, trial types, and experimental groups. The line plot shows mean modulation indices ± S. E. for each frequency pair and separately for males and females. Red stars mark significant differences between males and females. The red line marks the significance threshold. Please note that axes scaling of the comodulogram is different from that in Figure 4.19, Figure 4.20, and Figure 4.21. Here coloured shading is chosen to enhance visibility of modulation index graduation. DB: Delta-Beta; DG: Delta-Gamma; TB: Theta-Beta; TG: Theta-Gamma; BG: Beta-Gamma.

Attention Network Test – Correlations between modulation indices and reaction times. Exact correlations for each network and condition can be found in Table 4.7. Potentially relevant patterns of correlations between modulation indices and reaction times emerged within the alerting network for theta-gamma coupling and beta-gamma coupling as well as within the executive control network for beta-gamma coupling. The orienting network revealed nearly no significant correlations.

For the alerting network, females' reaction times did correlate positively with theta-gamma phase-amplitude coupling strength within the left hemisphere, for both cue types (no cue [$r^2 = .15$], double cue [$r^2 = .18$]), but only in block 2. Furthermore females' reaction times did correlate positively with beta-gamma phase-amplitude coupling strength within the left hemisphere during the entire experiment (both blocks and both cue types; $.08 \leq r^2 \geq .18$). Even though not reaching significance for double cues in block 1, this correlation was almost as large as the others, also being positive. Males did not show consistent correlation patterns within the alerting network and exhibited rather negative correlations, compared to females, which exhibited rather positive correlations.

For the executive control network, females' reaction times did again correlate positively with modulation indices within the left hemisphere. This was only significant for congruent and incongruent trials in block 2. However, all correlations in the left hemisphere were positive similar in magnitude ($.06 \leq r^2 \geq .23$). Males on the contrary, exhibited negative correlations between reaction times and beta-gamma phase-amplitude coupling within the left hemisphere, which were only significant in one case (block 1, congruent trials), but nevertheless were highly similar, all being negative and of similar magnitude ($.03 \leq r^2 \geq .20$).

4.4 Discussion

This study examined whether stress influences working memory and cognitive inhibition performance, both being core executive functions. Furthermore, it was examined whether phase-amplitude cross-frequency coupling is a physiological marker of these core executive functions and is similarly influenced by stress like behavioural measures are expected to be. To test the specificity of expected associations between stress, executive functions, and phase-amplitude coupling, the same relationship was investigated for the entire attention system according to Posner and Petersen (1990).

The stress manipulation was successful. Only high responders had statistically significant increased cortisol levels compared to the baseline measurements and additionally exhibited cortisol increases that are considered biologically significant (Miller et al., 2013). In contrast to the previous experiment, low responders in this study are subjects truly exhibiting a low cortisol response, which is below the biological significance criterion (1.5 nmol/l), not statistically significant, but nevertheless reflects an absolute increase of cortisol levels in response to the SECPT in each subject. The warm water control group was neither physiologically nor psychologically stressed. Cortisol level only slightly decreased over the course of the experiment, as is normal for humans in the afternoon hours. Subjective

Table 4.7: Spearman's rho correlations between modulation indices and reaction times in the attention network test for each attention network (a) alerting, b) orienting, c) executive control) separately for each hemisphere, frequency pair, block, and cue or trial type. Significant correlations are printed in bold.

a) Alerting			**Females**					**Males**				
			DB	DG	TB	TG	BG	DB	DG	TB	TG	BG
Left Hemisphere	Block 1	No Cue	**-.43**	.13	-.36	.19	**.37**	.06	.02	-.31	-.14	-.22
		Double Cue	.17	.04	-.13	.06	.28	-.25	-.19	.07	-.22	**-.42**
	Block 2	No Cue	.33	.04	-.22	**.39**	**.43**	-.23	-.04	-.23	.06	-.17
		Double Cue	.14	.02	.21	**.43**	**.42**	.03	.04	-.16	**-.47**	-.17
Right Hemisphere	Block 1	No Cue	.01	-.22	-.11	-.13	.07	.08	-.17	.03	-.29	-.15
		Double Cue	.05	.07	.19	.02	.00	-.16	-.10	-.16	-.14	-.12
	Block 2	No Cue	.07	-.15	.02	.11	.00	-.29	.32	-.34	-.04	.06
		Double Cue	.05	-.24	-.17	-.09	.02	-.03	-.01	**-.63**	-.07	-.08

b) Orienting			**Females**					**Males**				
			DB	DG	TB	TG	BG	DB	DG	TB	TG	BG
Left Hemisphere	Block 1	Centre Cue	-.08	-.12	.06	-.18	.28	.01	-.21	-.02	.17	-.31
		Spatial Cue	-.01	-.22	.16	.14	.26	.02	.05	.00	.14	-.34
	Block 2	Centre Cue	-.10	-.11	-.27	-.03	.35	.28	.02	.07	-.26	-.28
		Spatial Cue	.25	.04	.01	-.15	.26	-.26	**-.40**	.02	**-.42**	-.26
Right Hemisphere	Block 1	Centre Cue	.21	.27	-.25	-.16	-.08	-.36	-.14	.07	-.28	.05
		Spatial Cue	.02	-.13	-.06	-.20	-.20	-.27	.02	-.30	-.02	-.05
	Block 2	Centre Cue	-.20	-.14	-.28	.13	.00	-.13	-.09	-.15	-.09	.13
		Spatial Cue	.06	-.17	.12	-.14	-.10	-.04	-.10	-.20	-.18	-.01

c) Executive Control			**Females**					**Males**				
			DB	DG	TB	TG	BG	DB	DG	TB	TG	BG
Left Hemisphere	Block 1	Neutral	-.11	-.21	.06	-.21	.31	-.01	.07	-.25	-.09	-.34
		Congruent	-.11	.24	-.20	.12	.24	-.30	-.09	-.04	-.22	**-.45**
		Incongruent	.25	.03	-.05	.01	.32	.04	-.06	.01	-.16	-.28
	Block 2	Neutral	-.07	-.16	-.04	.04	.30	.22	**-.41**	.26	-.32	-.18
		Congruent	.02	-.17	.09	.36	**.38**	-.28	-.16	-.34	-.03	-.29
		Incongruent	.05	.33	.04	-.03	**.48**	-.18	-.18	-.06	-.19	-.17
Right Hemisphere	Block 1	Neutral	.09	.18	.01	.33	-.19	-.27	.26	-.20	-.31	-.11
		Congruent	.04	-.20	-.16	.21	.12	.07	-.20	.08	-.22	-.04
		Incongruent	.12	-.03	-.03	-.23	-.13	.00	-.04	-.33	.15	-.03
	Block 2	Neutral	.08	**-.41**	-.07	.33	-.11	-.22	.04	**-.47**	-.07	-.05
		Congruent	.34	.21	-.09	.12	.09	-.27	-.02	-.24	-.23	.05
		Incongruent	-.02	**-.50**	.11	-.23	-.09	.06	.01	-.17	-.08	.06

$p < .05$

stress ratings reflect the endocrinological stress response: warm water controls were neither stressed, nor did they feel pain, unpleasantness, or difficulty in the situation in contrast to both low and high responders, which were subjectively stressed. Interestingly, low responders reported significantly less stress than pain, unpleasantness, and difficulty in the situation, which is reflected in the low cortisol increase. Warm water controls, having to face the same reserved experimenter but not go through the difficult and painful cold water procedure, reported more unpleasantness than pain and experience of difficulty in the situation.

In addition to the endocrinological stress response, the cardiovascular stress response to the SECPT was assessed via blood pressure measurements. As expected, systolic and diastolic blood pressure significantly increase in subjects being exposed to the cold water, serving as a third manipulation check (Velasco et al., 1997).

4.4.1 Working Memory, Stress, and Phase-Amplitude Coupling

Typical Sternberg results were replicated in this experiment, underlining the validity of the working memory task. Subjects generally responded faster and made less errors in low workload trials than in high workload trials. They generally responded faster but made more errors in match trials than in non-match trials. Reaction time data is explained by an exhaustive serial search of the encoded list of consonants for a possible match (Lisman & Idiart, 1995; Sternberg, 1975). Error data indicates that subjects more often falsely reject a probe, assumingly not knowing whether the probe had been part of the list, than they do falsely remember having seen a probe they did not actually see.

Stress did not generally influence working memory performance. The only responder group differences that were found existed throughout the whole experiment and were thereby not caused by the SECPT. Furthermore, that effect explained only 3 % of variance and was therefore very small, especially when compared to other behavioural effects (e. g. workload explaining 53 % of variance). The effect revealed that the warm water control group consisted of subjects that responded faster than subjects allocated to the cold water condition. This performance advantage was especially present in more difficult trial types.

There were barely any sex differences in working memory performance, with the exception that men committed more errors to matches (not remembering correctly having seen the probe in the list) than to non-matches (thinking they had seen the probe in the list, even if it was not presented). Women committed equally often errors to matches and non-matches. Sexes committed overall the same amount of errors. The interaction explained 5 % of variance.

Phase-amplitude coupling analyses replicated the finding of highly significant beta-gamma coupling in the third executive functioning domain – working memory. In addition to having been replicated within the same, purely male, sample in the previous study, here beta-gamma coupling is replicated in an independent sample, additionally comprised of females. Therefore this finding is very

promising and strengthens the assumption that beta-gamma coupling is accompanying executive functioning.

Again, there is neither a clear modulation of phase-amplitude coupling strength by the task demands nor by stress. Nevertheless, a small stress effect, explaining about 3 % of variance, is observed in this paradigm. None of the groups and conditions differed in their coupling strength, except for male low responders who showed markedly increased phase-amplitude coupling after the SECPT compared to before the SECPT in the left hemisphere. Due to this increase they then – in block 2 – differed in their coupling strength from female low responders, warm water controls, and high responders (Figure 4.23). This indicates that male subjects who are stressed but cope quite well with this stressor (low responders) benefit from the experienced stress. The benefit is here defined as higher coupling strength, which is assumed but has not yet proven, to measure neuronal information transfer efficiency. Likewise, two other sex differences became apparent. Females had higher coupling strength than males in the right hemisphere when they belonged to high responders (valid in block 1) and low responders (valid in block 2). These two differences were rather small compared to the differences driven by the male low responders coupling strength increase in block 2.

Theta-beta coupling, even though not found to be generally significant in the entire sample, exhibited an interesting correlation pattern with reaction times in the Sternberg working memory task. Throughout the left hemisphere, phase-amplitude coupling strength for this frequency pair was negatively correlated with reaction times of the sample. These correlations became significant only for high workloads, displaying effects sizes between $.06 \leq r^2 \geq .10$. This reveals that the faster the reaction times, the stronger theta-beta coupling strength.

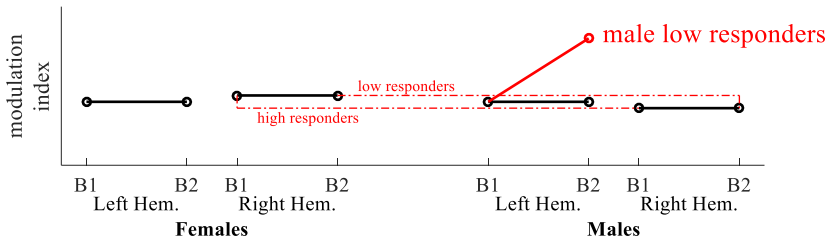

Figure 4.23: Simplified schematic depiction of the hemisphere by block by responder group by sex interaction (cf. Figure 4.15). Only male low responders show significantly increased phase-amplitude coupling in the left hemisphere in block 2, after the SECPT. Thereby they differ from all other groups at this time point. Furthermore, females show slightly stronger coupling than males in the right hemisphere, but this is only true within high responders in block 1 and low responders in block 2. Black lines display the average of all responder groups. B1: Block 1 (before SECPT); B2: Block 2 (after SECPT); Hem.: Hemisphere.

Similar to the flexibility task reported in the previous study, beta-gamma coupling was positively correlated with reaction times within the left hemisphere. However, significant correlations did not occur in block 1 and disappeared in block 2 as for the flexibility task, but were solely present in match but not in non-match trials (with the exception of block 2 match trials).[26] This correlation reveals that coupling strength increases as reaction times increase. Phase-amplitude coupling was only calculated for correct trials. Therefore, match trials are trials in which previously presented stimuli are correctly recognized. In non-match trials false probes are correctly rejected. This correlational pattern might be explained by the varying positions of the matching probe in the encoded list. Subjects see either three or five consonants and the matching probe appears equally often at each possible position. The exhaustive serial search hypothesis assumes that subjects replay all items of the encoded list in the correct order, and stop the search when the probe stimuli matches a stimuli of the list. That is, matches in early positions are detected faster (Sternberg, 1975). If phase-amplitude coupling is only present until subjects identify the match in the encoded list, then coupling should be present until the response and absent after the response. Then presence of coupling would be shorter for trials where matches appear in early positions. Shorter presence goes along with less coupling strength (cf. chapter 2) and thus shorter reaction times should be associated with less coupling strength. Furthermore, reaction times in non-match trials should be rather homogenous, because the entire list must always be scanned; hence non-significant correlations are found for non-matches. Descriptively, variance of reaction times is consistently, but only slightly, smaller for non-matches compared to matches (cf. Table 4.2). The positive correlation was driven by female participants (Figure 4.16). Men rather showed null or even negative correlations, but most importantly no clear pattern in the left hemisphere. Even though insignificant, correlations for males in the right hemisphere between phase-amplitude coupling strength and reaction times were rather negative in block 1 and disappeared in block 2. This sex difference is both interesting and problematic as will be further discussed in section 4.4.2.

How do phase-amplitude coupling findings compare to behavioural findings? For reaction times, it was found that warm water controls responded generally faster, but did not commit more errors than both other groups. This speed advantage was only significant in non-match trials in low workloads and match trials in high workloads. For phase-amplitude coupling, male low responders stick out. They exhibit stronger coupling in block 2. Thus, electrophysiological and behavioural results do not correspond. This is the third experiment, this time in an independent sample comprised of males and females, that shows that behavioural and phase-amplitude coupling data do not easily match. However, in contrast to the previous experiment, group differences in phase-amplitude coupling are driven by experimental blocks and therefore possibly represent stress effects. Group differences regarding behavioural data on the other side are hard to explain, but are very small, especially when comparing them to usual effects sizes of behavioural data.

[26] Whether the missing correlation between reaction times and phase-amplitude coupling strength in block 2 match trials is systematic or originates from coincidence cannot be conclusively clarified here and awaits replication.

In summary, there is a subtle hint, coming from electrophysiological coupling data that low responders might profit from the experienced stress. This association relies on the assumption that coupling strength reflects neuronal information transfer efficiency. More importantly, beta-gamma coupling is replicated for the third core executive function working memory, showing that it is a robust phenomenon during executive functioning. Even though behaviour and phase-amplitude coupling vary according to task demands, stress experience, and sex, the patterns of variation do not reveal a clear picture. This conclusion resembles the one formulated in the previous chapter. A thorough disquisition of possible reasons will be presented in the General Discussion.

4.4.2 Attention, Cognitive Inhibition, Stress, and Phase-Amplitude Coupling

Typical findings for the attention network test were replicated. Reaction times became faster the more precise the warning cue was. The longest reaction times were detected when no cue was presented. Alerting the subject via warning cue while maintaining diffused attention did decrease reaction times, but less than cues that also oriented attention to the correct target position. Furthermore, subjects responded fastest to targets that were not flanked by symbols similar to the target. However, if the flankers are identical to the target, and therefore do not evoke an inappropriate response, reaction times are almost as fast as without distracting flankers. Flankers which evoke incorrect responses slow down reaction times massively. It was further found that participants are able to improve their performance in this task by practice. Practice especially decreases the effect of flankers. Subjects are better capable of responding rapidly irrespective of flanker type.

Stress did not affect performance in the attention network test. While it was not necessarily expected to influence alerting and orienting, it was indeed expected to worsen executive control. Not many studies have investigated stress effects on cognitive inhibition using the flanker task as is done in the attention network test. The earlier reported meta-analysis of acute stress effects on executive functioning (Shields et al., 2016) reports exactly one study using the flanker paradigm (Sato, Takenaka, & Kawahara, 2012). According to the meta-analysis, Sato et al. (2012) report slightly enhanced inhibition after stress; however, the confidence interval of the effect size calculated in the meta-analysis is very large and includes a null effect. Heat stress was found to worsen executive control, but whether heat actually elicited psychological or physiological stress was not assessed (Sun et al., 2012). Another study found generally faster reaction times in a selective attention task after a TSST (Cornelisse et al., 2011). This TSST did not elicit an endocrinological stress response, but led to increased subjective stress. In summary, even though there is more evidence for detrimental stress effects on cognitive inhibition, it is not yet clear whether the flanker paradigm is an ideal task to measure these effects.

In contrast to stress, sex modulated performance in the attention network test, explaining 8 % of variance. Males generally responded faster than females. Furthermore, males' reaction times did not differ between central and double cues. Both cue types alert the subject and give temporal information about when the target will appear but either orient the subject to the centre of the screen or diffuse

attention to the entire screen. While women profit from diffused attention, men's reaction times did not differ between diffused and focal attention. There are nearly no studies reporting sex differences in the attention network test, few exceptions are, for example, Liu, Hu, Fan, and Wang (2013) or Neuhaus et al. (2009), which however do report other sex differences than were found in this experiment. A possible explanation for the here found sex differences might be the advantage of spatial ability in males (Linn & Petersen, 1985; Voyer, Voyer, & Bryden, 1995).

It was again beta-gamma coupling that was found to be strongly present. None of the other frequency pairs exhibited significant coupling. Because phase-amplitude coupling was calculated averaged over the whole trial, this result is not surprising. In each trial, a flanker task has to be solved and therefore in each trial executive control is potentially needed. To average phase-amplitude coupling across the entire trial might appear unpropitious when having aimed to disentangle basic attention processes from executive control. However, the cue-target interval in the attention network test is only 500 ms. Chapter 2 had shown that this trial length is too short for finding coupling even if it is present. This topic will be discussed at full length in the General Discussion.

The first central research question addressed by this work was whether stress modulates phase-amplitude coupling and executive functions. No support for the hypotheses that stress decreased cognitive inhibition ability was found, neither electrophysiologically or behaviourally. The second key research question was whether phase-amplitude coupling strength and inhibition performance correspond. It was found that behavioural and electrophysiological data indeed correspond for the attention network test. Male participants performed overall significantly faster than female participants. Error rates are naturally low in this task: subjects simply have to determine the direction of an arrow, which is visually present throughout the response period. That means males' performance was generally better than females'. Beta-gamma phase-amplitude coupling was correspondently generally higher in males than in females. This relationship was present during the entire task and did not depend on or changed for certain task conditions (block, cue types, trials types). It was further present in the left and right hemisphere. The hypotheses that phase-amplitude coupling reflects a cognitive mode that enables organisms to successfully execute higher cognitions by paralleling different basic processes, seems to be confirmed here. Males showed overall stronger coupling while simultaneously exhibiting overall better performance than females. Small task-dependent differences in reaction times between sexes, e. g. males showing no difference in reaction times between centre and double cue, were not reflected in phase-amplitude coupling.

In line with these results, male participants do show predominantly negative correlations between reaction times and phase-amplitude coupling strength, particularly for beta-gamma coupling and particularly in the left hemisphere. Females, on the contrary, show rather positive correlations between reaction times and phase-amplitude coupling, also particularly for beta-gamma coupling and for the left hemisphere. This is the same finding as for the Sternberg task.

There is no simple explanation for this difference between correlation directions. As was already discussed in the previous chapter, both correlation directions are conceivable and logically explainable. It was initially guessed that negative correlations would be found, showing that the higher the coupling, the better the information processing, the faster the reaction times. However, it is also conceivable that the higher the coupling, the more executive control is required to successfully solve the task, i. e. the more difficult the task is and hence the longer the reaction times. Additionally, a second explanation for positive correlations is conceivable. According to this explanation, phase-amplitude coupling would be present as long as the task is executed, that is, until a response is made. The longer the reaction times, the longer phase-amplitude coupling is present, and hence for longer periods of phase-amplitude coupling a higher modulation index is found.

However, there is no reason to assume that different mechanism should be valid for males and females. Even though there is the possibility, it is rather unlikely that very basic cognitive principles will differ between sexes. Correlation coefficients represent on average small to medium effect sizes (r^2 = .04), ranging between 0 to 40 % explained variance, and should be replicated before further interpretations are made.

Results indicate that coupling strength is higher for the executive control network than for both other attention networks (alerting and orienting; Figure 4.22). This finding complies with theoretical considerations of beta-gamma phase-amplitude coupling to be a specific physiological marker of executive functions, which can differentiate between executive functions and other cognitive domains (e. g. attention). The finding that beta-gamma coupling is markedly (and also statistically, see Appendix F) weaker during basic attention processes than during executive control processes seems therefore to be a proof of concept. However, there is a very simple, methodological explanation for this finding. In chapter 2, it was shown that the modulation index increases with increasing data length. For each block and cue condition in the alerting and orienting network, 48 trials of 3100 ms length were concatenated, resulting in a data length of 149 seconds for calculating the modulation index. For each block and target condition in the executive control network, 64 trials of 3100 ms length were concatenated, resulting in a data length of 198 seconds for calculating the modulation index. That is, data length for the executive control network is 33 % longer than data for alerting and orienting (cf. Figure 4.24). It is therefore expected to find higher phase-amplitude coupling for executive control than for alerting and orienting, simply because of data length.

Descriptive differences in coupling strength between cue and target types did not differ significantly. This might be caused by methodological aspects. Reaction time data was analysed in a fully crossed ANOVA, disentangling performance for all cue and target types. Phase-amplitude coupling data on the contrary was analysed in three ANOVAs separately for each attention network and averaged across the remaining cue and target types (cue type and trials type effects cannot be disentangled). This was done to include sufficient amount of trials per condition and in order to keep calculation time in reasonable limits.

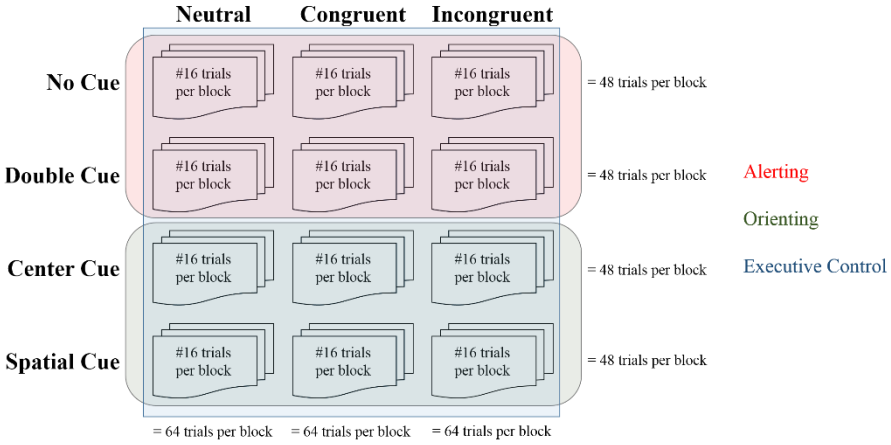

Figure 4.24: Schematic depiction of trials which were analysed for alerting, orienting and executive control networks. This schema depicts which trial types overlap between the three networks and which do not. It also depicts the maximal amount of trials contributing to each task condition. Each trial belongs to exactly one cue type and one target type simultaneously.

In summary, no stress effects were found for the attention system, including executive control, but clear and precisely interpretable sex effects on behavioural and electrophysiological data were found, which show that coupling strength can indeed be used to infer behavioural performance from phase-amplitude coupling data. Correlations between coupling strength and reaction times reveal patterns which are difficult to interpret, especially regarding sex differences becoming apparent in the direction of correlations.

4.4.3 Preliminary Conclusion

Briefly, this study showed that beta-gamma coupling is indeed an electrophysiological marker accompanying executive functions. Unfortunately, the aim of testing its specificity to executive function and demarcating it from a second cognitive domain (the attention system) failed out of methodological reasons. For the attention network test, a clear association between coupling strength and performance has been found. It should be emphasized that the here advocated clear pattern does only refer to sex differences and coupling strength and did not systematically vary with task demands or stress. Sex differences found in the Sternberg task were much more specific than in the attention network test. This could explain why no systematic phase-amplitude coupling strength variation is found in the Sternberg task, while it is in the attention network test.

It seems that for the Sternberg task, as well as for flexibility and behavioural inhibition, other parameters of phase-amplitude coupling should be investigated as coupling strength did not vary systematically with task demands. Some major thematic and methodologic topics will be taken up in the General Discussion.

5 General Discussion

All information is imperfect. We have to treat it with humility.
Bronowski, 2011

5.1 Summary of the Findings

The introduction thoroughly presented the relevance and importance of the studied topic: Are executive functions implemented via phase-amplitude coupling and can the repeatedly found influence of stress on executive functions be explained by a modulation of phase-amplitude coupling strength?

Chapter 2 showed that there are at least two phase-amplitude coupling measures that meet the requirements of being specific and sensitive to coupling strength and coupling width. The simulation study also drew attention to several confounding factors which influence coupling strength. One example is data length, which possibly explains relevant results of chapter 4.

Chapters 3 and 4 comprehensively investigated the topic of executive functions, phase-amplitude coupling and stress in two independent samples. Executive functions were reliably accompanied by beta-gamma coupling. In all tasks, typical behavioural results were replicated and validity of the task was thereby confirmed. Solely the go-nogo task was unfavourably designed for interpreting behavioural results. Behavioural results of all other studies showed that trials where executive functions are needed are more difficult for subjects, such that they displayed longer reaction times or more errors.

As expected, groups generally did not differ in their performance in any of the four tasks. It was hypothesized that stressed participants, especially those with a marked physiological stress response, would (1) perform less flexibly, (2) show better behavioural inhibition, (3) show less cognitive inhibition, and (4) show worse working memory performance after SECPT compared to before SECPT and after SECPT compared to the control group. However, stress was not found to influence executive functions, except to enhance flexibility performance.

It was hypothesized that phase-amplitude coupling strength would vary in a similar manner as performance varies, for example, stronger coupling in trials that demand executive functions compared to those that merely require simple responses. Overall no such association was found. For task switching, coupling should have been stronger in switch compared to repeat trials. This pattern was only found for the warm water control group. For the go-nogo task, stronger coupling was expected in nogo compared to go trials. In specific cases, the opposite pattern was found, but overall findings revealed no systematic differences. Stronger coupling was expected in higher workloads of the working memory task. No clear expectations were made for matches versus non-matches. No coupling strength modulation due to workload was found and also findings for probe types did not reveal a consistent pattern. For the attention network test, it was expected to find stronger coupling strength in incongruent compared to congruent and neutral trials, but findings revealed no differences. It was expected that coupling strength would not vary according to cue types, disentangling the basic attention processes of alerting and

orienting. These should not be dependent on phase-amplitude coupling. Indeed, no modulation of coupling strength by cue types was found.

It was hypothesized that groups would not differ in their coupling strength before the SECPT. This was indeed the case, except for the task switching paradigm, where groups did differ in their general coupling strength. Stressed participants, especially those with a marked physiological stress response were expected to show (1) less coupling in task switching, (2) more coupling in the go-nogo task, (3) less coupling in the attention network test for executive control, (4) no change in the attention network test for alerting and orienting, as well as (5) less coupling in the Sternberg task after SECPT compared to before SECPT and after SECPT compared to the control group. Analyses however revealed no change for task switching and the attention network test for executive control. For the go-nogo task, increased coupling was found, but only for the warm water control group. No changes were revealed for the attention network test for alerting and orienting. For the Sternberg task, increased coupling in male low responders were found, contradicting the expectations.

Finally, it was hypothesized that performance in the form of reaction times should negatively correlate with coupling strength. Strong phase-amplitude coupling, reflecting the efficiency of executive functions, should be associated with fast reactions. Positive correlations were found for flexibility and working memory. No correlations could be calculated for behavioural inhibition. For cognitive inhibition males revealed negative correlations while females revealed positive ones. Virtually no relevant correlations were found for orienting. For alerting only females showed relevant correlation patterns.

5.2 Are Executive Functions Implemented via Phase-Amplitude Coupling?

One of the primary aims of this thesis was to establish knowledge about the presence of phase-amplitude coupling during the carrying out of executive functions. In two independent studies, each being comprised of two core executive function tasks (flexibility and behavioural inhibition as well as cognitive inhibition and working memory), beta-gamma phase-amplitude coupling was found to be a robust phenomenon, detected in the left and right prefrontal hemispheres. A wide frequency spectrum, consisting of 137 frequency pairs, was screened for phase-amplitude coupling. These frequencies ranged from delta to beta for phase-providing frequencies and from beta to gamma for amplitude-providing frequencies. Having explored such a broad frequency spectrum, presumably no other relevant frequency pairs exhibiting coupling have been missed. Only very slow modulating frequencies below 3 Hz had to be excluded due to methodological reasons.[27]

[27] When wanting to reliably estimate phase-amplitude coupling, trial length should be at least as long as three cycles of the lowest frequency which is extracted. That is, when wanting to extract the phase of a 1 Hz oscillation, one should have at least 3000 ms of continuous data (Cohen, 2014, pp. 416–417). To improve the signal-to-noise ratio, one should average several trials consisting of continuous data.

The second goal of this thesis was to find out whether coupling strength would vary with task demands, i. e. being stronger in those trials that actually demand executive control (e. g. switch trials in the task switching paradigm) and being weaker in those trials that do not demand any executive control (e. g. repeat trials in the task switching paradigm). Overall phase-amplitude coupling strength did not systematically vary with task demands. There are at least three possible explanations for this finding. Firstly, the robust presence of beta-gamma phase-amplitude coupling could be an epiphenomenon just co-occurring with executive functioning but not being causally related to it. In this case, coupling strength would not be expected to vary with task demands. Secondly, it could simply be that methodological decisions have blurred the actually present association between coupling strength and task demands. Thirdly, it could be that coupling strength is an inappropriate parameter for seeing an association between task demands and phase-amplitude coupling. A reasonable alternative could be the preferred coupling phase or phase precision (= modulation width). To conclude the exploratory analysis presented in this thesis, these possibilities will now be discussed. They also apply for explaining findings regarding stress and attention, which will be discussed later on.

5.2.1 Beta-Gamma Coupling an Epiphenomenon?

There could be truly no phase-amplitude coupling strength modulation due to task demands. The analyses conducted in this thesis had enough power to find small, relevant effects of at least 3 % explained variance. Furthermore, this is not the first study to find significant phase-amplitude coupling but no systematic variation of coupling strength with tasks demands or correlation of reaction times with coupling strength (Tang et al., 2016; Yanagisawa et al., 2012). Yanagisawa et al. (2012) even report neither preferred coupling phase nor coupling strength to be predictive of performance in a motor execution task. However, before jumping to the conclusion that phase-amplitude coupling is simply co-occurring with executive functions, the other two possibilities, which are not mutually exclusive, should be investigated.

5.2.2 Critical Review of Methodology: did methodological decisions blur the association between coupling strength and task demands?

In the here presented thesis, phase-amplitude coupling was solely analysed in successfully completed trials; that is, only when executive functions had correctly guided actions. Differences in coupling strength could come into being when comparing accurate with erroneous performance. Unfortunately error rates were too low to reliably analyse phase-amplitude coupling in error trials. It could be important to design more difficult tasks to conduct this comparison. Other studies already reported that phase-amplitude coupling was higher in correct than in erroneous trials (Li et al., 2012, 2012; van Wingerden et al., 2014; Voloh et al., 2015). Furthermore, it is reported that coupling is significantly higher for later on remembered items in comparison to later on forgotten items (Friese et al., 2013; Köster et al., 2014). Lega et al. (2016) report that a subset of electrodes shows increased

coupling during successful encoding while other subsets show increased coupling during unsuccessful encoding.

Not only for analysing error trials it is important to design more difficult tasks. The here used tasks might have been too easy to consistently evoke the demand for executive functioning. On the other hand, in reaction time data executive function effects became visible. Nevertheless, Oei et al. (2006) and Lai et al. (2014) found stress effects only for high workloads. Their maximal workload exceeded the here used workload of five single letters. For task switching, the cue-target interval was comparably long; difficulty of switching decreases as the preparation period increases (Rogers & Monsell, 1995). Task difficulty might also explain why only the prefrontal cortex was engaged in the tasks. Tasks might have been too simple, to require different brain areas for solution.

Coupling was calculated over the entire trial length, including a baseline period, the period of stimuli encoding, response selection and execution, and a variable time after participants had responded. For the first investigation of this topic, it is reasonable to include the entire trial: one will not falsely focus on a trial segment that might turn out to be irrelevant. Calculating coupling separately for the entire trial length and each possibly relevant trial segment would have exceeded the available computing capacity. The decision to include the entire trial proved to be useful, as robust and consistent beta-gamma coupling was revealed by it in all executive function domains. Nevertheless, one should be aware that transient coupling between other frequency pairs could have been hidden by this decision. More precise and even additional coupling patterns could have occurred, had more restricted periods within the trials been analysed. That is why follow up analyses should investigate trial segments that are of major interest, like the cue-target interval in the task switching paradigm or the maintenance period in the working memory task. Former studies already reported phase-amplitude coupling to occur time-locked to stimulus onset (Demiralp et al., 2007; van Wingerden et al., 2014) or at a specific location in a t-maze (Tort et al., 2008). It could be further interesting to compare different epochs within a trial, e. g. a baseline period compared to the maintenance period in the working memory task. Yanagisawa et al. (2012), for example, found phase-amplitude coupling being present before a motor response and then decreasing towards the execution of a motor response (temporal variation). To extract very short segments will be difficult as chapter 2 had shown that one needs more than 12 seconds of data to be able to extract significant phase-amplitude coupling. For very short segments, the amount of trials needs to be increased. Alternatively, it would be favourable to find phase-amplitude coupling measures that are able to detect time-resolved phase-amplitude coupling, such as the event-related phase-amplitude coupling (ERPAC) measure promoted by Voytek, D'Esposito, Crone, and Knight (2013).

Furthermore, when looking at each participant’s data, it became evident that only a portion of participants exhibited beta-gamma phase-amplitude coupling, while others either showed coupling between other frequency pairs or no significant coupling at all. Why some subjects do and others do not show coupling cannot be clarified by the here presented studies. It is not the first study to find only a portion of subjects exhibiting significant coupling. For example, Maris et al. (2011) found subjects to

have up to four reliable phase-amplitude coupling patterns, but also subjects exhibiting none. Interestingly, a lot more participants exhibited reliable phase-amplitude coupling pattern during the maintenance period of the Sternberg task, compared to the baseline period. Tort et al. (2008) finds phase-amplitude coupling in the striatum for four of six rats; in the hippocampus all rats exhibit significant coupling. Regarding this thesis, it would certainly be helpful to investigate whether coupling strength systematically varies according to task demands when only the subjects that showed significant beta-gamma phase-amplitude coupling are included. This strategy was e. g. pursued by Osipova, Hermes, and Jensen (2008). The follow up analysis can be done very efficiently on the same data that has already been collected and for which phase-amplitude coupling has already been calculated. Solely the sample size would be further reduced, decreasing statistical power.

In this thesis, the broad range of frequency pairs for which coupling was calculated (137 pairs for the initial screening and 185 for the final calculations of the fronto-frontal phase-amplitude coupling) were later on drastically reduced to five averaged frequency pairs: delta-beta, delta-gamma, theta-beta, theta-gamma, and beta-gamma. This reduction fits the comodulogram of phase-amplitude coupling averaged over all subjects and conditions. It furthermore suits the logarithmic classification of frequency bands according to Penttonen and Buzsáki (2003). However, when studying the individual comodulograms, it becomes apparent that significant coupling for each individual occurs in much more restricted frequency areas. Averaging phase-amplitude coupling across such a broad area could have blurred a potential coupling strength modulation by task demands. It could be therefore useful to not average coupling across a broad frequency range, but to choose individual frequency ranges according to the comodulogram of each participant. That is, to average the range of frequency pairs at which each participant shows significant or maximal coupling. When following this analysis strategy, one would necessarily need to decide whether to include subjects without any significant coupling in a pre-specified frequency area. This pre-specified frequency area could, for example, be as broad as was chosen in the present thesis.

5.2.3 Alternative Parameters to Coupling Strength

After all, coupling strength could be an inappropriate parameter. Other parameters, like the preferred coupling phase, may be a better measure for disentangling efficiency of phase-amplitude coupling. Preferred coupling phase refers to the instantaneous phase of the phase-providing frequency at which the instantaneous amplitude of the amplitude-providing frequency is strongest. In the studies presented in this thesis, the preferred coupling phase belonged to the decreasing phase of the beta frequency and varied little across studies and tasks. Without having conducted a systematic review, it can be reported that all kinds of preferred coupling phases have already been found: the trough (Cohen, 2008; Colgin et al., 2009; Szczepanski et al., 2014; Whittingstall & Logothetis, 2009), the peak (Demiralp et al., 2007; Popov et al., 2012; Scheffzük et al., 2011; Siegel, Warden, & Miller, 2009), the

decreasing phase (Colgin et al., 2009; Mizuhara & Yamaguchi, 2011), and the rising phase (Monto, 2012) of the lower phase-providing frequency.

Apparently, there is no main preferred coupling phase throughout the brain. The preferred coupling phase rather seems to systematically vary between neuronal networks, frequencies, or task demands. Already mentioned in the introduction of chapter 3, Dürschmid et al. (2013) found that the preferred coupling phase discriminated between trials, requiring high and low cognitive control. Coupling phase furthermore significantly correlated with reaction times. Another study found the preferred coupling phase to differ according to trials types (go-nogo task; van Wingerden et al., 2014). Yet another reported that the depth of anaesthesia might be predicted from the preferred coupling phase of delta-gamma phase-amplitude coupling (Molaee-Ardekani, Senhadji, Shamsollahi, Wodey, & Vosoughi-Vahdat, 2007). Van der Meij et al. (2012) conclude from their investigation that different networks are held separately by assigning each a unique preferred coupling phase.

Phase precision is independent of the preferred coupling phase, which solely gives back where in the phase-providing frequency cycle the amplitude of the amplitude-providing frequency peaks. If the amplitude of the amplitude-providing frequency is strong at a narrow range of phases of the phase-providing frequency it is defined as precise. If it is strong at a wider range of phases it is defined as imprecise. The higher the phase precision, the narrower the modulation width. For this parameter caution is advised because increased phase precision can also occur due to higher coupling strength. Even though both parameters are technically independent, they can determine each other. This was the case in a study finding that in a memory task the preferred phase did not massively change, but rather became more precise in the last 20 trials compared to the first 20 trials (Tort, Komorowski, Manns, Kopell, & Eichenbaum, 2009). However, increased precision went along with stronger coupling. Van Wingerden et al. (2014) found the preferred coupling phase to be more precise in trials where animals responded correctly compared to trials where they made a mistake.

Hence, rather than solely investigating coupling strength, one should also investigate preferred coupling phase and phase precision. Is the coupling width more narrow, i. e. more precise, during trials which require executive control compared to those which do not need cognitive control? At the outset, it was emphasized that the two possible explanations for not having found coupling strength variation according to task demands are not mutually exclusive. There are indeed studies finding both parameters to simultaneously provide valuable information (Dürschmid et al., 2013; Lega et al., 2016; van Wingerden et al., 2014). It is therefore advisable to always analyse both parameters.

5.3 Does Stress modulate Executive Functions via Influencing Phase-Amplitude Coupling?

After having established knowledge about the mere presence of phase-amplitude coupling, the second major goal of this thesis was to investigate whether stress would influence phase-amplitude

coupling and thereby modulate overt executive function performance. The General Introduction had thoroughly described the thematic. Acute stress induces the release of cortisol from the adrenal cortex and cortisol readily enters the brain and is able to influence neuronal activity. Seemingly cortisol influences those neuronal processes that are active, which justifies the assumption that stress could influence executive functions if they are carried out during or shortly after a stressful episode.[28] The literature strongly suggests that executive functions are modulated by stress. A meta-analysis concluded that flexibility, cognitive inhibition, and working memory are impeded by stress while behavioural inhibition benefits from stress. Even though the 95 % confidence intervals numerically excluded null effects, stress effects are rather small (Shields et al., 2016)[29]. Despite the conclusion of the meta-analysis, stress has been found to exert beneficial, detrimental, and no effects on each core executive function (cf. section 3.1 and 4.1).

In the here presented studies executive functions were barely influenced by the applied socially evaluated cold pressor stress, with two exceptions. Flexibility benefitted from stress on a behavioural level; the effect was not reflected in the phase-amplitude coupling data. For working memory a presumably beneficial effect of stress on beta-gamma phase-amplitude coupling was found for male low responders. These exhibited stronger coupling in the Sternberg task after the stress induction procedure compared to before and compared to all other experimental groups. Similarly to flexibility, this effect was not mirrored in behavioural data.

The above discussed aspects, commenting on why no systematic modulation of coupling strength by task demands has been found so far, do apply for stress effects in an analogous manner. Again, a re-analysis of the data is strongly recommended before definitely excluding the possibility of systematic stress effects on phase-amplitude coupling.

Like it was already shown for event-related potential data (Dierolf, 2014), stress effects changing neuronal information processing, do not need to necessarily influence overt behaviour. They could even be missing precisely because changed neuronal information processing is preventing stress effects from becoming apparent in behaviour. Even though it makes interpretations easier when electrophysiological markers directly relate to overt behaviour, this relationship is naturally not necessary. However, a statistical dependency between two electrophysiological signals, which phase-amplitude coupling technically is, can only become a relevant electrophysiological marker if it has some kind of relation to cognitive or emotional functioning. Without such an association, its presence might be admired, but it does not help to explain human inner experience or behaviour. Thereby only one association needs to be present. For example, a correlation between reaction times and phase-amplitude

[28] Genomic stress effects are also able to exert long-lasting effects (hours to days), which however are not the focus of this work.

[29] Effect size Hedges' g is reported by Shields et al. (2016), which is comparable to Cohen's d. Effect sizes up to $d < .50$ are considered small according to the conventions of Cohen (1988). Reported effects sizes are g = -.30 [95 % CI: -.58, -.02] for flexibility, g = .30 [95 % CI: approx. .20, .40] for behavioural inhibition, g = -.21 [95 % CI: approx. -.30, -.10] for cognitive inhibition, and g = -.20 [95 % CI: -.33, -.06] working memory.

coupling strength or the variation of coupling strength due to task demands or just a temporal variation of coupling strength during the cognitive task.

Even though stress did not modulate overt behaviour in the expected way, the stress induction was highly successful in inducing psychological as well as physiological stress in the experimental groups. Cortisol increases in the first reported study (chapter 3), are weaker than usually found in the current state-of-the-art stress induction procedure (TSST; Dickerson & Kemeny, 2004), but are nevertheless substantial. Cortisol increases in the second study are nearly as high as usually reported for the TSST. Because statistical power was sufficient for all conducted analyses, null effects can be confidently assumed. It might be that stress effects do only become evident when tasks relate to personally important topics. This was shown by Pattyn et al. (2014), who found increased error rates after stress, but only in trials that were specifically emotionally relevant to the participants. Contrary to this assumption, many of the previous studies found stress effects for neutral material (Oei et al., 2006; Plessow et al., 2012; Scholz et al., 2009).

Summarizing, stress did not influence executive function performance, as was expected due to the results of the meta-analysis. Additionally, phase-amplitude coupling showed no consistent pattern of coupling strength modulation due to stress. There are two exceptions: flexibility performance and coupling strength in working memory (see above). Even though these results are contradicting to former behavioural results concerning stress and executive functions, the data is self-consistent: stress was not generally able to disturb phase-amplitude coupling, which is thought to be a prerequisite for well performing executive functions. In this case it would be expected that stress would also leave executive functioning performance unaffected, and indeed virtually no effects were found. It should be kept in mind that the relationship between phase-amplitude coupling and executive functioning is solely correlational and wording is framed according to the hypothesis made beforehand. A critical note should be given to the inconsistency of flexibility and working memory results. Performance and phase-amplitude coupling findings were inconsistent insofar as solely performance or coupling was affected by stress but never both.

5.4 Is Beta-Gamma Coupling Specific to Executive Functions?

To study cognitive inhibition the attention network test was chosen because it comes along with the advantage of measuring the entire attention system according to Posner and Petersen (1990). By applying this task, the specificity of beta-gamma coupling for executive functions in comparison to more basic cognitive functions like alerting and orienting can be determined.

Unfortunately, coupling during basic attention processes and during cognitive inhibition could not be disentangled due to methodological reasons discussed in section 4.4.2. Therefore the specificity of beta-gamma coupling for executive functions has not yet been verified. This test for specificity is necessary to be able to state that beta-gamma coupling is specifically associated with executive

functions. It also could be associated with basic cognitive processes or mere motor responses, as suggested by the work of de Hemptinne et al. (2015). In the case of this thesis, data from the go-nogo task contradicts the motor response assumption, as beta-gamma coupling was found in either trial: the go trial where motor responses had to be made and the nogo-trial where motor responses had to be withheld.

Even though not yet being able to test the specificity of beta-gamma coupling, results of the attention network test revealed one of the most interesting findings of this thesis. There was a clear performance advantage for male compared to female participants, males responding generally faster. At the same time, males displayed generally stronger beta-gamma coupling. This finding shows that coupling strength can indeed be an indicator of performance. The here found association does not prove a causal relationship but strongly suggests a dependency. It is a promising result that should be further investigated. As sex differences are rarely reported for the attention network test (Fan et al., 2002; Fan et al., 2005; Fan et al., 2007; Fan, Fossella, Sommer, Wu, & Posner, 2003; Posner & Rothbart, 2007), the causes for finding these differences should be determined in further research.

5.5 Beta-Gamma Coupling versus Theta-Gamma Coupling

Why did former studies mostly report theta-gamma coupling and barely beta-gamma coupling as was so robustly found here? Methodological decisions could be the reason. Most former studies used a fixed narrow bandwidth not only for the phase-providing frequencies (as was done here), but also for the amplitude-providing frequencies (unlike here). Chapter 2 reported that an amplitude-modulated oscillation has a characteristic frequency spectrum that includes a peak at its centre frequency as well as peaks of the modulating side bands (see Figure 2.10). When destroying this frequency spectrum by narrow band-pass filtering, a potential amplitude modulation cannot be detected (Aru et al., 2015; Berman et al., 2012; Berman et al., 2015). Thereby, studies that used fixed narrow bandwidth for the amplitude-providing frequencies will only be able to detect phase-amplitude coupling with low modulating frequencies. For example, if amplitude providing frequencies are band-pass filtered from 15 Hz to 100 Hz in 5 Hz steps (15 Hz, 20 Hz, 25 Hz, etc.) with a fixed bandwidth of ± 5 Hz around the centre frequency, phase-amplitude coupling cannot be found for beta-gamma or even alpha-gamma coupling. The modulating, phase-providing frequencies will have centre frequencies below 5 Hz.

The explanation above does clarify why most former studies did not report beta-gamma coupling. Yet it does not explain why in this study the otherwise so omnipresent theta-gamma coupling has not been found. Several reasons are conceivable. First, theta-gamma coupling was indeed present for some subjects, but it was not a characteristic for the entire sample. Second, many of the studies finding theta-gamma coupling investigate neuronal activity via ECoG or LFPs (mesoscopic level), and much less with scalp EEG or MEG (macroscopic level). Along with the second argument, oftentimes neural activity was calculated in subcortical structures, which cannot be detected by scalp EEG, as was

used in this thesis. Third, except for two study (Knyazev, 2011; Popov et al., 2012), none of the formerly reported studies calculate phase-amplitude coupling in the source space as was done in this thesis, but phase-amplitude coupling is calculated in the sensor space. Fourth, oftentimes only theta-gamma coupling is investigated and its significance is not always tested. Studying solely theta-gamma coupling bears the risk of missing other relevant coupling patterns that might be much stronger than theta-gamma coupling. Without permutation testing, one cannot be sure to report meaningful phase-amplitude coupling. The impression of omnipresent theta-gamma coupling might arise by the combination of all these factors. Despite the ubiquitous theta-gamma coupling findings, there are also studies reporting beta-gamma coupling (de Hemptinne et al., 2015; Lopez-Azcarate et al., 2010; Özkurt & Schnitzler, 2011) and additionally, virtually all other frequency combinations have been reported (Cohen et al., 2009; Jirsa & Müller, 2013; Malekmohammadi, Elias, & Pouratian, 2015; Miyakoshi et al., 2013; Roux et al., 2013). Beta-gamma coupling studies are restricted to Parkinsonian patients, where phase-amplitude coupling was measured within the subthalamic nulceus (STN).

In the previous paragraph, it was stated that it might be the type of electrophysiological data that explains why no theta-gamma coupling was found in the present thesis. However, theta-gamma coupling, especially in working memory tasks, has also been found on the macroscopic level (Cohen et al., 2009; Köster et al., 2014; Mizuhara & Yamaguchi, 2011; Rajji et al., 2016). On the other side, when restricting the selection of 82 phase-amplitude coupling studies (Appendix A) to studies investigating scalp EEG, healthy human subjects, and applying permutation testing, only four of eleven studies report exclusively theta-gamma coupling (Kirihara et al., 2012; Köster et al., 2014; Mizuhara & Yamaguchi, 2011; Rajji et al., 2016). Thereby all of these studies solely investigated theta-gamma coupling, and three investigated working memory or memory (Köster et al., 2014; Mizuhara & Yamaguchi, 2011; Rajji et al., 2016). Six of the eleven studies report several significant frequency pairs to couple, amongst these is also theta-gamma coupling (Allen et al., 2011; Cohen et al., 2009; Jirsa & Müller, 2013; Monto, Palva, Voipio, & Palva, 2008; Nakatani et al., 2014; van Zaen, Murray, Meuli, & Vesin, 2013). None of these studies specifically investigated memory. In an investigation of anaesthesia exclusively slow wave to alpha coupling was found (Mukamel et al., 2011).

As mentioned above analyses presented here are conducted on latent variables, i. e. on theoretical brain sources. Virtually all other studies conducted their analyses on sensor level. This aspect could be the cause of different findings regarding coupling frequencies. By comparing the same data set analysed in sensor and in source space, it can be tested whether the independent component analysis is truly a cause for finding different results. Furthermore, it can be tested whether ICA produces clearer results and larger effects sizes. Only then is its cost justified (time and computational costs).

5.6 Phase-Amplitude Coupling within the Prefrontal Cortex

Averaged over the entire sample, phase-amplitude coupling was solely found within a source, but not between different sources. This could potentially be indicative of artefactual coupling, insofar

as coupling might necessarily occur when calculating it within the same signal. However, this supposition is implausible, first and foremost, because within the midline frontal source, no significant phase-amplitude coupling was found. Therefore it can be excluded that coupling necessarily occurs when calculating it within the same signal. As discussed above, only a portion of subjects displayed significant fronto-frontal phase-amplitude coupling. This fact additionally proves that finding phase-amplitude coupling within the same signal is not a necessity. It can therefore be reasoned that fronto-frontal coupling is not an artefact.

The prefrontal cortex on its own and a fronto-parietal network were repeatedly associated with executive functions (see General Introduction, section 1.2). Hence, coupling had been calculated within prefrontal sources and between prefrontal and parietal sources. In this first exploratory analysis of this topic, it had been chosen to calculate coupling within – not between – hemispheres (as well as for medial sources). Beta-gamma coupling was only consistently present within the left and right prefrontal sources. This implies that phase-amplitude coupling which accompanied the carrying out of executive functions in four different tasks (task switching, go-nogo, flanker, and working memory) especially relies on the prefrontal cortex, while the fronto-parietal network does not seem to play a major role. Supporting this finding, Posner and Rothbart (2007) locate the executive control network solely in the prefrontal cortex, while both other attention networks are associated with the fronto-parietal network.

Statistical analyses showed that phase-amplitude coupling was equally present in the left and right prefrontal cortex, even though some hemispheric differences became evident. That is why future analysis should investigate whether the frontal sources interact via phase-amplitude coupling. Not only do the here presented results suggest this next step, former studies have also reported cross-frequency coupling between frontal regions. In a working memory task, phase-amplitude coupling was found between frontocentral sites (modulating, phase-providing frequency) and frontolateral sites (Mizuhara & Yamaguchi, 2011). Theta-gamma phase-amplitude coupling between prefrontal cortex and anterior cingulate was furthermore found in macaques executing an attention shifting task (Voloh et al., 2015). By comparing healthy human subjects with subjects diagnosed with schizophrenia, Reinhart, Zhu, Park, and Woodman (2015) found that theta-theta phase-phase coupling between frontocentral and frontolateral regions were a marker of the goodness cognitive control functioning. Measuring scalp EEG from 20 healthy human subjects executing an inhibition task, Cohen and Ridderinkhof (2013) found amplitude-amplitude coupling between frontocentral and frontolateral theta. Coupling was only evident in incongruent, but not in congruent trials. Furthermore, the stronger the coupling was, the smaller the conflict adaption effect[30]. They also detected theta-gamma amplitude-amplitude coupling within the fronto-parietal network, which occurred after subjects had responded.

[30] "The conflict adaption effect reflects the phenomenon that prior context situations influence the interference effects in subsequent trials." (Wittfoth, Schardt, Fahle, & Herrmann, 2009, p. 1202)

5.7 Conclusion

Robust beta-gamma coupling has been found. It might be the mechanism Fuster (1980) and Ridderinkhof et al. (2004) asked for: namely, a mechanism by which executive functions are implemented in the human brain. The test of specificity needs to be repeated. Minor phase-amplitude coupling strength modulations have been detected, not displaying a systematic pattern and preponderantly explaining only 3 % of variance. Overall coupling strength did not systematically vary with task demands or with stress. Before concluding that coupling strength truly does not predict performance in executive function tasks, the above discussed aspects have to be investigated. Independent of this follow-up analyses, of which many, but not all, can be conducted on the present data, the role of the preferred coupling phases and phase precision, as well as coupling between prefrontal sources, should be analysed. Lastly, it is strongly advisable to compare source level analyses with sensor level analyses. Firstly, to investigate whether the extensive procedures following the independent component analysis (reclustering of independent components) and the loss of subjects due to this procedure is worth the cost. Secondly, to find out whether differences in results presented in this thesis and results of former studies, are due to the application of the independent component analysis. For example, one major difference is the finding of beta being the modulating phase-providing frequency instead of slower frequencies.

Because beta-gamma coupling was so consistently found and also promising correlation patterns with participants' reaction times were found, this topic should urgently be further investigated. The next steps have been outlined in the previous discussion. Results of the follow up analysis should enable the scientific community to confidently judge in what way beta-gamma coupling and executive functioning are intertwined and whether stress actually influences beta-gamma coupling, or whether coupling is unaffected by stress like most of the executive functions were in the studies presented here.

REFERENCES

Achard, S., Salvador, R., Whitcher, B., Suckling, J., & Bullmore, E. (2006). A resilient, low-frequency, small-world human brain functional network with highly connected association cortical hubs. *The Journal of neuroscience : the official journal of the Society for Neuroscience*, *26*(1), 63–72. doi:10.1523/jneurosci.3874-05.2006

al'Absi, M., Hugdahl, K., & Lovallo, W. R. (2002). Adrenocortical stress responses and altered working memory performance. *Psychophysiology*, *39*(1), 95–99. doi:10.1017/S0048577202001543

Alexander, J. K., Hillier, A., Smith, R. M., Tivarus, M. E., & Beversdorf, D. Q. (2007). Beta-adrenergic modulation of cognitive flexibility during stress. *Journal of cognitive neuroscience*, *19*(3), 468–478. doi:10.1162/jocn.2007.19.3.468

Alexander-Bloch, A. F., Gogtay, N., Meunier, D., Birn, R., Clasen, L., Lalonde, F.,. . . Bullmore, E. T. (2010). Disrupted modularity and local connectivity of brain functional networks in childhood-onset schizophrenia. *Frontiers in systems neuroscience*, *4*, 147. doi:10.3389/fnsys.2010.00147

Allen, E. A., Liu, J., Kiehl, K. A., Gelernter, J., Pearlson, G. D., Perrone-Bizzozero, N. I., & Calhoun, V. D. (2011). Components of cross-frequency modulation in health and disease. *Frontiers in systems neuroscience*, *5*, 59. doi:10.3389/fnsys.2011.00059

Andren, L., Lindstedt, G., Bjorkman, M., Borg, K. O., & Hansson, L. (1982). Effect of noise on blood pressure and 'stress' hormones. *Clinical science (London, England : 1979)*, *62*(2), 137–141. doi:10.1042/cs0620137

Arnsten, A. F. T. (2009). Stress signalling pathways that impair prefrontal cortex structure and function. *Nature reviews. Neuroscience*, *10*(6), 410–422. doi:10.1038/nrn2648

Artoni, F., Menicucci, D., Delorme, A., Makeig, S., & Micera, S. (2014). RELICA: a method for estimating the reliability of independent components. *NeuroImage*, *103*, 391–400. doi:10.1016/j.neuroimage.2014.09.010

Aru, J., Aru, J., Priesemann, V., Wibral, M., Lana, L., Pipa, G.,. . . Vicente, R. (2015). Untangling cross-frequency coupling in neuroscience. *Current opinion in neurobiology*, *31*, 51–61. doi:10.1016/j.conb.2014.08.002

Axmacher, N., Henseler, M. M., Jensen, O., Weinreich, I., Elger, C. E., & Fell, J. (2010). Cross-frequency coupling supports multi-item working memory in the human hippocampus. *Proceedings of the National Academy of Sciences of the United States of America*, *107*(7), 3228–3233. doi:10.1073/pnas.0911531107

Baddeley. (2000). The episodic buffer: a new component of working memory? *Trends in cognitive sciences*, *4*(11), 417–423. doi:10.1016/S1364-6613(00)01538-2

Baddeley, A. D., & Hitch, G. (1974). Working Memory. In G. H. Bower (Ed.), *The Psychology of learning and motivation. Advances in research and theory (Vol. 8)* (pp. 47–89). New York: Academic Press.

Bassett, D. S., Meyer-Lindenberg, A., Achard, S., Duke, T., & Bullmore, E. (2006). Adaptive reconfiguration of fractal small-world human brain functional networks. *Proceedings of the National*

Academy of Sciences of the United States of America, *103*(51), 19518–19523. doi:10.1073/pnas.0606005103

Bassett, D. S., & Bullmore, E. (2006). Small-world brain networks. *The Neuroscientist : a review journal bringing neurobiology, neurology and psychiatry*, *12*(6), 512–523. doi:10.1177/1073858406293182

Behrmann, M., & Plaut, D. C. (2015). A vision of graded hemispheric specialization. *Annals of the New York Academy of Sciences*, *1359*, 30–46. doi:10.1111/nyas.12833

Beilock, S. L., & Decaro, M. S. (2007). From poor performance to success under stress: working memory, strategy selection, and mathematical problem solving under pressure. *Journal of experimental psychology. Learning, memory, and cognition*, *33*(6), 983–998. doi:10.1037/0278-7393.33.6.983

Bell, A. J., & Sejnowski, T. J. (1995). An information-maximization approach to blind separation and blind deconvolution. *Neural computation*, *7*(6), 1129–1159. doi:10.1162/neco.1995.7.6.1129

Berger, H. (1929). Über das Elektrenkephalogramm des Menschen. *Archiv für Psychiatrie und Nervenkrankheiten*, *87*(1), 527–570. doi:10.1007/BF01797193

Berman, J. I., McDaniel, J., Liu, S., Cornew, L., Gaetz, W., Roberts, T. P., & Edgar, J. C. (2012). Variable bandwidth filtering for improved sensitivity of cross-frequency coupling metrics. *Brain connectivity*, *2*(3), 155–163. doi:10.1089/brain.2012.0085

Berman, J. I., Liu, S., Bloy, L., Blaskey, L., Roberts, T. P. L., & Edgar, J. C. (2015). Alpha-to-gamma phase-amplitude coupling methods and application to autism spectrum disorder. *Brain connectivity*, *5*(2), 80–90. doi:10.1089/brain.2014.0242

Beste, C., Yildiz, A., Meissner, T. W., & Wolf, O. T. (2013). Stress improves task processing efficiency in dual-tasks. *Behavioural brain research*, *252*, 260–265. doi:10.1016/j.bbr.2013.06.013

Beutelspacher, A. (2015). *Kryptologie: Eine Einführung in die Wissenschaft vom Verschlüsseln, Verbergen und Verheimlichen* (10., aktualisierte Auflage). Wiesbaden, Germany: Springer Spektrum.

Bigdely-Shamlo, N., Mullen, T., Kreutz-Delgado, K., & Makeig, S. (2013). Measure projection analysis: a probabilistic approach to EEG source comparison and multi-subject inference. *NeuroImage*, *72*, 287–303. doi:10.1016/j.neuroimage.2013.01.040

Boudreau, T., Tulach, J., & Wielenga, G. The Benefits of Modular Programming (year unknown). Retrieved September 26, 2016. Retrieved from http://www.webreference.com/programming/modular_programming/index.html

Bronowski, J. (2011). *The ascent of man* ([New ed.]). London: BBC Books.

Brookes, M. J., Wood, J. R., Stevenson, C. M., Zumer, J. M., White, T. P., Liddle, P. F., & Morris, P. G. (2011). Changes in brain network activity during working memory tasks: a magnetoencephalography study. *NeuroImage*, *55*(4), 1804–1815. doi:10.1016/j.neuroimage.2010.10.074

Bruns, A. (2004). Fourier-, Hilbert- and wavelet-based signal analysis: are they really different approaches? *Journal of Neuroscience Methods*, *137*(2), 321–332. doi:10.1016/j.jneumeth.2004.03.002

Bruns, A., & Eckhorn, R. (2004). Task-related coupling from high- to low-frequency signals among visual cortical areas in human subdural recordings. *International Journal of Psychophysiology*, *51*(2), 97–116. doi:10.1016/j.ijpsycho.2003.07.001

Buckert, M., Kudielka, B. M., Reuter, M., & Fiebach, C. J. (2012). The COMT Val158Met polymorphism modulates working memory performance under acute stress. *Psychoneuroendocrinology*, *37*(11), 1810–1821. doi:10.1016/j.psyneuen.2012.03.014

Burgess, A. P., & Ali, L. (2002). Functional connectivity of gamma EEG activity is modulated at low frequency during conscious recollection. *International journal of psychophysiology : official journal of the International Organization of Psychophysiology*, *46*(2), 91–100. doi:10.1016/S0167-8760(02)00108-3

Button, K. S., Ioannidis, J. P. A., Mokrysz, C., Nosek, B. A., Flint, J., Robinson, E. S. J., & Munafo, M. R. (2013a). Confidence and precision increase with high statistical power. *Nature reviews. Neuroscience*, *14*(8), 585–586. doi:10.1038/nrn3475-c4

Button, K. S., Ioannidis, J. P. A., Mokrysz, C., Nosek, B. A., Flint, J., Robinson, E. S. J., & Munafo, M. R. (2013b). Power failure: why small sample size undermines the reliability of neuroscience. *Nature reviews. Neuroscience*, *14*(5), 365–376. doi:10.1038/nrn3475

Buzsáki, G. (2006). *Rhythms of the brain*. Oxford, New York: Oxford University Press.

Cabeza, R., & Nyberg, L. (2000). Imaging cognition II: An empirical review of 275 PET and fMRI studies. *Journal of cognitive neuroscience*, *12*(1), 1–47. doi:10.1162/08989290051137585

Cai, W., Ryali, S., Chen, T., Li, C.-S. R., & Menon, V. (2014). Dissociable roles of right inferior frontal cortex and anterior insula in inhibitory control: evidence from intrinsic and task-related functional parcellation, connectivity, and response profile analyses across multiple datasets. *The Journal of neuroscience : the official journal of the Society for Neuroscience*, *34*(44), 14652–14667. doi:10.1523/JNEUROSCI.3048-14.2014

Cannon, W. B. (1935). Stresses and strains of homeostasis. *The American Journal of the Medical Sciences*, *189*(1), 1–14. doi:10.1097/00000441-193501000-00001

Canolty, R. T., Edwards, E., Dalal, S. S., Soltani, M., Nagarajan, S. S., Kirsch, H. E.,. . . Knight, R. T. (2006). High gamma power is phase-locked to theta oscillations in human neocortex. *Science (New York, N.Y.)*, *313*(5793), 1626–1628. doi:10.1126/science.1128115

Canolty, R. T., & Knight, R. T. (2010). The functional role of cross-frequency coupling. *Trends in cognitive sciences*, *14*(11), 506–515. doi:10.1016/j.tics.2010.09.001

Canolty, R. T., Soltani, M., Dalal, S. S., Edwards, E., Dronkers, N. F., Nagarajan, S. S.,. . . Knight, R. T. (2007). Spatiotemporal dynamics of word processing in the human brain. *Frontiers in neuroscience*, *1*(1), 185–196. doi:10.3389/neuro.01.1.1.014.2007

Chatrian, G. E., Lettich, E., & Nelson, P. L. (1985). Ten Percent Electrode System for Topographic Studies of Spontaneous and Evoked EEG Activities. *American Journal of EEG Technology*. (25), 83–92. doi:10.1080/00029238.1985.11080163

Chen, Z. J., He, Y., Rosa-Neto, P., Germann, J., & Evans, A. C. (2008). Revealing modular architecture of human brain structural networks by using cortical thickness from MRI. *Cerebral cortex (New York, N.Y. : 1991)*, *18*(10), 2374–2381. doi:10.1093/cercor/bhn003

Chrousos, G. P. (2009). Stress and disorders of the stress system. *Nature Reviews Endocrinology*, *5*(7), 374–381. doi:10.1038/nrendo.2009.106

Cohen, J. (1988). *Statistical power analysis for the behavioral sciences* (2. ed.). Hillsdale, NJ: Erlbaum.

Cohen, M. X. (2008). Assessing transient cross-frequency coupling in EEG data. *Journal of Neuroscience Methods*, *168*(2), 494–499. doi:10.1016/j.jneumeth.2007.10.012

Cohen, M. X. (2011). It's about Time. *Frontiers in human neuroscience*, *5*, 2. doi:10.3389/fnhum.2011.00002

Cohen, M. X., Elger, C. E., & Fell, J. (2009). Oscillatory activity and phase-amplitude coupling in the human medial frontal cortex during decision making. *Journal of cognitive neuroscience*, *21*(2), 390–402. doi:10.1162/jocn.2008.21020

Cohen, M. X., & Ridderinkhof, K. R. (2013). EEG source reconstruction reveals frontal-parietal dynamics of spatial conflict processing. *PloS one*, *8*(2), e57293. doi:10.1371/journal.pone.0057293

Cohen, M. X. (2014). *Analyzing neural time series data: Theory and practice*. *Issues in clinical and cognitive neuropsychology*. Cambrige, Massachusetts: The MIT Press.

Colgin, L. L., Denninger, T., Fyhn, M., Hafting, T., Bonnevie, T., Jensen, O.,. . . Moser, E. I. (2009). Frequency of gamma oscillations routes flow of information in the hippocampus. *Nature*, *462*(7271), 353–357. doi:10.1038/nature08573

Cornelisse, S., Joëls, M., & Smeets, T. (2011). A randomized trial on mineralocorticoid receptor blockade in men: effects on stress responses, selective attention, and memory. *Neuropsychopharmacology : official publication of the American College of Neuropsychopharmacology*, *36*(13), 2720–2728. doi:10.1038/npp.2011.162;

Cousijn, H., Rijpkema, M., Qin, S., van Wingen, G. A., & Fernández, G. (2012). Phasic deactivation of the medial temporal lobe enables working memory processing under stress. *NeuroImage*, *59*(2), 1161–1167. doi:10.1016/j.neuroimage.2011.09.027

Criaud, M., & Boulinguez, P. (2013). Have we been asking the right questions when assessing response inhibition in go/no-go tasks with fMRI? A meta-analysis and critical review. *Neuroscience and biobehavioral reviews*, *37*(1), 11–23. doi:10.1016/j.neubiorev.2012.11.003

Crossley, N. A., Mechelli, A., Vertes, P. E., Winton-Brown, T. T., Patel, A. X., Ginestet, C. E.,. . . Bullmore, E. T. (2013). Cognitive relevance of the community structure of the human brain functional coactivation network. *Proceedings of the National Academy of Sciences of the United States of America*, *110*(28), 11583–11588. doi:10.1073/pnas.1220826110

Dallman, M. F. (2005). Fast glucocorticoid actions on brain: back to the future. *Frontiers in neuroendocrinology*, *26*(3-4), 103–108. doi:10.1016/j.yfrne.2005.08.001

de Hemptinne, C., Swann, N. C., Ostrem, J. L., Ryapolova-Webb, E. S., San Luciano, M., Galifianakis, N. B., & Starr, P. A. (2015). Therapeutic deep brain stimulation reduces cortical phase-amplitude coupling in Parkinson's disease. *Nature neuroscience*, *18*(5), 779–786. doi:10.1038/nn.3997

de Kloet, E. R. (2013). Functional profile of the binary brain corticosteroid receptor system: mediating, multitasking, coordinating, integrating. *European journal of pharmacology*, *719*(1-3), 53–62. doi:10.1016/j.ejphar.2013.04.053

de Kloet, E. R., Holsboer, F., & Joëls, M. (2005). Stress and the brain: from adaptation to disease. *Nature reviews. Neuroscience*, *6*(6), 463–475. doi:10.1038/nrn1683

de Veld, D. M. J., Riksen-Walraven, J. M., & de Weerth, C. (2014). Acute psychosocial stress and children's memory. *Stress (Amsterdam, Netherlands)*, *17*(4), 305–313. doi:10.3109/10253890.2014.919446

Debener, S., Makeig, S., Delorme, A., & Engel, A. K. (2005). What is novel in the novelty oddball paradigm? Functional significance of the novelty P3 event-related potential as revealed by independent component analysis. *Brain research. Cognitive brain research*, *22*(3), 309–321. doi:10.1016/j.cogbrainres.2004.09.006

Debener, S., Thorne, J., Schneider, T. R., & Viola, F. C. (2010). Using ICA for the Analysis of Multi-Channel EEG Data. In M. Ullsperger & S. Debener (Eds.), *Simultaneous EEG and fMRI. Recording, analysis, and application* (pp. 121–133). New York: Oxford University Press.

Dedovic, K., Duchesne, A., Andrews, J., Engert, V., & Pruessner, J. C. (2009). The brain and the stress axis: the neural correlates of cortisol regulation in response to stress. *NeuroImage*, *47*(3), 864–871. doi:10.1016/j.neuroimage.2009.05.074

Delahaye, M., Lemoine, P., Cartwright, S., Deuring, G., Beck, J., Pflueger, M.,. . . Hachtel, H. (2015). Learning aptitude, spatial orientation and cognitive flexibility tested in a virtual labyrinth after virtual stress induction. *BMC psychology*, *3*(1), 22. doi:10.1186/s40359-015-0080-5

Delorme, A., & Makeig, S. (2003). EEG changes accompanying learned regulation of 12-Hz EEG activity. *IEEE transactions on neural systems and rehabilitation engineering : a publication of the IEEE Engineering in Medicine and Biology Society*, *11*(2), 133–137. doi:10.1109/TNSRE.2003.814428

Delorme, A., & Makeig, S. (2004). EEGLAB: An open source toolbox for analysis of single-trial EEG dynamics including independent component analysis. *Journal of Neuroscience Methods*, *134*(1), 9–21. doi:10.1016/j.jneumeth.2003.10.009

Delorme, A., Palmer, J., Onton, J., Oostenveld, R., & Makeig, S. (2012). Independent EEG sources are dipolar. *PloS one*, *7*(2), e30135. doi:10.1371/journal.pone.0030135

Delorme, A., Sejnowski, T., & Makeig, S. (2007). Enhanced detection of artifacts in EEG data using higher-order statistics and independent component analysis. *NeuroImage*, *34*(4), 1443–1449. doi:10.1016/j.neuroimage.2006.11.004

Demiralp, T., Bayraktaroglu, Z., Lenz, D., Junge, S., Busch, N. A., Maess, B.,. . . Herrmann, C. S. (2007). Gamma amplitudes are coupled to theta phase in human EEG during visual perception. *International journal of psychophysiology : official journal of the International Organization of Psychophysiology*, *64*(1), 24–30. doi:10.1016/j.ijpsycho.2006.07.005

Diamond, A. (2013). Executive functions. *Annual review of psychology*, *64*, 135–168. doi:10.1146/annurev-psych-113011-143750

Dickerson, S. S., & Kemeny, M. E. (2004). Acute Stressors and Cortisol Responses: A Theoretical Integration and Synthesis of Laboratory Research. *Psychological Bulletin*, *130*(3), 355–391. doi:10.1037/0033-2909.130.3.355

Dierolf, A. M. (2014). *The Relation between Stress and Aggression and The Role of Inhibitory Control and Social Information Processing within a Psychophysiological Approach* (Dissertation). Universität Trier, Trier. Retrieved from http://ubt.opus.hbz-nrw.de/volltexte/2014/897/

Dierolf, A. M., Arlt, L. E., Roelofs, K., Kolsch, M., Hülsemann, M. J., Schächinger, H., & Naumann, E. (2016). Effects of basal and acute cortisol on cognitive flexibility in an emotional task switching paradigm in men. *Hormones and behavior*, *81*, 12–19. doi:10.1016/j.yhbeh.2016.02.002

Diorio, D., Viau, V., & Meaney, M. J. (1993). The role of the medial prefrontal cortex (cingulate gyrus) in the regulation of hypothalamic-pituitary-adrenal responses to stress. *The Journal of neuroscience : the official journal of the Society for Neuroscience*, *13*(9), 3839–3847.

Dressendörfer, R. A., Kirschbaum, C., Rohde, W., Stahl, F., & Strasburger, C. J. (1992). Synthesis of a cortisol-biotin conjugate and evaluation as a tracer in an immunoassay for salivary cortisol measurement. *The Journal of Steroid Biochemistry and Molecular Biology*, *43*(7), 683–692. doi:10.1016/0960-0760(92)90294-S

Duncko, R., Johnson, L., Merikangas, K., & Grillon, C. (2009). Working memory performance after acute exposure to the cold pressor stress in healthy volunteers. *Neurobiology of Learning and Memory*, *91*(4), 377–381. doi:10.1016/j.nlm.2009.01.006

Dunn, O. J. (1961). Multiple Comparisons among Means. *Journal of the American Statistical Association*, *56*(293), 52–64. doi:10.1080/01621459.1961.10482090

Dürschmid, S., Quandt, F., Krämer, U. M., Hinrichs, H., Heinze, H.-J., Schulz, R.,. . . Knight, R. T. (2014). Oscillatory dynamics track motor performance improvement in human cortex. *PloS one*, *9*(2), e89576. doi:10.1371/journal.pone.0089576

Dürschmid, S., Zaehle, T., Kopitzki, K., Voges, J., Schmitt, F. C., Heinze, H.-J.,. . . Hinrichs, H. (2013). Phase-amplitude cross-frequency coupling in the human nucleus accumbens tracks action monitoring during cognitive control. *Frontiers in human neuroscience*, *7*, 635. doi:10.3389/fnhum.2013.00635

Edwards, M. S., Moore, P., Champion, J. C., & Edwards, E. J. (2015). Effects of trait anxiety and situational stress on attentional shifting are buffered by working memory capacity. *Anxiety, stress, and coping*, *28*(1), 1–16. doi:10.1080/10615806.2014.911846

Eguiluz, V. M., Chialvo, D. R., Cecchi, G. A., Baliki, M., & Apkarian, A. V. (2005). Scale-free brain functional networks. *Physical review letters*, *94*(1), 18102. doi:10.1103/PhysRevLett.94.018102

Elzinga, B. M., & Roelofs, K. (2005). Cortisol-induced impairments of working memory require acute sympathetic activation. *Behavioral neuroscience*, *119*(1), 98–103. doi:10.1037/0735-7044.119.1.98

Eriksen, B. A., & Eriksen, C. W. (1974). Effects of noise letters upon the identification of a target letter in a nonsearch task. *Perception & Psychophysics*, *16*(1), 143–149. doi:10.3758/BF03203267

Fair, D. A., Cohen, A. L., Power, J. D., Dosenbach, N. U. F., Church, J. A., Miezin, F. M.,. . . Petersen, S. E. (2009). Functional brain networks develop from a "local to distributed" organization. *PLoS computational biology*, *5*(5), e1000381. doi:10.1371/journal.pcbi.1000381

Fairbairn, J. (2007). *Stress, cortisol and executive function: a study of pre-adolescent school children* (Dissertation). University College London, London.

Fan, J., Byrne, J., Worden, M. S., Guise, K. G., McCandliss, B. D., Fossella, J., & Posner, M. I. (2007). The relation of brain oscillations to attentional networks. *The Journal of neuroscience : the official journal of the Society for Neuroscience*, *27*(23), 6197–6206. doi:10.1523/jneurosci.1833-07.2007

Fan, J., Fossella, J., Sommer, T., Wu, Y., & Posner, M. I. (2003). Mapping the genetic variation of executive attention onto brain activity. *Proceedings of the National Academy of Sciences of the United States of America*, *100*(12), 7406–7411. doi:10.1073/pnas.0732088100

Fan, J., McCandliss, B. D., Fossella, J., Flombaum, J. I., & Posner, M. I. (2005). The activation of attentional networks. *NeuroImage*, *26*(2), 471–479. doi:10.1016/j.neuroimage.2005.02.004

Fan, J., McCandliss, B. D., Sommer, T., Raz, A., & Posner, M. I. (2002). Testing the efficiency and independence of attentional networks. *Journal of cognitive neuroscience*, *14*(3), 340–347. doi:10.1162/089892902317361886

Fechtner, J. (2012). *The Role of Cognitive Control and Approach-Avoidance Motivation in the Relationship between Stress and Aggression - A Psychophysiological Investigation* (Dissertation). Universität Trier, Trier. Retrieved from http://ubt.opus.hbz-nrw.de/volltexte/2013/786/

Foster, B. L., & Parvizi, J. (2012). Resting oscillations and cross-frequency coupling in the human posteromedial cortex. *NeuroImage*, *60*(1), 384–391. doi:10.1016/j.neuroimage.2011.12.019

Fox, M. D., Snyder, A. Z., Vincent, J. L., Corbetta, M., van Essen, D. C., & Raichle, M. E. (2005). The human brain is intrinsically organized into dynamic, anticorrelated functional networks. *Proceedings of the National Academy of Sciences of the United States of America*, *102*(27), 9673–9678. doi:10.1073/pnas.0504136102

Friedman, N. P., Miyake, A., Young, S. E., Defries, J. C., Corley, R. P., & Hewitt, J. K. (2008). Individual differences in executive functions are almost entirely genetic in origin. *Journal of experimental psychology. General*, *137*(2), 201–225. doi:10.1037/0096-3445.137.2.201

Fries, E., Dettenborn, L., & Kirschbaum, C. (2009). The cortisol awakening response (CAR): facts and future directions. *International journal of psychophysiology : official journal of the International Organization of Psychophysiology*, *72*(1), 67–73. doi:10.1016/j.ijpsycho.2008.03.014

Friese, U., Köster, M., Hassler, U., Martens, U., Trujillo-Barreto, N., & Gruber, T. (2013). Successful memory encoding is associated with increased cross-frequency coupling between frontal theta and posterior gamma oscillations in human scalp-recorded EEG. *NeuroImage*, *66*, 642–647. doi:10.1016/j.neuroimage.2012.11.002

Fuster, J. M. (1980). *The prefrontal cortex: Anatomy, physiology, and neuropsychology of the frontal lobe*. New York: Raven Press.

Galin, D., Ornstein, R., Herron, J., & Johnstone, J. (1982). Sex and handedness differences in EEG measures of hemispheric specialization. *Brain and Language*, *16*(1), 19–55. doi:10.1016/0093-934X(82)90070-0

Gärtner, M., Rohde-Liebenau, L., Grimm, S., & Bajbouj, M. (2014). Working memory-related frontal theta activity is decreased under acute stress. *Psychoneuroendocrinology*, *43*, 105–113. doi:10.1016/j.psyneuen.2014.02.009

Gathmann, B., Schulte, F. P., Maderwald, S., Pawlikowski, M., Starcke, K., Schäfer, L. C.,. . . Brand, M. (2014). Stress and decision making: neural correlates of the interaction between stress, executive functions, and decision making under risk. *Experimental brain research*, *232*(3), 957–973. doi:10.1007/s00221-013-3808-6

Geisser, S., & Greenhouse, S. W. (1958). An Extension of Box's Results on the Use of the F Distribution in Multivariate Analysis. *The Annals of Mathematical Statistics*, *29*(3), 885–891. doi:10.1214/aoms/1177706545

Genazzani, A. R., Mannella, P., & Simoncini, T. (2007). Drospirenone and its antialdosterone properties. *Climacteric : the journal of the International Menopause Society*, *10 Suppl 1*, 11–18. doi:10.1080/13697130601114891

Gogtay, N., Giedd, J. N., Lusk, L., Hayashi, K. M., Greenstein, D., Vaituzis, A. C.,. . . Thompson, P. M. (2004). Dynamic mapping of human cortical development during childhood through early adulthood. *Proceedings of the National Academy of Sciences of the United States of America*, *101*(21), 8174–8179. doi:10.1073/pnas.0402680101

Groeneweg, F. L., Karst, H., de Kloet, E. R., & Joëls, M. (2011). Rapid non-genomic effects of corticosteroids and their role in the central stress response. *The Journal of endocrinology*, *209*(2), 153–167. doi:10.1530/joe-10-0472

Hagemann, D. (1999). *Tonische Asymmetrien corticaler Aktiviertheit und affektive Dispositionen: Eine empirische Untersuchung latenter State- und Traitvariablen*. Berlin: Logos Vlg. Berlin.

Hager, W. (1987). Grundlagen einer Versuchsplanung. In G. Lüer (Ed.), *UTB für Wissenschaft. Grosse Reihe. Allgemeine experimentelle Psychologie. Eine Einführung in die methodischen Grundlagen mit praktischen Übungen für das experimentelle Praktikum* (pp. 254–258). Stuttgart: Fischer.

Hagmann, P., Cammoun, L., Gigandet, X., Meuli, R., Honey, C. J., van Wedeen, J., & Sporns, O. (2008). Mapping the structural core of human cerebral cortex. *PLoS biology*, *6*(7), e159. doi:10.1371/journal.pbio.0060159

Haller, J., Mikics, E., & Makara, G. B. (2008). The effects of non-genomic glucocorticoid mechanisms on bodily functions and the central neural system. A critical evaluation of findings. *Frontiers in neuroendocrinology*, *29*(2), 273–291. doi:10.1016/j.yfrne.2007.10.004

Hays, W. L. (1973). *Statistics for the social sciences* (2nd ed.). New York: Holt, Rinehart and Winston.

He, B. J., Zempel, J. M., Snyder, A. Z., & Raichle, M. E. (2010). The temporal structures and functional significance of scale-free brain activity. *Neuron*, *66*(3), 353–369. doi:10.1016/j.neuron.2010.04.020

He, Y., Chen, Z. J., & Evans, A. C. (2007). Small-world anatomical networks in the human brain revealed by cortical thickness from MRI. *Cerebral cortex (New York, N.Y. : 1991)*, *17*(10), 2407–2419. doi:10.1093/cercor/bhl149

Hebb, D. O. (1949). *The organization of behavior: A neuropsychological theory*. New York, NY: Wiley.

Hebb, D. O. (1955). Drives and the C. N. S. (conceptual nervous system). *Psychological review*, *62*(4), 243–254. doi:10.1037/h0041823

Herculano-Houzel, S. (2009). The human brain in numbers: a linearly scaled-up primate brain. *Frontiers in human neuroscience*, *3*, 31. doi:10.3389/neuro.09.031.2009

Herman, J. P., & Cullinan, W. E. (1997). Neurocircuitry of stress: central control of the hypothalamo-pituitary-adrenocortical axis. *Trends in neurosciences*, *20*(2), 78–84. doi:10.1016/S0166-2236(96)10069-2

Het, S., Ramlow, G., & Wolf, O. T. (2005). A meta-analytic review of the effects of acute cortisol administration on human memory. *Psychoneuroendocrinology*, *30*(8), 771–784. doi:10.1016/j.psyneuen.2005.03.005

Hillier, A., Alexander, J. K., & Beversdorf, D. Q. (2006). The effect of auditory stressors on cognitive flexibility. *Neurocase*, *12*(4), 228–231. doi:10.1080/13554790600878887

Hoffman, R., & al'Absi, M. (2004). The effect of acute stress on subsequent neuropsychological test performance (2003). *Archives of clinical neuropsychology : the official journal of the National Academy of Neuropsychologists*, *19*(4), 497–506. doi:10.1016/j.acn.2003.07.005

Holmes, A., & Wellman, C. L. (2009). Stress-induced prefrontal reorganization and executive dysfunction in rodents. *Neuroscience and biobehavioral reviews*, *33*(6), 773–783. doi:10.1016/j.neubiorev.2008.11.005

Hopkins, W. D., Misiura, M., Pope, S. M., & Latash, E. M. (2015). Behavioral and brain asymmetries in primates: a preliminary evaluation of two evolutionary hypotheses. *Annals of the New York Academy of Sciences*, *1359*, 65–83. doi:10.1111/nyas.12936

Hülsemann, M. J. (2013). *Stress and Frequency Band Coupling in Resting EEG. Influence of Cortisol on Delta-Beta Coupling* (Master Thesis). Universität Trier, Trier.

Hyvärinen, A., Karhunen, J., & Oja, E. (2001). *Independent component analysis*. New York: J. Wiley.

Ishigami, Y., & Klein, R. M. (2010). Repeated measurement of the components of attention using two versions of the Attention Network Test (ANT): stability, isolability, robustness, and reliability. *Journal of Neuroscience Methods*, *190*(1), 117–128. doi:10.1016/j.jneumeth.2010.04.019

Ishizuka, K., Hillier, A., & Beversdorf, D. Q. (2007). Effect of the cold pressor test on memory and cognitive flexibility. *Neurocase*, *13*(3), 154–157. doi:10.1080/13554790701441403

Jackson, A. F., & Bolger, D. J. (2014). The neurophysiological bases of EEG and EEG measurement: a review for the rest of us. *Psychophysiology*, *51*(11), 1061–1071. doi:10.1111/psyp.12283

Jäncke, L. (2013). *Lehrbuch Kognitive Neurowissenschaften*. *Lehrbuch Psychologie*. Bern: Huber.

Jensen, O. (2006). Maintenance of multiple working memory items by temporal segmentation. *Neuroscience*, *139*(1), 237–249. doi:10.1016/j.neuroscience.2005.06.004

Jensen, O., & Lisman, J. E. (1998). An oscillatory short-term memory buffer model can account for data on the Sternberg task. *The Journal of neuroscience : the official journal of the Society for Neuroscience*, *18*(24), 10688–10699.

Jensen, O., & Colgin, L. L. (2007). Cross-frequency coupling between neuronal oscillations. *Trends in cognitive sciences*, *11*(7), 267–269. doi:10.1016/j.tics.2007.05.003

Jensen, O., & Tesche, C. D. (2002). Frontal theta activity in humans increases with memory load in a working memory task. *The European journal of neuroscience*, *15*(8), 1395–1399. doi:10.1046/j.1460-9568.2002.01975.x

Jirsa, V., & Müller, V. (2013). Cross-frequency coupling in real and virtual brain networks. *Frontiers in computational neuroscience*, *7*, 78. doi:10.3389/fncom.2013.00078

Joëls, M., & de Kloet, E. R. (1992). Control of neuronal excitability by corticosteroid hormones. *Trends in neurosciences*, *15*(1), 25–30. doi:10.1016/0166-2236(92)90345-9

Joëls, M., & de Kloet, E. R. (1994). Mineralocorticoid and glucocorticoid receptors in the brain. Implications for ion permeability and transmitter systems. *Progress in neurobiology*, *43*(1), 1–36. doi:10.1016/0301-0082(94)90014-0

Joëls, M., & Baram, T. Z. (2009). The neuro-symphony of stress. *Nature reviews. Neuroscience*, *10*(6), 459–466. doi:10.1038/nrn2632

Johnson, E. O., Kamilaris, T. C., Chrousos, G. P., & Gold, P. W. (1992). Mechanisms of stress: a dynamic overview of hormonal and behavioral homeostasis. *Neuroscience and biobehavioral reviews*, *16*(2), 115–130. doi:10.1016/S0149-7634(05)80175-7

Jung, T. P., Makeig, S., Humphries, C., Lee, T. W., McKeown, M. J., Iragui, V., & Sejnowski, T. J. (2000). Removing electroencephalographic artifacts by blind source separation. *Psychophysiology*, *37*(2), 163–178. doi:10.1111/1469-8986.3720163

Jung, T. P., Makeig, S., Westerfield, M., Townsend, J., Courchesne, E., & Sejnowski, T. J. (2001). Analysis and visualization of single-trial event-related potentials. *Human brain mapping*, *14*(3), 166–185. doi:10.1002/hbm.1050

Kaplan, R., Bush, D., Bonnefond, M., Bandettini, P. A., Barnes, G. R., Doeller, C. F., & Burgess, N. (2014). Medial prefrontal theta phase coupling during spatial memory retrieval. *Hippocampus*, *24*(6), 656–665. doi:10.1002/hipo.22255

Keller-Wood, M. (2015). Hypothalamic-Pituitary--Adrenal Axis-Feedback Control. *Comprehensive Physiology*, *5*(3), 1161–1182. doi:10.1002/cphy.c140065

Kern, S., Oakes, T. R., Stone, C. K., McAuliff, E. M., Kirschbaum, C., & Davidson, R. J. (2008). Glucose metabolic changes in the prefrontal cortex are associated with HPA axis response to a psychosocial stressor. *Psychoneuroendocrinology*, *33*(4), 517–529. doi:10.1016/j.psyneuen.2008.01.010

Kiesel, A., Steinhauser, M., Wendt, M., Falkenstein, M., Jost, K., Philipp, A. M., & Koch, I. (2010). Control and interference in task switching--a review. *Psychological Bulletin*, *136*(5), 849–874. doi:10.1037/a0019842

Kirihara, K., Rissling, A. J., Swerdlow, N. R., Braff, D. L., & Light, G. A. (2012). Hierarchical Organization of Gamma and Theta Oscillatory Dynamics in Schizophrenia. *Biological psychiatry*, *71*(10), 873–880. doi:10.1016/j.biopsych.2012.01.016

Kirschbaum, C., Pirke, K. M., & Hellhammer, D. H. (1993). The 'Trier Social Stress Test'--a tool for investigating psychobiological stress responses in a laboratory setting. *Neuropsychobiology*, *28*(1-2), 76–81. doi:10.1159/000119004

Kirschbaum, C., & Hellhammer, D. H. (2000). Salivary Cortisol. In G. Fink (Ed.), *Encyclopedia of stress* (1st ed., pp. 379–383). San Diego: Academic Press.

Knyazev, G. G. (2011). Cross-frequency coupling of brain oscillations: an impact of state anxiety. *International journal of psychophysiology : official journal of the International Organization of Psychophysiology*, *80*(3), 236–245. doi:10.1016/j.ijpsycho.2011.03.013

Kofman, O., Meiran, N., Greenberg, E., Balas, M., & Cohen, H. (2006). Enhanced performance on executive functions associated with examination stress: Evidence from task-switching and Stroop paradigms. *Cognition & Emotion*, *20*(5), 577–595. doi:10.1080/02699930500270913

Köster, M., Friese, U., Schöne, B., Trujillo-Barreto, N., & Gruber, T. (2014). Theta-gamma coupling during episodic retrieval in the human EEG. *Brain research*, *1577*, 57–68. doi:10.1016/j.brainres.2014.06.028

Kothe, C. A. (2013). The Artifact Subspace Reconstruction method. Retrieved September 26, 2016. Retrieved from http://sccn.ucsd.edu/eeglab/plugins/ASR.pdf

Kramer, M. A., & Eden, U. T. (2013). Assessment of cross-frequency coupling with confidence using generalized linear models. *Journal of Neuroscience Methods*, *220*(1), 64–74. doi:10.1016/j.jneumeth.2013.08.006

Kury, P. (2012). *Der überforderte Mensch: Eine Wissensgeschichte vom Stress zum Burnout*. *Campus Historische Studien: Vol. 66*. Frankfurt am Main: Campus.

Lai, V., Theppitak, C., Makizuka, T., Higuchi, Y., Movahed, M., Kumudini, G.,. . . Kumashiro, M. (2014). A normal intensity level of psycho-physiological stress can benefit working memory performance at high load. *International Journal of Industrial Ergonomics*, *44*(3), 362–367. doi:10.1016/j.ergon.2013.11.015

Lakatos, P., Shah, A. S., Knuth, K. H., Ulbert, I., Karmos, G., & Schroeder, C. E. (2005). An oscillatory hierarchy controlling neuronal excitability and stimulus processing in the auditory cortex. *Journal of neurophysiology*, *94*(3), 1904–1911. doi:10.1152/jn.00263.2005

Lee, J., & Yun, K. (2014). Alcohol reduces cross-frequency theta-phase gamma-amplitude coupling in resting electroencephalography. *Alcoholism, clinical and experimental research*, *38*(3), 770–776. doi:10.1111/acer.12310

Lega, B., Burke, J., Jacobs, J., & Kahana, M. J. (2016). Slow-Theta-to-Gamma Phase-Amplitude Coupling in Human Hippocampus Supports the Formation of New Episodic Memories. *Cerebral cortex (New York, N.Y. : 1991)*, *26*(1), 268–278. doi:10.1093/cercor/bhu232

Leibniz, G. W. (2013). *Neue Abhandlungen über den menschlichen Verstand : Buch I-II = Nouveaux Essais sur l'entendement humain: Livre I-II*. hrsg. und übers. von Wolf von Engelhardt und Hans Heinz Holz (Sonderausg). *Philosophische Schriften / Gottfried Wilhelm Leibniz: Vol. 3,1*. Darmstadt: Wiss. Buchges.

Lenartowicz, A., Kalar, D. J., Congdon, E., & Poldrack, R. A. (2010). Towards an ontology of cognitive control. *Topics in cognitive science*, *2*(4), 678–692. doi:10.1111/j.1756-8765.2010.01100.x

Leszczynski, M., Fell, J., & Axmacher, N. (2015). Rhythmic Working Memory Activation in the Human Hippocampus. *Cell reports*, *13*(6), 1272–1282. doi:10.1016/j.celrep.2015.09.081

Levy, B. J., & Wagner, A. D. (2011). Cognitive control and right ventrolateral prefrontal cortex: reflexive reorienting, motor inhibition, and action updating. *Annals of the New York Academy of Sciences*, *1224*, 40–62. doi:10.1111/j.1749-6632.2011.05958.x

Lewis, R. S., Nikolova, A., Chang, D. J., & Weekes, N. Y. (2008). Examination stress and components of working memory. *Stress (Amsterdam, Netherlands)*, *11*(2), 108–114. doi:10.1080/10253890701535160

Li, S., Bai, W., Liu, T., Yi, H., & Tian, X. (2012). Increases of theta-low gamma coupling in rat medial prefrontal cortex during working memory task. *Brain research bulletin*, *89*(3-4), 115–123. doi:10.1016/j.brainresbull.2012.07.012

Lieberman, K. W., Stokes, P. E., Fanelli, C. J., & Klevan, T. (1980). Reuptake of biogenic amines by brain slices: effect of hydrocortisone. *Psychopharmacology*, *70*(1), 59–61. doi:10.1007/BF00432370

Linn, M. C., & Petersen, A. C. (1985). Emergence and Characterization of Sex Differences in Spatial Ability: A Meta-Analysis. *Child Development*, *56*(6), 1479. doi:10.2307/1130467

Lisman, J. E., & Idiart, M. A. (1995). Storage of 7 +/- 2 short-term memories in oscillatory subcycles. *Science (New York, N.Y.)*, *267*(5203), 1512–1515. doi:10.1126/science.7878473

Lisman, J. E., & Jensen, O. (2013). The theta-gamma neural code. *Neuron*, *77*(6), 1002–1016. doi:10.1016/j.neuron.2013.03.007

Liston, C., McEwen, B. S., & Casey, B. J. (2009). Psychosocial stress reversibly disrupts prefrontal processing and attentional control. *Proceedings of the National Academy of Sciences of the United States of America*, *106*(3), 912–917. doi:10.1073/pnas.0807041106

Liu, G., Hu, P.-P., Fan, J., & Wang, K. (2013). Gender differences associated with orienting attentional networks in healthy subjects. *Chinese medical journal*, *126*(12), 2308–2312.

Lopez-Azcarate, J., Tainta, M., Rodriguez-Oroz, M. C., Valencia, M., Gonzalez, R., Guridi, J.,. . . Alegre, M. (2010). Coupling between beta and high-frequency activity in the human subthalamic nucleus may be a pathophysiological mechanism in Parkinson's disease. *The Journal of neuroscience : the official journal of the Society for Neuroscience*, *30*(19), 6667–6677. doi:10.1523/JNEUROSCI.5459-09.2010

Losel, R. M., Falkenstein, E., Feuring, M., Schultz, A., Tillmann, H.-C., Rossol-Haseroth, K., & Wehling, M. (2003). Nongenomic Steroid Action: Controversies, Questions, and Answers. *Physiological Reviews*, *83*(3), 965–1016. doi:10.1152/physrev.00003.2003

Lovallo, W. R. (1997). *Stress & health: Biological and psychological interactions*. *Behavioral medicine and health psychology series: v. 1*. Thousand Oaks, Calif.: Sage Publications.

Luethi, M., Meier, B., & Sandi, C. (2008). Stress effects on working memory, explicit memory, and implicit memory for neutral and emotional stimuli in healthy men. *Frontiers in behavioral neuroscience*, *2*, 5. doi:10.3389/neuro.08.005.2008

MacLeod, J. W., Lawrence, M. A., McConnell, M. M., Eskes, G. A., Klein, R. M., & Shore, D. I. (2010). Appraising the ANT: Psychometric and theoretical considerations of the Attention Network Test. *Neuropsychology*, *24*(5), 637–651. doi:10.1037/a0019803

Makara, G. B., & Haller, J. (2001). Non-genomic effects of glucocorticoids in the neural system. *Progress in neurobiology*, *65*(4), 367–390. doi:10.1016/S0301-0082(01)00012-0

Makeig, S., Jung, T. P., Bell, A. J., Ghahremani, D., & Sejnowski, T. J. (1997). Blind separation of auditory event-related brain responses into independent components. *Proceedings of the National Academy of Sciences of the United States of America*, *94*(20), 10979–10984. doi:10.1073/pnas.94.20.10979

Makeig, S., Westerfield, M., Jung, T. P., Covington, J., Townsend, J., Sejnowski, T. J., & Courchesne, E. (1999). Functionally independent components of the late positive event-related potential during visual spatial attention. *The Journal of neuroscience : the official journal of the Society for Neuroscience*, *19*(7), 2665–2680. doi:10.1098/rstb.1999.0469

Makeig, S., Westerfield, M., Jung, T. P., Enghoff, S., Townsend, J., Courchesne, E., & Sejnowski, T. J. (2002). Dynamic brain sources of visual evoked responses. *Science (New York, N.Y.)*, *295*(5555), 690–694. doi:10.1126/science.1066168

Makeig, S., Bell, A. J., Jung, T. P., & Sejnowski, T. J. (1996). Independent component analysis of electroencephalographic data. In D. S. Touretzky, M. C. Mozer, & M. E. Hasselmo (Eds.), *A Bradford book. Advances in Neural Information Processing Systems 8. Proceedings of the 1995 conference* (pp. 145–151). Cambridge, Mass., London: MIT Press.

Malekmohammadi, M., Elias, W. J., & Pouratian, N. (2015). Human thalamus regulates cortical activity via spatially specific and structurally constrained phase-amplitude coupling. *Cerebral cortex (New York, N.Y. : 1991)*, *25*(6), 1618–1628. doi:10.1093/cercor/bht358

Maris, E., van Vugt, M., & Kahana, M. (2011). Spatially distributed patterns of oscillatory coupling between high-frequency amplitudes and low-frequency phases in human iEEG. *NeuroImage*, *54*(2), 836–850. doi:10.1016/j.neuroimage.2010.09.029

McEwen, B. S. (2000a). Allostasis and Allostatic Load. In G. Fink (Ed.), *Encyclopedia of stress* (1st ed., pp. 145–149). San Diego: Academic Press.

McEwen, B. S. (2000b). Stress, Definitions and Concepts of. In G. Fink (Ed.), *Encyclopedia of stress* (1st ed., pp. 508–509). San Diego: Academic Press.

McEwen, B. S. (2007). Physiology and neurobiology of stress and adaptation: central role of the brain. *Physiological Reviews*, *87*(3), 873–904. doi:10.1152/physrev.00041.2006

McEwen, B. S., de Kloet, E. R., & Rostene, W. (1986). Adrenal steroid receptors and actions in the nervous system. *Physiological Reviews*, *66*(4), 1121–1188.

McEwen, B. S., Weiss, J. M., & Schwartz, L. S. (1968). Selective retention of corticosterone by limbic structures in rat brain. *Nature*, *220*(5170), 911–912. doi:10.1038/220911a0

McGaugh, J. L. (2000). Memory--a Century of Consolidation. *Science*, *287*(5451), 248–251. doi:10.1126/science.287.5451.248

McGinn, R. J., & Valiante, T. A. (2014). Phase-amplitude coupling and interlaminar synchrony are correlated in human neocortex. *The Journal of neuroscience : the official journal of the Society for Neuroscience*, *34*(48), 15923–15930. doi:10.1523/JNEUROSCI.2771-14.2014

McMorris, T., Swain, J., Smith, M., Corbett, J., Delves, S., Sale, C.,. . . Potter, J. (2006). Heat stress, plasma concentrations of adrenaline, noradrenaline, 5-hydroxytryptamine and cortisol, mood state and cognitive performance. *International journal of psychophysiology : official journal of the International Organization of Psychophysiology*, *61*(2), 204–215. doi:10.1016/j.ijpsycho.2005.10.002

McRae, A. L., Saladin, M. E., Brady, K. T., Upadhyaya, H., Back, S. E., & Timmerman, M. A. (2006). Stress reactivity: biological and subjective responses to the cold pressor and Trier Social stressors. *Human psychopharmacology*, *21*(6), 377–385. doi:10.1002/hup.778

Meaney, M. J., & Aitken, D. H. (1985). [3H]Dexamethasone binding in rat frontal cortex. *Brain research*, *328*(1), 176–180. doi:10.1016/0006-8993(85)91340-X

Mehring, C., Rickert, J., Vaadia, E., Cardosa de Oliveira, S., Aertsen, A., & Rotter, S. (2003). Inference of hand movements from local field potentials in monkey motor cortex. *Nature neuroscience*, *6*(12), 1253–1254. doi:10.1038/nn1158

Meyer, K., & Damasio, A. (2009). Convergence and divergence in a neural architecture for recognition and memory. *Trends in neurosciences*, *32*(7), 376–382. doi:10.1016/j.tins.2009.04.002

Miller, G. A. (1956). The magical number seven, plus or minus two: Some limits on our capacity for processing information. *Psychological review*, *63*(2), 81–97. doi:10.1037/h0043158

Miller, K. J., Sorensen, L. B., Ojemann, J. G., & den Nijs, M. (2009). Power-law scaling in the brain surface electric potential. *PLoS computational biology*, *5*(12), e1000609. doi:10.1371/journal.pcbi.1000609

Miller, R., Plessow, F., Kirschbaum, C., & Stalder, T. (2013). Classification criteria for distinguishing cortisol responders from nonresponders to psychosocial stress: evaluation of salivary cortisol pulse detection in panel designs. *Psychosomatic medicine*, *75*(9), 832–840. doi:10.1097/psy.0000000000000002

Miyake, A., Friedman, N. P., Emerson, M. J., Witzki, A. H., Howerter, A., & Wager, T. D. (2000). The unity and diversity of executive functions and their contributions to complex "Frontal Lobe" tasks: a latent variable analysis. *Cognitive psychology*, *41*(1), 49–100. doi:10.1006/cogp.1999.0734

Miyake, A., & Friedman, N. P. (2012). The Nature and Organization of Individual Differences in Executive Functions: Four General Conclusions. *Current directions in psychological science*, *21*(1), 8–14. doi:10.1177/0963721411429458

Miyakoshi, M. (2016). Makoto's preprocessing pipeline. Retrieved September 26, 2016. Retrieved from http://sccn.ucsd.edu/wiki/Makoto%27s_preprocessing_pipeline

Miyakoshi, M., Delorme, A., Mullen, T., Kojima, K., Makeig, S., & Asano, E. (2013). Automated detection of cross-frequency coupling in the electrocorticogram for clinical inspection. *Conference proceedings : ... Annual International Conference of the IEEE Engineering in Medicine and Biology Society. IEEE Engineering in Medicine and Biology Society. Annual Conference*, *2013*, 3282–3285. doi:10.1109/EMBC.2013.6610242

Mizuhara, H., & Yamaguchi, Y. (2011). Neuronal ensemble for visual working memory via interplay of slow and fast oscillations. *The European journal of neuroscience*, *33*(10), 1925–1934. doi:10.1111/j.1460-9568.2011.07681.x

Molaee-Ardekani, B., Senhadji, L., Shamsollahi, M.-B., Wodey, E., & Vosoughi-Vahdat, B. (2007). Delta waves differently modulate high frequency components of EEG oscillations in various unconsciousness levels. *Conference proceedings : ... Annual International Conference of the IEEE Engineering in Medicine and Biology Society. IEEE Engineering in Medicine and Biology Society. Annual Conference*, *2007*, 1294–1297. doi:10.1109/IEMBS.2007.4352534

Monsell, S. (2003). Task switching. *Trends in cognitive sciences*, *7*(3), 134–140. doi:10.1016/S1364-6613(03)00028-7

Monto, S. (2012). Nested synchrony-a novel cross-scale interaction among neuronal oscillations. *Frontiers in physiology*, *3*, 384. doi:10.3389/fphys.2012.00384

Monto, S., Palva, S., Voipio, J., & Palva, J. M. (2008). Very slow EEG fluctuations predict the dynamics of stimulus detection and oscillation amplitudes in humans. *The Journal of neuroscience : the official journal of the Society for Neuroscience*, *28*(33), 8268–8272. doi:10.1523/JNEUROSCI.1910-08.2008

Mormann, F., Fell, J., Axmacher, N., Weber, B., Lehnertz, K., Elger, C. E., & Fernandez, G. (2005). Phase/amplitude reset and theta-gamma interaction in the human medial temporal lobe during a continuous word recognition memory task. *Hippocampus*, *15*(7), 890–900. doi:10.1002/hipo.20117

Mukamel, E. A., Wong, K. F., Prerau, M. J., Brown, E. N., & Purdon, P. L. (2011). Phase-based measures of cross-frequency coupling in brain electrical dynamics under general anesthesia. *Conference proceedings : ... Annual International Conference of the IEEE Engineering in Medicine and Biology Society. IEEE Engineering in Medicine and Biology Society. Annual Conference*, *2011*, 1981–1984. doi:10.1109/IEMBS.2011.6090558

Müller-Linow, M., Hilgetag, C. C., & Hütt, M.-T. (2008). Organization of excitable dynamics in hierarchical biological networks. *PLoS computational biology*, *4*(9), e1000190. doi:10.1371/journal.pcbi.1000190

Myers, B., McKlveen, J. M., & Herman, J. P. (2014). Glucocorticoid actions on synapses, circuits, and behavior: implications for the energetics of stress. *Frontiers in neuroendocrinology*, *35*(2), 180–196. doi:10.1016/j.yfrne.2013.12.003

Nakatani, C., Raffone, A., & van Leeuwen, C. (2014). Efficiency of conscious access improves with coupling of slow and fast neural oscillations. *Journal of cognitive neuroscience*, *26*(5), 1168–1179. doi:10.1162/jocn_a_00540

Nee, D. E., Wager, T. D., & Jonides, J. (2007). Interference resolution: insights from a meta-analysis of neuroimaging tasks. *Cognitive, affective & behavioral neuroscience*, *7*(1), 1–17. doi:10.3758/CABN.7.1.1

Nestler, E. J., Hyman, S. E., & Malenka, R. C. (2009). *Molecular neuropharmacology: A foundation for clinical neuroscience* (2nd ed.). *McGraw Hill professional*. New York: McGraw-Hill Medical.

Neuhaus, A. H., Opgen-Rhein, C., Urbanek, C., Gross, M., Hahn, E., Ta, T. M. T.,. . . Dettling, M. (2009). Spatiotemporal mapping of sex differences during attentional processing. *Human brain mapping*, *30*(9), 2997–3008. doi:10.1002/hbm.20724

Niendam, T. A., Laird, A. R., Ray, K. L., Dean, Y. M., Glahn, D. C., & Carter, C. S. (2012). Meta-analytic evidence for a superordinate cognitive control network subserving diverse executive functions. *Cognitive, affective & behavioral neuroscience*, *12*(2), 241–268. doi:10.3758/s13415-011-0083-5

Nishikawa, T., Motter, A. E., Lai, Y.-C., & Hoppensteadt, F. C. (2003). Heterogeneity in oscillator networks: are smaller worlds easier to synchronize? *Physical review letters*, *91*(1), 14101. doi:10.1103/PhysRevLett.91.014101

Norman, A. W., Mizwicki, M. T., & Norman, D. P. G. (2004). Steroid-hormone rapid actions, membrane receptors and a conformational ensemble model. *Nature Reviews Drug Discovery*, *3*(1), 27–41. doi:10.1038/nrd1283

Novak, P., Lepicovska, V., & Dostalek, C. (1992). Periodic amplitude modulation of EEG. *Neuroscience letters*, *136*(2), 213–215. doi:10.1016/0304-3940(92)90051-8

Oei, N. Y. L., Everaerd, W. T. A. M., Elzinga, B. M., van Well, S., & Bermond, B. (2006). Psychosocial stress impairs working memory at high loads: an association with cortisol levels and memory retrieval. *Stress (Amsterdam, Netherlands)*, *9*(3), 133–141. doi:10.1080/10253890600965773

Oei, N. Y. L., Veer, I. M., Wolf, O. T., Spinhoven, P., Rombouts, S. A. R. B., & Elzinga, B. M. (2012). Stress shifts brain activation towards ventral 'affective' areas during emotional distraction. *Social cognitive and affective neuroscience*, *7*(4), 403–412. doi:10.1093/scan/nsr024

Olver, J. S., Pinney, M., Maruff, P., & Norman, T. R. (2015). Impairments of spatial working memory and attention following acute psychosocial stress. *Stress and health : journal of the International Society for the Investigation of Stress*, *31*(2), 115–123. doi:10.1002/smi.2533

Onslow, A. C. E., Bogacz, R., & Jones, M. W. (2011). Quantifying phase-amplitude coupling in neuronal network oscillations. *Progress in biophysics and molecular biology*, *105*(1-2), 49–57. doi:10.1016/j.pbiomolbio.2010.09.007

Onton, J., & Makeig, S. (2006). Information-based modeling of event-related brain dynamics. *Progress in brain research*, *159*, 99–120. doi:10.1016/S0079-6123(06)59007-7

Onton, J., & Makeig, S. (2014). EEGLAB Tutorial - II. Multiple Subject Processing: Chapter 05 - Component Clustering Tools. Retrieved September 26, 2016. Retrieved from http://sccn.ucsd.edu/wiki/Chapter_05:_Component_Clustering_Tools

Onton, J., Westerfield, M., Townsend, J., & Makeig, S. (2006). Imaging human EEG dynamics using independent component analysis. *Neuroscience and biobehavioral reviews*, *30*(6), 808–822. doi:10.1016/j.neubiorev.2006.06.007

Oostendorp, T. F., & van Oosterom, A. (1989). Source parameter estimation in inhomogeneous volume conductors of arbitrary shape. *IEEE transactions on bio-medical engineering*, *36*(3), 382–391. doi:10.1109/10.19859

Open Science Collaboration. (2015). Estimating the reproducibility of psychological science. *Science*, *349*(6251), aac4716. doi:10.1126/science.aac4716

O'Reilly, R. C. (1998). Six principles for biologically based computational models of cortical cognition. *Trends in cognitive sciences*, *2*(11), 455–462. doi:10.1016/S1364-6613(98)01241-8

Osipova, D., Hermes, D., & Jensen, O. (2008). Gamma power is phase-locked to posterior alpha activity. *PloS one*, *3*(12), e3990. doi:10.1371/journal.pone.0003990

Özkurt, T. E., & Schnitzler, A. (2011). A critical note on the definition of phase-amplitude cross-frequency coupling. *Journal of Neuroscience Methods*, *201*(2), 438–443. doi:10.1016/j.jneumeth.2011.08.014

Park, H.-J., & Friston, K. (2013). Structural and functional brain networks: from connections to cognition. *Science (New York, N.Y.)*, *342*(6158), 1238411. doi:10.1126/science.1238411

Park, J. Y., Jhung, K., Lee, J., & An, S. K. (2013). Theta-gamma coupling during a working memory task as compared to a simple vigilance task. *Neuroscience letters*, *532*, 39–43. doi:10.1016/j.neulet.2012.10.061

Park, J. Y., Lee, Y.-R., & Lee, J. (2011). The relationship between theta-gamma coupling and spatial memory ability in older adults. *Neuroscience letters*, *498*(1), 37–41. doi:10.1016/j.neulet.2011.04.056

Patel, P. D., Lopez, J. F., Lyons, D. M., Burke, S., Wallace, M., & Schatzberg, A. F. (2000). Glucocorticoid and mineralocorticoid receptor mRNA expression in squirrel monkey brain. *Journal of psychiatric research*, *34*(6), 383–392. doi:10.1016/S0022-3956(00)00035-2

Pattyn, N., Mairesse, O., Cortoos, A., Morais, J., Soetens, E., Roelands, B.,. . . Kolinsky, R. (2014). Cardiac reactivity and preserved performance under stress: two sides of the same coin? *International journal of psychophysiology : official journal of the International Organization of Psychophysiology*, *93*(1), 30–37. doi:10.1016/j.ijpsycho.2013.03.008

Penny, W. D., Duzel, E., Miller, K. J., & Ojemann, J. G. (2008). Testing for nested oscillation. *Journal of Neuroscience Methods*, *174*(1), 50–61. doi:10.1016/j.jneumeth.2008.06.035

Penttonen, M., & Buzsáki, G. (2003). Natural logarithmic relationship between brain oscillators. *Thalamus & Related Systems*, *2*(2), 145–152. doi:10.1016/S1472-9288(03)00007-4

Pesaran, B., Pezaris, J. S., Sahani, M., Mitra, P. P., & Andersen, R. A. (2002). Temporal structure in neuronal activity during working memory in macaque parietal cortex. *Nature neuroscience*, *5*(8), 805–811. doi:10.1038/nn890

Petersen, S. E., & Posner, M. I. (2012). The attention system of the human brain: 20 years after. *Annual review of neuroscience*, *35*, 73–89. doi:10.1146/annurev-neuro-062111-150525

Pfurtscheller, G. (1976). Ultralangsame Schwankungen innerhalb der rhythmischen Aktivität im Alpha-Band und deren mögliche Ursachen. *Pflugers Arch. (Pflügers Archiv European Journal of Physiology)*, *367*(1), 55–66. doi:10.1007/BF00583657

Plessow, F., Fischer, R., Kirschbaum, C., & Goschke, T. (2011). Inflexibly focused under stress: acute psychosocial stress increases shielding of action goals at the expense of reduced cognitive flexibility with increasing time lag to the stressor. *Journal of cognitive neuroscience*, *23*(11), 3218–3227. doi:10.1162/jocn_a_00024

Plessow, F., Kiesel, A., & Kirschbaum, C. (2012). The stressed prefrontal cortex and goal-directed behaviour: acute psychosocial stress impairs the flexible implementation of task goals. *Experimental brain research*, *216*(3), 397–408. doi:10.1007/s00221-011-2943-1

Plessow, F., Schade, S., Kirschbaum, C., & Fischer, R. (2012). Better not to deal with two tasks at the same time when stressed? Acute psychosocial stress reduces task shielding in dual-task performance. *Cognitive, affective & behavioral neuroscience*, *12*(3), 557–570. doi:10.3758/s13415-012-0098-6

Popov, T., Steffen, A., Weisz, N., Miller, G. A., & Rockstroh, B. (2012). Cross-frequency dynamics of neuromagnetic oscillatory activity: two mechanisms of emotion regulation. *Psychophysiology*, *49*(12), 1545–1557. doi:10.1111/j.1469-8986.2012.01484.x

Porcelli, A. J., Cruz, D., Wenberg, K., Patterson, M. D., Biswal, B. B., & Rypma, B. (2008). The effects of acute stress on human prefrontal working memory systems. *Physiology & behavior*, *95*(3), 282–289. doi:10.1016/j.physbeh.2008.04.027

Posner, M. I. (1980). Orienting of attention. *The Quarterly journal of experimental psychology*, *32*(1), 3–25. doi:10.1080/00335558008248231

Posner, M. I., & Petersen, S. E. (1990). The attention system of the human brain. *Annual review of neuroscience*, *13*, 25–42. doi:10.1146/annurev.ne.13.030190.000325

Posner, M. I., & Rothbart, M. K. (2007). Research on attention networks as a model for the integration of psychological science. *Annual review of psychology*, *58*, 1–23. doi:10.1146/annurev.psych.58.110405.085516

Preuss, T. M. (1995). Do rats have prefrontal cortex? The rose-woolsey-akert program reconsidered. *Journal of cognitive neuroscience*, *7*(1), 1–24. doi:10.1162/jocn.1995.7.1.1

Qi, X.-R., Kamphuis, W., Wang, S., Wang, Q., Lucassen, P. J., Zhou, J.-N., & Swaab, D. F. (2013). Aberrant stress hormone receptor balance in the human prefrontal cortex and hypothalamic paraventricular nucleus of depressed patients. *Psychoneuroendocrinology*, *38*(6), 863–870. doi:10.1016/j.psyneuen.2012.09.014

Qin, S., Cousijn, H., Rijpkema, M., Luo, J., Franke, B., Hermans, E. J., & Fernández, G. (2012). The effect of moderate acute psychological stress on working memory-related neural activity is modulated by a genetic variation in catecholaminergic function in humans. *Frontiers in integrative neuroscience*, *6*, 16. doi:10.3389/fnint.2012.00016

Qin, S., Hermans, E. J., van Marle, H. J. F., Luo, J., & Fernández, G. (2009). Acute psychological stress reduces working memory-related activity in the dorsolateral prefrontal cortex. *Biological psychiatry*, *66*(1), 25–32. doi:10.1016/j.biopsych.2009.03.006

Quinn, P. D., & Fromme, K. (2016). Individual differences in subjective alcohol responses and alcohol-related disinhibition. *Experimental and clinical psychopharmacology*, *24*(2), 90–99. doi:10.1037/pha0000065

Radvansky, G. A. (2015). *Human memory* (2nd ed.). London: Routledge.

Rajji, T. K., Zomorrodi, R., Barr, M. S., Blumberger, D. M., Mulsant, B. H., & Daskalakis, Z. J. (2016). Ordering Information in Working Memory and Modulation of Gamma by Theta Oscillations in Humans. *Cerebral cortex (New York, N.Y. : 1991).* doi:10.1093/cercor/bhv326

Rasch, B., Friese, M., Hofmann, W., & Naumann, E. (2006). *Quantitative Methoden 2: Einführung in die Statistik* (2., erw. Aufl.). *Springer-Lehrbuch*. Berlin, Heidelberg: Springer Medizin Verlag Heidelberg.

Raz, A., & Buhle, J. (2006). Typologies of attentional networks. *Nature reviews. Neuroscience*, *7*(5), 367–379. doi:10.1038/nrn1903

Reinhart, R. M. G., Zhu, J., Park, S., & Woodman, G. F. (2015). Synchronizing theta oscillations with direct-current stimulation strengthens adaptive control in the human brain. *Proceedings of the National Academy of Sciences of the United States of America*, *112*(30), 9448–9453. doi:10.1073/pnas.1504196112

Renner, K. H., & Beversdorf, D. Q. (2010). Effects of naturalistic stressors on cognitive flexibility and working memory task performance. *Neurocase*, *16*(4), 293–300. doi:10.1080/13554790903463601

Ridderinkhof, K. R., van den Wildenberg, W. P. M., Segalowitz, S. J., & Carter, C. S. (2004). Neurocognitive mechanisms of cognitive control: the role of prefrontal cortex in action selection, response inhibition, performance monitoring, and reward-based learning. *Brain and cognition*, *56*(2), 129–140. doi:10.1016/j.bandc.2004.09.016

Robinson, S. J., Sünram-Lea, S. I., Leach, J., & Owen-Lynch, P. J. (2008). The effects of exposure to an acute naturalistic stressor on working memory, state anxiety and salivary cortisol concentrations. *Stress (Amsterdam, Netherlands)*, *11*(2), 115–124. doi:10.1080/10253890701559970

Robinson, S. J., Leach, J., Owen-Lynch, P. J., & Sünram-Lea, S. I. (2013). Stress Reactivity and Cognitive Performance in a Simulated Firefighting Emergency. *Aviation, Space, and Environmental Medicine*, *84*(6), 592–599. doi:10.3357/ASEM.3391.2013

Rogers, R. D., & Monsell, S. (1995). Costs of a predictible switch between simple cognitive tasks. *Journal of Experimental Psychology: General*, *124*(2), 207–231. doi:10.1037/0096-3445.124.2.207

Rottschy, C., Langner, R., Dogan, I., Reetz, K., Laird, A. R., Schulz, J. B.,. . . Eickhoff, S. B. (2012). Modelling neural correlates of working memory: a coordinate-based meta-analysis. *NeuroImage*, *60*(1), 830–846. doi:10.1016/j.neuroimage.2011.11.050

Roux, F., Wibral, M., Singer, W., Aru, J., & Uhlhaas, P. J. (2013). The phase of thalamic alpha activity modulates cortical gamma-band activity: evidence from resting-state MEG recordings. *The Journal of neuroscience : the official journal of the Society for Neuroscience*, *33*(45), 17827–17835. doi:10.1523/JNEUROSCI.5778-12.2013

Roznowski, M., & Smith, M. L. (1993). A note on some psychometric properties of Sternberg task performance: Modifications to content. *Intelligence*, *17*(3), 389–398. doi:10.1016/0160-2896(93)90006-Q

Rubinov, M., & Sporns, O. (2010). Complex network measures of brain connectivity: uses and interpretations. *NeuroImage*, *52*(3), 1059–1069. doi:10.1016/j.neuroimage.2009.10.003

Sabb, F. W., Bearden, C. E., Glahn, D. C., Parker, D. S., Freimer, N., & Bilder, R. M. (2008). A collaborative knowledge base for cognitive phenomics. *Molecular psychiatry*, *13*(4), 350–360. doi:10.1038/sj.mp.4002124

Salvador, R., Suckling, J., Coleman, M. R., Pickard, J. D., Menon, D., & Bullmore, E. (2005). Neurophysiological architecture of functional magnetic resonance images of human brain. *Cerebral cortex (New York, N.Y. : 1991)*, *15*(9), 1332–1342. doi:10.1093/cercor/bhi016

Sánchez, M. M., Young, L. J., Plotsky, P. M., & Insel, T. R. (2000). Distribution of corticosteroid receptors in the rhesus brain: relative absence of glucocorticoid receptors in the hippocampal formation. *The Journal of neuroscience : the official journal of the Society for Neuroscience*, *20*(12), 4657–4668.

Sänger, J., Bechtold, L., Schoofs, D., Blaszkewicz, M., & Wascher, E. (2014). The influence of acute stress on attention mechanisms and its electrophysiological correlates. *Frontiers in behavioral neuroscience*, *8*, 353. doi:10.3389/fnbeh.2014.00353

Sapolsky, R. M., Romero, L. M., & Munck, A. U. (2000). How do glucocorticoids influence stress responses? Integrating permissive, suppressive, stimulatory, and preparative actions. *Endocrine reviews*, *21*(1), 55–89. doi:10.1210/edrv.21.1.0389

Sarrieau, A., Dussaillant, M., Agid, F., Philibert, D., Agid, Y., & Rostene, W. (1986). Autoradiographic localization of glucocorticosteroid and progesterone binding sites in the human post-mortem brain. *Journal of steroid biochemistry*, *25*(5B), 717–721. doi:10.1016/0022-4731(86)90300-6

Sarrieau, A., Dussaillant, M., Sapolsky, R. M., Aitken, D. H., Olivier, A., Lal, S.,. . . Meaney, M. J. (1988). Glucocorticoid binding sites in human temporal cortex. *Brain research*, *442*(1), 157–160. doi:10.1016/0006-8993(88)91444-8

Sato, H., Takenaka, I., & Kawahara, J. I. (2012). The effects of acute stress and perceptual load on distractor interference. *Quarterly journal of experimental psychology (2006)*, *65*(4), 617–623. doi:10.1080/17470218.2011.648944

Sauro, M. D., Jorgensen, R. S., & Pedlow, C. T. (2003). Stress, glucocorticoids, and memory: a meta-analytic review. *Stress (Amsterdam, Netherlands)*, *6*(4), 235–245. doi:10.1080/10253890310001616482

Scheffzük, C., Kukushka, V. I., Vyssotski, A. L., Draguhn, A., Tort, A. B. L., & Brankačk, J. (2011). Selective coupling between theta phase and neocortical fast gamma oscillations during REM-sleep in mice. *PloS one*, *6*(12), e28489. doi:10.1371/journal.pone.0028489

Schlader, Z. J., Gagnon, D., Adams, A., Rivas, E., Cullum, C. M., & Crandall, C. G. (2015). Cognitive and perceptual responses during passive heat stress in younger and older adults. *American journal of physiology. Regulatory, integrative and comparative physiology*, *308*(10), R847-54. doi:10.1152/ajpregu.00010.2015.

Schmidt, S. (2009). Shall we really do it again?: The powerful concept of replication is neglected in the social sciences. *Review of General Psychology*, *13*(2), 90–100. doi:10.1037/a0015108

Scholz, U., La Marca, R., Nater, U. M., Aberle, I., Ehlert, U., Hornung, R.,. . . Kliegel, M. (2009). Go no-go performance under psychosocial stress: beneficial effects of implementation intentions. *Neurobiology of Learning and Memory*, *91*(1), 89–92. doi:10.1016/j.nlm.2008.09.002

Schoofs, D., Pabst, S., Brand, M., & Wolf, O. T. (2013). Working memory is differentially affected by stress in men and women. *Behavioural brain research*, *241*, 144–153. doi:10.1016/j.bbr.2012.12.004

Schoofs, D., Preuss, D., & Wolf, O. T. (2008). Psychosocial stress induces working memory impairments in an n-back paradigm. *Psychoneuroendocrinology*, *33*(5), 643–653. doi:10.1016/j.psyneuen.2008.02.004

Schoofs, D., Wolf, O. T., & Smeets, T. (2009). Cold pressor stress impairs performance on working memory tasks requiring executive functions in healthy young men. *Behavioral neuroscience*, *123*(5), 1066–1075. doi:10.1037/a0016980

Schutter, D. J., & Knyazev, G. G. (2012). Cross-frequency coupling of brain oscillations in studying motivation and emotion. *Motivation and emotion*, *36*(1), 46–54. doi:10.1007/s11031-011-9237-6

Schwabe, L., Haddad, L., & Schachinger, H. (2008). HPA axis activation by a socially evaluated cold-pressor test. *Psychoneuroendocrinology*, *33*(6), 890–895. doi:10.1016/j.psyneuen.2008.03.001

Schwabe, L., Höffken, O., Tegenthoff, M., & Wolf, O. T. (2013). Stress-induced enhancement of response inhibition depends on mineralocorticoid receptor activation. *Psychoneuroendocrinology*, *38*(10), 2319–2326. doi:10.1016/j.psyneuen.2013.05.001

Schwabe, L., Joels, M., Roozendaal, B., Wolf, O. T., & Oitzl, M. S. (2012). Stress effects on memory: an update and integration. *Neuroscience and biobehavioral reviews*, *36*(7), 1740–1749. doi:10.1016/j.neubiorev.2011.07.002

Schwarz, A. J., Gass, N., Sartorius, A., Risterucci, C., Spedding, M., Schenker, E.,. . . Weber-Fahr, W. (2013). Anti-correlated cortical networks of intrinsic connectivity in the rat brain. *Brain connectivity*, *3*(5), 503–511. doi:10.1089/brain.2013.0168

Schweisthal, O. W. (2007). *Der Cortisol Awakening Response in der Diagnostik stressbezogener Erkrankungen* (Dissertation). Universität Trier, Trier. Retrieved from http://ubt.opus.hbz-nrw.de/volltexte/2007/442/

Seehagen, S., Schneider, S., Rudolph, J., Ernst, S., & Zmyj, N. (2015). Stress impairs cognitive flexibility in infants. *Proceedings of the National Academy of Sciences of the United States of America*, *112*(41), 12882–12886. doi:10.1073/pnas.1508345112

Selye, H., & McKeown, T. (1935). Studies on the Physiology of the Maternal Placenta in the Rat. *Proceedings of the Royal Society of London. Series B, Biological Sciences*, *119*(812), 1–31. doi:10.1098/rspb.1935.0073

Selye, H., & Pentz, E. I. (1943). Pathogenetical Correlations between Periarteritis Nodosa, Renal Hypertension and Rheumatic Lesions. *Canadian Medical Association journal*, *49*(4), 264–272.

Selye, H. (1936). A Syndrome produced by Diverse Nocuous Agents. *Nature*, *138*(3479), 32. doi:10.1038/138032a0

Selye, H. (1939). The Effect Of Adaption To Various Damaging Agents On The Female Sex Organs in The Rat. *Endocrinology*, *25*(4), 615–624. doi:10.1210/endo-25-4-615

Selye, H. (1946). The general adaption syndrome and the diseases of adaption. *The Journal of Clinical Endocrinology & Metabolism*, *6*(2), 117–230. doi:10.1210/jcem-6-2-117

Selye, H. (1977). *Stress: Lebensregeln vom Entdecker d. Stress-Syndroms*. *Rororo: 7072 : rororo-Sachbuch*. Reinbek bei Hamburg: Rowohlt.

Shields, G. S., Bonner, J. C., & Moons, W. G. (2015). Does cortisol influence core executive functions? A meta-analysis of acute cortisol administration effects on working memory, inhibition, and set-shifting. *Psychoneuroendocrinology*, *58*, 91–103. doi:10.1016/j.psyneuen.2015.04.017

Shields, G. S., Sazma, M. A., & Yonelinas, A. P. (2016). The Effects of Acute Stress on Core Executive Functions: A Meta-Analysis and Comparison with Cortisol. *Neuroscience and biobehavioral reviews*. doi:10.1016/j.neubiorev.2016.06.038

Shields, G. S., Trainor, B. C., Lam, J. C. W., & Yonelinas, A. P. (2016). Acute Stress Impairs Cognitive Flexibility in Men, Not Women. *Stress (Amsterdam, Netherlands)*, 1–18. doi:10.1080/10253890.2016.1192603

Siegel, M., Warden, M. R., & Miller, E. K. (2009). Phase-dependent neuronal coding of objects in short-term memory. *Proceedings of the National Academy of Sciences of the United States of America*, *106*(50), 21341–21346. doi:10.1073/pnas.0908193106

Silbernagl, S., & Despopoulos, A. (2012). *Taschenatlas Physiologie* (8., überarb. und erw. Aufl.). Stuttgart: Thieme.

Sinclair, D., Tsai, S. Y., Woon, H. G., & Weickert, C. S. (2011). Abnormal glucocorticoid receptor mRNA and protein isoform expression in the prefrontal cortex in psychiatric illness. *Neuropsychopharmacology : official publication of the American College of Neuropsychopharmacology*, *36*(13), 2698–2709. doi:10.1038/npp.2011.160

Smeets, T., Jelicic, M., & Merckelbach, H. (2006). The effect of acute stress on memory depends on word valence. *International journal of psychophysiology : official journal of the International Organization of Psychophysiology*, *62*(1), 30–37. doi:10.1016/j.ijpsycho.2005.11.007

Soto, J. L. P., & Jerbi, K. (2012). Investigation of cross-frequency phase-amplitude coupling in visuomotor networks using magnetoencephalography. *Conference proceedings : ... Annual International Conference of the IEEE Engineering in Medicine and Biology Society. IEEE Engineering in Medicine and Biology Society. Annual Conference*, *2012*, 1550–1553. doi:10.1109/EMBC.2012.6346238

Spaak, E., Bonnefond, M., Maier, A., Leopold, D. A., & Jensen, O. (2012). Layer-specific entrainment of gamma-band neural activity by the alpha rhythm in monkey visual cortex. *Current biology : CB*, *22*(24), 2313–2318. doi:10.1016/j.cub.2012.10.020

Spadone, S., Pasquale, F. de, Mantini, D., & Della Penna, S. (2012). A K-means multivariate approach for clustering independent components from magnetoencephalographic data. *NeuroImage*, *62*(3), 1912–1923. doi:10.1016/j.neuroimage.2012.05.051

Sporns, O. (2011). *Networks of the brain*. Cambridge, Mass.: MIT Press.

Sporns, O., & Zwi, J. D. (2004). The small world of the cerebral cortex. *Neuroinformatics*, *2*(2), 145–162. doi:10.1385/NI:2:2:145

Stam, C. J. (2004). Functional connectivity patterns of human magnetoencephalographic recordings: A 'small-world' network? *Neuroscience letters*, *355*(1-2), 25–28. doi:10.1016/j.neulet.2003.10.063

Staresina, B. P., Bergmann, T. O., Bonnefond, M., van der Meij, R., Jensen, O., Deuker, L.,. . . Fell, J. (2015). Hierarchical nesting of slow oscillations, spindles and ripples in the human hippocampus during sleep. *Nature neuroscience*, *18*(11), 1679–1686. doi:10.1038/nn.4119

Stauble, M. R., Thompson, L. A., & Morgan, G. (2013). Increases in cortisol are positively associated with gains in encoding and maintenance working memory performance in young men. *Stress (Amsterdam, Netherlands)*, *16*(4), 402–410. doi:10.3109/10253890.2013.780236

Steinhauser, M., Maier, M., & Hübner, R. (2007). Cognitive control under stress: How stress affects strategies of task-set reconfiguration. *Psychological science*, *18*(6), 540–545. doi:10.1111/j.1467-9280.2007.01935.x

Sternberg, S. (1966). High-speed scanning in human memory. *Science*, *153*(3736), 652–654. doi:10.1126/science.153.3736.652

Sternberg, S. (1975). Memory scanning: New findings and current controversies. *Quarterly Journal of Experimental Psychology*, *27*(1), 1–32. doi:10.1080/14640747508400459

Sun, G., Yang, X., Jiang, Q., Liu, K., Li, B., Li, L.,. . . Li, M. (2012). Hyperthermia impairs the executive function using the Attention Network Test. *International journal of hyperthermia : the official journal of European Society for Hyperthermic Oncology, North American Hyperthermia Group*, *28*(7), 621–626. doi:10.3109/02656736.2012.705217

Szczepanski, S. M., Crone, N. E., Kuperman, R. A., Auguste, K. I., Parvizi, J., & Knight, R. T. (2014). Dynamic changes in phase-amplitude coupling facilitate spatial attention control in fronto-parietal cortex. *PLoS biology*, *12*(8), e1001936. doi:10.1371/journal.pbio.1001936

Tang, H., Yu, H.-Y., Chou, C.-C., Crone, N. E., Madsen, J. R., Anderson, W. S., & Kreiman, G. (2016). Cascade of neural processing orchestrates cognitive control in human frontal cortex. *eLife*, *5*. doi:10.7554/eLife.12352

Tausk, M. (1951). Hat die Nebenniere tatsächlich eine Verteidungsfunktion? *Das Hormon : Zeitschrift für Endokrinologie mit Beiträgen über Vitaminforschung*, *4*(3), 1–24.

Taverniers, J., van Ruysseveldt, J., Smeets, T., & Grumbkow, J. von. (2010). High-intensity stress elicits robust cortisol increases, and impairs working memory and visuo-spatial declarative memory in Special Forces candidates: A field experiment. *Stress (Amsterdam, Netherlands)*, *13*(4), 323–333. doi:10.3109/10253891003642394

Thompson, R. F. (2000). *The brain: A neuroscience primer* (3rd ed.). New York, N.Y.: Worth Publishers.

Toro, R., Fox, P. T., & Paus, T. (2008). Functional coactivation map of the human brain. *Cerebral cortex (New York, N.Y. : 1991)*, *18*(11), 2553–2559. doi:10.1093/cercor/bhn014

Tort, A. B. L., Komorowski, R., Eichenbaum, H., & Kopell, N. (2010). Measuring phase-amplitude coupling between neuronal oscillations of different frequencies. *Journal of neurophysiology*, *104*(2), 1195–1210. doi:10.1152/jn.00106.2010.

Tort, A. B. L., Komorowski, R. W., Manns, J. R., Kopell, N. J., & Eichenbaum, H. (2009). Theta-gamma coupling increases during the learning of item-context associations. *Proceedings of the National Academy of Sciences of the United States of America*, *106*(49), 20942–20947. doi:10.1073/pnas.0911331106

Tort, A. B. L., Kramer, M. A., Thorn, C., Gibson, D. J., Kubota, Y., Graybiel, A. M., & Kopell, N. J. (2008). Dynamic cross-frequency couplings of local field potential oscillations in rat striatum and hippocampus during performance of a T-maze task. *Proceedings of the National Academy of Sciences of the United States of America*, *105*(51), 20517–20522. doi:10.1073/pnas.0810524105

Tukey, J. W. (1977). *Exploratory data analysis*. *Addison-Wesley series in behavioral science*. Reading, Mass.: Addison-Wesley Pub. Co.

van der Meij, R., Kahana, M., & Maris, E. (2012). Phase-amplitude coupling in human electrocorticography is spatially distributed and phase diverse. *The Journal of neuroscience : the official journal of the Society for Neuroscience*, *32*(1), 111–123. doi:10.1523/JNEUROSCI.4816-11.2012

van Wingerden, M., van der Meij, R., Kalenscher, T., Maris, E., & Pennartz, C. M. A. (2014). Phase-amplitude coupling in rat orbitofrontal cortex discriminates between correct and incorrect decisions during associative learning. *The Journal of neuroscience : the official journal of the Society for Neuroscience*, *34*(2), 493–505. doi:10.1523/JNEUROSCI.2098-13.2014

van Zaen, J., Murray, M. M., Meuli, R. A., & Vesin, J.-M. (2013). Adaptive filtering methods for identifying cross-frequency couplings in human EEG. *PloS one*, *8*(4), e60513. doi:10.1371/journal.pone.0060513

Vanhatalo, S., Palva, J. M., Holmes, M. D., Miller, J. W., Voipio, J., & Kaila, K. (2004). Infraslow oscillations modulate excitability and interictal epileptic activity in the human cortex during sleep. *Proceedings of the National Academy of Sciences of the United States of America*, *101*(14), 5053–5057. doi:10.1073/pnas.0305375101

Velasco, M., Gomez, J., Blanco, M., & Rodriguez, I. (1997). The cold pressor test: pharmacological and therapeutic aspects. *American journal of therapeutics*, *4*(1), 34–38. doi:10.1097/00045391-199701000-00008

Voloh, B., Valiante, T. A., Everling, S., & Womelsdorf, T. (2015). Theta-gamma coordination between anterior cingulate and prefrontal cortex indexes correct attention shifts. *Proceedings of the National Academy of Sciences of the United States of America*, *112*(27), 8457–8462. doi:10.1073/pnas.1500438112

von Stein, A., & Sarnthein, J. (2000). Different frequencies for different scales of cortical integration: From local gamma to long range alpha/theta synchronization. *International Journal of Psychophysiology*, *38*(3), 301–313. doi:10.1016/S0167-8760(00)00172-0

Vosskuhl, J., Huster, R. J., & Herrmann, C. S. (2015). Increase in short-term memory capacity induced by down-regulating individual theta frequency via transcranial alternating current stimulation. *Frontiers in human neuroscience*, *9*, 257. doi:10.3389/fnhum.2015.00257

Voyer, D., Voyer, S., & Bryden, M. P. (1995). Magnitude of sex differences in spatial abilities: A meta-analysis and consideration of critical variables. *Psychological Bulletin*, *117*(2), 250–270. doi:10.1037/0033-2909.117.2.250

Voytek, B., D'Esposito, M., Crone, N., & Knight, R. T. (2013). A method for event-related phase/amplitude coupling. *NeuroImage*, *64*, 416–424. doi:10.1016/j.neuroimage.2012.09.023

Voytek, B., Kayser, A. S., Badre, D., Fegen, D., Chang, E. F., Crone, N. E.,. . . D'Esposito, M. (2015). Oscillatory dynamics coordinating human frontal networks in support of goal maintenance. *Nature neuroscience*, *18*(9), 1318–1324. doi:10.1038/nn.4071

Wager, T. D., Jonides, J., & Reading, S. (2004). Neuroimaging studies of shifting attention: a meta-analysis. *NeuroImage*, *22*(4), 1679–1693. doi:10.1016/j.neuroimage.2004.03.052

Wager, T. D., & Smith, E. E. (2003). Neuroimaging studies of working memory: a meta-analysis. *Cognitive, affective & behavioral neuroscience*, *3*(4), 255–274. doi:10.3758/CABN.3.4.255

Wang, C., Qiu, W., Zheng, Y., Li, H., Li, Y., Feng, B.,. . . Cao, J.-M. (2013). Extraneuronal monoamine transporter mediates the permissive action of cortisol in the Guinea pig trachea: possible involvement of tracheal chondrocytes. *PloS one*, *8*(10), e76193. doi:10.1371/journal.pone.0076193

Watts, D. J., & Strogatz, S. H. (1998). Collective dynamics of 'small-world' networks. *Nature*, *393*(6684), 440–442. doi:10.1038/30918

Webster, J. C., & Cidlowski, J. A. (1999). Mechanisms of Glucocorticoid-receptor-mediated Repression of Gene Expression. *Trends in endocrinology and metabolism: TEM*, *10*(10), 396–402. doi:10.1016/S1043-2760(99)00186-1

Webster, M. J., Knable, M. B., O'Grady, J., Orthmann, J., & Weickert, C. S. (2002). Regional specificity of brain glucocorticoid receptor mRNA alterations in subjects with schizophrenia and mood disorders. *Molecular psychiatry*, *7*(9), 985-94, 924. doi:10.1038/sj.mp.4001139

Weerda, R., Muehlhan, M., Wolf, O. T., & Thiel, C. M. (2010). Effects of acute psychosocial stress on working memory related brain activity in men. *Human brain mapping*, *31*(9), 1418–1429. doi:10.1002/hbm.20945

Weitzman, E. D., Fukushima, D., Nogeire, C., Roffwarg, H., Gallagher, T. F., & Hellman, L. (1971). Twenty-four hour pattern of the episodic secretion of cortisol in normal subjects. *The Journal of clinical endocrinology and metabolism*, *33*(1), 14–22. doi:10.1210/jcem-33-1-14

White, J. G., Southgate, E., Thomson, J. N., & Brenner, S. (1986). The Structure of the Nervous System of the Nematode Caenorhabditis elegans. *Philosophical Transactions of the Royal Society B: Biological Sciences*, *314*(1165), 1–340. doi:10.1098/rstb.1986.0056

Whittingstall, K., & Logothetis, N. K. (2009). Frequency-band coupling in surface EEG reflects spiking activity in monkey visual cortex. *Neuron*, *64*(2), 281–289. doi:10.1016/j.neuron.2009.08.016

Widmann, A., Schröger, E., & Maess, B. (2015). Digital filter design for electrophysiological data – a practical approach. *Journal of Neuroscience Methods*, *250*, 34–46. doi:10.1016/j.jneumeth.2014.08.002

Winkler, I., Debener, S., Muller, K.-R., & Tangermann, M. (2015). On the influence of high-pass filtering on ICA-based artifact reduction in EEG-ERP. *Conference proceedings : ... Annual International Conference of the IEEE Engineering in Medicine and Biology Society. IEEE Engineering in Medicine and Biology Society. Annual Conference*, *2015*, 4101–4105. doi:10.1109/EMBC.2015.7319296

Wittfoth, M., Schardt, D. M., Fahle, M., & Herrmann, M. (2009). How the brain resolves high conflict situations: double conflict involvement of dorsolateral prefrontal cortex. *NeuroImage*, *44*(3), 1201–1209. doi:10.1016/j.neuroimage.2008.09.026

Worden, M. S. (2011). Attention Network Test (ANT). In J. S. Kreutzer, B. Caplan, & J. DeLuca (Eds.), *Springer reference. Encyclopedia of clinical neuropsychology* (pp. 296–297). New York, London: Springer. doi:10.1007/978-0-387-79948-3_1268

World Medical Association. (2013). World Medical Association Declaration of Helsinki: ethical principles for medical research involving human subjects. *JAMA*, *310*(20), 2191–2194. doi:10.1001/jama.2013.281053

Wu, J., Yuan, Y., Duan, H., Qin, S., Buchanan, T. W., Zhang, K., & Zhang, L. (2014). Long-term academic stress increases the late component of error processing: an ERP study. *Biological psychology*, *99*, 77–82. doi:10.1016/j.biopsycho.2014.03.002

Yanagisawa, T., Yamashita, O., Hirata, M., Kishima, H., Saitoh, Y., Goto, T.,. . . Kamitani, Y. (2012). Regulation of motor representation by phase-amplitude coupling in the sensorimotor cortex. *The Journal of neuroscience : the official journal of the Society for Neuroscience*, *32*(44), 15467–15475. doi:10.1523/JNEUROSCI.2929-12.2012

Yarkoni, T., Poldrack, R. A., Nichols, T. E., van Essen, D. C., & Wager, T. D. (2011). Large-scale automated synthesis of human functional neuroimaging data. *Nature methods*, *8*(8), 665–670. doi:10.1038/nmeth.1635

Yildiz, A., Wolf, O. T., & Beste, C. (2014). Stress intensifies demands on response selection during action cascading processes. *Psychoneuroendocrinology*, *42*, 178–187. doi:10.1016/j.psyneuen.2014.01.022

Young, C. K., & Eggermont, J. J. (2009). Coupling of mesoscopic brain oscillations: recent advances in analytical and theoretical perspectives. *Progress in neurobiology*, *89*(1), 61–78. doi:10.1016/j.pneurobio.2009.06.002

Zhang, K., & Sejnowski, T. J. (2000). A universal scaling law between gray matter and white matter of cerebral cortex. *Proceedings of the National Academy of Sciences of the United States of America*, *97*(10), 5621–5626. doi:10.1073/pnas.090504197

Zhivomirov, H. (2013). Pink, Red, Blue and Violet Noise Generation with Matlab Implementation. Retrieved September 26, 2016. Retrieved from http://www.mathworks.com/matlabcentral/fileexchange/42919-pink--red--blue-and-violet-noise-generation-with-matlab-implementation/content/rednoise.m

Ziegler, G., Dahnke, R., Jäncke, L., Yotter, R. A., May, A., & Gaser, C. (2012). Brain structural trajectories over the adult lifespan. *Human brain mapping*, *33*(10), 2377–2389. doi:10.1002/hbm.21374

APPENDIX A

List of 82 studies applying various phase-amplitude coupling measures

1. Allen, E. A., Liu, J., Kiehl, K. A., Gelernter, J., Pearlson, G. D., Perrone-Bizzozero, N. I., & Calhoun, V. D. (2011). Components of cross-frequency modulation in health and disease. *Frontiers in systems neuroscience*, *5*, 59. doi:10.3389/fnsys.2011.00059
2. Axmacher, N., Henseler, M. M., Jensen, O., Weinreich, I., Elger, C. E., & Fell, J. (2010). Cross-frequency coupling supports multi-item working memory in the human hippocampus. *Proceedings of the National Academy of Sciences of the United States of America*, *107*(7), 3228–3233. doi:10.1073/pnas.0911531107
3. Berman, J. I., Liu, S., Bloy, L., Blaskey, L., Roberts, T. P. L., & Edgar, J. C. (2015). Alpha-to-gamma phase-amplitude coupling methods and application to autism spectrum disorder. *Brain connectivity*, *5*(2), 80–90. doi:10.1089/brain.2014.0242
4. Bruns, A., & Eckhorn, R. (2004). Task-related coupling from high- to low-frequency signals among visual cortical areas in human subdural recordings. *International Journal of Psychophysiology*, *51*(2), 97–116. doi:10.1016/j.ijpsycho.2003.07.001
5. Burgess, A. P., & Ali, L. (2002). Functional connectivity of gamma EEG activity is modulated at low frequency during conscious recollection. *International journal of psychophysiology : official journal of the International Organization of Psychophysiology*, *46*(2), 91–100.
6. Buzsaki, G., Buhl, D. L., Harris, K. D., Csicsvari, J., Czeh, B., & Morozov, A. (2003). Hippocampal network patterns of activity in the mouse. *Neuroscience*, *116*(1), 201–211.
7. Canolty, R. T., Edwards, E., Dalal, S. S., Soltani, M., Nagarajan, S. S., Kirsch, H. E.,. . . Knight, R. T. (2006). High gamma power is phase-locked to theta oscillations in human neocortex. *Science (New York, N.Y.)*, *313*(5793), 1626–1628. doi:10.1126/science.1128115
8. Chorlian, D. B., Porjesz, B., & Begleiter, H. (2006). Amplitude modulation of gamma band oscillations at alpha frequency produced by photic driving. *International journal of psychophysiology : official journal of the International Organization of Psychophysiology*, *61*(2), 262–278. doi:10.1016/j.ijpsycho.2005.11.002
9. Cohen, M. X. (2008). Assessing transient cross-frequency coupling in EEG data. *Journal of Neuroscience Methods*, *168*(2), 494–499. doi:10.1016/j.jneumeth.2007.10.012
10. Cohen, M. X., Elger, C. E., & Fell, J. (2009). Oscillatory activity and phase-amplitude coupling in the human medial frontal cortex during decision making. *Journal of cognitive neuroscience*, *21*(2), 390–402. doi:10.1162/jocn.2008.21020
11. Colgin, L. L., Denninger, T., Fyhn, M., Hafting, T., Bonnevie, T., Jensen, O.,. . . Moser, E. I. (2009). Frequency of gamma oscillations routes flow of information in the hippocampus. *Nature*, *462*(7271), 353–357. doi:10.1038/nature08573
12. de Hemptinne, C., Ryapolova-Webb, E. S., Air, E. L., Garcia, P. A., Miller, K. J., Ojemann, J. G.,. . . Starr, P. A. (2013). Exaggerated phase-amplitude coupling in the primary motor cortex in Parkinson disease. *Proceedings of the National Academy of Sciences of the United States of America*, *110*(12), 4780–4785. doi:10.1073/pnas.1214546110

13. de Hemptinne, C., Swann, N. C., Ostrem, J. L., Ryapolova-Webb, E. S., San Luciano, M., Galifianakis, N. B., & Starr, P. A. (2015). Therapeutic deep brain stimulation reduces cortical phase-amplitude coupling in Parkinson's disease. *Nature neuroscience*, *18*(5), 779–786. doi:10.1038/nn.3997
14. Demiralp, T., Bayraktaroglu, Z., Lenz, D., Junge, S., Busch, N. A., Maess, B.,. . . Herrmann, C. S. (2007). Gamma amplitudes are coupled to theta phase in human EEG during visual perception. *International journal of psychophysiology : official journal of the International Organization of Psychophysiology*, *64*(1), 24–30. doi:10.1016/j.ijpsycho.2006.07.005
15. Dimitriadis, S. I., Laskaris, N. A., Bitzidou, M. P., Tarnanas, I., & Tsolaki, M. N. (2015). A novel biomarker of amnestic MCI based on dynamic cross-frequency coupling patterns during cognitive brain responses. *Frontiers in neuroscience*, *9*, 350. doi:10.3389/fnins.2015.00350
16. Dürschmid, S., Quandt, F., Krämer, U. M., Hinrichs, H., Heinze, H.-J., Schulz, R.,. . . Knight, R. T. (2014). Oscillatory dynamics track motor performance improvement in human cortex. *PloS one*, *9*(2), e89576. doi:10.1371/journal.pone.0089576
17. Dürschmid, S., Zaehle, T., Kopitzki, K., Voges, J., Schmitt, F. C., Heinze, H.-J.,. . . Hinrichs, H. (2013). Phase-amplitude cross-frequency coupling in the human nucleus accumbens tracks action monitoring during cognitive control. *Frontiers in human neuroscience*, *7*, 635. doi:10.3389/fnhum.2013.00635
18. Foster, B. L., & Parvizi, J. (2012). Resting oscillations and cross-frequency coupling in the human posteromedial cortex. *NeuroImage*, *60*(1), 384–391. doi:10.1016/j.neuroimage.2011.12.019
19. Fraga, F. J., Falk, T. H., Kanda, P. A. M., & Anghinah, R. (2013). Characterizing Alzheimer's disease severity via resting-awake EEG amplitude modulation analysis. *PloS one*, *8*(8), e72240. doi:10.1371/journal.pone.0072240
20. Friese, U., Köster, M., Hassler, U., Martens, U., Trujillo-Barreto, N., & Gruber, T. (2013). Successful memory encoding is associated with increased cross-frequency coupling between frontal theta and posterior gamma oscillations in human scalp-recorded EEG. *NeuroImage*, *66*, 642–647. doi:10.1016/j.neuroimage.2012.11.002
21. Guirgis, M., Chinvarun, Y., Del Campo, M., Carlen, P. L., & Bardakjian, B. L. (2015). Defining regions of interest using cross-frequency coupling in extratemporal lobe epilepsy patients. *Journal of neural engineering*, *12*(2), 26011. doi:10.1088/1741-2560/12/2/026011
22. He, B. J., Zempel, J. M., Snyder, A. Z., & Raichle, M. E. (2010). The temporal structures and functional significance of scale-free brain activity. *Neuron*, *66*(3), 353–369. doi:10.1016/j.neuron.2010.04.020
23. Helfrich, R. F., Herrmann, C. S., Engel, A. K., & Schneider, T. R. (2016). Different coupling modes mediate cortical cross-frequency interactions. *NeuroImage*, *140*, 76–82. doi:10.1016/j.neuroimage.2015.11.035
24. Herman, P. A., Lundqvist, M., & Lansner, A. (2013). Nested theta to gamma oscillations and precise spatiotemporal firing during memory retrieval in a simulated attractor network. *Brain research*, *1536*, 68–87. doi:10.1016/j.brainres.2013.08.002
25. Jirsa, V., & Müller, V. (2013). Cross-frequency coupling in real and virtual brain networks. *Frontiers in computational neuroscience*, *7*, 78. doi:10.3389/fncom.2013.00078

26. Kaplan, R., Bush, D., Bonnefond, M., Bandettini, P. A., Barnes, G. R., Doeller, C. F., & Burgess, N. (2014). Medial prefrontal theta phase coupling during spatial memory retrieval. *Hippocampus*, *24*(6), 656–665. doi:10.1002/hipo.22255
27. Kirihara, K., Rissling, A. J., Swerdlow, N. R., Braff, D. L., & Light, G. A. (2012). Hierarchical Organization of Gamma and Theta Oscillatory Dynamics in Schizophrenia. *Biological psychiatry*, *71*(10), 873–880. doi:10.1016/j.biopsych.2012.01.016
28. Knyazev, G. G. (2011). Cross-frequency coupling of brain oscillations: an impact of state anxiety. *International journal of psychophysiology : official journal of the International Organization of Psychophysiology*, *80*(3), 236–245. doi:10.1016/j.ijpsycho.2011.03.013
29. Köster, M., Friese, U., Schöne, B., Trujillo-Barreto, N., & Gruber, T. (2014). Theta-gamma coupling during episodic retrieval in the human EEG. *Brain research*, *1577*, 57–68. doi:10.1016/j.brainres.2014.06.028
30. Lakatos, P., Shah, A. S., Knuth, K. H., Ulbert, I., Karmos, G., & Schroeder, C. E. (2005). An oscillatory hierarchy controlling neuronal excitability and stimulus processing in the auditory cortex. *Journal of neurophysiology*, *94*(3), 1904–1911. doi:10.1152/jn.00263.2005
31. Lee, J., & Jeong, J. (2013). Correlation of risk-taking propensity with cross-frequency phase-amplitude coupling in the resting EEG. *Clinical neurophysiology : official journal of the International Federation of Clinical Neurophysiology*, *124*(11), 2172–2180. doi:10.1016/j.clinph.2013.05.007
32. Lee, J., & Yun, K. (2014). Alcohol reduces cross-frequency theta-phase gamma-amplitude coupling in resting electroencephalography. *Alcoholism, clinical and experimental research*, *38*(3), 770–776. doi:10.1111/acer.12310
33. Lega, B., Burke, J., Jacobs, J., & Kahana, M. J. (2016). Slow-Theta-to-Gamma Phase-Amplitude Coupling in Human Hippocampus Supports the Formation of New Episodic Memories. *Cerebral cortex (New York, N.Y. : 1991)*, *26*(1), 268–278. doi:10.1093/cercor/bhu232
34. Leszczynski, M., Fell, J., & Axmacher, N. (2015). Rhythmic Working Memory Activation in the Human Hippocampus. *Cell reports*, *13*(6), 1272–1282. doi:10.1016/j.celrep.2015.09.081
35. Li, S., Bai, W., Liu, T., Yi, H., & Tian, X. (2012). Increases of theta-low gamma coupling in rat medial prefrontal cortex during working memory task. *Brain research bulletin*, *89*(3-4), 115–123. doi:10.1016/j.brainresbull.2012.07.012
36. Lopez-Azcarate, J., Tainta, M., Rodriguez-Oroz, M. C., Valencia, M., Gonzalez, R., Guridi, J.,. . . Alegre, M. (2010). Coupling between beta and high-frequency activity in the human subthalamic nucleus may be a pathophysiological mechanism in Parkinson's disease. *The Journal of neuroscience : the official journal of the Society for Neuroscience*, *30*(19), 6667–6677. doi:10.1523/JNEUROSCI.5459-09.2010
37. Malekmohammadi, M., Elias, W. J., & Pouratian, N. (2015). Human thalamus regulates cortical activity via spatially specific and structurally constrained phase-amplitude coupling. *Cerebral cortex (New York, N.Y. : 1991)*, *25*(6), 1618–1628. doi:10.1093/cercor/bht358
38. Maris, E., van Vugt, M., & Kahana, M. (2011). Spatially distributed patterns of oscillatory coupling between high-frequency amplitudes and low-frequency phases in human iEEG. *NeuroImage*, *54*(2), 836–850. doi:10.1016/j.neuroimage.2010.09.029

39. McGinn, R. J., & Valiante, T. A. (2014). Phase-amplitude coupling and interlaminar synchrony are correlated in human neocortex. *The Journal of neuroscience : the official journal of the Society for Neuroscience*, *34*(48), 15923–15930. doi:10.1523/JNEUROSCI.2771-14.2014
40. Miller, K. J., Hermes, D., Honey, C. J., Sharma, M., Rao, R. P. N., den Nijs, M.,. . . Leuthardt, E. C. (2010). Dynamic modulation of local population activity by rhythm phase in human occipital cortex during a visual search task. *Frontiers in human neuroscience*, *4*, 197. doi:10.3389/fnhum.2010.00197
41. Miyakoshi, M., Delorme, A., Mullen, T., Kojima, K., Makeig, S., & Asano, E. (2013). Automated detection of cross-frequency coupling in the electrocorticogram for clinical inspection. *Conference proceedings : ... Annual International Conference of the IEEE Engineering in Medicine and Biology Society. IEEE Engineering in Medicine and Biology Society. Annual Conference*, *2013*, 3282–3285. doi:10.1109/EMBC.2013.6610242
42. Mizuhara, H., & Yamaguchi, Y. (2011). Neuronal ensemble for visual working memory via interplay of slow and fast oscillations. *The European journal of neuroscience*, *33*(10), 1925–1934. doi:10.1111/j.1460-9568.2011.07681.x
43. Monto, S. (2012). Nested synchrony-a novel cross-scale interaction among neuronal oscillations. *Frontiers in physiology*, *3*, 384. doi:10.3389/fphys.2012.00384
44. Monto, S., Palva, S., Voipio, J., & Palva, J. M. (2008). Very slow EEG fluctuations predict the dynamics of stimulus detection and oscillation amplitudes in humans. *The Journal of neuroscience : the official journal of the Society for Neuroscience*, *28*(33), 8268–8272. doi:10.1523/JNEUROSCI.1910-08.2008
45. Mormann, F., Fell, J., Axmacher, N., Weber, B., Lehnertz, K., Elger, C. E., & Fernandez, G. (2005). Phase/amplitude reset and theta-gamma interaction in the human medial temporal lobe during a continuous word recognition memory task. *Hippocampus*, *15*(7), 890–900. doi:10.1002/hipo.20117
46. Mukamel, E. A., Pirondini, E., Babadi, B., Wong, K. F. K., Pierce, E. T., Harrell, P. G.,. . . Purdon, P. L. (2014). A transition in brain state during propofol-induced unconsciousness. *The Journal of neuroscience : the official journal of the Society for Neuroscience*, *34*(3), 839–845. doi:10.1523/JNEUROSCI.5813-12.2014
47. Mukamel, E. A., Wong, K. F., Prerau, M. J., Brown, E. N., & Purdon, P. L. (2011). Phase-based measures of cross-frequency coupling in brain electrical dynamics under general anesthesia. *Conference proceedings : ... Annual International Conference of the IEEE Engineering in Medicine and Biology Society. IEEE Engineering in Medicine and Biology Society. Annual Conference*, *2011*, 1981–1984. doi:10.1109/IEMBS.2011.6090558
48. Nakatani, C., Raffone, A., & van Leeuwen, C. (2014). Efficiency of conscious access improves with coupling of slow and fast neural oscillations. *Journal of cognitive neuroscience*, *26*(5), 1168–1179. doi:10.1162/jocn_a_00540
49. Novak, P., Lepicovska, V., & Dostalek, C. (1992). Periodic amplitude modulation of EEG. *Neuroscience letters*, *136*(2), 213–215.
50. Osipova, D., Hermes, D., & Jensen, O. (2008). Gamma power is phase-locked to posterior alpha activity. *PloS one*, *3*(12), e3990. doi:10.1371/journal.pone.0003990

51. Özkurt, T. E., & Schnitzler, A. (2011). A critical note on the definition of phase-amplitude cross-frequency coupling. *Journal of Neuroscience Methods*, *201*(2), 438–443. doi:10.1016/j.jneumeth.2011.08.014
52. Papadaniil, C. D., Kosmidou, V. E., Tsolaki, A., Tsolaki, M., Kompatsiaris, I. Y., & Hadjileontiadis, L. J. (2015). Phase-amplitude cross-frequency coupling in EEG-derived cortical time series upon an auditory perception task. *Conference proceedings : ... Annual International Conference of the IEEE Engineering in Medicine and Biology Society. IEEE Engineering in Medicine and Biology Society. Annual Conference*, *2015*, 4150–4153. doi:10.1109/EMBC.2015.7319308
53. Park, J. Y., Jhung, K., Lee, J., & An, S. K. (2013). Theta-gamma coupling during a working memory task as compared to a simple vigilance task. *Neuroscience letters*, *532*, 39–43. doi:10.1016/j.neulet.2012.10.061
54. Park, J. Y., Lee, Y.-R., & Lee, J. (2011). The relationship between theta-gamma coupling and spatial memory ability in older adults. *Neuroscience letters*, *498*(1), 37–41. doi:10.1016/j.neulet.2011.04.056
55. Popov, T., Steffen, A., Weisz, N., Miller, G. A., & Rockstroh, B. (2012). Cross-frequency dynamics of neuromagnetic oscillatory activity: two mechanisms of emotion regulation. *Psychophysiology*, *49*(12), 1545–1557. doi:10.1111/j.1469-8986.2012.01484.x
56. Rajji, T. K., Zomorrodi, R., Barr, M. S., Blumberger, D. M., Mulsant, B. H., & Daskalakis, Z. J. (2016). Ordering Information in Working Memory and Modulation of Gamma by Theta Oscillations in Humans. *Cerebral cortex (New York, N.Y. : 1991).* doi:10.1093/cercor/bhv326
57. Roux, F., Wibral, M., Singer, W., Aru, J., & Uhlhaas, P. J. (2013). The phase of thalamic alpha activity modulates cortical gamma-band activity: evidence from resting-state MEG recordings. *The Journal of neuroscience : the official journal of the Society for Neuroscience*, *33*(45), 17827–17835. doi:10.1523/JNEUROSCI.5778-12.2013
58. Schack, B., Vath, N., Petsche, H., Geissler, H.-G., & Möller, E. (2002). Phase-coupling of theta–gamma EEG rhythms during short-term memory processing. *International Journal of Psychophysiology*, *44*(2), 143–163. doi:10.1016/S0167-8760(01)00199-4
59. Scheffzük, C., Kukushka, V. I., Vyssotski, A. L., Draguhn, A., Tort, A. B. L., & Brankačk, J. (2011). Selective coupling between theta phase and neocortical fast gamma oscillations during REM-sleep in mice. *PloS one*, *6*(12), e28489. doi:10.1371/journal.pone.0028489
60. Siegel, M., Warden, M. R., & Miller, E. K. (2009). Phase-dependent neuronal coding of objects in short-term memory. *Proceedings of the National Academy of Sciences of the United States of America*, *106*(50), 21341–21346. doi:10.1073/pnas.0908193106
61. Soto, J. L. P., & Jerbi, K. (2012). Investigation of cross-frequency phase-amplitude coupling in visuomotor networks using magnetoencephalography. *Conference proceedings : ... Annual International Conference of the IEEE Engineering in Medicine and Biology Society. IEEE Engineering in Medicine and Biology Society. Annual Conference*, *2012*, 1550–1553. doi:10.1109/EMBC.2012.6346238
62. Spaak, E., Bonnefond, M., Maier, A., Leopold, D. A., & Jensen, O. (2012). Layer-specific entrainment of gamma-band neural activity by the alpha rhythm in monkey visual cortex. *Current biology : CB*, *22*(24), 2313–2318. doi:10.1016/j.cub.2012.10.020

63. Staresina, B. P., Bergmann, T. O., Bonnefond, M., van der Meij, R., Jensen, O., Deuker, L.,. . . Fell, J. (2015). Hierarchical nesting of slow oscillations, spindles and ripples in the human hippocampus during sleep. *Nature neuroscience*, *18*(11), 1679–1686. doi:10.1038/nn.4119
64. Szczepanski, S. M., Crone, N. E., Kuperman, R. A., Auguste, K. I., Parvizi, J., & Knight, R. T. (2014). Dynamic changes in phase-amplitude coupling facilitate spatial attention control in fronto-parietal cortex. *PLoS biology*, *12*(8), e1001936. doi:10.1371/journal.pbio.1001936
65. Tang, H., Yu, H.-Y., Chou, C.-C., Crone, N. E., Madsen, J. R., Anderson, W. S., & Kreiman, G. (2016). Cascade of neural processing orchestrates cognitive control in human frontal cortex. *eLife*, *5*. doi:10.7554/eLife.12352
66. Tort, A. B. L., Komorowski, R. W., Manns, J. R., Kopell, N. J., & Eichenbaum, H. (2009). Theta-gamma coupling increases during the learning of item-context associations. *Proceedings of the National Academy of Sciences of the United States of America*, *106*(49), 20942–20947. doi:10.1073/pnas.0911331106
67. Tort, A. B. L., Kramer, M. A., Thorn, C., Gibson, D. J., Kubota, Y., Graybiel, A. M., & Kopell, N. J. (2008). Dynamic cross-frequency couplings of local field potential oscillations in rat striatum and hippocampus during performance of a T-maze task. *Proceedings of the National Academy of Sciences of the United States of America*, *105*(51), 20517–20522. doi:10.1073/pnas.0810524105
68. van der Meij, R., Kahana, M., & Maris, E. (2012). Phase-amplitude coupling in human electrocorticography is spatially distributed and phase diverse. *The Journal of neuroscience : the official journal of the Society for Neuroscience*, *32*(1), 111–123. doi:10.1523/JNEUROSCI.4816-11.2012
69. van Wingerden, M., van der Meij, R., Kalenscher, T., Maris, E., & Pennartz, C. M. A. (2014). Phase-amplitude coupling in rat orbitofrontal cortex discriminates between correct and incorrect decisions during associative learning. *The Journal of neuroscience : the official journal of the Society for Neuroscience*, *34*(2), 493–505. doi:10.1523/JNEUROSCI.2098-13.2014
70. van Zaen, J., Murray, M. M., Meuli, R. A., & Vesin, J.-M. (2013). Adaptive filtering methods for identifying cross-frequency couplings in human EEG. *PloS one*, *8*(4), e60513. doi:10.1371/journal.pone.0060513
71. Vanhatalo, S., Palva, J. M., Holmes, M. D., Miller, J. W., Voipio, J., & Kaila, K. (2004). Infraslow oscillations modulate excitability and interictal epileptic activity in the human cortex during sleep. *Proceedings of the National Academy of Sciences of the United States of America*, *101*(14), 5053–5057. doi:10.1073/pnas.0305375101
72. Voloh, B., Valiante, T. A., Everling, S., & Womelsdorf, T. (2015). Theta-gamma coordination between anterior cingulate and prefrontal cortex indexes correct attention shifts. *Proceedings of the National Academy of Sciences of the United States of America*, *112*(27), 8457–8462. doi:10.1073/pnas.1500438112
73. Vosskuhl, J., Huster, R. J., & Herrmann, C. S. (2015). Increase in short-term memory capacity induced by down-regulating individual theta frequency via transcranial alternating current stimulation. *Frontiers in human neuroscience*, *9*, 257. doi:10.3389/fnhum.2015.00257
74. Voytek, B., Canolty, R. T., Shestyuk, A., Crone, N. E., Parvizi, J., & Knight, R. T. (2010). Shifts in gamma phase-amplitude coupling frequency from theta to alpha over posterior cortex during visual tasks. *Frontiers in human neuroscience*, *4*, 191. doi:10.3389/fnhum.2010.00191

75. Voytek, B., D'Esposito, M., Crone, N., & Knight, R. T. (2013). A method for event-related phase/amplitude coupling. *NeuroImage*, *64*, 416–424. doi:10.1016/j.neuroimage.2012.09.023
76. Voytek, B., Kayser, A. S., Badre, D., Fegen, D., Chang, E. F., Crone, N. E.,. . . D'Esposito, M. (2015). Oscillatory dynamics coordinating human frontal networks in support of goal maintenance. *Nature neuroscience*, *18*(9), 1318–1324. doi:10.1038/nn.4071
77. Voytek, B., Kramer, M. A., Case, J., Lepage, K. Q., Tempesta, Z. R., Knight, R. T., & Gazzaley, A. (2015). Age-Related Changes in 1/f Neural Electrophysiological Noise. *The Journal of neuroscience : the official journal of the Society for Neuroscience*, *35*(38), 13257–13265. doi:10.1523/JNEUROSCI.2332-14.2015
78. Whittingstall, K., & Logothetis, N. K. (2009). Frequency-band coupling in surface EEG reflects spiking activity in monkey visual cortex. *Neuron*, *64*(2), 281–289. doi:10.1016/j.neuron.2009.08.016
79. Wulff, P., Ponomarenko, A. A., Bartos, M., Korotkova, T. M., Fuchs, E. C., Bahner, F.,. . . Monyer, H. (2009). Hippocampal theta rhythm and its coupling with gamma oscillations require fast inhibition onto parvalbumin-positive interneurons. *Proceedings of the National Academy of Sciences of the United States of America*, *106*(9), 3561–3566. doi:10.1073/pnas.0813176106
80. Xu, X., Zheng, C., An, L., Wang, R., & Zhang, T. (2016). Effects of Dopamine and Serotonin Systems on Modulating Neural Oscillations in Hippocampus-Prefrontal Cortex Pathway in Rats. *Brain topography*, *29*(4), 539–551. doi:10.1007/s10548-016-0485-3
81. Yanagisawa, T., Yamashita, O., Hirata, M., Kishima, H., Saitoh, Y., Goto, T.,. . . Kamitani, Y. (2012). Regulation of motor representation by phase-amplitude coupling in the sensorimotor cortex. *The Journal of neuroscience : the official journal of the Society for Neuroscience*, *32*(44), 15467–15475. doi:10.1523/JNEUROSCI.2929-12.2012
82. Zheng, C., & Zhang, T. (2015). Synaptic plasticity-related neural oscillations on hippocampus-prefrontal cortex pathway in depression. *Neuroscience*, *292*, 170–180. doi:10.1016/j.neuroscience.2015.01.071

APPENDIX B

K-Means Clustering Approach

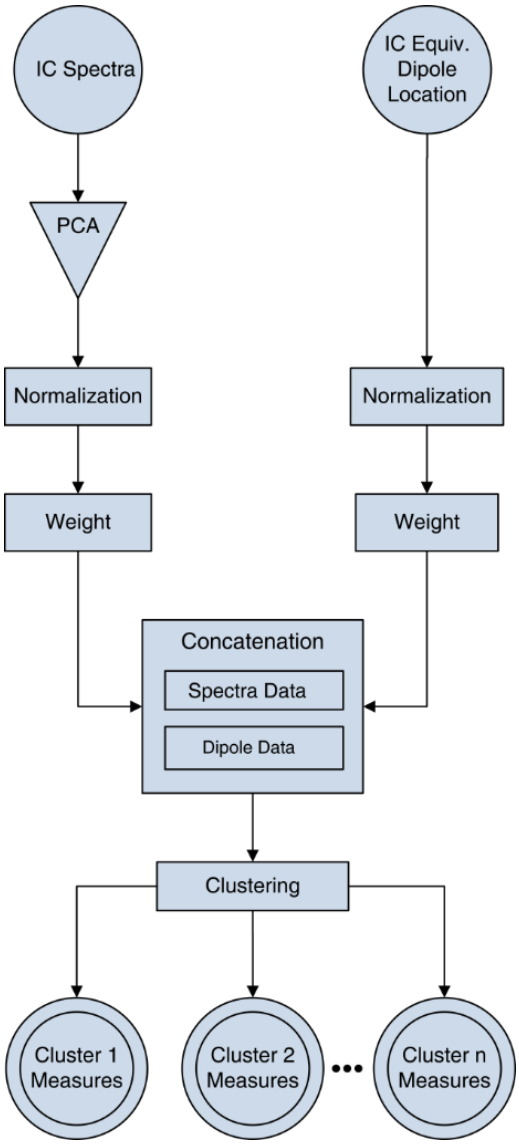

Figure 5.1: Steps of a k-means clustering approach (based on the principal component analysis). Process to define ICs with spatially close dipole positions and similar spectra of IC activations. Reprinted and adapted from NeuroImage, 72, Bigdely-Shamlo et al., Measure projection analysis: A probabilistic approach to EEG source comparison and multi-subjects inference, p. 290, Copyright 2013, with permission from Elsevier.

APPENDIX C

Reclustering Process

1 Mean cluster scalp maps were visually inspected and one cluster was chosen for each of the following topographical regions of interest: frontal left, parietal left, frontal midline, parietal midline, frontal right, parietal right. If two clusters were equally suitable for one region of interest these two clusters were combined.

2 For each subject all independent component scalp maps were screened and each IC that could potentially fit into the cluster according to its scalp map, its distance to the cluster centroid (MNI x- and y- coordinates; z-coordinate was omitted because Dipfit2 is imprecise for the z-direction), and according to its location (Talairach Client; http://www.talairach.org) was looked at in more detail.

3 Frequency spectra of all ICs for each subject (automatically clustered and if applicable manually found) were checked whether they had a peak below beta frequency. This criteria was established, because extracted instantaneous phases of band-pass filtered signals are only meaningful, if the correspondent frequency band has a peak in the spectrum (Aru et al., 2015).

4 It was made sure that the component(s) did not contain strong muscle artefacts. If a component fit perfectly by all criteria, but had slight muscle artefacts, it was included to prevent having to exclude a subject.

5 If more than one component was left for a subject, these were rated according to their location (minimal distance to cluster centroid) and residual variance (the lower the better). In ambiguous cases, the automatically clustered component had priority.

During reclustering some ICs were identified that fit ideally into a cluster (according to dipole localization, spectra, scalp map, and IC activation), but were localized slightly above the head. As dipole fitting in the z-direction is imprecise, these ICs were nevertheless included. This was done to prevent having to exclude subjects from the analyses.

APPENDIX D

Dipole Location within a standardised brain (MNI template): Each blue circle represents a subject; the red circle represents the cluster centroid.

Task Switching Paradigm

Left Frontal Cluster

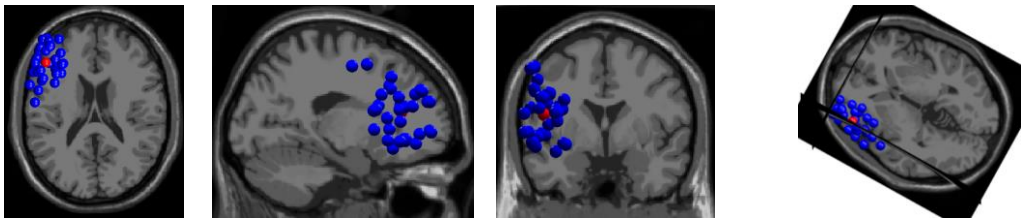

Midline Frontal Cluster

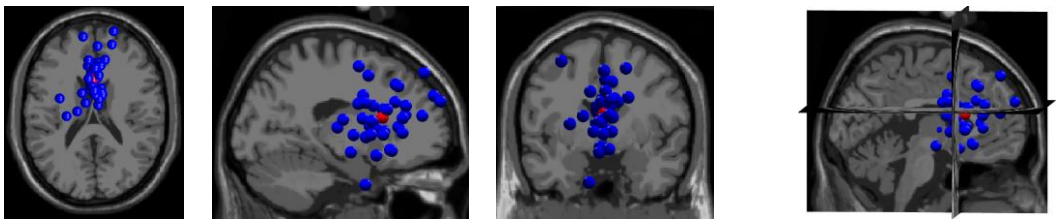

Right Frontal Cluster

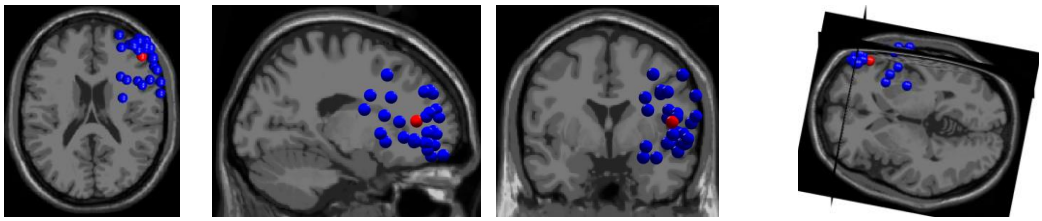

Left Parietal Cluster

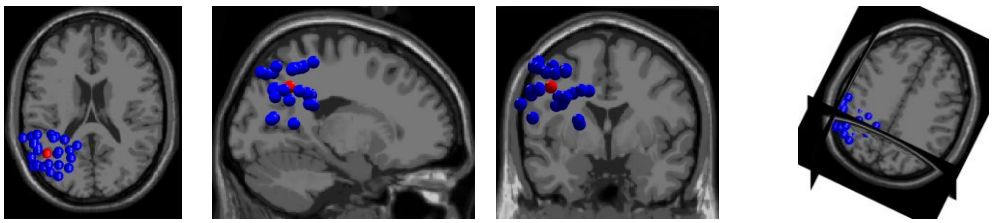

Midline Parietal Cluster

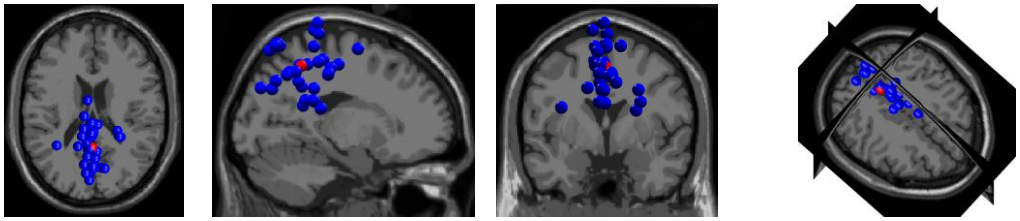

Right Parietal Cluster

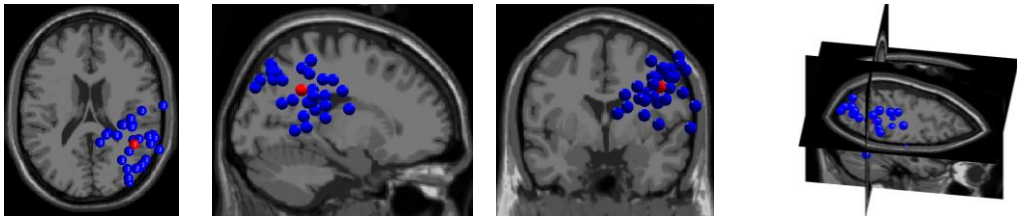

Go-Nogo Paradigm

Left Frontal Cluster

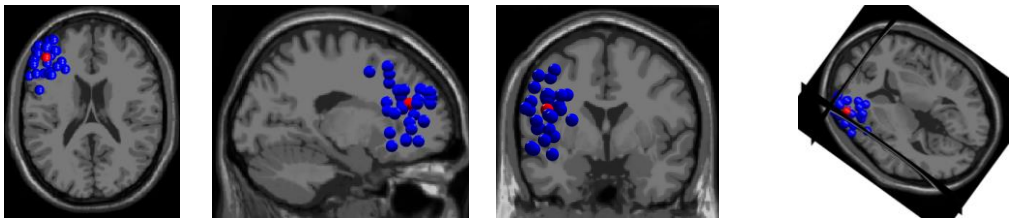

Midline Frontal Cluster

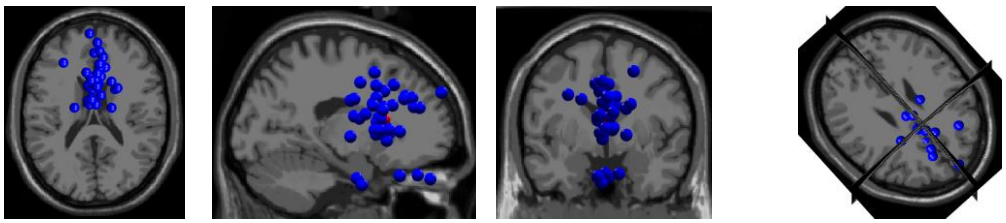

Right Frontal Cluster

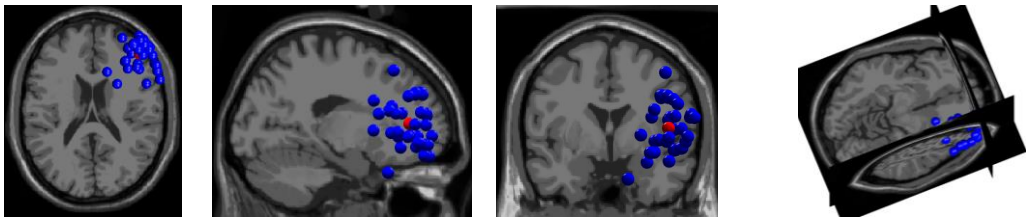

Left Parietal Cluster

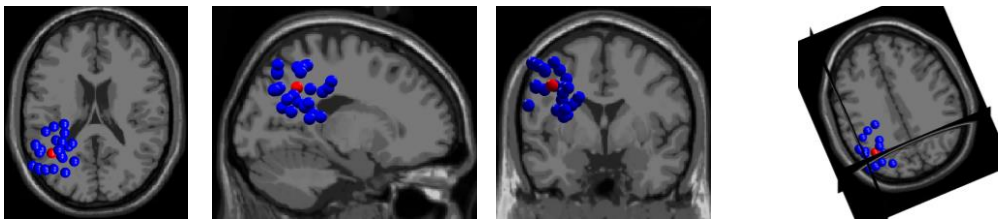

Midline Parietal Cluster

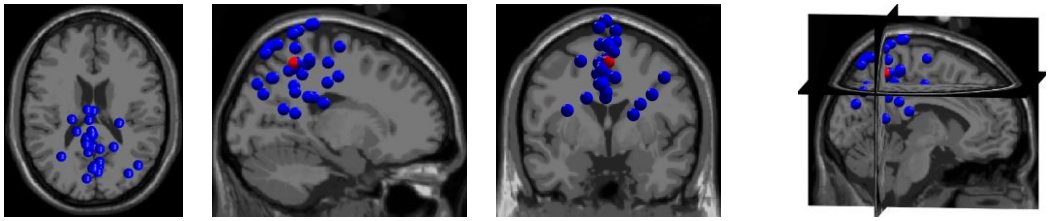

Right Parietal Cluster

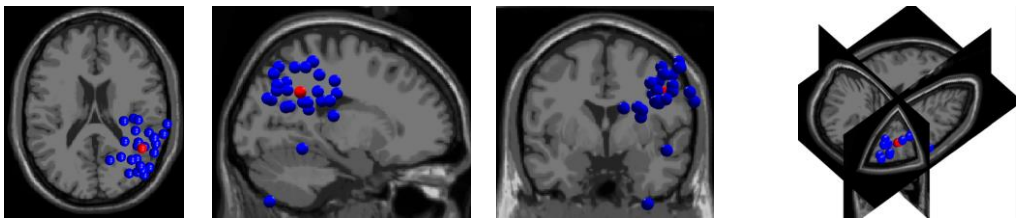

APPENDIX E

Dipole Location within a standardised brain (MNI template): Each blue circle represents a subject; the red circle represents the cluster centroid.

Sternberg Working Memory Task

Left Frontal Cluster

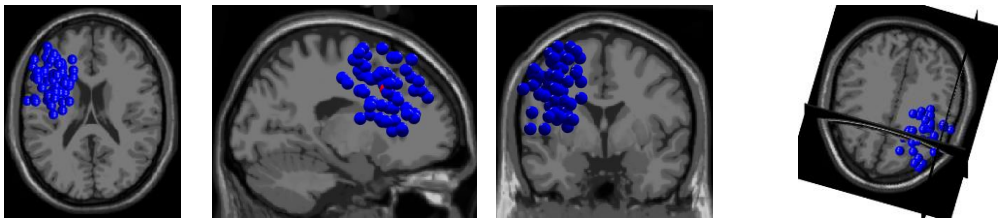

Midline Frontal Cluster

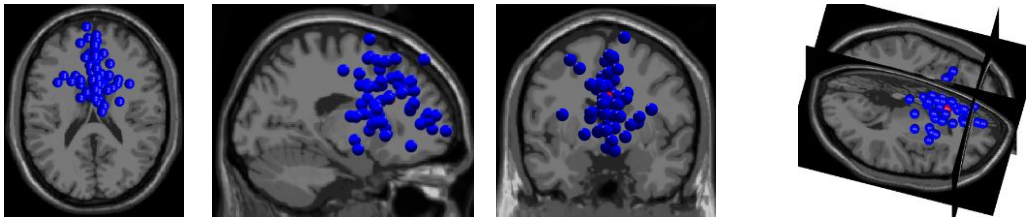

Right Frontal Cluster

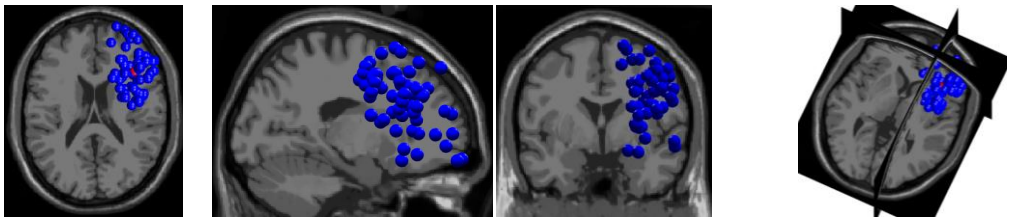

Left Parietal Cluster

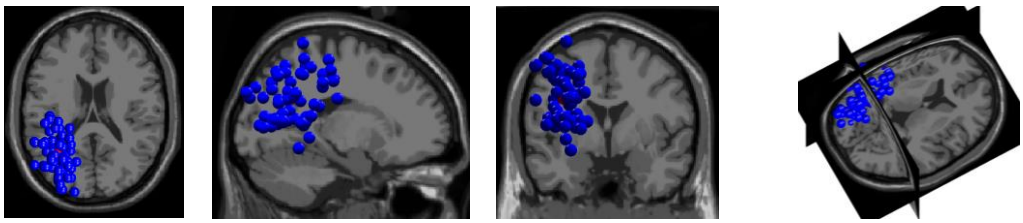

Midline Parietal Cluster

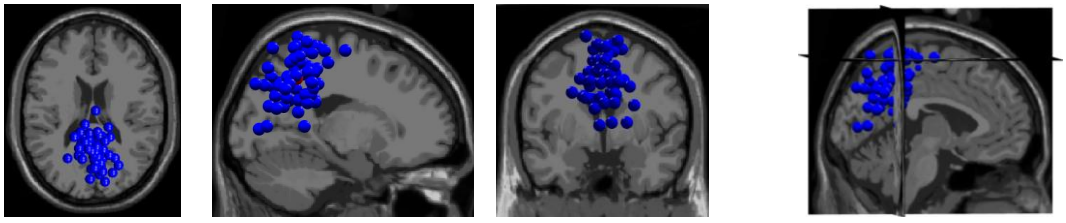

Right Parietal Cluster

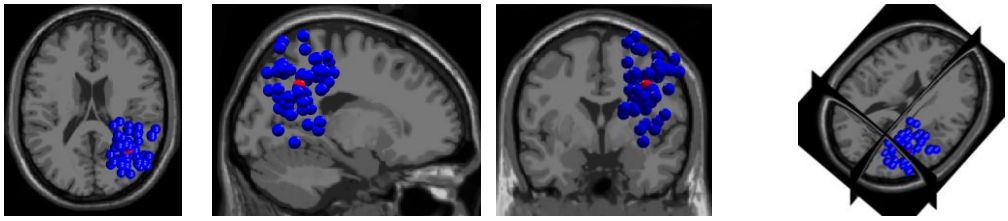

Attention Network Test

Left Frontal Cluster

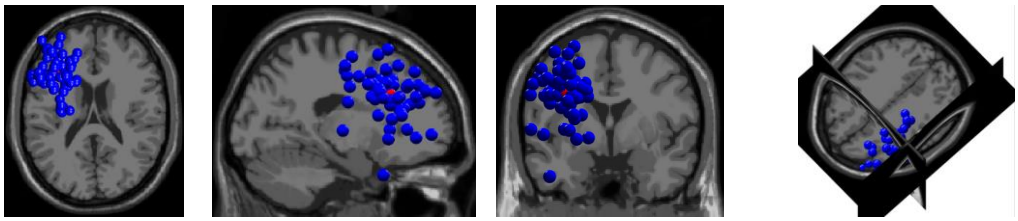

Midline Frontal Cluster

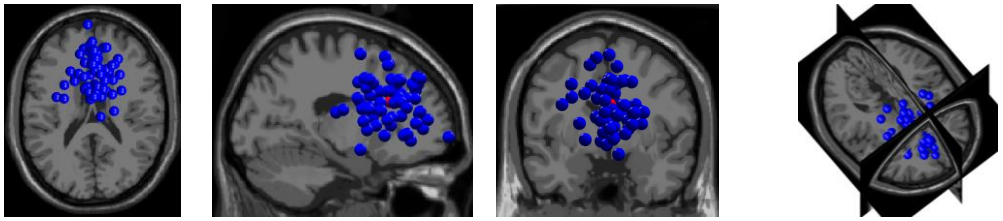

Right Frontal Cluster

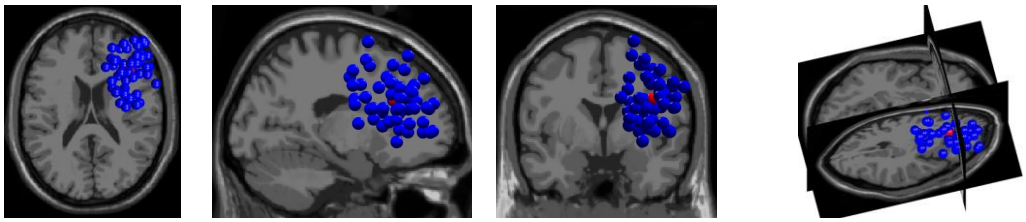

Left Parietal Cluster

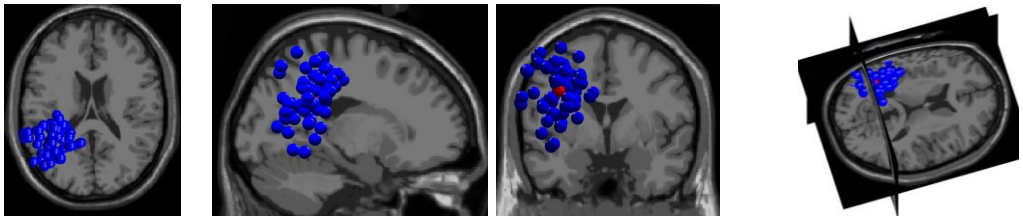

Midline Parietal Cluster

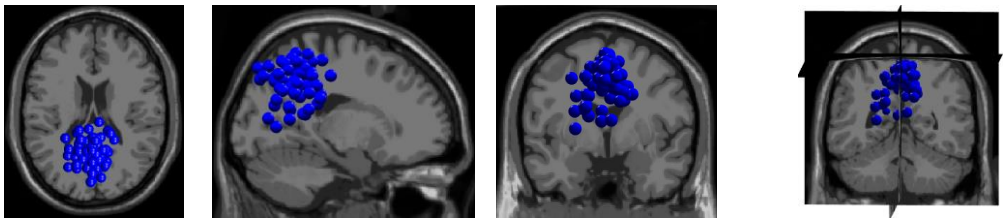

Right Parietal Cluster

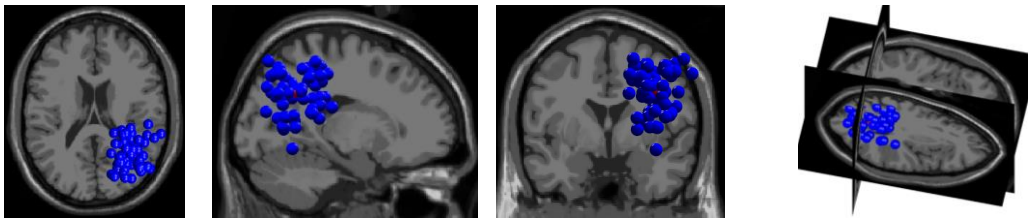

APPENDIX F

Follow-up ANOVA for comparing coupling strength between attention networks

Statistical Analysis. After having explored phase-amplitude coupling for each attention network independently, another ANOVA was calculated to compare modulation indices between attention networks. Therefore modulation indices for each participants were averaged over hemispheres, blocks, and cue or target types. A 3 x 5 x 2 ANOVA with the repeated measurement factors attention network (alerting, orienting, executive control) and frequency pair (delta-beta, delta-gamma, theta-beta, theta-gamma, beta-gamma) as well as the between-subjects factor sex (male, female) was conducted. The factor responder group was omitted in this analyses, as it had not been shown to explain any variance in the previous analyses.

Results. Again main effects frequency pair and sex as well as their interaction became significant as was already shown in the analyses of section 4.3.5 (data can be inferred from the analyses reported in that section; p. 119 ff.). The main effect attention network was significant ($F_{(2,106)} = 38.81$, $p < .001$, $\omega^2 = .31$, $\text{Dunn}_{\text{crit}} = .18$) and interacted with sex ($F_{(2,106)} = 4.67$, $p = .016$, $\omega^2 = .04$, $\text{Dunn}_{\text{crit}} = .29$) and frequency pair ($F_{(8,424)} = 20.00$, $p < .001$, $\omega^2 = .16$, $\text{Dunn}_{\text{crit}} = .89$). The three-way interaction attention network by frequency pair by sex (Table 5.1) became only marginally significant and did not explain more than 2 % of variance. These effects reveal, coupling within alerting and orienting networks is similar, while it is significantly weaker for these both networks than for the executive control network (alerting = orienting < executive control). This is true for both sexes, even though males show generally higher coupling strength than females.

Table 5.1: Mean modulation indices (S. E.) in the attention network test for each attention network, frequency pair and sex. Averaged over hemispheres, blocks, cue or target types, and responder groups. Values printed in bold represent significant coupling. Males and females do not differ in the pattern of coupling strength differences, but only in their overall coupling strength, men exhibiting stronger coupling.

	Female			**Male**		
	Alerting	Orienting	Executive Control	Alerting	Orienting	Executive Control
Delta-Beta	0.92 (0.21)	0.74 (0.18)	1.08 (0.25)	0.95 (0.22)	.90 (0.19)	1.31 (0.26)
Delta-Gamma	0.20 (0.09)	0.21 (0.10)	0.24 (0.11)	0.35 (0.10)	.29 (0.10)	0.49 (0.12)
Theta-Beta	0.45 (0.12)	0.42 (0.14)	0.65 (0.17)	0.47 (0.13)	.56 (0.15)	0.74 (0.18)
Theta-Gamma	0.23 (0.12)	0.18 (0.11)	0.27 (0.15)	0.42 (0.13)	.43 (0.12)	0.56 (0.16)
Beta-Gamma	**3.99 (1.66)**	**3.76 (1.68)**	**5.17 (2.12)**	**9.38 (1.75)**	**9.67 (1.78)**	**12.28 (2.32)**

Erklärung

nach § 9, Abs. 1 der Promotionsordnung des Fachbereichs I der Universität Trier vom 13.11.2008.

Ich versichere, dass ich die vorliegende Dissertation selbstständig verfasst und keine anderen als die angegebenen Quellen und Hilfsmittel benutzt habe. Die Arbeit wurde an keiner anderen Universität zur Erlangung eines akademischen Grades eingereicht.

Trier, 26. September 2016

Mareike J. Hülsemann